UNIVERSITY OF BELGRADE

FACULTY OF MEDICINE

Aleksa Z. Leković

MACHINE LEARNING ALGORITHMS IN FORENSIC EXPERTISE: ASSESSING NOOSE KNOT'S POSITION IN SUICIDAL HANGINGS THROUGH FRACTURE PATTERNS OF THE THYROHYOID COMPLEX AND THE CERVICAL SPINE

Doctoral Dissertation

Belgrade, 2024

УНИВЕРЗИТЕТ У БЕОГРАДУ

МЕДИЦИНСКИ ФАКУЛТЕТ

Алекса З. Лековић

АЛГОРИТМИ МАШИНСКОГ УЧЕЊА У ФОРЕНЗИЧКОЈ ЕКСПЕРТИЗИ: ПРОЦЕНА ПОЛОЖАЈА ЧВОРА ОМЧЕ У САМОУБИЛАЧКИМ ВЕШАЊИМА НА ОСНОВУ РАСПОРЕДА ПРЕЛОМА ТИРЕОХИОИДНОГ КОМПЛЕКСА И ВРАТНЕ КИЧМЕ

докторска дисертација

Београд, 2024.

PhD Advisor:

Full Professor Slobodan Nikolić

University of Belgrade – Faculty of Medicine

Members of the Evaluation Committee

1. **Prof. Marija Djurić,**
   Full Professor, University of Belgrade - Faculty of Medicine
2. **Prof. Djordje Alempijević,**
   Full Professor, University of Belgrade - Faculty of Medicine
3. **Assist. Prof. Arso Vukićević**,
   Assistant Professor, University of Kragujevac – Faculty of Engineering

Date of the public presentation: _____

Ментор:

проф. др Слободан Николић

Универзитет у Београду – Медицински факултет

Чланови комисије за оцену и одбрану докторске дисертације

1. **проф. др Марија Ђурић**,
   редовни професор, Медицински факултет Универзитета у Београду
2. **проф. др Ђорђе Алемпијевић,**
   редовни професор, Медицински факултет Универзитета у Београду
3. **доц. др Арсо Вукићевић**,
   доцент, Факултет инжењерских наука Универзитета у Крагујевцу

Датум јавне одбране докторске дисертације: _____

I want to express my gratitude to Professor Slobodan Nikolić, my mentor, for his selfless support and advice, which were of great assistance to me during this research but also in overcoming challenges in my scientific and professional work in general.

I am thankful to Professor Marija Djurić and colleagues from the Center of Bone Biology of our Faculty for their sincere support during the dissertation preparation.

I want to thank Assistant Professor Arso Vukićević for the assistance in the application, analysis, and interpretation of machine learning methods, which are an integral part of this research.

For their unconditional support in everything I like to do, I thank my parents and sister.

I dedicate this thesis to my dear Marija, with love.

Belgrade,

October 1, 2024

Професору Слободану Николићу, свом ментору, захваљујем се на несебичној подршци и саветима који су ми били од велике помоћи током овог истраживања, али и у савладавању изазова у мом научном и у стручном раду уопште.

Захваљујем се професорки Марији Ђурић и колегама из Центра за биологију кости нашег Факултета на искреној подршци током израде дисертације.

Доценту Арси Вукићевићу захваљујем се на пруженој помоћи у примени, анализи и интерпретацији метода машинског учења, које су саставни део овог истраживања.

На безусловној подршци у свему што волим да радим захваљујем се својим родитељима и сестри.

Овај рад посвећујем својој драгој Марији, с љубављу.

Београд,

1. октобар 2024. године

Title of the doctoral dissertation:

MACHINE LEARNING ALGORITHMS IN FORENSIC EXPERTISE: ASSESSING NOOSE KNOT'S POSITION IN SUICIDAL HANGINGS THROUGH FRACTURE PATTERNS OF THE THYROHYOID COMPLEX AND THE CERVICAL SPINE

Abstract

Background and Aim: In hanging, a noose can be formed with the knot located on the posterior side of the neck (typical hanging), anterior, or lateral side (atypical hangings). Upon neck compression, characteristic but nonspecific injuries of hard neck structures occur, particularly the hyoid bone's greater horns, the thyroid cartilage's superior horns, and the cervical spine. In the evaluation of deaths by hanging, it can be important to determine the position of the knot in a noose. This is particularly useful if the ligature is not found, or a ligature mark is subtle or absent. However, previous research failed to clearly determine if the distribution of fractures of the neck hard tissue structures that occur in hanging directly relates to the noose's knot position and if there are distinct patterns of these injuries that would correspond to the localization and direction of a force applied to the neck by the noose. Also, the subject's age, body height, and weight could impact the occurrence of these fractures. The hemorrhages at the origin of the sternocleidomastoid muscles at the clavicles could also aid in the knot position assessment. So far, machine learning models have not been used to associate the fracture distribution patterns with the knot position and thus supplement standard statistical analyses. Machine learning algorithms, capable of detecting complex and non-obvious associations between variables, might help in these cases. So, this research aimed to analyze the characteristics and distribution of neck's hard structure fractures with regards to the knot in a noose position in suicidal hangings and to determine the performance of machine learning models in assessing the knot position based on the presence of the fractures and their distribution, as well as to consider the significance of subjects' body weight and height, and presence of sternocleidomastoid muscle's origin hemorrhage in the knot position assessment.

Material and Methods: The research comprised of three separate parts. In all three parts, retrospectively obtained single-institution autopsy data on subjects' sex, age, and distribution of greater hyoid bone's horns (GHH), superior thyroid cartilage's horns (STH), and cervical spine (cS) fractures in suicidal hangings with a short drop or without a drop were analyzed. In the first part of the study, which included 1235 cases of suicidal hanging, the mentioned variables were analyzed by standard statistical and machine learning-based analyses in a stepwise manner to discriminate between a) typical (posterior) and atypical (anterior and lateral) hangings, b) anterior and lateral hangings, and c) left and right lateral hangings. The study's second part, which included 368 cases, comprised the subset with additional data on body weight and body height. To assess the contribution of body weight and height in knot position-related fracture patterns (in addition to standard statistical analyses), two analogous machine learning models (MLm), one considering these anthropometric characteristics and one without this data, were developed. The machine learning analysis was performed to discriminate between the typical and atypical knot positions. The third part of the study, which included 126 cases of suicidal hangings, comprised a subset with data on hemorrhage of the sternocleidomastoid muscle's (SCMm)

origin at the clavicles. As in the previous step, analogous MLm models were developed to discriminate between the typical and atypical knot position, one considering data on SCMm origin hemorrhages and analogous model not considering it. In all three study parts, the following machine learning algorithms were used: Genetic Algorithm-optimized Artificial Neural Network (GA-ANN) developed in MATLAB, and algorithms developed in SPSS – Multilayer Perceptron-ANN (MLP-ANN), Decision Tree (DT), k Nearest Neighbors (kNN), and Naïve Bayes (NB).

Results: The accuracy of machine learning models in the first step (discrimination between the typical and atypical hangings) was very modest (c. 60%) but increased subsequently in discriminating between atypical and lateral hangings, and particularly in distinguishing between left lateral from right lateral knot position: ANNs and k-NN models performed excellently in this step, with overall classification accuracies above 90%. Age was a statistically significant predictor of GHH and cS fractures but not STH fractures. Body weight was a statistically significant predictor only of STH fracture and SCMm origin hemorrhage occurrence. However, input on body weight, height, and SCMm origin hemorrhage presence and distribution did not improve MLm's performance in discriminating between the hangings with typical and atypical knot positions. In the second part of the study, the developed MLm that considered body height and weight did not perform statistically better than analogous MLm that did not consider them, on the ROC curve analysis. The same holds for the third part of the study – the developed MLm that considered SCMm origin hemorrhages did not perform statistically better than analogous MLm that did not consider this variable. Supplemented by conventional statistical analysis, the entire research showed that cervical spine and unilateral GHH fractures were independently associated with atypical knot position compared to hangings with typical knot position. In lateral hangings, the knot position was associated with ipsilateral GHH fracture and ipsilateral SCMm hemorrhage, as well as with the contralateral STH fracture.

Conclusion: Valid machine learning models can be developed to determine the noose knot position in hangings with a short drop or without a drop by thyrohyoid complex and cervical spine fracture patterns. This contributes to a better understanding of biomechanical processes in hanging. While the subject's age should be considered, this study indicated that body weight and height are of no detrimental value in assessing the thyrohyoid and cervical spine fracture patterns in suicidal hangings. The most apparent fracture distribution patterns observed were significantly more frequent unilateral fracture of the hyoid bone's greater horn and the cervical spine fracture in atypical hangings. When comparing only lateral hangings, the greater hyoid bone's horn fracture on the side of the knot and thyroid cartilage's superior horn fracture contralateral to it were significantly more frequent. The SCMm origin hemorrhages tend to occur more often on the side of the knot if it is placed on the lateral side of the neck.

Keywords: Forensic Pathology, Expertise, Autopsy, Hanging, Suicide, Machine Learning, Thyrohyoid Complex, Cervical Spine, Fracture, Pattern.

Scientific field: ***Medicine***
Specific scientific field: ***Skeletal Biology***

UDK number: _____

Наслов докторске дисертације:

АЛГОРИТМИ МАШИНСКОГ УЧЕЊА У ФОРЕНЗИЧКОЈ ЕКСПЕРТИЗИ: ПРОЦЕНА ПОЛОЖАЈА ЧВОРА ОМЧЕ У САМОУБИЛАЧКИМ ВЕШАЊИМА НА ОСНОВУ РАСПОРЕДА ПРЕЛОМА ТИРЕОХИОИДНОГ КОМПЛЕКСА И ВРАТНЕ КИЧМЕ

Сажетак

Увод и циљ: При вешању омча може да се постави тако да се чвор налази на задњој страни врата (типична вешања), предњој или латералној (атипична вешања). При стезању врата, долази до карактеристичних, али не и специфичних повреда чврстих структура врата и то великих рогова хиоидне кости и горњих рогова тиреоидне хрскавице, али и вратне кичме. При анализи смрти услед вешања може бити значајно да се утврди место чвора омче. То је нарочито корисно уколико омча није нађена на лицу места или је траг стезања слабо изражен или не постоји уопште. Међутим, досадашња истраживања нису јасно утврдила да ли је распоред прелома чврстих структура врата насталих током акта вешања у директној вези са позицијом чвора омче и да ли постоји нарочит распоред, односно дистрибуција прелома у односу на правац и место дејства силе којом омча притиска врат. Притом, на настанак ових прелома могли би да утичу старост особе, њена висина и тежина. На положај чвора омче током вешања, могла би да укажу и крварења припоја стерноклеидомастоидних мишића *(SCMm)* за клавикуле. До сада, модели машинског учења *(MLm)* нису коришћени да открију повезаност између распореда прелома чврстих структура врата и позиције чвора и на тај начин буду допуна стандардним статистичким анализама. Алгоритми машинског учења, способни да открију сложене везе између ових варијабли, које нису очигледне, могли би да буду корисни у овим случајевима. Стога, ово истраживање је имало за циљ да анализира карактеристике и распоред прелома чврстих структура врата у односу на место чвора омче код самоубилачких вешања и да утврди перформансе модела машинског учења у процени положаја чвора на основу постојања ових прелома и њиховог распореда, као и да испита значај тежине и висине вешаника и крварења припоја стерноклеидомастоидних мишића за клавикуле у процени положаја чвора омче.

Материјал и методе: Истраживање је спроведено у три засебна дела. У сва три дела, анализирани су ретроспективно прикупљени подаци о полу, старости, распореду прелома великих рогова хиоидне кости *(GHH)*, горњих рогова тиреоидне хрскавице *(STH)* и вратне кичме *(cS)* у обдукованих особа које су извршиле самоубиство вешањем са кратким замахом или без њега. У првом делу студије, који је обухватио 1235 случајева, наведене варијабле анализиране су стандардним статистичким методама и методама машинског учења, поступном анализом, ради дискриминације између: а) типичне (задње) и атипичне (предње и бочне) позиције чвора, б) предње и бочне позиције чвора и в) леве и десне бочне позиције чвора. У другом делу студије испитивано је 368 случајева са додатним подацима о тежини и висини вешаника. Да би се проценио значај тежине и висине у односу на распоред прелома и место чвора (уз стандардне анализе) направљена су два *MLm*-а, један који у обзир узима ове две варијабле и други, аналогни, који их не анализира. Анализа машинског учења коришћена је за дискриминацију између случајева са типичном и са атипичном

позицијом чвора. У трећи део студије укључено је 126 случајева са подацима о крварењима припоја *SCMm* за клавикуле. Као и у претходном кораку, направљени су аналогни модели за дискриминацију између случајева са типичном и са атипичном позицијом чвора, један који у обзир узима податке о постојању и распореду ових крварења и други који не анализира ове варијабле. У сва три дела истраживања коришћени су следећи модели машинског учења: *Genetic Algorithm-optimized Artificial Neural Network (GA-ANN)* направљен у *MATLAB*-у и модели направљени у *SPSS*-у – *Multilayer Perceptron-ANN (MLP-ANN), Decision Tree (DT), k Nearest Neighbors (kNN),* и *Naïve Bayes (NB).*

Резултати: Прецизност класификације модела машинског учења у првом кораку (дискриминација између типичне и атипичне позиције чвора) била је врло умерена (око 60%), али се потом повећала: *ANN* и *k-NN MLm* одлично су разликовали леву од десне позиције чвора, уз прецизности веће од 90%. Старост особе била је значајан предиктор настанка *GHH* и *cS* прелома, али не и настанка прелома *STH.* Тежина особе била је значајан предиктор само прелома *STH* и крварења припоја *SCMm*. Међутим, подаци о тежини особе и постојању и распореду крварења припоја *SCMm* нису побољшали перформансе *MLm* у дискриминацији између типичне и атипичне позиције чвора. У другом делу истраживања, *MLm* који су у обзир узимали податке о тежини и висини вешаника нису били статистички значајно бољи, на основу анализе *ROC* криве. Исти резултат добијен је и у трећем делу истраживања – *MLm* који су у обзир узимали крварења припоја *SCMm* нису били статистички значајно бољи у односу на моделе који у обзир нису узимали ове варијабле. Уз конвенционалну статистичку анализу, резултати целокупног истраживања показали су да су прелом вратне кичме и једнострани преломи *GHH* били независно повезани са предњом у односу на задњу позицију чвора. Код бочних позиција чвора, постојала је повезаност стране чвора са преломом ипсилатералног *GHH* и крварењем припоја ипсилатералног *SCMm,* као и са преломом контралатералног *STH*.

Закључак: Могуће је направити валидне моделе машинског учења за одређивање позиције чвора омче код вешања са кратким замахом или без њега, а на основу прелома чврстих структура врата. Све ово доприноси бољем разумевању биомеханичких процеса током акта вешања. Резултати овог истраживања указују да телесна висина и тежина нису од пресудног значаја код процене положаја чвора на основу распореда прелома, док старост особе треба узимати у обзир. Најочигледнији уочени обрасци прелома били су унилатерални прелом великог рога хиоидне кости и прелом вратне кичме, који су чешћи код атипичне позиције чвора. При поређењу латералних вешања, прелом великог рога хиоидне кости на страни чвора и контралатералног горњег рога тиреоидне хрскавице били су значајно чешћи. Крварење припоја стерноклеидомастоидних мишића чешће је било на страни чвора, уколико је чвор био постављен на бочној страни врата.

Кључне речи: форензичка патологија, експертиза, обдукција, вешање, самоубиство, машинско учење, тиреохиоидни комплекс, вратна кичма, прелом, образац.

Научна област: **Медицина**
Ужа научна област: **Биологија скелета**

УДК број: _____

Table of Contents

1. INTRODUCTION

1.1. Asphyxia

Etymological roots of the coined term *asphyxia* stem from two Greek words: *-a* (*without*) and *-sphuxis* (*a pulse*), meaning "pulseless" or "absence of pulsation" [1–3]. Under the umbrella term "asphyxia" are, however, considered various conditions of natural and violent causes that result in the inability of cells to receive or utilize the oxygen (O_2) [2, 4, 5] – this impairment can be a consequence of the reduced amount of available (atmospheric) oxygen, blockage and obstruction of various segments of the respiratory system, restriction of respiratory movements, diseases of the lung and thorax (e.g., pneumonia), reduced cardiac function, reduced oxygen transport capacity (e.g., severe anemia or bleeding), direct blockage of oxygen utilization by cells (cellular respiration) [2, 3].

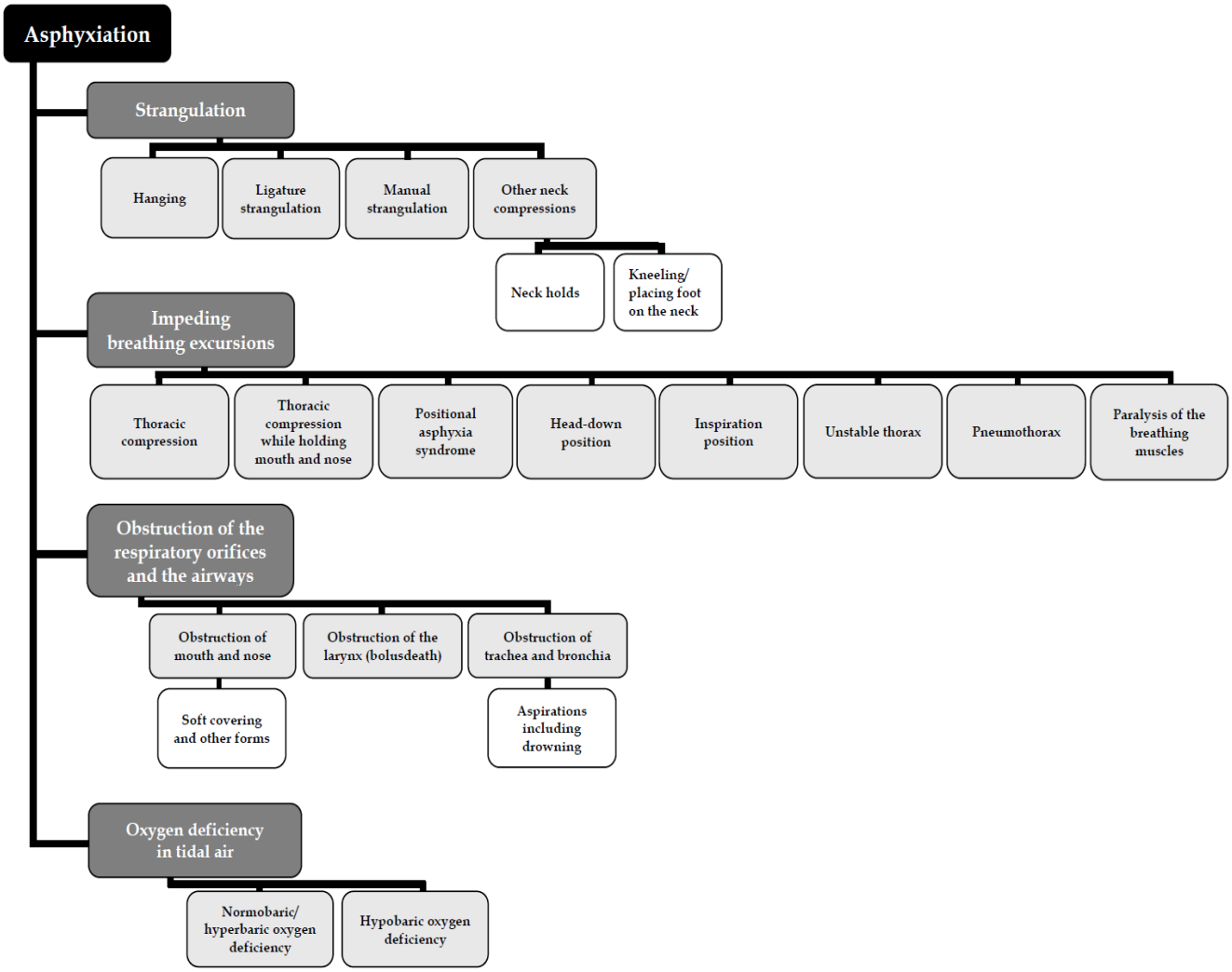

Figure 1.1. *Classification of asphyxiation. In: Madea B, Keil W, Lunetta P, Kettner M. Asphyxiation. In: Madea B (Ed). Handbook of Forensic Medicine, 2nd ed. Hoboken, NJ: Wiley, 2022, p. 510.* [2] *Reproduced with permission from John Wiley & Sons (not part of the governing CC license).*

But, apart from the severe destructive head and brain injuries, it is easy to claim that practically every fatal condition is eventually accompanied by a hypoxic-ischemic brain death [2]. In the context of forensic medicine and pathology, under the broadest terms, asphyxia and asphyxiation refer to the state of *oxygen deficiency* caused by *specific traumas* that *directly* result in hypoxic-ischemic brain injury and death. So, these conditions, in a stricter term, stem from the *injury*, are of *violent manners* (Latin, *asphyxia violenta*), and can be caused by physical (e.g., electrocution, lightning strike), chemical (e.g., cyanide or strychnine poisoning) or mechanical means [2, 6].

Although violent asphyxia deaths have always been widespread in forensic medicine, up to date, even many primary reference textbooks provided different classifications of asphyxiation [2, 3, 7–11]. One of these, a comprehensive classification used by Madea et al. [2] is shown in Figure 1.1. The most significant issue was to form a single and uniform, standardized classification system of the violent asphyxia caused by *mechanical means* – due to simple differences in didactics, different approaches to injury pathophysiology understanding, or a non-uniform English-language use. The best overview of the problem was probably given by Sauvageau and Boghossian in 2010, where a new classification system was proposed, which was presented in 2011 as the "INFOR (International Network for Forensic Research) classification" [4, 12]. This classification system of "Asphyxia in forensic context" is shown in Figure 1.2 and accompanying Table 1.1. So, violent asphyxia caused by *mechanical means* where external pressure is applied to the neck are strangulations [4, 12]. Depending on the origin of the external constricting force, three separate entities are recognized: hanging, ligature strangulation, and manual strangulation (Table 1.1) [4, 12].

1.2. Hanging

Hanging (suspension, Latin, suspensio) is a form of ligature strangulation in which the force applied to the neck is derived from the gravitational drag of the weight of the body or part of the body [3].

The majority of the hanging cases are suicidal [2, 3, 7, 9]. It is one of the most common suicide methods worldwide [13–18]. The World Health Organization (WHO) ranks it among the three most common causes of suicide in general [13]. This suicide method is favored by males [2]. Rarely, hangings can be accidental – in autoerotic asphyxia (a typical subject is a young or middle-aged male) [3, 12], and in children playing hazardous "hanging games" or in a child who accidentally entangled in a rope, or, for example, in a pacifier cord [3, 9]. Homicides are extremely rare, and a more common situation than this for a perpetrator is to hang the dead body of a previously strangled person to conceal foul play [3, 9, 19]. Judicial hangings have been quite a common practice throughout history and are nowadays almost entirely abandoned [3, 20].

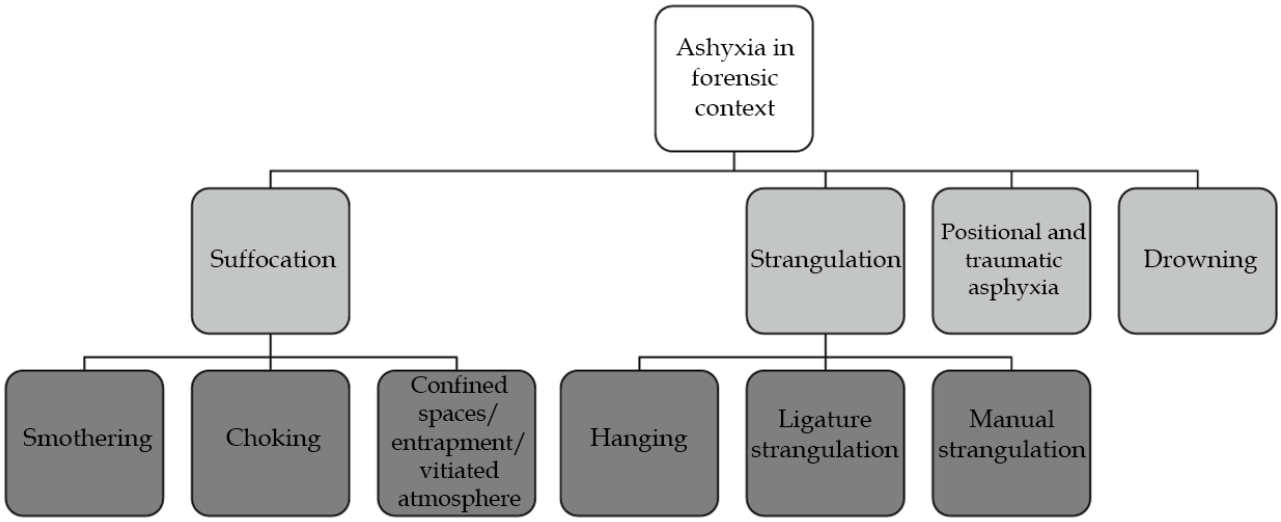

Figure 1.2. *INFOR Classification of asphyxia. From: Sauvageau A. Death by Hanging. In: Rutty G.N. (Ed). Essentials of Autopsy Practice. London: Springer-Verlage, 2014, p. 24.* [12] *Reproduced with permission from Springer Nature (not part of the governing CC license).*

Table 1.1. *Definitions of terms in the INFOR classification*

Term	**Definition**
Suffocation	A broad term encompassing different types of asphyxia, such as vitiated atmosphere and smothering, associated with deprivation of oxygen
Smothering	Asphyxia by obstruction of the air passages above the epiglottis, including the nose, mouth, and pharynx
Choking	Asphyxia by obstruction of the air passages below the epiglottis
Confined spaces/ entrapment / vitiated atmosphere	Asphyxia in an inadequate atmosphere by reduction of oxygen, displacement of oxygen by other gases, or by gases causing chemical interference with the oxygen uptake and utilization
Strangulation	Asphyxia by closure of the blood vessels and/or air passages of the neck as a result of external pressure on the neck
Hanging	A form of strangulation in which the pressure on the neck is applied by a constricting band tightened by the gravitational weight of the body or part of the body
Ligature strangulation	A form of strangulation in which the pressure on the neck is applied by a constricting band tightened by a force other than the body weight
Manual strangulation	Manual strangulation A form of strangulation caused by an external pressure
Positional or postural asphyxia	A type of asphyxia where the position of an individual compromises the ability to breathe
Traumatic asphyxia	A type of asphyxia caused by external chest compression by a heavy object
Drowning	Asphyxia by immersion in a liquid

From: Sauvageau A. Death by Hanging. In: Rutty G.N. (Ed). Essentials of Autopsy Practice. London: Springer-Verlage, 2014, p. 25. [12] *Reproduced with permission from Springer Nature (not part of the governing CC license).*

1.2.1. Circumstances and hanging scenarios

There are some distinct circumstances in hangings where the body can be found.

Complete and incomplete hangings: The suspension point in suicidal hangings is often not high enough to suspend the entire body (without any contact of the body with the floor/ground object/platform), and this is called a *complete* hanging [3, 6, 7, 9]. The entire body weight loads the noose and contributes to neck compression – strangulation [6]. In this scenario, there is a chair, ladder, or other climbing aid the subject uses to reach the formed ligature. Alternatively, which is a more common scenario, the victims can be found in standing, kneeling, sitting, or even lying positions, in which they successfully performed suicide by an *incomplete* hanging (Figure 1.3) [2, 3, 6, 9]. In this case, the partial suspension implies only the part of the body weight loads the ligature, and thus, the neck [12, 21].

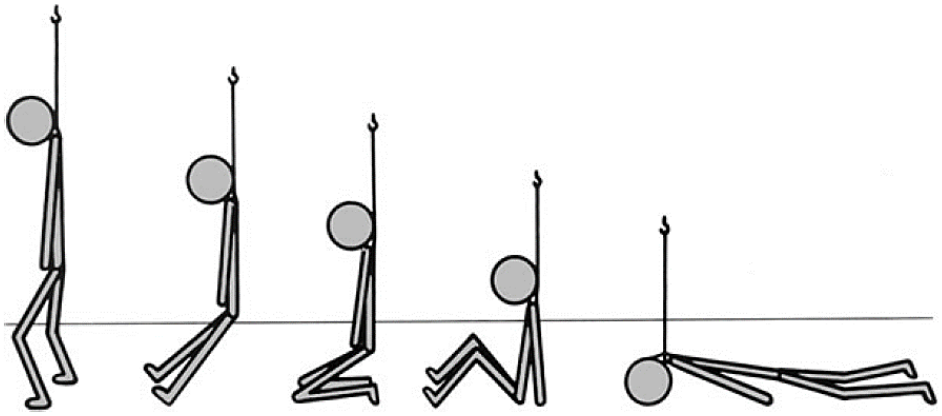

Figure 1.3. *Positions in (incomplete) hanging. From: Neck Trauma. In: Dettmeyer R.B, Verhoff M.A, Shutz H.F. Forensic Medicine Fundamentals and Perspectives. Heidelberg: Springer-Verlage, 2014, p. 171.* [9] *Reproduced with permission from Springer Nature (not part of the governing CC license).*

The proportion of the body weight that loads the ligature and the neck is reported to be 98% if a person stands and touches the ground only with toes, 66% if standing "feet-flat," 64 – 74% if kneeling, 18 – 32% if sitting, and 10 – 18% of body weight if lying down [12, 21].

The typical and atypical hangings: With regards to the position of a ligature's noose and knot, the hanging can be *typical* when the ligature slants upwards and backward symmetrically from the loop's lowest position located at the anterior midline of the neck to form the knot or the highest point (if there is no knot) at the posterior side of the head and neck, typically in the occipital or nuchal region. In the case of any other ligature's loop and knot position, the hanging is considered to be *atypical (Figure 1.4)* [2, 3, 6, 9]. This atypical position of the knot (or the ligature's highest point if the knot is not formed) can be placed in the anterior midline of the neck (the so-called *anterior* hangings) or on the lateral sides of the head and neck (approximately around the earlobes, the so-called *lateral* hangings) [6, 9].

The ligature: The ligature can be formed by a rope or improvised by virtually any available convenient material. For example, a necktie, cabled earphones, bedsheets, various clothes, a belt, a scarf, shoelaces. It can be turned around the neck once, twice, or several more times. When constructing a ligature, the noose can be formed by tying the fixed knot, creating a slip noose, or by creating an open noose, in which two ends at the highest point remain untangled and independently fixed [3, 6, 7, 9, 10].

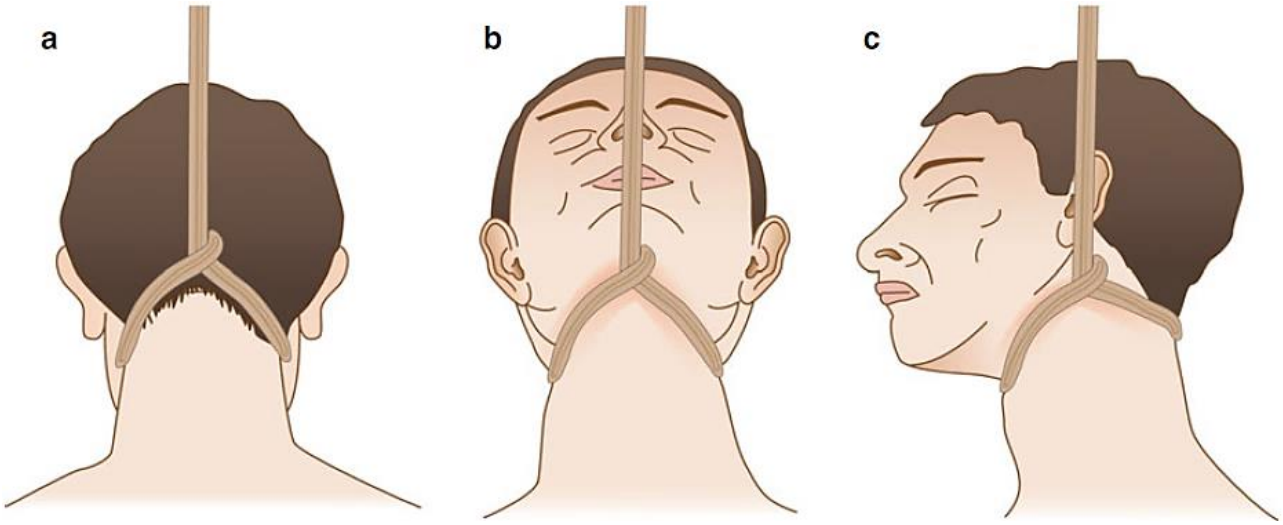

Figure 1.4. *(**a**) Typical and (**b, c**) atypical hanging. From: Neck Trauma. In: Dettmeyer R.B, Verhoff M.A, Shutz H.F. Forensic Medicine Fundamentals and Perspectives. Heidelberg: Springer-Verlage, 2014, p. 176.* [9] *Reproduced with permission from Springer Nature (not part of the governing CC license).*

The short drop and the long drop hangings: One of the most important characteristics regarding the case circumstances is distinguishing between the short drop hanging and the long drop hanging. The former is characteristic of suicides and accidents. In a *short drop*, the distance the hanged person's body, or to be more exact – the person's *neck* travels from the moment the suspension is initiated until the noose is completely tightened and fixed around the neck (that is, the final point of suspension) is no more than about one meter, or there is no drop at all (*N. B.* the short drop hangings can be complete or incomplete) [2]. On the other hand, long drop hangings are characteristic of executions and only rarely occur in the context of suicide or accident [3, 6, 12, 22]. The executions by hanging were performed for many centuries in an unstandardized manner with many flaws, and even with sentenced persons surviving being hanged [20]. In fact, the drop was introduced in the early 19th century, with the initially proposed length of about 0.3 – 0.45 meters [20]. In the following decades, the long drop method was introduced, with some adjustments, to make hanging a systematic, more efficient, and more humane execution method [12, 20]. Formulas and tables were proposed to calculate the required drop for a given subject's body weight. As the name self-describes, the distance the hanged person's neck travels are significantly greater. According to the proposed calculations, for example, a person weighing c. 80 kg would require a drop of at least c. 2.5 m [20]. In addition to the drop increase, the preferred position of the knot was changed to be placed submental (i.e., anterior atypical hanging) [20]. The proposals and conclusions were made after a better understanding of the biomechanics and a principal injury caused by this long drop method – the severe injury of the cervical spine resulting in instantaneous death, entirely different from the death mechanism in suicidal hangings with the short drop, considered in the further text [6, 12, 20, 22].

1.2.2. Mechanism of death by short drop hangings

The understanding of death mechanisms in hangings lies in two groups of evidence. The first is experimental data from the studies conducted around the end of the 19th and throughout the 20th century [2, 7, 12, 23–29]. The other is a contemporary analysis of

recorded videos of suicidal hangings initiated by Anny Sauvageau, who founded the Working Group on Human Asphyxia in the year 2006 [12, 25, 30–33].

The proposed mechanism of airway constriction was soon challenged by the occlusion of the large-caliber cervical blood vessels and eventually with the reflex cardiac arrest through the carotid sinus reflex [2, 3, 6, 12, 25]. The three proposed mechanisms are not considered mutually exclusive, and one could superimpose on others [3].

Airway occlusion: It was demonstrated that a weight load of about 15 kg is sufficient to close the trachea [3, 23]. But, in hangings, the airway occlusion stems from the lifting of the larynx by pushing the base of the tongue upwards and backward against the pharynx walls, which results in the so-called *tamponada oris* [3, 6, 9] occludes the opening of larynx.

Occlusion of the large-caliber neck blood vessels: The internal jugular veins lie relatively superficial, and the complete occlusion of their thin-walled lumens occurs with a load of as much as 2 kg [3, 23, 25]. Once the blood outflow from the head (and brain) is impeded by neck compression, the continuous blood inflow from the partially or wholly patent carotid arteries leads to congestion above the level of the ligature [2, 3, 9]. This eventually prevents the oxygenated blood from perfusing the brain and causes neuronal hypoxia [2]. This is a reason why it is possible to perform an incomplete hanging in a lying down position – the human head, on average, weighs about 5 kg [6]. To occlude the major neck arteries, a higher weight load is required – experiments showed that the load for common carotid arteries is at least 3.5 – 7.5 kg (often reported to be 5 kg), and for the vertebral arteries a much higher, at least 16 – 35 kg (usually referenced at about 30 kg) [2, 3, 21, 23, 26–28]. These results mainly refer to typical knot position, but it has been demonstrated that a force of about 30 kg is enough "to occlude at least two out of four arteries supplying the brain" in atypical (lateral) hangings [2]. The complete occlusion of all arteries is not necessary for a rapid, irreversible neuronal injury, as it occurs if the brain perfusion drops by 3 to 4 times from the standard values [2].

The carotid sinus reflex: The direct mechanical trauma to the carotid sinus could trigger the reflex cardiac arrest. The mechanical stimulation of baroreceptors and nerve endings in the carotid sinus, located in the *tunica adventitia* of the internal carotid artery just distal from its origin, triggers the cardioinhibitory reflex. From the sinus, the afferent impulses are transmitted via the sensory fibers of the carotid sinus nerve (Hering's nerve), the branch of the glossopharyngeal nerve (CN IX). These afferent fibers terminate in the *nucleus tractus solitarii* in the *medulla oblongata*, while the efferent impulses traverse through the *n. vagus* (CN X) [2, 3, 9, 34–37].

But in fact, and as previously stated, many evidence-based conclusions on the mechanism of death and agonal sequence stem from an analysis of cases of hangings that were video-recorded and the recent work on this issue of the Working Group on Human Asphyxia [4, 12, 25, 30–33]. The hanged person typically becomes unconscious after about ten seconds and then develops generalized tonic-clonic convulsions, followed by decerebrate and decorticate rigidity, with the last observable movement about 4 minutes after the hanging. There are also periods of deep rhythmic abdominal respiratory movements throughout the first two minutes [2, 12]. The exact reported agonal sequence is shown in Table 1.2. Previously, it has been reported that cardiac activity was detected for

up to 20 minutes after suspension. However, the evidence on the "point of irreversibility" for now only shows that a person could recover after about 38 s ± 15 s after the suspension was initiated, in the period of decorticate rigidity [12, 31].

Table 1.2. *The agonal sequence in strangulation (based on a review of 14 cases of filmed hanging)*

	Average time
Loss of consciousness	10 s ± 3 s
Convulsions	14 s ± 3 s
Decerebrate rigidity	19 s ± 5 s
Start of deep rhythmic abdominal respiratory movements	19 s ± 5 s
Decorticate rigidity	38 s ± 15 s
Loss of muscle tone	1 min 17 s ± 25 s
End of deep rhythmic abdominal respiratory movements	1 min 51 s ± 30 s
Last muscle movement	4 min 12 s ± 2 min 29 s

From: Sauvageau A. Death by Hanging. In: Rutty G.N. (Ed). Essentials of Autopsy Practice. London: Springer-Verlage, 2014, p. 28. [12] *Reproduced with permission from Springer Nature (not part of the governing CC license).*

1.2.3. Autopsy evaluation of deaths by hanging

In evaluating suspected deaths by hanging on autopsy, as in any case in which a neck injury is suspected, the general autopsy procedure is modified and supplemented by a so-called special autopsy of the neck organs [2, 3, 5, 7, 9, 38]. It is, nevertheless, preceded by looking at the ligature (if still present) and the detailed routine external examination of the whole body, particularly the skin of the neck, and eventually by creating "the artificial bloodless field" at the beginning of the internal autopsy examination. This bloodless field is achieved by opening the cranial vault, removing the brain and incising the dural sinuses on one side, and disconnecting the heart from its major blood vessels on the other [2, 3, 9, 10]. By this process, the blood is allowed to drain on both ends passively, rostral and caudal from the neck [2, 3, 9], which significantly decreases the possibility of creating artifactual hemorrhages in the neck structures (an excellent example of bleeding being a relative vital sign).

The general findings are typical in all deaths preceded by a very short agony and are characteristic but non-specific of asphyxia in general and of hanging, for example, the fluidity of the blood [6] (considered by some to be irrelevant and *a myth* [3]), well-pronounced *livores mortis,* congestion and edema, cyanosis, and petechial hemorrhages. So, observing them in general is of no definite significance alone (for example, many can be detected in sudden cardiac deaths) [2, 3, 6, 9]. Their distribution (or even absence) can be of more use, as will be pointed out.

1.2.3.1. Findings on the external examination

Findings above the level of the ligature: The appearance is directly related to the underlying hemodynamic disturbance [9]. If the constriction by ligature causes partial occlusion of the major blood vessels of the neck – completely occluding jugular veins but allowing some inflow of the blood through the carotid arteries – the previously described congestion ensues above the ligature level [2, 3, 7, 9, 10]. The impaired blood outflow, in addition to the transudation and consequent tissue edema, probably by combined effects of anoxia and shifting of the oxyhemoglobin curve, potentiates the formation of the reduced hemoglobin (carbaminohemoglobin) and causes pronounced cyanosis of the head and the segment of the neck rostral to the ligature level [3]. The impaired outflow can result in a dramatic increase in the intravascular pressure, which can lead to rupture of the venules and/or capillaries, appreciable in the conjunctivae, sclerae, and skin of the forehead. This is macroscopically observable as a petechial hemorrhage in these regions [2, 3, 6, 9]. Due to the same reason, overt bleeding from the ears and nose can occur [7, 9]. The petechial hemorrhage appears suddenly but requires compression to last at least 10 – 20 seconds [2, 3, 9]. These findings are present in cases of incomplete cessation of head circulation and are hence observable in incomplete and atypical hangings. Contrary, full suspension with typical knot position and complete cessation of blood inflow to the head as a rule results in total absence of the described findings (a so-called "pale hangman," Figure 1.3) [2, 3, 6, 9]. In fact, finding them in such a case must raise a suspicion of foul play [3, 9]. Additional findings include hypersalivation and saliva dripping from the angle of the lips on a tilted side of the head [2, 6, 9, 35].

Findings at the level of the ligature: The typical finding at the site of the ligature compression is the postmortal formed ligature mark, a parchment-like, brown-yellowish, or dark-reddish *furrow,* due to skin desiccation [3, 6, 9]. This is present only if the ligature is not removed quickly and if the constricting force is not minimal [6]. If present, it is usually overt and is significant for several reasons. It shows the position of the noose's loop and the position of the knot in a noose – the lowest portion corresponds to the site of the loop, while the opposite, highest point indicates the position of the knot (if it was made) or the highest level of suspension (Figure 1.5) [9]. If there is no tightly constricted fixed knot or a slip noose, the ligature mark does not encircle the entire neck circumference [2, 3, 9, 10]. It is rarely placed horizontally, except in a tightly entangled fixed/slip noose, multiple turns of the ligature, or a specifically tilted body position in incomplete hanging [3, 9]. There may be excoriations around the ligature mark, which are of no value in terms of vitality [9]. If there are several turns of the ligature, the skin between them may get pinched. In this skin ridge, the presence of hemorrhages is a significant relative sign of vitality [2, 3, 6, 9].

Findings below the level of the ligature: Since the hypostasis is typically well-pronounced, its distribution can aid in reconstructing the body's position or indicate if the body was moved and position manipulated. In complete suspensions, the characteristic "gloves and socks" distribution of the hypostasis can be observed [3, 6, 9]. In incomplete hangings, the distribution can be more complex and corresponds to the body position, compression points and tilting, if *livores* were fixed. At the most dependent areas, *vibices* can be observed (postmortem phenomenon) [6].

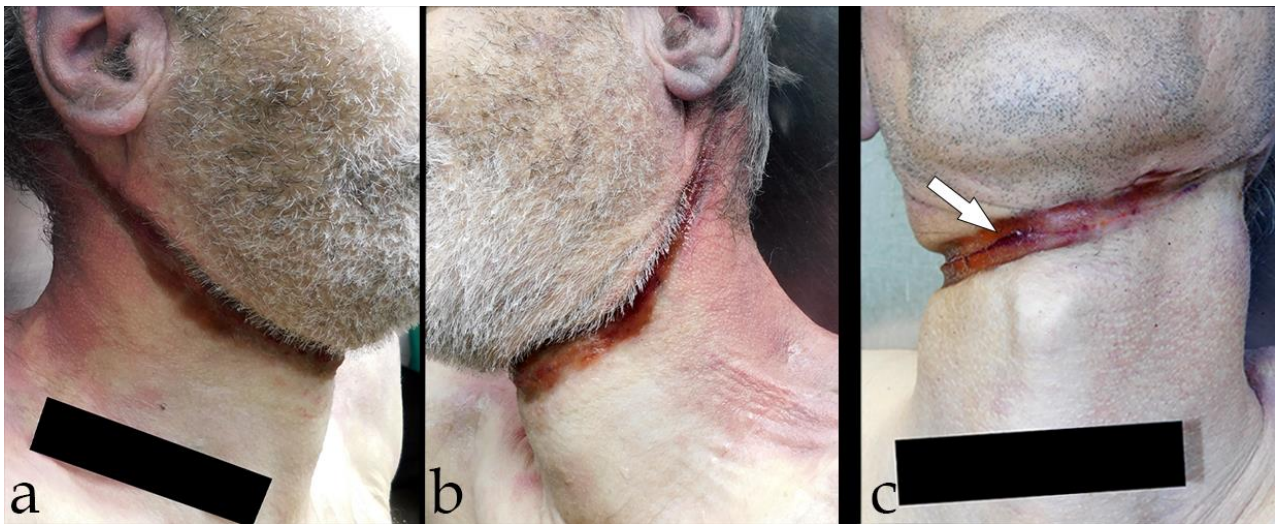

Figure 1.5. *(**a** and **b**) A furrow in the case of a typical hanging – the ligature mark has the lowest point in the anterior neck midline (above the laryngeal prominence) and runs symmetrically backwards and upwards, fading behind the earlobes – indicating the highest point or the knot in the noose was in the occipital region. (**c**) A furrow in the case of atypical (left lateral) hanging – the placement of the ligature mark indicates the lowest part was on the right lateral side of the neck, while the knot was placed in the left auricular region. The white arrow indicates the pinched ridge of the neck skin.*
From: Institute of Forensic Medicine, University of Belgrade, Faculty of Medicine, Belgrade, Serbia.

1.2.3.2. Findings on the internal examination

Findings above the level of the ligature: If the described hemodynamic disturbance – acute congestion above the ligature level occurs in the head region, the petechial hemorrhages can be detected under the temporal muscles' fasciae and in the leptomeninges. Congestion can also result in appreciable brain edema [2, 3, 6, 7, 9, 10]. All the findings in the neck region will be considered separately.

The special neck autopsy procedure and local findings: The layer-by-layer dissection is performed. Below the level of the ligature, subcutaneous tissue emphysema can occur due to Macklin effect [39], while at the ligature level, drying out of the soft tissue can be seen [6]. Moving to deeper layers of the neck, particular attention should be given to the sternocleidomastoid muscles and the upper belly of the omohyoid muscles [2, 3, 6, 9, 38]. Hemorrhages can be observed in muscles at the ligature level, but the most important are the periosteal hemorrhages of the clavicles at the origin of sternocleidomastoid muscles (Figure 1.6) [2, 3, 6, 9]. They represent the local relative vital signs and can be of various extents. This injury seems to occur due to hyperextension of the muscle – indicating the site of the knot in a noose [3, 40]. Further, in situ dissection includes the search for vessel injuries, the Amussat's sign (transversal intimal tears of carotid arteries), although rare, being the most characteristic [41, 42], the analysis of deeper neck muscles, the thyroid gland, and larynx (signs of congestion and mechanical trauma) [9]. Then, the *en bloc* evisceration of the tongue, hyoid bone, larynx, and upper segments of the trachea and esophagus is done for further inspection (see the next paragraph) [2, 3, 9]. Eventually, the revealed cervical portion of the spinal column is inspected. The cervical spine injuries in short drop hangings are more often confined to the lower half of the column (between the third and seventh cervical vertebra) and range from tearing of the anterior longitudinal ligament, widening of the intervertebral space or fractures without a dislocation [43–46]. The injury seems to be the most common in anterior atypical hangings. Still, it is different from the cervical spine injury

in long drop judicial hangings, where the fracture of the upper spine segments occurs, with a fragment dislocation (the dens), with medullar injury, or even partial or complete decapitation [22, 43]. The Hangman's fracture, spondylolisthesis of the second cervical vertebra, and symmetrical fractures of the pedicles are also characteristic of upper segment injuries [6, 22]. The fractures should be considered intravital only if accompanied by a hemorrhage in the surrounding soft tissue [6].

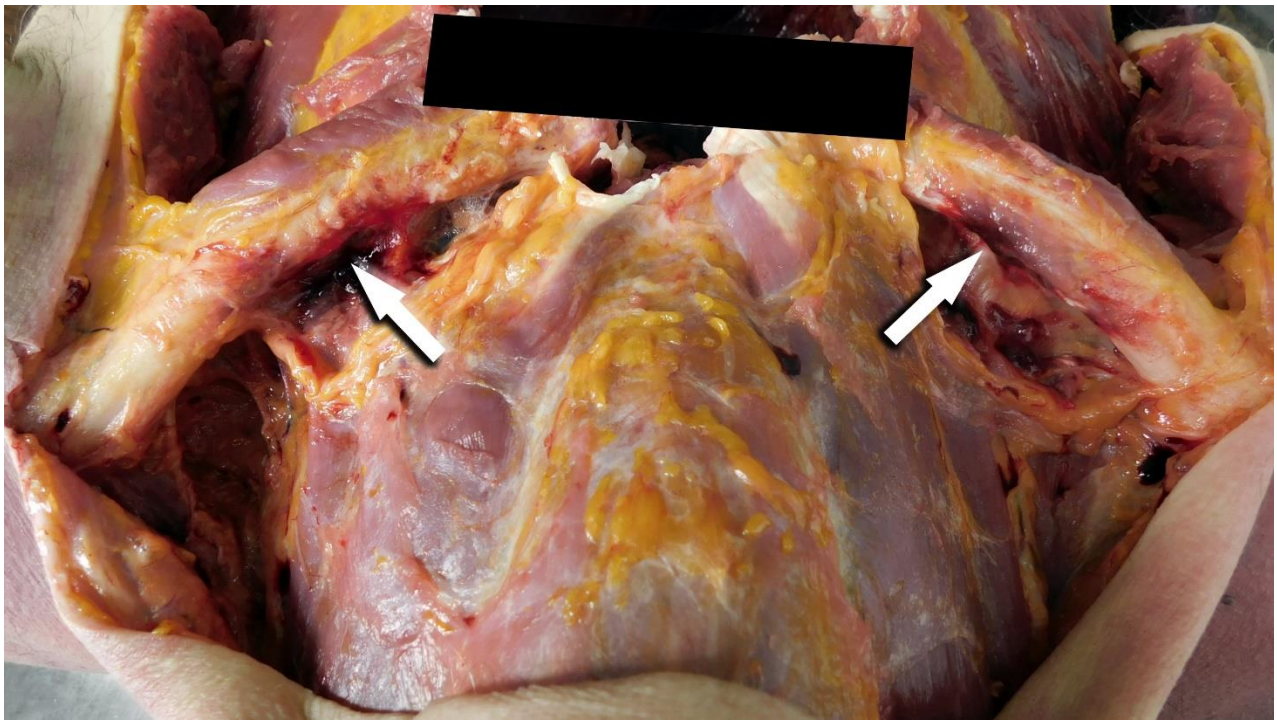

Figure 1.6. *Dissection of the neck – white arrows indicate visible collarbones subperiosteal hemorrhages, at the origin of sternocleidomastoid muscles.*
From: Institute of Forensic Medicine, University of Belgrade, Faculty of Medicine, Belgrade, Serbia.

The laryngohyoid complex injuries: The typical injuries are confined to the hyoid bone's greater horns and the thyroid cartilage's superior horns [3]. Interconnected with ligaments and soft tissue, they form an interdependent biomechanical functional unit [6, 9, 47]. The more detailed anatomy of the thyrohyoid complex is described in the following subsection of the introduction (section 1.3). Of forensic relevance is the detection of fractures, recognition of signs of intravital fracture occurrence (Figures 1.7 and 1.8), and familiarity with pitfalls – misinterpretation of anatomy variations, such as the Eagle syndrome, the hypoplasia or absence of superior thyroid horns, and the misinterpretation of the palpable triticeal cartilage as a fracture fragment [3, 6, 9, 38, 48]. Detecting horn fractures on autopsy is typically straightforward after the horns are dissected and defleshed (Figure 1.7). To make things more straightforward, they are relevant only if surrounded by a soft-tissue hemorrhage, making them more easily observable [6, 9]. The extensivity of the bleeding may vary, and artificial bloodless field creation is of great importance here, too. The horns can fracture by direct compression, laterally oriented or anteroposteriorly oriented force, or by an indirectly acting stretching through ligamentous structures (membranes) [2, 3]. The displacement direction of the fragments cannot be established on autopsy due to direct manipulation and artifactual displacement, but postmortem imaging may prove especially useful regarding this [49, 50]. The horns can fracture at any site. However, the hyoid bone's

greater horns most often fracture on the borderline between the middle and distal thirds, within 1 cm from the tip, and at the junction with the hyoid bone's body. The superior horns of the thyroid cartilage tend to fracture near its base [3, 9]. However, no particular pattern in fractures has been established concerning the position of the knot in a noose [46, 51–58]. It is well demonstrated that the frequency of horn fractures increases with age (ossification and calcification, increased brittleness), but the association with other basic anthropometrics – sex, body weight, and body height remain ambiguous [9, 51, 53, 58–61]. To make things more complicated, despite numerous autopsy studies, the thyrohyoid complex fracture prevalence estimation remains unordinary inconsistent – reported prevalences range from less than 5% to over 75% of cases [46, 52, 56–58, 62–73]!

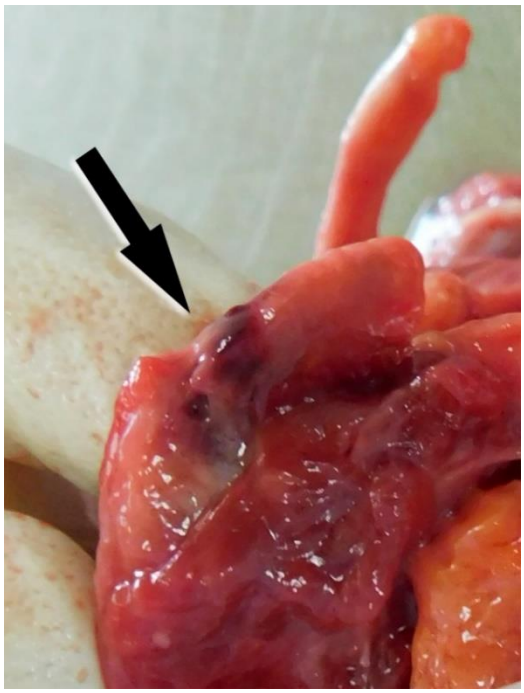

Figure 1.7. *Defleshing the thyrohyoid complex on autopsy. The black arrow shows the site of the fracture of the right greater horn of the hyoid bone, with macroscopically visible hemorrhage in the surrounding soft tissue. The hemorrhage is a sign of intravital horn injury, and eases detection of the fracture.*
From: Institute of Forensic Medicine, University of Belgrade, Faculty of Medicine, Belgrade, Serbia.

Findings below the level of the ligature: The general organ hyperemia is seen in all organs and tissues [6]. Particular attention should be given to remote signs of the agonal sequence in hanging. Due to hyperextension of the spine and convulsions, the rupture of the vessels in the ventral sides of the intervertebral discs in the lumbosacral region can occur, particularly in younger individuals. This macroscopically visible bleeding is called Simon's hemorrhage [6, 12, 30, 43, 74].

1.3. Hyoid bone and thyroid cartilage anatomy

The hyoid bone (Latin, *os hyoideum*) is U- or V-shaped (i.e., curved) and located under the base of the tongue, in the body midline [3, 9, 34, 47, 58]. It is the only bone of the human skeleton which does not form a direct connection with any other bone [34, 47]. However, it forms complex indirect connections with several surrounding structures by fibrous connections (Figure 1.8). The stylohyoid ligament connects it with the skull, the glossohyoid

membrane with the tongue, and, most importantly, a thyrohyoid membrane with the larynx (thyroid cartilage). Moreover, many muscles attach to it, including several tongue muscles, digastric muscle, stylohyoid muscle, thyrohyoid, sternohyoid, and omohyoid muscle. The hyoid bone has a centrally placed body and two sets of horns (Latin, *cornua*) – greater and lesser horns [34, 47]. Of the most significant forensic relevance are the greater horns, as previously discussed. They are oriented horizontally backward from the sides of the body [47]. At the base, they are articulated with the hyoid bone's body and only in some entirely ossify and fuse with it over time

The thyroid cartilage (Latin, *cartilago thyroidea*) is one of the central structures of the larynx, which in addition comprises of cricoid and epiglottic cartilage, as well as paired structures, arytenoid, corniculate, and cuneiform cartilages. Thyroid cartilage is a hyaline cartilage and has two laminas fused at the midline to form the laryngeal prominence [34, 47]. The angle of this fusion is more acute in males (about 90 degrees) than in females (about 120 degrees), making it more prominent in the former case [47]. Superior horns originate from the lateral aspects, at the junction of laminar upper and posterior margins, and are directed upwards. At the margin of laminar lower and posterior margins, the inferior horns originate, directed downwards to articulate with the cricoid cartilage [34, 47], but apart from this, they are of no forensic significance.

The thyrohyoid membrane is a principal structure that interconnects the thyroid cartilage and the hyoid bone. In its medial part, it is thicker, while the lateral portions are thin. The free posterior margins form a connection between the tip of the thyroid cartilage's superior horn and the hyoid bone's greater horn. It traverses by the interior aspect of the hyoid bone [47]. The thyrohyoid complex anatomy is shown in Figure 1.8.

1.4. Medicolegal significance of thyrohyoid complex fractures

These fractures are nonspecific neck injuries. They occur in other types of strangulation, in blunt-force neck trauma (agonal falls, traffic accidents, falls from height when it is typically not an isolated injury but often associated with polytrauma), or can even be iatrogenic (endotracheal intubation, Sellick maneuver) [2, 3, 9, 58, 71]. On the evaluation of strangulation deaths, including the hangings, the forensic medicine specialist is expected to provide direct answers to several important questions, such as were the detected injuries sustained while the subject was alive, can a self-infliction be ruled out, and do the autopsy findings suggest the particular and expected circumstances or rule them out (including the position of the body and hence the knot position) [2, 3, 9]. To provide answers, one relies on many findings, including the described autopsy findings such as distribution of the postmortem lividity, position and direction of the ligature mark, and potentially thyrohyoid fractures, as well. However, currently, the latter can be of significance only to state that such an injury (accompanied by the surrounding soft tissue hemorrhage) is consistent with strangulation (i.e., hanging). But as a non-specific to hangings, and strangulation in general, and without any recognized patterns regarding the knot in a noose position, other than the discussed above, the thyrohyoid complex (and cervical spine) fractures are of no other medicolegal significance *per se.* Initial attempts to observe the association of some distribution patterns of these fractures with the knot in a noose position were deemed unsuccessful, and this topic requires further research.

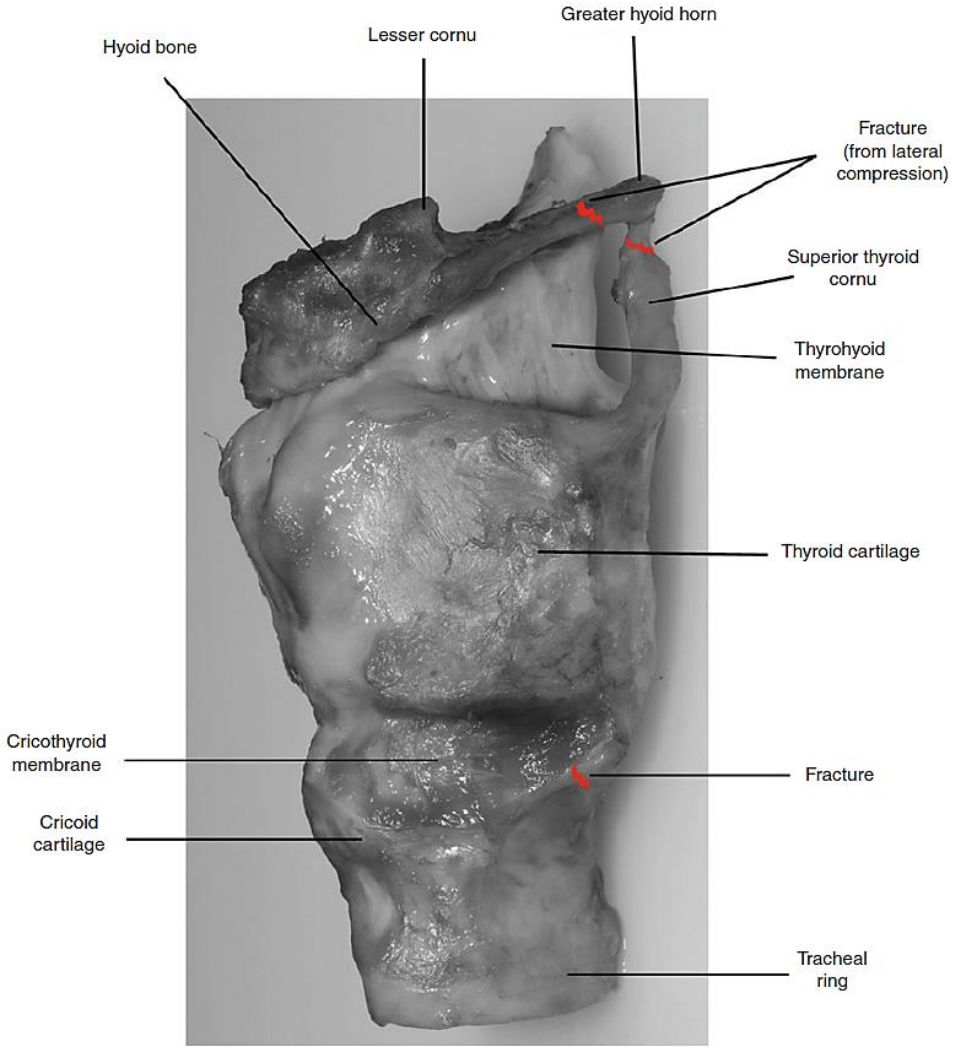

Figure 1.8. *Predilection sites for fractures of the larynx and hyoid bone from lateral compression. From: Neck Trauma. In: Dettmeyer R.B, Verhoff M.A, Shutz H.F. Forensic Medicine Fundamentals and Perspectives. Heidelberg: Springer-Verlage, 2014, p. 176.* [9] *Reproduced with permission from Springer Nature (not part of the governing CC license).*

1.5. Machine learning and forensic pathology

The concept of artificial intelligence (AI) was coined in 1956 and refers to the development of computer systems able to perform tasks that require human intelligence [75]. For example, this would encompass visual perception, speech recognition, and decision-making. The theory defines three main AI stages: 1. Narrow AI ("weak," capable of functioning within a strictly defined narrow function, e.g., Alexa), 2. General AI ("strong" machine capable of performing any intellectual task a human can – not yet achieved), and 3. Super AI (a stage when a computer surpasses human capacities) [75]. AI is an umbrella term, while one of its subcategories is called machine learning (ML). ML specifically refers to a computer program capable of learning how to produce behavior not explicitly programmed by the author (i.e., by a human). In the broadest sense, ML can learn patterns from data [75–77]. We can probably see this concept as a set of experience-based learning and numerous try-and-error attempts, which improve the capability for a correct final

decision (output) after each step (iteration) based on the previous observation and result. This concept of self-improvement by recognizing error and trying to minimize it is termed "Error backpropagation" [75]. Machine learning programs can detect non-obvious associations between variables, which would remain unobserved by common sense or even "conventional" statistical analyses. Patterns can be detected in complex data structures (e.g., nonlinear associations, interactions, subgroups). Thus, it can be a handy tool to overcome challenges for which traditional statistical methods are not well-suited [75, 76].

Each machine learning program is defined by an algorithm (set of rules and statistical techniques for learning and decision making), a model (mathematical equation, a formula providing output based on the available input), predictor feature(s) (a variable – distinct observation of interest), and response variable (the "feature" or the target output – outcome that should be predicted/classified) [75, 76]. For the ML program to function, the sample of cases from which it will learn needs to be divided into the training set – to train the model (learning) and a typically smaller testing set – a subgroup of cases from a sample that will be omitted from the "training sessions." It will contain "unseen" data to test the general ML model performance. [75–78]. The sample size ratio is usually 70% to 30% or 80% to 20% for training and test subset, respectively [75, 76, 79, 80]. The ML modeling requires a significantly large sample size and uniform data, preferably without any missing information for every included case in the sample. There are no precise rules for determining the required sample size for supervised machine learning model development, but a general rule is that the larger the sample is, the more accurate estimation will make [75–77].

Depending on how the ML models are trained, three distinct types are defined: supervised, unsupervised, and reinforcement learning. In the supervised ML, the author provides the machine with data on the actual outcome in the analyzed set. In the case of the research presented in this thesis, the machine learning program will be "familiar" with the position of the knot in a noose for each case, so it can explicitly learn which outcomes should be differentiated and would ideally provide high-accuracy classifications in the unseen data (Figure 1.7) - learning by example [75, 77]. The two latter ML forms are less interesting for the present research. Briefly, the unsupervised learning machine is not provided with the outcome for each case (so-called unlabeled data) and should classify by itself, without guidance from the author – it should determine how to best categorize dimensions into subtypes (e.g., diagnostic groups). It helps understand patterns (e.g., pixel patterns) and detect grouping (groups). In reinforcement learning, the essential principle is a trial-and-error learning method (text and speech understanding is an example of application) [76, 77].

Several different "supervised" machine learning algorithms (i.e., different sets of decision-making rules) exist, and the basic concepts of some will be described here.

Logistic regression can be considered as a "rudimental" machine learning algorithm. The binary outcome is defined (e.g., the fracture is present or absent, in mathematical terms "1" or "0"), and the significance of the input variable with the outcome is calculated and defined as an *odds ratio*. It can be useful to detect significant associations that can point to important input variables for other classification algorithms. It is, nevertheless, a "traditional" or a "conventional" statistical method [75–77].

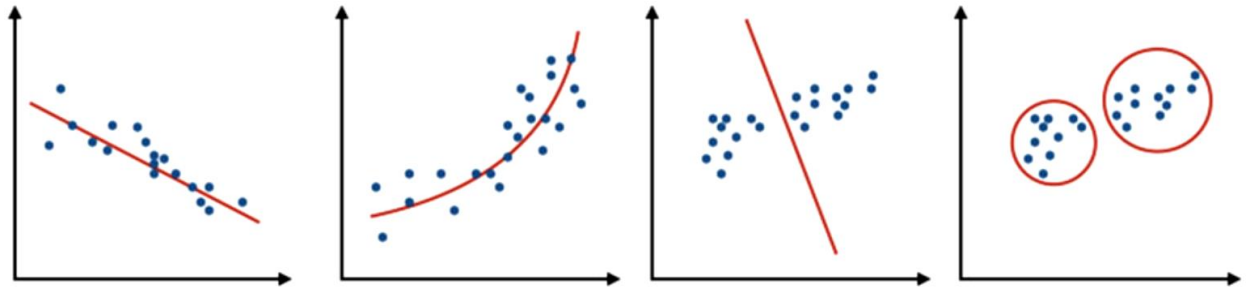

Figure 1.9. *Illustration of three machine learning problems, left to right: linear and nonlinear regression, classification, and clustering. From: Lidströmer N, Aresu F, Ashrafian H. Basic Concepts of Artificial Intelligence: Primed for Clinicians. In: Lidströmer N, Ashrafian H. (Eds). Artificial Intelligence in Medicine. Cham: Springer, 2022, p. 11.* [75] *Reproduced with permission from Springer Nature (not part of the governing CC license).*

Decision Tree is an algorithm whose model provides a branching set of rules in decision-making that resemble the inverted tree (Figure 1.10). If adequately modeled, it can perform classification tasks in a stepwise manner by several if-then decision steps, which is quite useful as it is easily understandable by common sense and directly points to the most significant inputs, with high visual interpretability – it is useful for identifying complex associations [75–77, 81].

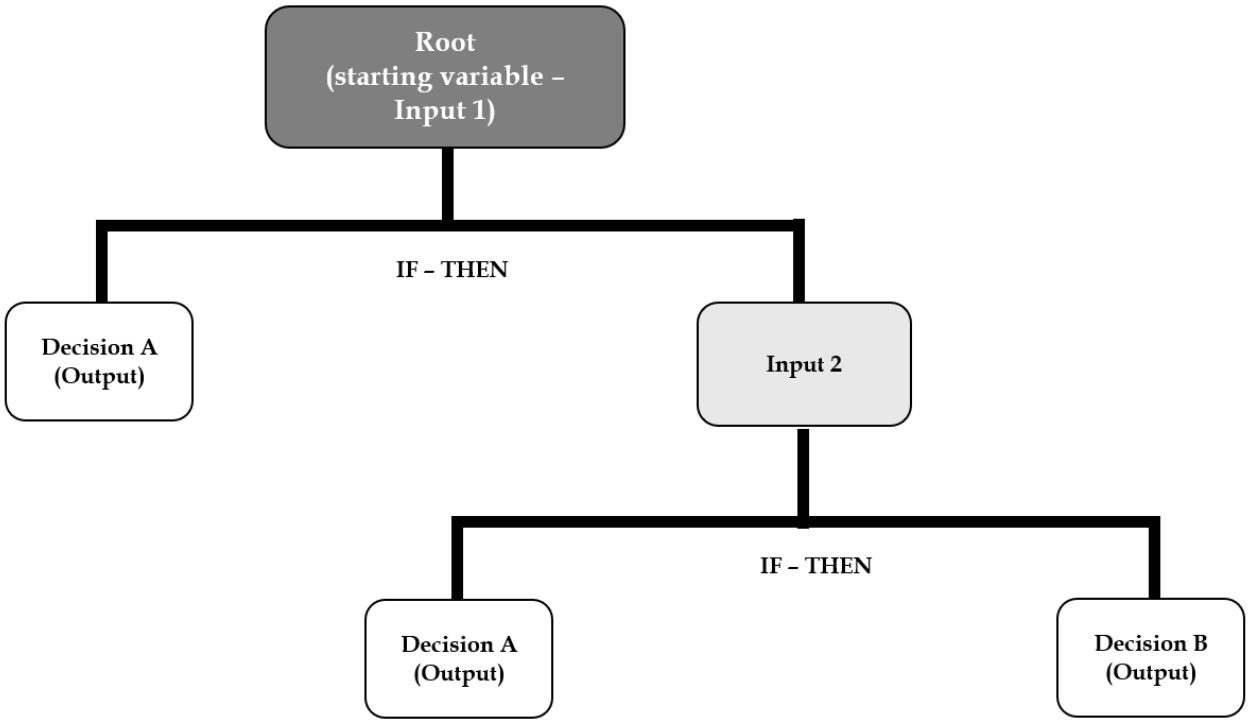

Figure 1.10. *A scheme of a simple "branching" decision tree machine learning model – a series of understandable if-then decision-making stops.*

Naïve Bayes is based on the Bayes' theorem, a distinct set of rules based on the probabilistic approach. The algorithm's initial assumption is that none of the inputs are interdependent (change in the value of one variable does not affect other variables) [75, 82].

K-Nearest Neighbor (k-NN) classifies cases based on the "distance" to the closest (most similar) neighbor points. It is referred to as a *lazy algorithm* because it memorizes the training set and does not learn a discriminative function [75, 83].

The artificial neural network (ANN) is probably the most complex of the algorithms. The inspiration for their design is based on the biological organization of neurons (synapses). Each neuron performs the calculation and provides individual output delivered to the next neuron. This one independently analyzes the output as a new input. Eventually, the single final output of the model is provided. During the training process, the weights are calculated for each transfer function and the best of many pathways in the network is selected. Several factors define the complexity of ANN, the most significant being the number of hidden layers – defining the number of interconnections and pathway complexity [75–77, 79, 80, 84].

However, the way the training is carried out is defined by the set of parameters (so-called hyperparameters) that are not learned but are predefined manually (before training) [75, 76]. These define how to optimize the weights (variable importance), how many times the algorithm can pass through the training data, and limiting the complexity of a model (e.g., number of hidden layers and neurons in ANN, number of nodes and a minimum sample size of the parent node in decision tree model) [75–77]. There are means by which this process of manual hyperparameter adjustment can be automatized and systematized – using a so-called genetic algorithm, which is inspired by the biological evolution process: the best model achieved in a single generation will be the starting point for the next one [79, 80, 84–86]. Of note is that there is no standardized set of these values that is uniformly appropriate – one of the reasons why this is an experimental method [76, 77].

A well-trained model should perform against the test data similarly to its average performance against the training data. The metrics for evaluation can be those dependent on the defined cutoff point (accuracy, sensitivity, specificity, positive and negative predictive value), as well as those independent of this – most notably the Receiver operating characteristics curve analysis [76].

In medicine, the primary interest is in AI-based (ML-based) image analysis (for example, radiology, histology, and dermatoscopy), which could improve or speed up diagnostics. For example, a highly accurate automated model that differentiates between benign and malignant lesions based on a routinely analyzed microscopy slide scan or some other macroscopic image would be of great direct clinical value. But it can also be useful for the classification based on non-image data (sets of numerical and categorical data) [75–78, 87]. In forensic medicine, AI-based problem solving was attempted, for example, in research on the sex and age estimation, dating of bruises, detection and classification of the pulmonary fat embolism, reconstruction of the pedestrian strike regarding the vehicle type, estimation of the postmortem interval, toxicology analysis [88–96].

However, up to the author's best knowledge, no attempts to classify the position of the knot in a noose in hanging by distribution and pattern of the fractures of the thyrohyoid complex and the cervical spine have been performed previously [62]. As the previous subsections of the introduction suggest, this type of research could have important implications for forensic pathology research and practice in death-by-hanging evaluation.

2. RESEARCH AIMS

I To analyze characteristics and distribution of thyrohyoid complex and cervical spine fractures with regards to the position of the knot in a noose in suicidal hangings by basic descriptive and inferential statistical methods.

II To determine the performance of machine learning algorithms in assessing the knot in a noose position based on the thyrohyoid complex and cervical spine fracture patterns in suicidal hangings.

III To determine the performance of machine learning algorithms in assessing the knot in a noose position while taking into account the body weight of hanged subjects, in addition to the fractures.

IV To determine the performance of machine learning algorithms in assessing the knot in a noose position while taking into account the presence of hemorrhages at the origin of sternocleidomastoid muscles on the clavicles, in addition to the fractures and the body weight of hanged subjects.

3. MATERIAL AND METHODS

This is a single-institution retrospective observational autopsy study on cases of suicidal hangings autopsied at the Institute of Forensic Medicine of the Faculty of Medicine of the University of Belgrade, Serbia. The data on autopsy cases relevant to the study was systematically collected for the period from 1995 to 2023, with several additional sporadic cases from the later period, which were observed during the conduction of the research. The data was obtained from autopsy records and supplementary documentation (police reports, photo documentation, and heteroanamnestic data), all archived at the Institute of Forensic Medicine. The study was approved by the Ethics Committee of the Faculty of Medicine, University of Belgrade, Serbia (N^0 25/V-7).

The entire study presented in this thesis is structured into three separate parts. Therefore, the general research structure and characteristics common for all three parts are described in the following sections of the Materials and Methods (from section 3.1. to section 3.3.). After these sections, the detailed design and any additional methodology or data analyses are described separately in a successive and logical order for each part of the study. If not otherwise mentioned, the principles described in the general methodology sections (3.1. – 3.3.) hold for each part of the study.

3.1. General case selection criteria and study sample

The study sample comprised autopsied cases of suicidal hanging with a short drop or without a drop, in whom autopsy findings, police investigation and report, circumstances, and heteroanamnestic data excluded potential foul play and concluded the hanging event and death were of suicidal manner. In all the cases, autopsy findings were consistent with hanging as a cause of death, and in those cases in whom the fractures of the thyrohyoid complex or cervical spine were observed on autopsy, the presence of a macroscopically visible soft-tissue hemorrhage surrounding these fractures was considered a sign of intravital injury (fracture) occurrence. Exclusion criteria in the case selection were: subject's age of fewer than 15 years, a long drop hanging, anatomy variations (congenital or acquired) of the thyrohyoid complex in which one or more horns – greater hyoid bone horns, and superior thyroid cartilage horns are absent or hypoplastic, Eagle syndrome, fractures of other laryngohyoid structures (for example, cricoid cartilage, hyoid bone body, lesser horns of the hyoid bone), pronounced putrefactive changes, as well as all the cases in which the position of the knot in a noose could not be determined by autopsy examination and police investigation.

Based on the assessed knot in a noose localization regarding the head anatomy, each included case was assigned to one of the four groups (Figure 3.1):

- Posterior knot position,
- Anterior knot position,
- Left lateral knot position,
- Right lateral knot position.

The position of the knot in a noose was classified as the *posterior* if the knot was estimated to be in the region behind the mastoid processes' projections, at the back side of the neck; as the *anterior* if the knot was located anteriorly to the projection of mandible angles; and, as the *left* or *right lateral* if the knot was located between the projections of an ipsilateral mastoid processus and mandible angle, as shown on Figure 3.2 (see section *3.2.1. The knot in a noose position assessment*). In this manner, the cases were divided into *typical (posterior)* hangings and *atypical (anterior, left lateral, and right lateral)* hangings.

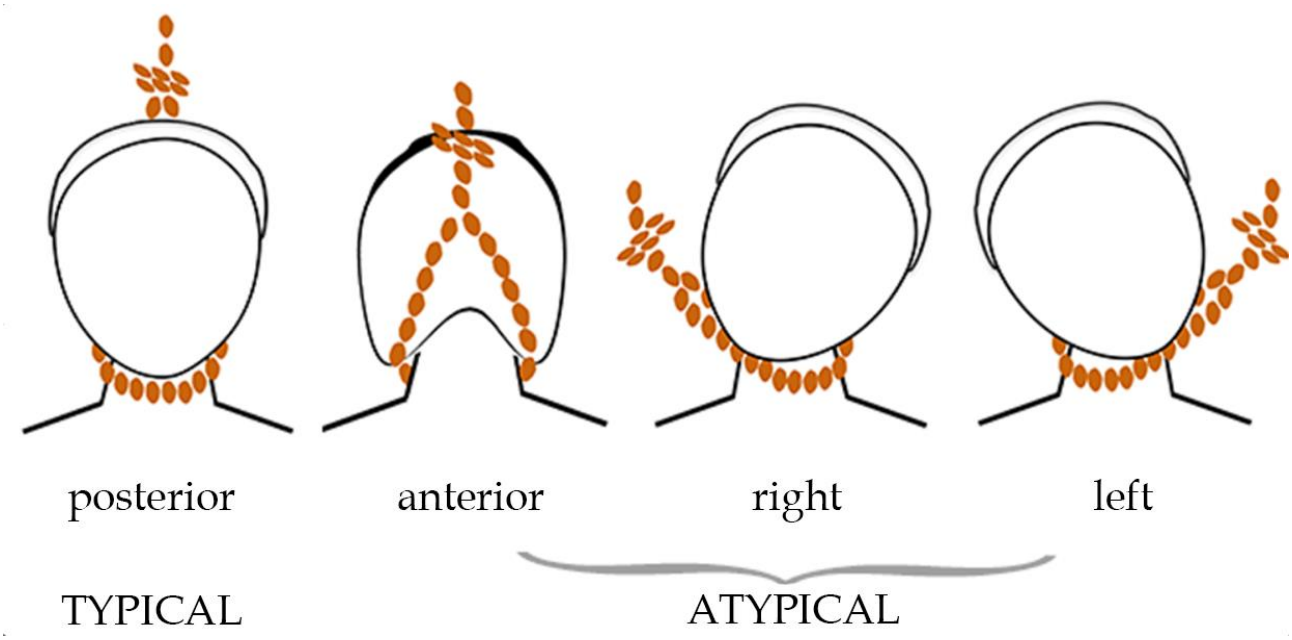

Figure 3.1. *The subjects were assigned to one of the four groups depending on the knot in a noose position: It can be in a typical (posterior) or atypical position (anterior or left/right lateral).*
Adopted from: Leković et al. [62]

3.2. Autopsy technique standard and uniformity of documented findings

At the Institute of Forensic Medicine in Belgrade, all autopsies are performed or supervised by at least two forensic pathologists, university teachers, with at least five years but usually more than ten years of forensic pathology practice as forensic medicine specialists. Moreover, at the Institute, all forensic pathologists perform the identical autopsy standard procedure, which in cases of suspected hanging deaths invariably includes a mandatory and detailed external neck examination followed by a standard layer-by-layer neck dissection. Therefore, the uniformity of recorded findings is ensured, as described in the following text.

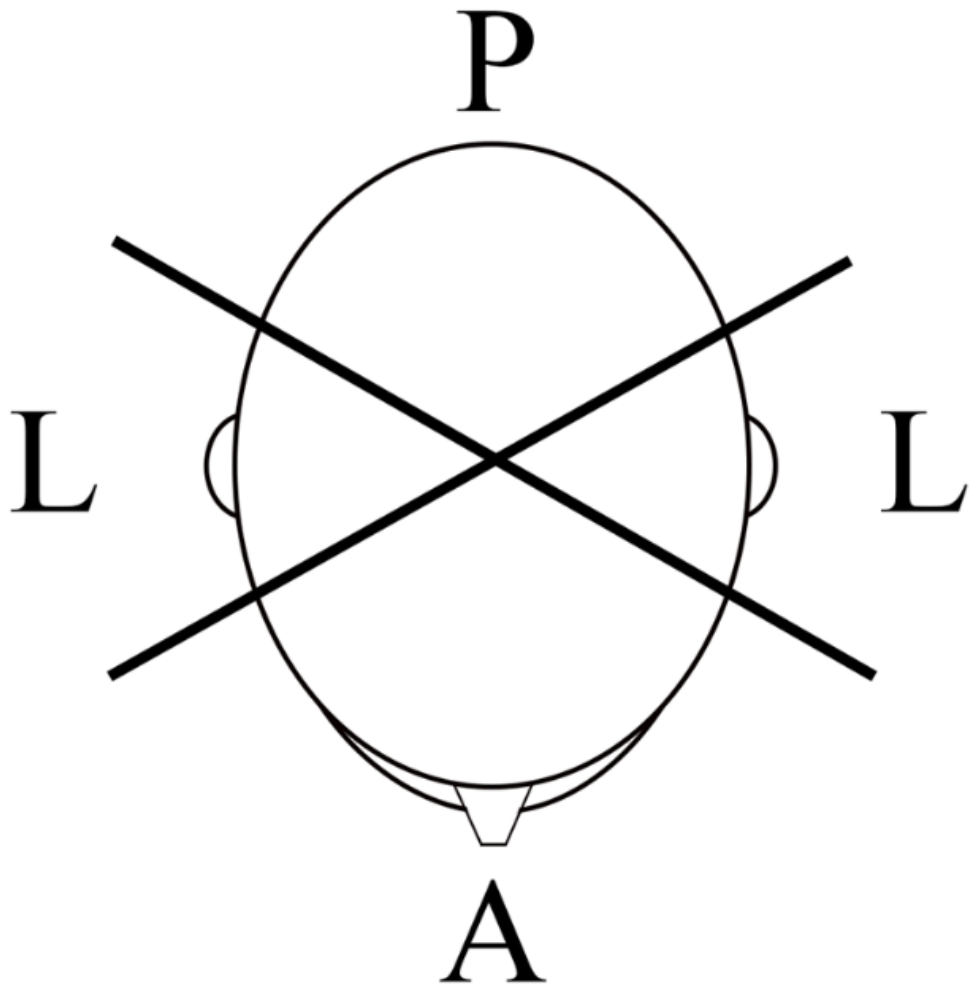

***Figure 3.2**. Scheme of the knot in a noose position classification as anterior (**A**), posterior (**P**), or lateral (**L**). The head is viewed from the top, ears can be seen on the sides and the nose in front. The drawn lines are crossing the mastoid processes in the back, and mandible angles in front (not directly visible from the top but crossing points are corresponding to their positions). Reproduced from: Leković et al.* [62]

3.2.1. External neck examination – the knot in a noose position assessment

On the external neck examination, if the fixed-knot noose is still in place, the position of the knot is noted. Regardless of this, the ligature skin mark (a furrow) is always precisely measured (width, depth) and described considering the distance from the fixed anatomical points of the head: chin tip, mandible angles, lower poles of earlobes' radices, and external occipital protuberance (if a furrow was present). In this manner, even if the noose was absent at the time of the autopsy examination, the position of the knot could be determined: it represents the point opposing the lowest and the deepest part of the ligature mark (illustrative example shown in Figure 1.5). If the mark in the form of the knot's impression is visible, this is noted, too. So, the noose knot's position is estimated based on the appearance and position of the skin ligature mark on the neck or by noting the position of the knot on autopsy if the noose was not removed before it.

3.2.2. Neck dissection – detection of the thyrohyoid complex and cervical spine fractures

The neck dissection is preceded by the autopsy of the head and cranial vault to ensure the so-called 'dry' neck dissection. Then, a standard layer-by-layer dissection of the anterolateral neck is performed. For this research, the following segments of this neck dissection technique should be highlighted:

- A layer-by-layer dissection of the skin and soft tissues, including each muscle layer of the anterolateral neck, is performed to expose the larynx. Then, the tongue, oropharynx, larynx, and initial tracheal segments are dissected and removed *en bloc* after *in situ* inspection. Afterward, the thyrohyoid structures are separated ('defleshed') from the soft tissue to reveal any fractures by inspection and palpation. The thyroid cartilage's superior horns and the hyoid bone's greater horns are invariably inspected, palpated, and checked for mobile fragments and fissures.
- After this, the cervical spine is exposed, and this segment is checked for the presence of an injury—a fracture.
- As previously mentioned, the fractures of the thyrohyoid complex and the cervical segment of the spinal column were considered to be intravital (that is, to have occurred due to hanging and neck compression by the noose) only if accompanied by the surrounding soft tissue hemorrhage. This prevented misinterpretation of artifactual fractures due to body transport or ma autopsy-related postmortem injury.

3.3. General variable selection and coding

For all the included cases, the following data were noted: sex, age, position of the knot in a noose, and presence of the fracture of each (left and right) greater hyoid bone's horn, the fracture of each (left and right) superior thyroid cartilage's horn, and the fracture of the cervical spine, as per criteria described in the previous methodology (sub)sections. So, for each included case, it was determined if thyrohyoid complex fractures were present and exactly which horns were fractured (defining the side – left or right lateral). Based on the presence or absence of the mentioned thyrohyoid complex and cervical spine fractures, the following variables were coded for analysis:

- Unilateral superior thyroid horn fracture (Yes / No),
- Bilateral superior thyroid horn fractures (Yes / No),
- Total number of superior thyroid horn fractures (range 0 – 2),
- Unilateral greater hyoid horn fracture (Yes / No),
- Bilateral greater hyoid horn fractures (Yes / No),
- Total number of greater hyoid horn fractures (range 0 – 2),
- Total number of thyrohyoid fractures (a sum of variables listed 3rd and 6th, range 0 – 4),
- Isolated superior thyroid horn fracture(s) (Yes / No)
- Isolated greater hyoid horn fracture(s) (Yes / No)
- Simultaneous superior thyroid horn and greater hyoid horn fractures (Yes / No)
- Cervical spine fracture (Yes / No)

The coded variables and other noted data were used in all three parts of this study. Their further analyses are described in detail in the following (sub)sections of the *Material and Methods* for each study part separately. Again, if overlapping in terms of methodology, these analyses of the obtained data will be described in detail in the part where these are first applied, with subsequent briefer comments on any modifications in the following segments of the entire research.

3.4. PARTI I of the study: Separate analysis of the fracture patterns in knot's position assessment

3.4.1. Study design

The first part of the study represents analysis, which investigated the association of the noose knot's position with the subject's sex, age, and the presence of fractures of the superior horns of the thyroid cartilage (STH), greater horns of the hyoid bone (GHH), and the cervical spine. For the descriptive, inferential statistics analyses, as well as for machine learning models development, to determine the thyrohyoid and cervical spine fracture patterns with regards to the knot's position, this part of the study comprised stepwise, similar analyses of the entire study sample and three derived subsets, as described below:

- Dataset I — The entire sample – all cases that fulfilled the defined study criteria. A total of 1235 subjects were included. Therefore, this Dataset (I) comprised the cases without any thyrohyoid and cervical spine fractures and cases with these fractures. The subjects were divided into two groups to be compared based on the noose knot's position: (1) typical (posterior) hangings and (2) atypical (lateral and anterior) hangings.
- Dataset II — This is a subgroup of the entire sample, including only cases with at least one thyrohyoid or cervical spine fracture. A total of 773 subjects were included in this subgroup. The exclusion of subjects without thyrohyoid and cervical spine fractures may eliminate potential failure of fracture pattern detection or underestimation. The cases were divided into the same two groups for comparison (typical and atypical hangings).
- Dataset III — The subgroup comprised only atypical hanging cases with at least one thyrohyoid or cervical spine fracture and comprised 340 subjects. The subjects were divided into two groups to be compared based on the noose knot's position: (1) anterior hangings and (2) lateral hangings.
- Dataset IV — The subgroup comprised only lateral hanging cases with at least one thyrohyoid or cervical spine fracture and included 286 subjects. The subjects were divided into two groups to be compared based on the knot position: (1) left lateral and (2) right lateral hangings. To try to discriminate between the two groups, additional variables needed to be coded, defining on which side the fractures occurred: left or right superior thyroid and greater hyoid horns. Furthermore, based on the statistical analysis results of the machine learning model experiments, we included two additional variables: (1) the presence of a single (unilateral) greater hyoid bone horn fracture ipsilateral to the knot position and (2) the presence of a single (unilateral) superior thyroid cartilage horn fracture contralateral to the position of the knot.

3.4.2. Statistical analysis

Descriptive statistics were used to analyze the samples (datasets) and assess the frequency and distribution of thyrohyoid and cervical spine fractures regarding the position of the knot in a noose. Nominal data were represented as absolute frequencies and proportions (%), and numerical data as mean (± SD) or median (range), as appropriate per type (categorical or continuous) and normality of distribution. The normality of the continuous numerical data distribution was analyzed by *Q-Q* plots and the Kolmogorov-Smirnov test. Inferential statistical analysis of the coded variables and other obtained data between the defined study groups was performed using Pearson's $\chi 2$ test, Student's t-test for two independent samples, and the Mann-Whitney U test. To determine the association between the thyrohyoid and cervical spine fracture patterns with the position of the knot in a noose, each of the four datasets was analyzed separately in the noted order (I to IV). The χ^2 test, t-test for two independent samples, Mann-Whitney U test, and Student's t-test for two independent samples were used.

For each dataset, the univariable logistic regression analysis was performed to detect whether the dichotomous variables coded above, and the subjects' age were associated with the position of the knot in the noose. Variables with p-values ≤ 0.1 on univariable analysis were included in the multivariable analysis. Results were expressed as odds ratio (OR) with 95% confidence interval (CI). Additionally, a Receiver Operating Characteristic (ROC) Curve analysis was performed to assess the predictive value of subjects' age on the occurrence of thyrohyoid fracture in general and, separately, on the occurrence of superior thyroid cartilage horn fractures and greater hyoid horn fractures. The highest Youden's index [97] was criterion for selection of a threshold value. Separately from these analyses, occurrence of the fractures was analyzed between the subjects older than 40 years of age and the younger – previous studies reported the fractures tend to occur more often above this threshold. A two-tailed p-value < 0.05 was considered statistically significant.

Finally, using the same coded variables and case group divisions, the machine learning algorithm models were assessed for classification – predicting the knot position (see below).

3.4.3. Machine learning algorithms development and assessment

According to the aim of this study, using the age, sex, coded variables, and case group divisions, the machine learning algorithm models were developed for each of the four datasets and assessed for classification performance – predicting the knot in a noose position. All the coded variables were included as potential inputs for the training of considered algorithms. Before the training, if necessary, the unbalanced dataset was balanced using the Synthetic Minority Oversampling Technique (SMOTE) algorithm in the Weka software (v. 3.8): we used the ten nearest neighbors and set the seed for random sampling to 4. Each dataset was divided into Training and (independent) Test groups, with a ratio of 70% to 30%, respectively, by manually repeating the randomization until there were no statistically significant differences in the analyzed variables between the two groups. The characteristics and comparison of the variables between the training and test groups are reported in the Supplementary material.

For each developed dataset, the Artificial Neural Network (ANN) model with hyperparameter setting finetuning by Genetic algorithm (GA), previously utilized, modified and provided to the PhD candidate by Vukićević AM [79, 80, 84], was developed in MATLAB (v. 2021b). Finetuning of the algorithm by the GA is done in an evolutionary manner – the GA starts a model optimization from an initial guess of hyperparameters (initial population), which are used as inputs for the objective function (OF). The OF ensembles the model with respect to the current guess of hyperparameters and computes the model accuracy – aiming to maximize it [79, 80, 85]. The number of generations of the GA optimization was set to 10. Of the developed models, the one with the highest accuracy in the test sample was selected, with the condition that there was no statistically significant difference in the ROC curve analysis of the outcome predicted probabilities between the training and test group. In a case where no model with insignificantly different performance between the training and test groups was achieved, the GA-optimized ANN development process was repeated until the criteria were met. The ANN developed in this manner also selects input variables that were considered and included in the final model, and the selected variables are reported in the results section.

Then, using SPSS software (IBM, v. 29), for each dataset, another ANN (Multilayer Perceptron – Artificial Neural Network, MLP-ANN) was developed, as well as the following machine learning algorithms: k - Nearest Neighbors (k-NN), Decision Tree (DT), and Naïve Bayes (NB). The development of the machine learning models in SPSS was done by repeated manual or automatic hyperparameter settings. As previously stated, each dataset used for machine learning models' analysis was divided into a training group (70% of the dataset) and an independent test group (30% of the dataset) by repeated randomization until no statistically significant difference between analyzed variables exists, and this division was also used in SPSS, in any developed machine learning model for which the statistical program allows the setting to be modified. Again, the model with the highest accuracy in the test group with no statistically significant difference in the ROC curve analysis of the outcome predicted probabilities between the training and test groups was selected. During the analysis in SPSS, at least ten repeated model development attempts were made using the same available settings adjustment for each selected model. Up to the top five ranked variables for each developed model are also reported based on their relative importance in the model. The utilized models' developed in SPSS basic hyperparameter settings are reported: for MLP-ANN number of hidden layers, number of neurons in a hidden layer, activation function, training type, training algorithm, initial learning rate, and momentum; for DT growing method, tree depth, min. samples of parent node, min. samples of child node, number of nodes, and number of terminal nodes; for k-NN number of neighbors to consider, distance metrics, and search algorithm (feature selection – stopping criterion); and for NB maximum memory, number of bins for scale predictors, and number of selected predictors.

All the developed ML models' performances were evaluated by calculating the accuracy, sensitivity, specificity, positive predictive value (PPV), negative predictive value (NPV), positive (LR+) and negative likelihood ratio (LR-), and Area Under the Receiver Operating Characteristic (ROC) curve (AUC), overall, and for the test and train group. The ROC curve analysis of the outcome predicted probabilities for each dataset was compared between the ANN developed in MATLAB and the ANN developed in SPSS. Statistical analysis was performed using SPSS software (IBM, v. 29). The calculation of the ML models' performances and the ROC curve comparisons were done in R (v. 4.2) using the EZR GUI.

3.5. PART II of the study: Analysis of the body weight's significance in knot position-related fracture patterns assessment

3.5.1. Study design

The second part of the study represents a similar analysis but only of cases in which, in addition to the subjects' sex, age, and thyrohyoid and cervical spine fractures, data on their body weight and height could be obtained (the body weight has been measured systematically and accurately only for the past ten years at the Institute). Therefore, this study part's entire sample was smaller than the previous part and comprised 368 included cases. Analyses were focused on the contribution of body weight to predicting the knot in a noose position through the thyrohyoid and cervical spine fracture patterns. So, the cases were again analyzed stepwise, firstly on the entire sample (with data on the body weight and height) and then on subsets formed identically to the previous study part (Dataset I – IV; see Section 3.4.1.). For discrimination between datasets of the first study part, the datasets in the second part were labeled with the suffix '-w' (e.g., Dataset I-w), indicating analysis of the weight's significance. The following sample subsets were formed:

- Dataset I-w – a total of 368 cases were included. Again, it included the cases without thyrohyoid and cervical spine fractures and cases with these fractures. The subjects were divided into the same two groups to be compared: (1) typical (posterior) hangings and (2) atypical (lateral and anterior) hangings.
- Dataset II-w – a total of 242 cases were included. It is a subgroup that included only cases with at least one thyrohyoid or cervical spine fracture. The subjects were divided into the same two groups to be compared: (1) typical (posterior) hangings and (2) atypical (lateral and anterior) hangings.
- Dataset III-w – a total of 114 cases were included. There were only atypical hanging cases with at least one thyrohyoid or cervical spine fracture, and the cases were divided into two groups to be compared: (1) anterior hangings and (2) lateral hangings.
- Dataset IV-w – a total of 106 cases were included. There were only lateral hanging cases with at least one thyrohyoid or cervical spine fracture, and the subjects were divided into the following two groups: (1) left lateral and (2) right lateral hangings. Identically to the previous step (as for Dataset IV), additional variables were coded to define on which side the fractures occurred and if these were unilateral or contralateral (see Section 3.4.1.).

3.5.2. Statistical analysis

The basic descriptive and inferential statistical analyses of each of the four datasets that correspond to the statistical analyses in the first part of the study were performed, with two additional variables considered: the subjects' body weight and height.

In addition, the ROC curve analyses were performed to assess the predictive value of subjects' age, body weight, and body height on the occurrence of thyrohyoid fracture in general and, separately, on the occurrence of superior thyroid cartilage horn fractures and greater hyoid horn fractures.

3.5.3. Machine learning algorithms development and assessment

Due to a smaller sample size from the previous part of the research, machine learning model development was performed only in the first two steps: for Dataset I-w and Dataset II-w. So, cases without fractures and cases with fractures were included in the first step, while subjects without any thyrohyoid complex or cervical spine fracture were excluded in the second step. Therefore, all machine learning algorithms were assessed in classification performances between the cases where the knot was located posteriorly (typical hangings) and cases where the knot was located either laterally or anteriorly (atypical hangings).

The machine learning algorithm development approach was the same as previously described (see Section 3.4.3.), with one additional element: for each machine learning algorithm, two different models were developed – one that considered subjects' body weight and height and one 'analogous' that did not have input on these variables. If the settings allowed this, forcing the input variable (subject's body weight) was performed in cases where the model did not automatically consider the variable. The two 'analogous' models of each algorithm, one taking into account the body weight and one not considering it, were also analyzed by comparing their ROC curves on predicted outcome probabilities in test samples. This provided additional information on the significance of considering the body weight in assessing the knot in a noose position based on the thyrohyoid and cervical fracture patterns.

3.6. PART III of the study: Analysis of the sternocleidomastoid muscles' origin hemorrhage in knot position-related fracture patterns assessment

3.6.1. Study design and the sternocleidomastoid muscle origin site hemorrhage detection

The third part of the study represents an analysis similar to the previous ones but with additional variables: in addition to the subject's age, body weight, body height, and presence of the thyrohyoid and cervical spine fractures, the presence of the hemorrhage at the origin sites of the sternocleidomastoid muscles at the clavicles was analyzed with regards to the knot in a noose prediction. The presence of the macroscopically visible hemorrhage at the sternocleidomastoid muscle origin site — the periosteum of the clavicles, left and right — was noted only in cases in which the presence or absence of these hemorrhages was explicitly documented in the autopsy report or by the analyzed autopsy photographs. This was done to obtain as uniform and as reliable data as possible. Because of this, this sample was the smallest of the three study parts and comprised 126 cases. For statistical analysis of these muscle hemorrhages, the following additional variables were coded:

- Unilateral sternocleidomastoid muscle hemorrhage (Yes / No)
- Bilateral sternocleidomastoid muscle hemorrhages (Yes / No)
- Total number of sternocleidomastoid muscle hemorrhages (range, 0 – 2)

The cases were again analyzed stepwise, firstly on the entire sample and then on subsets formed identically as in the previous two study parts. For discrimination between the marking of datasets of the preceding study parts, the datasets in the third part were labeled

with the suffix '-m' (e.g., Dataset I-m), indicating analysis of the muscles' hemorrhage significance. The following sample subsets were formed:

- Dataset I-m – a total of 126 cases were included. Identically to the previous parts of the study, the cases without thyrohyoid and cervical spine fractures and cases with these fractures were included.
- Dataset II-m – a total of 117 cases were included. It is a subgroup that included only cases with at least one thyrohyoid or cervical spine fracture or hemorrhage of at least one sternocleidomastoid muscle, and these cases were divided into the same two groups to be compared: (1) typical and (2) atypical hangings.
- Dataset III-m - a total of 58 cases were included. There were only atypical hanging cases with at least one thyrohyoid or cervical spine fracture or hemorrhage of at least one sternocleidomastoid muscle, and the cases were divided into the same two groups to be compared: (1) anterior hangings and (2) lateral hangings.
- Dataset IV-m – a total of 52 cases were included. There were only lateral hanging cases with at least one thyrohyoid or cervical spine fracture or hemorrhage of at least one sternocleidomastoid muscle's origin site at the clavicle, and the cases were divided into the following two groups: (1) left lateral and (2) right lateral hangings. In addition to the variable coding for the fourth dataset, which was identical to the previous study parts, additional variables were defined – indicating if each (left and right) sternocleidomastoid muscle had visible hemorrhage and if the hemorrhage occurred at the side ipsilateral to the position of the knot in a noose.

3.6.2. Statistical analysis

The basic descriptive and inferential statistical analyses of each of the four datasets that correspond to the statistical analyses in the second part of the study were performed, with additional variables considered: regarding the presence of the sternocleidomastoid muscle origin site hemorrhages. In addition, the ROC curve analyses were performed to assess the predictive value of subjects' age, body weight, and body height on the occurrence of the sternocleidomastoid muscle origin site hemorrhages.

3.6.3. Machine learning algorithms development and assessment

Because of the size of the sample in the third study part, machine learning model development was limited to and performed only in the first step: for Dataset I-m. So, the algorithms were developed to attempt classification between the atypical and typical knot in a noose position on the sample that included subjects with thyrohyoid and cervical spine fractures, as well as the subjects without these fractures. But in each considered case, there was information on the presence of the sternocleidomastoid muscle origin hemorrhages. Similarly to the second part of the study, in the machine learning algorithms analysis, two 'analogous' models were developed: one machine learning model that took into account the presence of sternocleidomastoid muscle hemorrhages and one machine learning model that did not have data (variables) regarding the hemorrhages. These two 'analogous' models of each algorithm were analyzed by comparing their ROC curves on predicted outcome probabilities in the test samples. This provided additional information on the significance of sternocleidomastoid origin site hemorrhages in assessing the knot in a noose position based on the thyrohyoid and cervical fracture patterns.

4. RESULTS

The results are reported for each study part separately, in the order following the one in the Material and Methods.

4.1. PART I of the study: Separate analysis of the fracture patterns in knot's position assessment

The basic subjects' characteristics: sex, age, overall thyrohyoid and cervical spine fracture occurrence, and ligature knot position prevalence in all the subjects included in this study are shown in Table 4.1.1.

4.1.1. Descriptive, basic inferential, and logistic regression analysis of the thyrohyoid and cervical spine fracture patterns

The distribution of the analyzed thyrohyoid and cervical spine fractures in terms of the coded variables (see section 3.3. of the Material and Methods) for study subgroups (Datasets I – III) is shown in Table 4.1.2. Due to the additional variable coding, the analysis of the subgroup of subjects with lateral knot position (Dataset IV) is shown separately in Table 4.1.3. As most of the descriptive information is given in these tables, only the additional statistically significant associations and binary logistic regression analyses are highlighted here.

4.1.1.1. The entire sample (hangings with and without fractures) – Dataset I

Considering the entire sample (all 1,235 cases), the fractures of the thyrohyoid complex were significantly more frequent in those older than 40 years of age compared to the younger (N = 591, 63.8% subjects older than 40 years of age vs. N = 158, 51.3% subjects younger than 40 years of age, $\chi^2 = 15.03$, $p < 0.001$). And, this was true for occurrence of STH fractures considered separately (N = 430, 46.4% of subjects older than 40 years vs. N = 120, 39.0% of subjects younger than 40 years of age, $\chi^2 = 5.16$, $p < 0.05$), as well as for the occurrence of GHH fractures considered separately (N= 352, 38.0% of subjects older than 40 years of age vs. N=73, 23.7% of subjects younger than 40 years of age). The cervical spine fractures were significantly more frequent in cases older than 40 years of age, as well (N = 40, 4.3% vs. N = 4, 1.3%, $\chi^2 = 6.12$, $p < 0.05$). The overall occurrence of thyrohyoid fractures did not significantly differ between the two groups (typical vs. atypical hangings, $\chi^2 = 0.001$, $df = 1$, $p > 0.05$) and the distribution of subjects older than 40 years of age was equal between these groups ($\chi^2 = 3.31$, $df = 1$, $p > 0.05$).

On the ROC analysis, age was a statistically significant predictor of the thyrohyoid fracture occurrence in general, as well as for the occurrence of GHH fractures considered separately but was not a statistically significant predictor for STH fracture occurrence alone – the ROC curve analyses are shown in Figure 4.1.1.

Table 4.1.1. *Basic subjects' and injury characteristics – the entire study sample (Dataset I).*

N = 1,235		
Sex	Male Female	937 (75.9%) 298 (24.1%)
Age (years)		54.3 ± 17.9
THYROHYOID AND CERVICAL SPINE FRACTURES		
Thyrohyoid fractures present	Yes No	749 (60.6 %) 486 (39.4 %)
STH fracture present	Yes No	550 (44.5%) 685 (55.5%)
GHH fracture present	Yes No	425 (34.4%) 810 (65.6%)
Isolated STH fracture(s)	Yes No	324 (26.2%) 911 (73.8%)
Isolated GHH fracture(s)	Yes No	199 (16.1%) 1,036 (83.9%)
Simultaneous STH and GHH fractures	Yes No	226 (18.3%) 1,009 (81.7%)
Left GHH fracture	Yes No	248 (20.1 %) 987 (79.9 %)
Right GHH fracture	Yes No	263 (21.3%) 972 (78.7%)
Left STH fracture	Yes No	371 (30.0%) 864 (70.0%)
Right STH fracture	Yes No	360 (29.1%) 875 (70.9%)
Cervical Spine fracture	Yes No	44 (3.6%) 1,191 (96.4%)
KNOT POSITION		
Anterior		116 (9.4%)
Posterior		707 (57.2%)
Left lateral		208 (16.8%)
Right lateral		204 (16.6%)

Note: The data is presented as frequency and ratio.
Abbreviations: STH – Superior thyroid cartilage horn; GHH – Greater hyoid bone horn.
Most of the data previously reported and table adopted from: Leković et al. [62]

Age was fair but significant predictor for thyrohyoid fracture occurrence (AUC 0.557, 95% CI 0.524 – 0.591, p <0.05) – cutoff value was age of ≥ 36.5 years (sensitivity 85.7%, specificity 27.0%), as well as for GHH fractures alone (AUC 0.571, 95% CI 0.538 – 0.601, p <0.001) – cutoff value was age of ≥ 37.5 years (sensitivity 87.8%, specificity 25.6%). Contrary, age was not a significant predictor in STH fracture occurrence (AUC 0.518, 95% CI 0.486 – 0.550, p >0.05). Considering the entire sample, age was a good predictor of cervical spine fracture occurrence – with AUC of 0.709 (95% CI 0.639 – 0.779), p < 0.001. This ROC analysis is shown in the same figure. Regarding the cervical spine fracture occurrence, the threshold value was the age of ≥ 64.5 years, with a sensitivity of 65.9%, and a specificity of 70.6%.

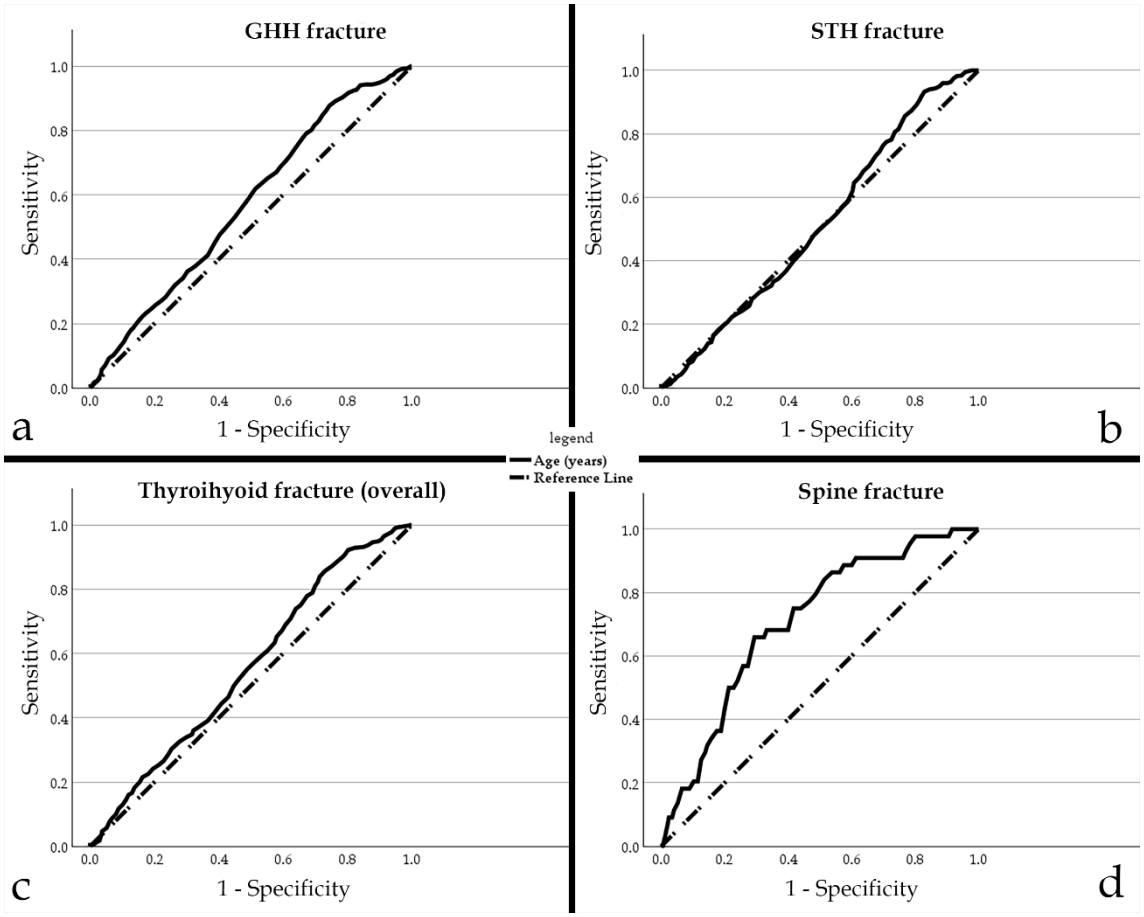

Figure 4.1.1. *The ROC curve analyses of the subjects' age as a predictor for (**a**) the occurrence of GHH fractures, (**b**) the occurrence of STH fractures (**c**) the occurrence of thyrohyoid fractures in general, and (**d**) the cervical spine fracture occurrence, in the entire study sample (Dataset I).*
Abbreviations: *GHH – Greater hyoid bone horn, STH – Superior thyroid cartilage horn.*

On the univariable binary logistic regression analysis, significantly associated with the atypical knot position were older age (OR = 1.008, 95% CI 1.002 – 1.015; $p < 0.05$), cervical spine fracture (OR = 4.797, 95% CI 2.348 – 9.801; $p < 0.001$), unilateral GHH fracture (OR = 1.615, 95% CI 1.255 – 2.076; $p < 0.001$), simultaneous STH and GHH fractures (OR = 1.528, 95% CI 1.144 – 2.041; $p < 0.01$), and absence of isolated STH fractures (OR = 0.640, 95% CI 0.492 – 0.833; $p < 0.001$).

On the multivariable logistic regression analysis, the cervical spine fracture (aOR = 4.326, 95% CI 2.097 – 8.927; $p < 0.001$) and unilateral GHH fracture (aOR = 1.368, 95% CI 1.004 – 1.863 $p < 0.05$) remained significantly associated with the atypical knot position, adjusted for subjects age (aOR = 1.005, 95% CI 0.999 – 1.012; $p > 0.05$), simultaneous STH and GHH fractures (aOR 1.166, 95% CI 0.827 – 1.643), and isolated STH fractures (aOR 0.790, 95% CI 0.553 – 1.054). This model correctly classified 60.7% of cases ($\chi^2 = 52.94$, df = 5, $p < 0.001$; Hosmer & Lemeshow Test: $\chi^2 = 13.61$, df = 8, $p > 0.05$).

4.1.1.2. The hangings with thyrohyoid or cervical spine fractures – Dataset II

In the subgroup of subjects in which at least one thyrohyoid or cervical spine fracture was observed, subjects older than 40 years were equally distributed between the two groups (typical vs. atypical hangings, $\chi^2 = 0.001$, df = 1, $p > 0.05$).

On the univariable logistic regression analysis, significantly associated with the atypical knot position were older age (OR = 1.012, 95% CI 1.003 – 1.020; $p < 0.05$), unilateral GHH fracture (OR = 1.703, 95% CI 1.277 – 2.270; $p < 0.001$), simultaneous STH and GHH fractures OR = 1.521, 95% CI 1.114 – 2.077; $p < 0.01$, cervical spine fracture (OR = 4.700, 95% CI 2.287 – 9.658; $p < 0.001$), and absence of isolated STH fractures (OR = 0.524, 95% CI 0.390 – 0.703; $p < 0.001$).

On the multivariable logistic regression analysis, the cervical spine fracture (OR = 5.085, 95% CI 2.281 – 11,337; $p < 0.001$), and unilateral GHH fracture (OR = 1.674, 95% CI 1.033 – 2.712; $p < 0.05$) remained significantly associated with the atypical knot position, independently of subjects age (OR = 1.008, 95% CI 0.999 – 1.017; $p > 0.05$), simultaneous STH and GHH fractures (OR = 1.284, 95% CI 0.873 – 1.980; $p > 0.05$), or isolated STH fractures (OR = 1.025, 95% CI 0.593 – 1.769; $p > 0.05$). This model correctly classified 61.8% of cases ($\chi^2 = 42.98$, df = 5, $p < 0.001$; Hosmer & Lemeshow Test: $\chi^2 = 12.85$, df = 8, $p > 0.05$).

4.1.1.3. The atypical hangings with thyrohyoid or cervical spine fractures – Dataset III

The subgroup of Dataset III comprised only atypical hanging cases with at least one thyrohyoid or cervical spine fracture, and here, the anterior and lateral hanging groups were compared in between. Subjects older than 40 years of age were equally distributed between the two groups ($\chi^2 = 0.25$, df = 1, $p > 0.05$).

On the univariable binary logistic regression analysis, significantly associated with the anterior knot position were cervical spine fracture (OR = 15.698, 95% CI 7.103 – 34.692; $p < 0.001$) and the absence of unilateral and isolated STH fractures (OR = 0.536, 95% CI 0.291 – 0.988; $p < 0.05$, and OR = 0.404, 95% CI 0.195 – 0.836; $p < 0.05$, respectively). The presence of unilateral GHH fracture was not significantly different between the groups but was included in multivariable logistic regression analysis since the p-value was less than 0.1 in univariable binary logistic regression analysis.

On the multivariable binary logistic regression analysis, the cervical spine fracture (aOR = 10.157, 95% CI 4.032 – 25.588; $p < 0.001$) remained significantly associated with the anterior knot position, independently of the unilateral and isolated STH fractures (aOR = 1.066, 95% CI 0.509 – 2.231; $p > 0.05$, and aOR = 0.398, 95% CI 0.133 – 1.195; $p > 0.05$, respectively), as well as of the unilateral GHH fracture (aOR = 0.508, 95% CI 0.209 – 1.236; $p > 0.05$). This model correctly classified 87.4 % of cases ($\chi^2 = 51.41$, df = 4, $p < 0.001$; Hosmer & Lemeshow Test: $\chi^2 = 2.21$, df = 4, $p > 0.05$).

Table 4.1.2. *The descriptives of the coded variables: thyrohyoid and cervical fractures and basic subject characteristics for Datasets I, II, and III.*

		DATASET I THE ENTIRE SAMPLE			*DATASET II HANGINGS WITH FRACTURES*			*DATASET III ATYPICAL HANGINGS*		
		Knot Position			***Knot Position***			***Knot Position***		
		Typical *N = 707 (57.3 %)*	***Atypical*** *N = 528 (42.7 %)*	***p-value***	***Typical*** *N = 433 (56.0%)*	***Atypical*** *N = 340 (44.0%)*	***p-value***	***Anterior*** *N = 54 (15.9 %)*	***Lateral*** *N = 286 (84.1 %)*	***p-value***
Sex	Male	527 (74.5%)	410 (77.7%)		329 (76.0%)	271 (79.7%)		38 (70.4%)	233 (81.5%)	
	Female	180 (25.5%)	118 (23.3%)		104 (24.0%)	69 (20.3%)		16 (29.6%)	53 (18.5%)	
Age (years)		**53.1 ± 18.1**	**55.7 ± 17.5**	**< 0.05**	**54.6 ± 17.2**	**57.9 ± 16.4**	**< 0.05**	60.5 (28 – 88)	57.0 (16 – 94)	
THYROHYOID AND CERVICAL SPINE FRACTURE PATTERNS										
Isolated	Yes	**211 (29.8%)**	**113 (21.4%)**	**< 0.001**	**211 (48.7%)**	**113 (33.2%)**	**< 0.001**	**10 (18.5%)**	**103 (36.0%)**	**< 0.05**
***STH** fracture(s)*	No	**496 (70.2%)**	**415 (78.6%)**		**222 (51.3%)**	**227 (55.8%)**		**44 (81.5%)**	**183 (64.0%)**	
Unilateral	Yes	213 (30.1%)	156 (29.5%)		**213 (49.2%)**	**156 (45.9%)**		**18 (33.3%)**	**138 (48.3%)**	**< 0.05**
***STH** fracture*	No	494 (69.9%)	372 (70.5%)		220 (50.8%)	184 (54.1%)		**36 (66.7%)**	**148 (51.7%)**	
Bilateral	Yes	108 (15.3%)	73 (13.8%)		108 (24.9%)	73 (21.5%)		8 (14.8%)	65 (22.7%)	
***STH** fracture*	No	599 (84.7%)	455 (86.2%)		325 (75.1%)	267 (78.5%)		46 (85.2%)	221 (77.3%)	
Total N⁰ of STH fractures (0 – 2)		0 (0 – 2)	0 (0 – 2)		**1 (0 – 2)**	**0 (0 – 2)**	**< 0.05**	**0 (0 – 2)**	**1 (0 – 2)**	**< 0.05**
Isolated	Yes	108 (15.3%)	91 (17.2%)		108 (24.9%)	91 (26.8%)		13 (24.1%)	78 (27.3%)	
***GHH** fracture(s)*	No	599 (84.7%)	437 (82.8%)		325 (75.1%)	249 (73.2%)		41 (75.9%)	208 (72.7%)	
Unilateral	Yes	**165 (23.3%)**	**174 (30.0%)**	**< 0.001**	**165 (38.1%)**	**174 (51.2%)**	**< 0.001**	22 (40.7%)	152 (53.1%)	
***GHH** fracture*	No	**542 (76.6%)**	**354 (67.0%)**		**268 (61.9%)**	**166 (48.8%)**		32 (53.1%)	134 (46.9%)	
Bilateral	Yes	53 (7.5%)	33 (6.3%)		53 (12.2%)	33 (9.7%)		7 (13.0%)	26 (9.1%)	
***GHH** fracture*	No	654 (92.5%)	495 (93.8)		380 (87.8%)	307 (90.3%)		47 (87.0%)	260 (90.9%)	
Total N⁰ of GHH fractures (0 – 2)		**0 (0 – 2)**	**0 (0 – 2)**	**< 0.05**	**1 (0 – 2)**	**0 (0 – 2)**	**< 0.001**	1 (0 – 2)	1 (0 – 2)	
Total N⁰ of TyHy fractures (0 – 4)		1 (0 – 4)	1 (0 – 4)		1 (0 – 4)	1 (0 – 4)		**1 (0 – 4)**	**1 (0 – 4)**	**< 0.05**
Simultaneous	Yes	**110 (15.6%)**	**116 (22.0%)**	**< 0.01**	**110 (25.4%)**	**116 (34.1%)**	**< 0.01**	16 (29.6%)	100 (35.0%)	
***STH and GHH** fractures*	No	**597 (84.4%)**	**412 (78.0%)**		**323 (74.6%)**	**224 (65.9%)**		38 (70.4%)	186 (65.0%)	
Contralateral thyrohyoid fracture								Yes: 2 (3.7%) / No: 52 (96.3%)	Yes: 28 (9.8%) / No: 258 (90.2%)	
***Cervical spine** fracture*	Yes	10 (1.4%)	34 (6.4%)	< 0.001	10 (2.3%)	34 (10.0%)	< 0.001	**22 (40.7%)**	**12 (4.2%)**	**< 0.001**
	No	**697 (98.6%)**	**494 (93.6%)**		**423 (97.7%)**	**306 (90%)**		**32 (59.3%)**	**274 (95.8%)**	

Note: The categorical data is presented as frequency and ratio, and numerical as average ± standard deviation or median and range. For comparison of categorical data, the χ^2 test was performed, while the Student's t-test for two independent samples or Mann-Whitney U test were performed for numerical data. The missing p values are > 0.05. ***Abbreviations:*** STH – Superior thyroid cartilage horn; GHH – Greater hyoid bone horn; TyHy – Thyrohyoid. From: Leković et al. [62]

4.1.1.4. *The lateral hangings with thyrohyoid or cervical spine fractures – Dataset IV*

Subjects older than 40 years of age were equally distributed between the two groups ($\chi^2 = 1.16$, df = 1, $p > 0.05$).

On the univariable binary logistic regression analysis, significantly associated with the left lateral hangings were fractures of the left greater hyoid horn (OR = 1.701, 95% CI 1.040 – 2.781; $p < 0.05$), and right superior thyroid horn (OR = 1.607, 95% CI 1.006 – 2.566; $p < 0.05$).

On the multivariable logistic regression analysis, both variables remained independently associated with the left lateral hangings (aOR = 1.832, 95% CI 1.126 – 2.979, $p < 0.05$, and aOR = 1.940, 95% CI 1.164 – 3.232, $p < 0.05$, for right STH, and left GHH, respectively). This model correctly classified 55.9 % of cases ($\chi^2 = 10.566$, df = 2, $p < 0.05$; Hosmer & Lemeshow Test: $\chi^2 = 0.965$, df = 2, $p > 0.05$).

Table 4.1.3. *Characteristics of lateral hanging cases with thyrohyoid or cervical spine fractures (Dataset IV).*

N = 286			***Left lateral N = 140 (49.0%)***	***Right lateral N = 146 (51.0%)***	***p-value***
Sex	Male	233 (81.5%)	119 (85.0%)	114 (78.1%)	
	Female	53 (18.5%)	21 (15.0%)	32 (21.9%)	
Age (years)		57.0 (16 – 94)	57.0 (18 – 94)	59.0 (16 – 94)	
THYROHYOID AND CERVICAL SPINE FRACTURE PATTERNS					
Thyrohyoid fractures present	Yes	281 (98.3%)	137 (97.9%)	144 (98.6%)	
	No	5 (1.7%)	3 (2.1%)	2 (1.4%)	
GHH fracture present	Yes	178 (62.2%)	87 (48.9%)	91 (51.1%)	
	No	108 (37.8%)	53 (49.1%)	55 (50.9%)	
STH fracture present	Yes	203 (71.0%)	105 (51.7%)	98 (48.3%)	
	No	83 (29.0%)	35 (42.2%)	48 (57.8%)	
Ipsilateral GHH fracture	Yes	90 (31.5%)	41 (45.6%)	49 (54.4%)	
	No	196 (68.5%)	99 (50.5%)	97 (49.5%)	
Contralateral STH fracture	Yes	80 (28.0%)	41 (51.2%)	39 (48.8%)	
	No	206 (72.0%)	99 (48.1%)	107 (51.9%)	
Left GHH fracture	Yes	99 (34.6%)	**57 (40.7%)**	**42 (28.8%)**	**< 0.05**
	No	187 (65.4%)	**83 (59.3%)**	**104 (71.2%)**	
Right GHH fracture	Yes	105 (36.7%)	46 (32.9%)	59 (40.4%)	
	No	181 (63.3%)	94 (67.1%)	87 (59.6%)	
Left STH fracture	Yes	136 (47.6%)	64 (45.7%)	72 (49.3%)	
	No	150 (52.4%)	76 (54.3%)	74 (50.7%)	
Right STH fracture	Yes	132 (46.2%)	**73 (52.1%)**	**59 (40.4%)**	**< 0.05**
	No	154 (53.8%)	**67 (47.9%)**	**87 (59.6%)**	
Cervical spine fracture	Yes	12 (4.2%)	7 (5.0%)	5 (3.4%)	
	No	274 (95.8%)	133 (95.0%)	141 (96.6%)	

Note: *The categorical data is presented as frequency and ratio, and numerical as median and range. For comparison of categorical data, the χ^2 test was performed, while the Mann-Whitney U test was performed for numerical data. The missing p values are > 0.05.*
Abbreviations: *STH – Superior thyroid cartilage horn; GHH – Greater hyoid bone horn.*
Most of the data previously published in: Leković et al. [62]

4.1.2. Machine learning algorithms

The characteristics of all the datasets and the coded variables used in the algorithms considering the training and test groups are given in Supplement A. The distribution of the subjects in Datasets I, II, and IV regarding the frequencies of two defined outcomes (knot position) did not require these samples to be balanced (see Tables 4.1.2, and 4.1.3, and Supplement A for sample sizes and proportions). In Dataset III the SMOTE algorithm was performed to oversample the significantly less frequent group of cases of anterior hangings and reduce the frequency disproportion: the initial ratio of 1:5.3 (54 (15.9%) anterior hangings to 286 (84.1%) lateral hangings) was preprocessed to form the sample of 371 cases with the ratio of 1:4.4 (85 (22.9%) anterior hangings to 286 (77.1%) lateral hangings).

In the following text, the results for all the four Datasets (I – IV) will be presented in the following order: (1) performance characteristics of the GA-optimized Artificial Neural Network developed in MATLAB, (2) performance characteristics of all machine learning algorithms developed in SPSS, followed by ROC analysis comparisons between the GA-optimized ANN models developed in MATLAB and the MLP-ANN models developed in SPSS. At the end of the results section of the first study part, the variable ranking in the machine learning models developed in SPSS, and the hyperparameter settings of these models will be reported.

4.1.2.1. Genetic Algorithm-optimized Artificial Neural Networks

In accordance with the previous paragraph, Tables from 4.1.4 to 4.1.7. show performance characteristic analysis of the GA-optimized ANNs, for Datasets I – IV, respectively.

Table 4.1.4. *Performance characteristics of ANN developed in MATLAB for knot position classification in the entire sample (Dataset I).*

GA-optimized ANN		***Accuracy (95% CI)***	***Sn***	***Sp***	***PPV***	***NPV***	***LR+***	***LR-***	***AUC (95% CI)***
DATASET I *Whole sample (w&w/o fractures)*	**Overall**	60.6% (57.8–63.3)	25.2%	87.0%	0.6	0.6	1.9	0.9	0.61 (0.58–0.64)
	Test	60.5% (55.4–65.6)	24.4%	88.1%	0.6	0.5	2.0	0.9	0.60 (0.54–0.66)
	Training	60.6% (57.2–63.9)	25.5%	86.5%	0.6	0.6	1.9	0.9	0.62 (0.58–0.65)

Note: *The atypical knot position was considered as the positive state in confusion matrix performance calculations. There was no statistically significant difference in ROC curve analysis of the predicted outcome probabilities between the training and the test group ($p > 0.05$).*

Abbreviations: *GA – Genetic algorithm; w&w/o – with and without; Sn – sensitivity; Sp – specificity; PPV – positive predictive value, NPV – negative predictive value, LR+ – positive likelihood ratio, negative LR- – negative likelihood ratio, AUC – Area under the curve, CI – Confidence Interval.*

The GA-optimized ANN for Dataset I selected following variables (n = 6) to be included in the model: subject's sex and age, presence of unilateral GHH fracture, presence of bilateral GHH fracture, the total number of GHH fractures, and the total number of thyrohyoid fractures.

Table 4.1.5. *Performance characteristics of ANN developed in MATLAB for knot position classification in atypical hangings (Dataset II).*

GA-optimized ANN		*Accuracy (95% CI)*	*Sn*	*Sp*	*PPV*	*NPV*	*LR+*	*LR-*	*AUC (95% CI)*
DATASET II	**Overall**	62.6% (59.1-66.0)	45.0%	76.4%	60.0%	63.9%	1.9	0.7	0.64 (0.60-0.68)
Hangings with fractures	**Test**	62.7% (56.1-68.9)	49.0%	72.6%	56.5%	66.2%	1.7	0.7	0.64 (0.57-0.71)
	Training	62.6% (58.4-66.7)	43.4%	78.2%	61.8%	63.0%	1.9	0.7	0.64 (0.59-0.69)

Note: *The atypical knot position was considered as the positive state in confusion matrix performance calculations. There was no statistically significant difference in ROC curve analysis of the predicted outcome probabilities between the training and the test group ($p > 0.05$).*
Abbreviations: *GA – Genetic algorithm; Sn – sensitivity; Sp – specificity; PPV – positive predictive value, NPV – negative predictive value, LR+ – positive likelihood ratio, negative LR- – negative likelihood ratio, AUC – Area under the curve, CI – Confidence Interval.*

The GA-optimized ANN for Dataset I selected following variables (n = 6) to be included in the model: subject's age, presence of bilateral STH fracture, the total number of STH fractures, presence of unilateral GHH fracture, presence of simultaneous STH and GHH fractures, and the presence of the cervical spine fracture.

Table 4.1.6. *Performance characteristics of ANN developed in MATLAB for knot position classification in the atypical hangings with fractures (Dataset III).*

GA-optimized ANN		*Accuracy (95% CI)*	*Sn*	*Sp*	*PPV*	*NPV*	*LR+*	*LR-*	*AUC (95% CI)*
DATASET III	**Overall**	84.4% (80.3-87.9)	42.4%	96.9%	80.0%	85.0%	13.5	0.6	0.78 (0.72-0.84)
Atypical hangings with fractures	**Test**	85.0% (77.0-91.0)	40.0%	97.7%	83.3%	85.1%	17.6	0.6	0.74 (0.61-0.86)
	Training	84.1% (79.1-88.3)	43.3%	96.5%	84.9%	84.1%	12.3	0.6	0.80 (0.73-0.87)

Note: *The anterior knot position was considered as the positive state in confusion matrix performance calculations. There was no statistically significant difference in ROC curve analysis of the predicted outcome probabilities between the training and the test group ($p > 0.05$).*
Abbreviations: *GA – Genetic algorithm Sn – sensitivity; Sp – specificity; PPV – positive predictive value, NPV – negative predictive value, LR+ – positive likelihood ratio, negative LR- – negative likelihood ratio, AUC – Area under the curve, CI – Confidence Interval.*

The GA-optimized ANN for Dataset II selected following variables (n = 7) to be included in the model: subject's sex and age, presence of unilateral and bilateral STH fractures, presence of unilateral GHH fracture, the total number of thyrohyoid fractures, as well as the cervical spine fracture.

Table 4.1.7. *Performance characteristics of ANN developed in MATLAB for knot position classification in atypical hangings with fractures (Dataset IV).*

GA-optimized ANN		***Accuracy (95% CI)***	***Sn***	***Sp***	***PPV***	***NPV***	***LR+***	***LR-***	***AUC (95% CI)***
DATASET IV *Lateral hangings with fractures*	**Overall**	92.3% (88.6-95.1)	94.3%	90.4%	90.4%	94.3%	9.8	<0.1	0.96 (0.93-0.99)
	Test	91.8% (83.8-96.6)	92.3%	91.3%	90.0%	93.3%	10.6	<0.1	0.96 (0.90-1.00)
	Training	92.5% (88.0-95.8)	95.0%	90.0%	94.7%	92.5%	9.5	<0.1	0.96 (0.93-0.99)

Note: *The left lateral knot position was considered as the positive state in confusion matrix performance calculations. There was no statistically significant difference in ROC curve analysis of the predicted outcome probabilities between the training and the test group ($p > 0.05$).*

Abbreviations: *GA – Genetic algorithm; Sn – sensitivity; Sp – specificity; PPV – positive predictive value, NPV – negative predictive value, LR+ – positive likelihood ratio, negative LR- – negative likelihood ratio, AUC – Area under the curve, CI – Confidence Interval.*

The GA-optimized ANN for Dataset IV selected following variables (n = 13) to be included in the model: subject's sex and age, presence of right STH fracture, presence of unilateral STH fracture, presence of bilateral STH fracture, presence of STH fracture contralateral to the knot position, presence of left GHH fracture, presence of right GHH fracture, presence of unilateral GHH fracture, presence of bilateral GHH fracture, presence of isolated GHH fracture, presence of GHH fracture ipsilateral to the knot position, and presence of simultaneous STH and GHH fracture.

4.1.2.2. MLP-ANN, Decision Tree, k-NN, and Naïve Bayes algorithms

Tables 4.1.8 – 4.1.11. provide information on the performance characteristics of the machine learning algorithms developed in SPSS software, for Datasets I – IV, respectively.

Table 4.1.8. *The performance characteristics of the machine learning models developed in SPSS, for the knot in a noose position classification in Dataset I.*

MLAs – Dataset I *The entire sample (w & w/o fractures)*		***Accuracy (95% CI)***	***Sn***	***Sp***	***PPV***	***NPV***	***LR+***	***LR-***	***AUC (95% CI)***
MLP-ANN	**Overall**	60.3% (57.5-63.1)	14.4%	94.6%	66.7%	59.7%	2.7	0.9	0.59 (0.56-0.63)
	Test	60.0% (54.8-65.0)	13.1%	95.7%	70.9%	50.6%	3.1	0.9	0.57 (0.51-0.63)
	Training	60.5% (57.1-63.7)	14.9%	94.2%	65.5%	59.9%	2.6	0.9	0.61 (0.57-0.63)
Decision Tree	**Overall**	61.7% (58.9-64.4)	24.1%	89.8%	63.8%	61.3%	2.4	0.8	0.59 (0.56-0.62)
	Test	59.2 (54.0-64.2)	18.8%	90.0%	58.5%	59.2%	1.9	0.9	0.57 (0.51-0.63)
	Training	62.8% (59.5-66.0)	26.4%	89.7%	65.5%	62.2%	2.6	0.8	0.60 (0.56-0.64)

MLAs – Dataset I *The entire sample (w & w/o fractures)*		***Accuracy (95% CI)***	***Sn***	***Sp***	***PPV***	***NPV***	***LR+***	***LR-***	***AUC (95% CI)***
k-NN	**Overall**	62.1% (59.3-64.8)	43.8%	75.8%	57.5%	64.3%	1.8	0.7	0.59 (0.56-0.62)
	Test	60.0% (54.8-65.0)	41.9%	73.8%	54.9%	62.5%	1.6	0.8	0.59 (0.53-0.65)
	Training	63.0% (59.7-66.2)	44.6%	76.7%	58.6%	65.1%	1.9	0.7	0.58 (0.55-0.63)
Naïve Bayes	**Overall**	62.5% (59.7-65.2)	40.3%	79.1%	59.0%	64.0%	1.9	0.8	0.64 (0.61-0.67)
	Test	61.2% (56.2-66.0)	38.3%	78.0%	56.1%	63.2%	1.7	0.8	0.64 (0.58-0.70)
	Training	63.1% (59.8-66.4)	41.3%	79.6%	60.3%	64.3%	2.0	0.7	0.64 (0.60-0.67)
Logistic Regression	**Overall**	60.7% (57.9-63.5)	25.6%	87.7%	59.5%	61.0%	2.0	0.8	0.59 (0.56-0.62)

Notes: *The atypical knot position was considered as a positive state in confusion matrix performance calculations. There was no statistically significant difference in Area under the ROC curve analysis between training and test samples ($p > 0.05$). Some data previously published in Leković et al.* [62]

Abbreviations: *MLP–ANN – Multilayer Perceptron – Artificial Neural Network, k-NN – k Nearest Neighbors, Logistic Regression – Multivariable Logistic Regression analysis, w&w/o – with and without, Sn – sensitivity, Sp – specificity, PPV – positive predictive value, NPV – negative predictive value, LR+ – positive likelihood ratio, negative LR- – negative likelihood ratio, AUC – Area under the curve, CI – Confidence Interval.*

Table 4.1.9. *The performance characteristics of the machine learning models developed in SPSS, for the knot in a noose position classification in Dataset II.*

MLAs – Dataset II *Hangings with fractures*		***Accuracy (95% CI)***	***Sn***	***Sp***	***PPV***	***NPV***	***LR+***	***LR-***	***AUC (95% CI)***
MLP-ANN	**Overall**	62.2% (58.7-65.7)	39.4%	80.1%	60.9%	62.7%	1.9	0.8	0.64 (0.60-0.68)
	Test	62.2% (55.7-68.5)	44.9%	74.8%	56.4%	65.2%	1.8	0.7	0.65 (0.58-0.72)
	Training	62.2% (58.0-66.3)	37.2%	82.6%	63.4%	61.8%	2.1	0.8	0.64 (0.59-0.69)
Decision Tree	**Overall**	62.0% (58.4-65.4)	37.9%	80.8%	60.8%	62.4%	2.0	0.8	0.62 (0.58-0.66)
	Test	62.2% (55.7-68.5)	42.9%	76.3%	56.8%	64.8%	1.8	0.7	0.63 (0.56-0.70)
	Training	61.9% (57.6-66.0)	36.0%	82.9%	63.0%	61.4%	2.1	0.8	0.62 (0.57-0.66)
k-NN	**Overall**	62.1% (58.6-65.5)	44.7%	75.8%	59.1%	63.6%	1.8	0.7	0.61 (0.57-0.65)
	Test	60.9% (54.4-67.2)	45.9%	71.9%	54.2%	64.7%	1.6	0.8	0.64 (0.56-0.71)
	Training	62.6% (58.4-66.7)	44.2%	77.5%	61.5%	63.1%	2.0	0.7	0.59 (0.54-0-64)
Naïve Bayes	**Overall**	65.6% (62.1-68.9)	51.8%	76.4%	63.3%	66.9%	2.2	0.6	0.70 (0.66-0.73)

MLAs – Dataset II *Hangings with fractures*		***Accuracy*** ***(95% CI)***	***Sn***	***Sp***	***PPV***	***NPV***	***LR+***	***LR-***	***AUC*** ***(95% CI)***
Naïve Bayes	**Test**	61.7% (55.2-67.8)	44.0%	74.3%	55.0%	65.0%	1.7	0.8	0.73 (0.67-0.80)
	Training	67.4% (63.2-71.3)	55.0%	77.5%	66.7%	67.8%	2.4	0.6	0.68 (0.64-0.73)
Logistic Regression	**Overall**	61.8% (58.3-65.3)	39.1%	79.7%	60.2%	62.5%	1.9	0.8	0.65 (0.58-0.72)

Notes: *The atypical knot position was considered as a positive state in confusion matrix performance calculations. There was no statistically significant difference in Area under the ROC curve analysis between training and test samples (p > 0.05).*
Abbreviations: *MLP–ANN – Multilayer Perceptron – Artificial Neural Network, k-NN – k Nearest Neighbors, Logistic Regression – Multivariable Logistic Regression analysis, Sn – sensitivity, Sp – specificity, PPV – positive predictive value, NPV – negative predictive value, LR+ – positive likelihood ratio, negative LR- – negative likelihood ratio, AUC – Area under the curve, CI – Confidence Interval. Some data was previously published in Leković et al.* [62]

Table 4.1.10. *The performance characteristics of the machine learning models developed in SPSS, for the knot in a noose position classification in Dataset III.*

MLAs – Dataset III *Atypical hangings with fractures*		***Accuracy*** ***(95% CI)***	***Sn***	***Sp***	***PPV***	***NPV***	***LR+***	***LR-***	***AUC*** ***(95% CI)***
MLP-ANN	**Overall**	84.6% (80.6-88.2)	42.4%	97.2%	81.8%	85.0%	15.1	0.6	82.4 (0.75-0.87)
	Test	84.1% (76.0-90.3)	40.0%	96.6%	85.0%	84.1%	11.7	0.6	0.81 (0.72-0.90)
	Training	84.9% (79.9-89.0)	43.3%	97.5%	83.9%	85.0%	17.1	0.6	0.83 (0.77-0.89)
Decision Tree	**Overall**	83.6% (79.4-87.2)	42.4%	95.8%	75.0%	84.8%	10.1	0.6	0.69 (0.62-0.76)
	Test	83.2% (75.0-89.6)	40.0%	95.5%	71.4%	84.8%	8.8	0.6	0.68 (0.54-0.81)
	Training	83.7% (78.6-88.0)	43.3%	96.0%	76.5%	84.8%	10.7	0.6	0.70 (0.61-0.78)
k-NN	**Overall**	84.4% (80.3-87.9)	42.4%	96.9%	80.0%	85.0%	13.5	0.6	0.69 (0.62-0.76)
	Test	83.2% (75.0-89.6)	40.0%	95.5%	71.4%	84.8%	8.8	0.6	0.68 (0.54-0.81)
	Training	84.9% (79.9-89.0)	43.3%	97.5%	83.9%	85.0%	17.2	0.6	0.70 (0.61-0.79)
Naïve Bayes	**Overall**	87.1% (83.0-90.4)	40.7%	95.8%	64.7%	89.5%	9.7	0.6	0.68 (0.59-0.77)
	Test	86.7% (78.4-92.7)	41.2%	96.3%	70.0%	88.6%	11.1	0.6	0.62 (0.46-0.78)
	Training	87.2% (82.3-91.1)	40.5%	95.6%	62.5%	89.9%	9.2	0.6	0.71 (0.60-0.82)
Logistic Regression	**Overall**	87.4% (83.3-90.7)	40.7%	96.2%	66.7%	89.6%	10.6	0.6	0.72 (0.63-0.81)

Notes: *The anterior knot position was considered as a positive state in confusion matrix performance calculations. There was no statistically significant difference in Area under the ROC curve analysis between training and test samples (p > 0.05).* ***Abbreviations:*** *MLP–ANN – Multilayer Perceptron – Artificial Neural Network, k-NN – k Nearest Neighbors, Logistic Regression – Multivariable Logistic Regression analysis, Sn – sensitivity, Sp – specificity, PPV – positive predictive value, NPV – negative predictive value, LR+ – positive likelihood ratio, negative LR- – negative likelihood ratio, AUC – Area under the curve, CI – Confidence Interval. Some data was previously published in Leković et al.* [62]

Table 4.1.11. *The performance characteristics of the machine learning models developed in SPSS, for the knot in a noose position classification in Dataset IV.*

MLAs – Dataset IV *Lateral hangings with fractures*		***Accuracy (95% CI)***	***Sn***	***Sp***	***PPV***	***NPV***	***LR+***	***LR-***	***AUC (95% CI)***
MLP-ANN	**Overall**	94.1% (90.7-96.5)	95.0%	93.2%	93.0%	95.1%	13.9	<0.1	0.99 (0.99-1.00)
	Test	91.8% (83.8-96.6)	92.3%	91.3%	90.0%	93.3%	10.6	<0.1	0.98 (0.96-1.00)
	Training	95.0% (91.0-97.6)	96.0%	94.0%	94.2%	95.9%	16.0	<0.1	0.99 (0.99-100)
Decision Tree	**Overall**	79.4% (74.2-83.9)	85.7%	73.3%	75.5%	84.3%	3.2	0.2	0.89 (0.85-0.92)
	Test	77.6% (67.3-86.0)	82.1%	73.9%	72.7%	82.9%	3.1	0.2	0.87 (0.80-0.94)
	Training	80.1% (73.9-85.4)	87.1%	73.0%	76.5%	84.9%	3.2	0.2	0.90 (0.85-0.94)
k-NN	**Overall**	88.8% (84.6-92.2)	97.9%	80.1%	82.5%	97.5%	4.9	<0.1	0.96 (0.94-0.98)
	Test	90.6% (82.3-95.8)	100%	82.6%	83.0%	100%	5.8	<0.1	0.97 (0.93-1.00)
	Training	88.1% (82.8-92.2)	97.0%	79.0%	82.4%	96.3%	4.6	<0.1	0.95 (0.93-0.98)
Naïve Bayes	**Overall**	60.8% (54.9-66.5)	58.6%	63.0%	60.3%	61.3%	1.6	0.7	0.63 (0.57-0.66)
	Test	56.5% (45.3-67.2)	59.1%	53.7%	57.8%	55.0%	1.3	0.8	0.59 (0.47-0.71)
	Training	62.7% (55.6-69.4)	58.3%	66.7%	61.5%	63.6%	1.7	0.6	0.64 (0.57-0.72)
Logistic Regression	**Overall**	55.9% (50.0-61.8)	75.7%	37.0%	53.5%	61.4%	1.2	0.7	0.59 (0.53-0.66)

Notes: *The left lateral knot position was considered as a positive state in confusion matrix performance calculations. There was no statistically significant difference in Area under the ROC curve analysis between training and test samples ($p > 0.05$).* ***Abbreviations:*** *MLP–ANN – Multilayer Perceptron – Artificial Neural Network, k-NN – k Nearest Neighbors, Logistic Regression – Multivariable Logistic Regression analysis, Sn – sensitivity, Sp – specificity, PPV – positive predictive value, NPV – negative predictive value, LR+ – positive likelihood ratio, negative LR- – negative likelihood ratio, AUC – Area under the curve, CI – Confidence Interval. Some data was previously published in Leković et al.* [62]

Figure 4.1.2. shows ROC curve analysis of each reported ML algorithm, separately for all four datasets (I – IV).

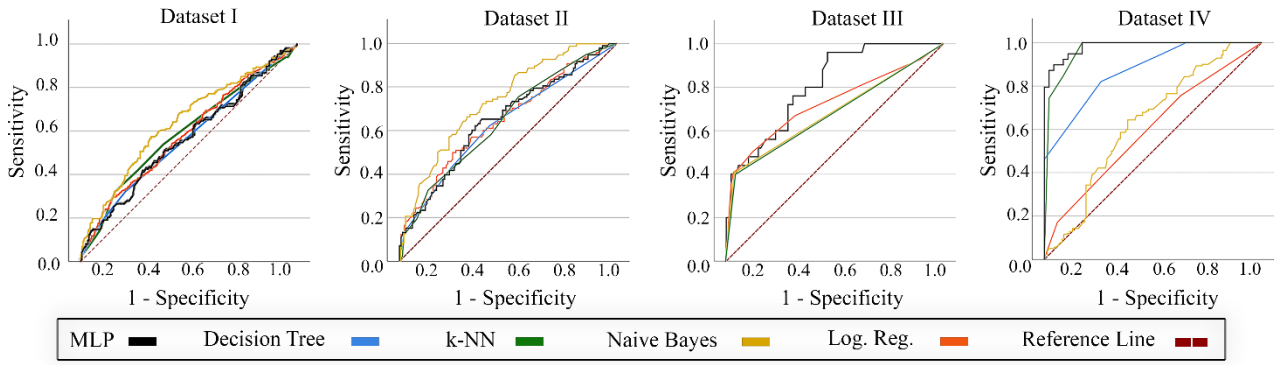

Figure 4.1.2. *The Receiver Operating Characteristic (ROC) and Area under the curve (AUC) analysis of developed machine learning models in Test samples of each of four datasets. The AUCs with 95% Confidence Intervals are listed in Tables 4.1.8 – 4.1.11. There was no statistically significant difference in analysis between any Training and Test sample (p > 0.05). Abbreviations: MLP – Multilayer Perceptron- Artificial Neural Network, k-NN – k Nearest Neighbors, Log. Reg. – Multivariable logistic regression analysis. Previously published in: Leković et al.* [62]

4.1.2.3. GA-optimized ANN and MLP-ANN ROC analysis comparison

There comparison analysis between the ROC curves of the GA-optimized ANN models and the ROC curves of the MLP-ANN models for all four datasets are shown in Figure 4.1.3. (all p-values were > 0.05).

4.1.2.4. Machine learning models' variable importance and settings

Table 4.1.12. lists up to the top five ranked input variables for each of these algorithms, according to the variable's independent importance.

The hyperparameters settings for all used algorithms developed in SPSS (MLP-ANN, DT, k-NN, and NB), in all four datasets (I – IV, respectively) are shown in Table 4.1.13.

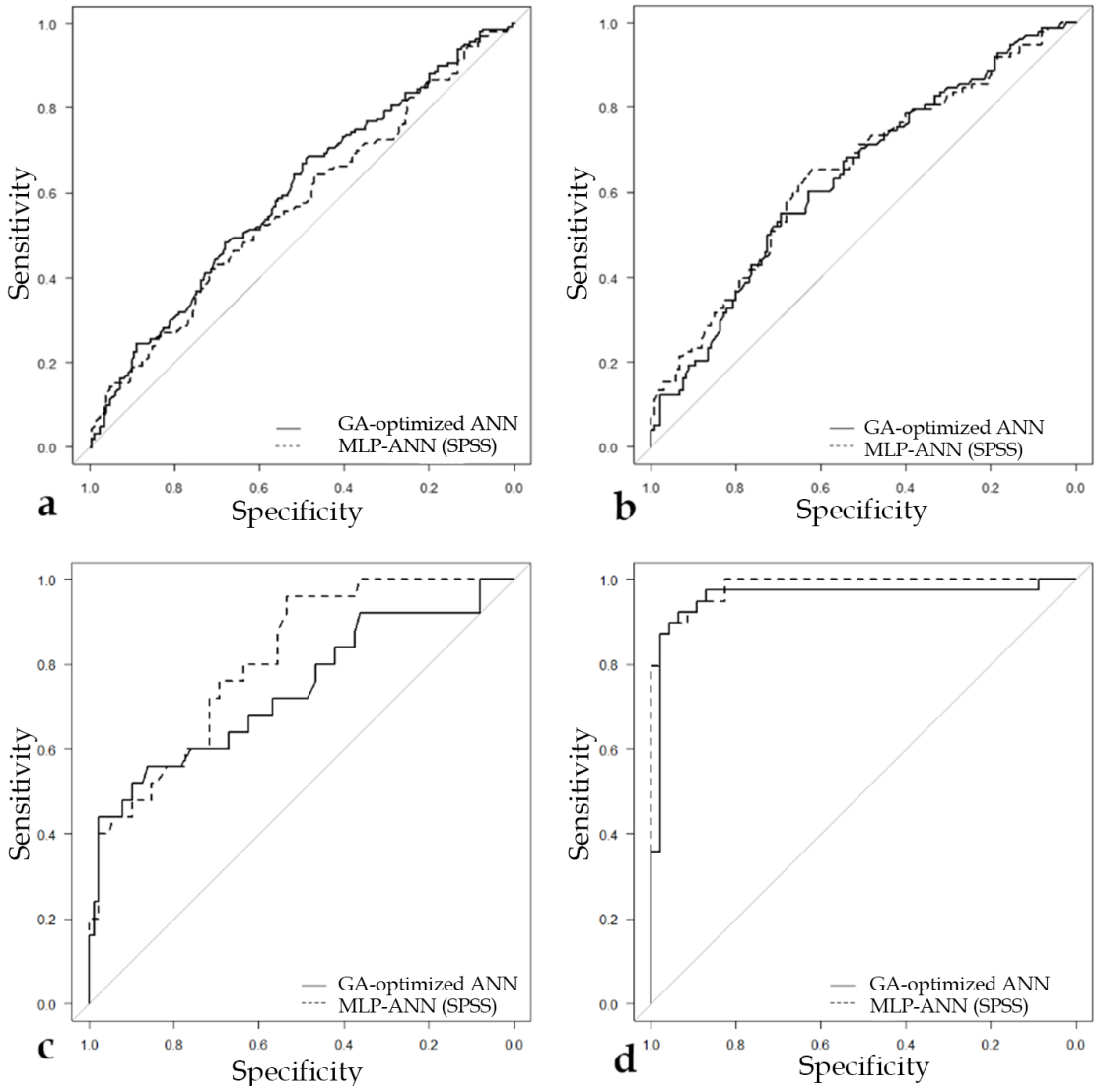

Figure 4.1.3. *The comparison of the ROC curves of two Artificial Neural Network models developed for the knot position classification (atypical vs. typical hangings) in Datasets I and II (**a** and **b**, respectively), (**c**) in Dataset III (anterior vs. lateral hangings), and (**d**) in Dataset IV (left lateral vs. right lateral hangings): the GA-optimized ANN developed in MATLAB and the MLP-ANN developed in SPSS.*

There was no statistically significant difference between any of the two ROC curves:
Dataset I, Z = 1.2835, p > 0.05;
Dataset II, Z = -0.48081, p > 0.05;
Dataset III, Z = -1.6003, p > 0.05;
Dataset IV, Z = -1.2091, p > 0.05.

Table 4.1.12. *The top five ranked input variables based on their relative importance for utilized machine learning models.*

	DATASET I				***DATASET II***				***DATASET III***				***DATASET IV***			
	MLP	**DT**	**k-NN**	**NB**	**MLP**	**DT**	**k-NN**	**NB**	**MLP**	**DT**	**k-NN**	**NB**	**MLP**	**DT**	**k-NN**	**NB**
1st	Tot.Fr.N^0	Spine	sTy&Hy	iTy	iTy	sTy&Hy	sTy&Hy	BL-Ty	Spine	Spine	BL-Ty	Spine	IL-Hy	IL-Hy	Tot.Fr.N^0	Sex
2nd	Spine	sTy&Hy	Spine	Hy N^0	Ty N0	Tot.Fr.N^0	Spine	BL-Hy	Age	Tot.Fr.N^0	Tot.Fr.N^0	Age	CL-Ty	Hy N^0	L-Hy	L-Hy
3rd	Age	UL-Hy	BL-Hy	Sex	Age	UL-Hy	BL-Hy	Sex	Ty N0	/	Spine	Sex	R-Hy	UL-Hy	Spine	Hy N^0
4th	Hy N^0	Age	Age	Tot.Fr.N^0	sTy&Hy	Spine	Age	UL-Ty	iTy	/	/	BL-Hy	Tot.Fr.N^0	R-Hy	IL-Hy	Age
5th	BL-Ty	Tot.Fr.N^0	/	BL-Hy	Tot.Fr.N^0	Hy N^0	/	Spine	Tot.Fr.N^0	/	/	iHy	L-Hy	iTy	sTy&Hy	L-Ty

Note: *Some models included less than 5 variables, and these empty fields in table are labeled by "/" sign.*

Abbreviations: *BL-Hy – bilateral greater hyoid horn fractures, BL-Ty – bilateral superior thyroid horn fractures, CL-Ty - superior thyroid cartilage horn contralateral to the knot position, Hy N^0 – Total number of greater hyoid horn fractures, iTy – isolated superior thyroid horn fracture(s), IL-Hy - greater hyoid bone horn ipsilateral to the knot position, IL-Ty – superior thyroid cartilage horn ipsilateral to the knot position, L-Hy – left greater hyoid bone horn, L-Ty – left superior thyroid cartilage horn, R-Hy – right greater hyoid bone horn, sTy&Hy – simultaneous superior thyroid horn and greater hyoid horn fractures, Spine – Cervical spine fracture, Tot.Fr.N^0 – Total number of thyrohyoid fractures, Ty N^0 – Total number of superior thyroid horn fractures, UL-Hy – unilateral greater hyoid horn fracture, UL-Ty – unilateral superior thyroid horn fracture. From: Leković et al.* [62]

Table 4.1.13. *Hyperparameter settings in the reported machine learning algorithms (developed in SPSS).*

		N⁰ of hidden layers	*N⁰ of neurons in a hidden layer*	*Activation function*	*Training type*	*Training algorithm*	*Initial learning rate*	*Momentum*
MLP ANN	**DATASET I**	1	9	Hyperbolic tangent	Online	Gradient descent	0.4	0.78
	DATASET II	1	8	Hyperbolic tangent	Mini batch	Gradient descent	0.4	0.85
	DATASET III	1	6	Scale conjugate gradient	Batch	Gradient descent	0.54	0.321
	DATASET IV	1	7	Hyperbolic tangent	Online	Gradient descent	0.54	0.321

		Growing method	*Tree depth*	*Min. samples of parent node*	*Min. samples of child node*	*Nº of nodes*	*Nº of terminal nodes*
Decision Tree	**DATASET I**	CRT	4	100	10	9	5
	DATASET II	CRT	3	100	10	7	4
	DATASET III	CRT	2	65	10	7	4
	DATASET IV	CRT	4	50	7	11	6

		Nº of Neighbors to consider	**Distance metrics**	**Search Algorithm (Feature selection - Stopping criterion)**
k-NN	**DATASET I**	13	Euclidean	Change in Absolute Error Ratio ≤0.01
	DATASET II	12	Euclidean	Change in Absolute Error Ratio ≤0.01
	DATASET III	12	Euclidean	Change in Absolute Error Ratio ≤0.01
	DATASET IV	4	Euclidean	Select all features

		Maximum memory (Mb)	**N⁰ of bins for scale predictors**	**N⁰ of selected predictors**
Naïve Bayes	**DATASET I**	1024	50	10
	DATASET II	1024	50	6
	DATASET III	1024	12	1
	DATASET IV	1024	10	5

Abbreviations: *MLP-ANN - Multilayer Perceptron – Artificial neural network, k-NN – k Nearest Neighbors. From: Leković et al.* [62]

4.2. PART II of the study: Analysis of the body weight's significance in knot position-related fracture patterns assessment

The basic subjects' characteristics: sex, age, body weight and body height, overall thyrohyoid and cervical spine fracture occurrence, and ligature knot position prevalence in the subjects included in this study part are shown in Table 4.2.1.

Table 4.2.1. *Basic subjects' and injury characteristics – the study sample of Dataset I-w.*

N = 368

Sex	Male	283 (76.9%)
	Female	85 (23.1%)
Age (years)		57.0 (16-94)
Body weight (kg)		70 (34-148)
Body height (cm)		176.0 (145-205)
THYROHYOID AND CERVICAL SPINE FRACTURES		
Thyrohyoid fractures present	Yes	236 (64.1%)
	No	132 (35.9%)
STH fracture present	Yes	178 (48.4%)
	No	190 (51.6%)
GHH fracture present	Yes	133 (36.1%)
	No	235 (63.9%)
Isolated STH fracture(s)	Yes	103 (28.0%)
	No	265 (72.0%)
Isolated GHH fracture(s)	Yes	58 (15.8%)
	No	310 (84.2%)
Simultaneous STH and GHH fractures	Yes	75 (20.4%)
	No	293 (79.6%)
Left GHH fracture	Yes	85 (23.1%)
	No	283 (76.9%)
Right GHH fracture	Yes	81 (22.0%)
	No	287 (78.0%)
Left STH fracture	Yes	116 (31.5%)
	No	252 (68.5%)
Right STH fracture	Yes	126 (34.2%)
	No	242 (65.8%)
Cervical Spine fracture	Yes	16 (4.3%)
	No	352 (95.7%)
KNOT POSITION		
Anterior		18 (4.9%)
Posterior		197 (53.5%)
Left lateral		82 (22.3%)
Right lateral		71 (19.3%)

Note: *The data is presented as frequency and ratio.*
Abbreviations: *STH – Superior thyroid cartilage horn; GHH – Greater hyoid bone horn.*

4.2.1. Descriptive, basic inferential, and logistic regression analysis of the thyrohyoid and cervical spine fracture patterns

Corresponding to the previous part of the study, the distribution of the analyzed thyrohyoid and cervical spine fractures in terms of the coded variables for study subgroups (Datasets I-w – III-w) is shown in Table 4.2.2, and Table 4.2.3 (Dataset IV-w), while the additional statistically significant associations and logistic regression analyses are reported here.

4.2.1.1. The entire sample (hangings with and without fractures) – Dataset I-w

In the Dataset I-w, comprising 368 hangings with and without thyrohyoid complex and cervical spine fractures, the fractures of the thyrohyoid complex were, in overall, significantly more frequent in subjects older than 40 years of age, compared to the younger subjects (N = 192, 69.6% subjects older than 40 years of age vs. N = 44, 47.8% of younger subjects, $\chi^2 = 14.17$, df = 1, $p < 0.001$). When considered separately, both, STH and GHH fractures were significantly more frequent in subjects older than 40 years of age compared to younger subjects (N = 144, 52.2% subjects older than 40 years of age vs. N = 34, 37.0% of younger subjects, $\chi^2 = 6.40$, df = 1, $p < 0.05$; and N = 116, 42.0% subjects older than 40 years of age vs. N = 17, 18,5% of younger subjects, $\chi^2 = 16.58$, df = 1, $p < 0.001$, respectively). However, between these two groups there was no significant difference in the frequency of cervical spine fractures (N = 14, 5.1% subjects older than 40 years of age vs. N = 2, 2.2% of younger subjects, $\chi^2 = 1.39$, df = 1, $p > 0.05$). The overall occurrence of thyrohyoid fractures did not significantly differ between the two analyzed groups (typical vs. atypical hangings, $\chi^2 = 2.655$, df = 1, $p > 0.05$) and the distribution of subjects older than 40 years of age was equal between these groups ($\chi^2 = 3.31$, df = 1, $p > 0.05$).

On the ROC analysis, subjects' age and body weight were statistically significant predictors for thyrohyoid and cervical fracture occurrence, while the subject's body height was not – the ROC curve analyses are shown in Figures 4.2.1 – 4.2.3. for subjects' age, body weight, and body height, respectively.

Age was a significant predictor for thyrohyoid fracture occurrence (AUC 0.616, 95% CI 0.556 – 0.677, $p < 0.001$) – cutoff value was age of ≥ 41.5 years (sensitivity 80.9%, specificity 39.4%), and for the occurrence of GHH fractures alone (AUC 0.653, 95% CI 0.595 – 0.710, $p < 0.001$) – cutoff value was age of ≥ 52.5 years (sensitivity 76.7%, specificity 51.9%) but, again, age was not a good predictor of STH fracture occurrence considered separately (AUC 0.528, 95% CI 0.469 – 0.587, $p > 0.05$). In this group of subjects (Dataset I-w), age was not a significant predictor of cervical spine fracture occurrence (AUC 0.618, 95% CI 0.490 – 0.746, $p > 0.05$).

Age showed a weak statistically significant positive correlation with the total number of thyrohyoid fractures (range 0-4 – sum of STH and GHH fractures, $\rho = 0.212$, $p < 0.001$), and with the total number of GHH fractures (range 0-2, $\rho = 0.248$, $p < 0.001$), but did not correlate with the number of STH fractures (range 0-2, $\rho = 0.183$, $p > 0.05$).

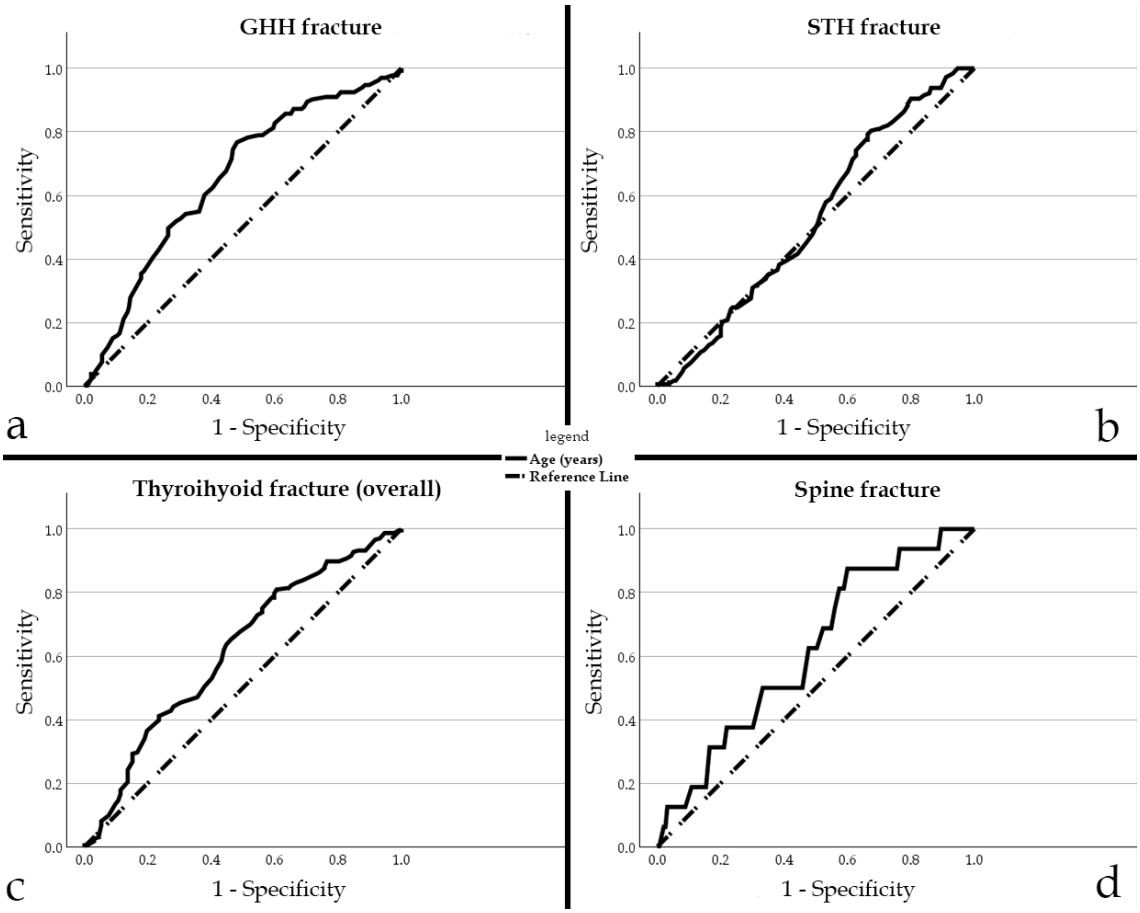

Figure 4.2.1. *The ROC curve analyses of the subjects' age as a predictor for (**a**) the occurrence of GHH fractures, (**b**) the occurrence of STH fractures, (**c**) the occurrence of thyrohyoid fractures in general, as well as (**d**) the cervical spine fracture occurrence, in the entire study sample(Part II of the study, Dataset I-w).*
Abbreviations: *GHH – Greater hyoid bone horn, STH – Superior thyroid cartilage horn.*

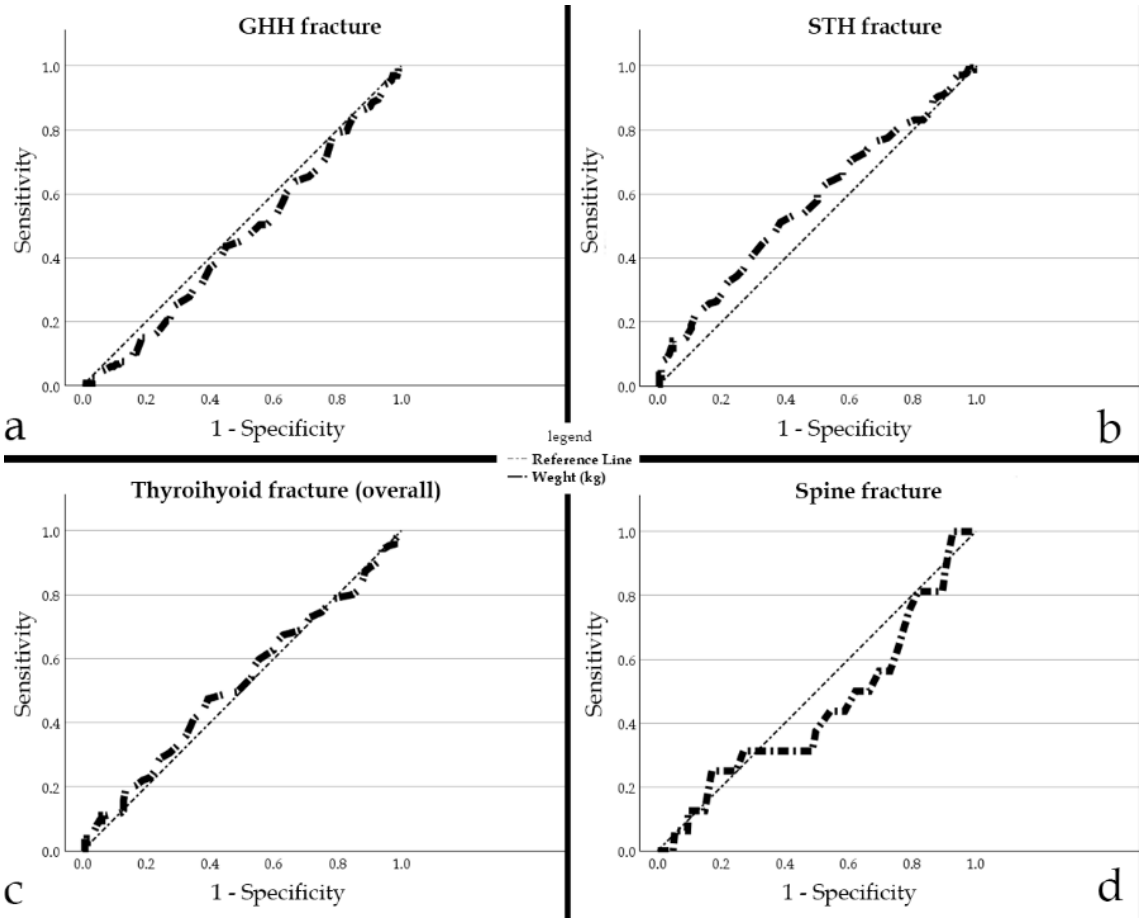

Figure 4.2.2. *The ROC curve analyses of the subjects' body weight as a predictor for (**a**) the occurrence of GHH fractures, (**b**) the occurrence of STH fractures, (**c**) the occurrence of thyrohyoid fractures in general, as well as (**d**) the cervical spine fracture occurrence, in the entire study sample (Part II of the study, Dataset I-w).* ***Abbreviations:*** *GHH – Greater hyoid bone horn, STH – Superior thyroid cartilage horn.*

Body weight was a statistically significant predictor only of STH fracture occurrence (AUC 0.573, 95% CI 0.514 – 0.631, $p < 0.05$) – cutoff value was body weight of ≥ 72.5 kg (sensitivity 51.1%, specificity 61.6%). Body weight was not a significant predictor of thyrohyoid fracture occurrence in general (AUC 0.520, 95% CI 0.459 – 0.580, $p > 0.05$), nor for the occurrence of GHH fractures alone (AUC 0.461, 95% CI 0.400 – 0.521, $p > 0.05$), and for the cervical spine fracture occurrence (AUC 0.448, 95% CI 0.297 – 0.599, $p > 0.05$).

Body weight showed significant but negligible positive correlation only with the total number of STH fractures (range 0 – 2, $\rho = 0.139$, $p < 0.05$).

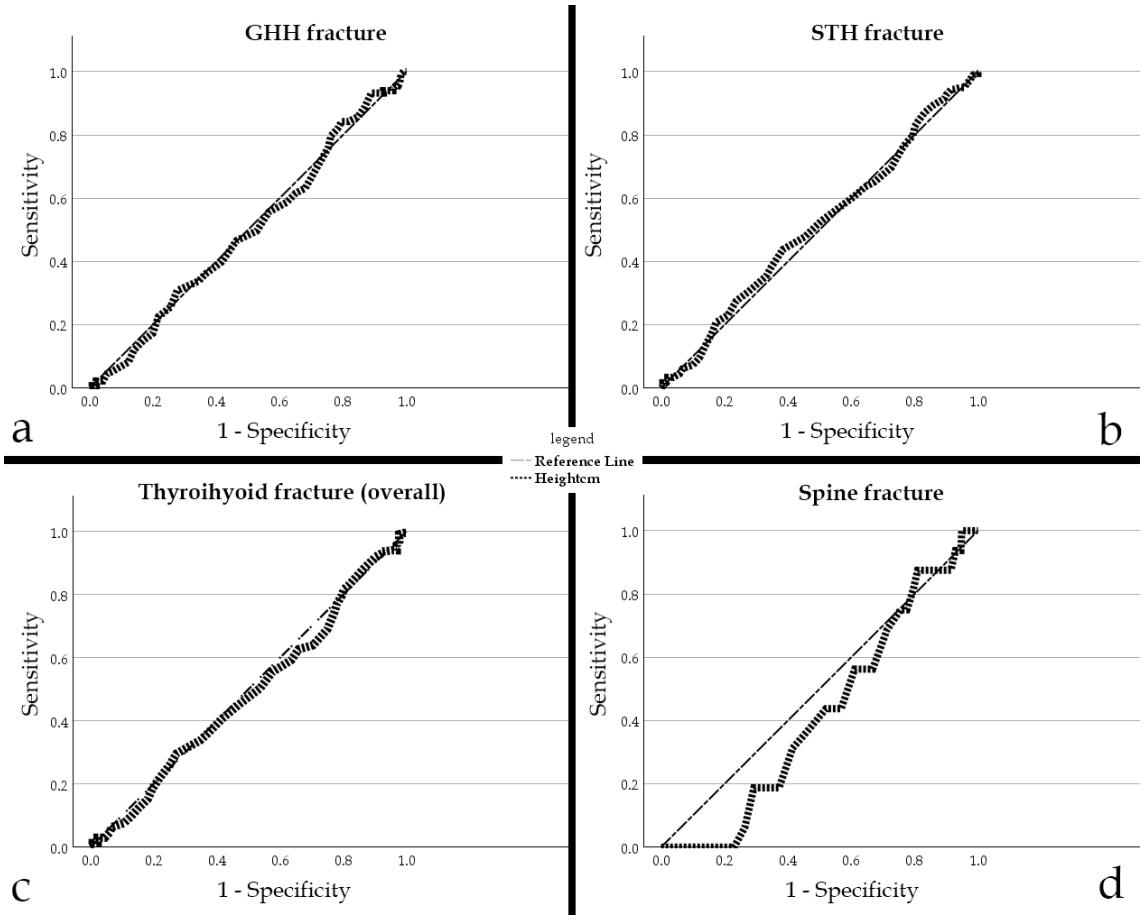

Figure 4.2.3. *The ROC curve analyses of the subjects' body height as a predictor for* ***(a)*** *the occurrence of GHH fractures* ***(b)*** *the occurrence of STH fractures,* ***(c)*** *the occurrence of thyrohyoid fractures in general, as well as* ***(d)*** *the cervical spine fracture occurrence, in the entire study sample (Part II of the study, Dataset I-w).* ***Abbreviations:*** *GHH – Greater hyoid bone horn, STH – Superior thyroid cartilage horn.*

Body height was not a significant predictor of cervical spine fracture occurrence (AUC 0.420, 95% CI 0.306 – 0.534, $p > 0.05$), of overall thyrohyoid fracture occurrence (AUC 0.486, 95% CI 0.424 – 0.547, $p > 0.05$), of GHH fracture occurrence considered separately (AUC 0.494, 95% CI 0.432 – 0.555, $p > 0.05$), nor of STH fracture occurrence considered separately (AUC 0.512, 95% CI 0.453 – 0.571, $p > 0.05$).

Body height did not significantly correlate with the number of thyrohyoid fractures, overall and when considered separately (STH and GHH, $p > 0.05$ – for all).

On the univariable logistic regression analysis, only unilateral GHH fracture was statistically significantly associated with the atypical knot position (OR = 1.791, 95% CI 1.126-2.848, $p < 0.05$). In the multivariable analysis the following variables were also included, as p-values were less than 0.1 in univariable binary logistic regression analyses: isolated STH fracture ($p = 0.068$), and simultaneous STH and GHH fractures ($p = 0.065$).

On the multivariable binary logistic regression analysis, the presence of unilateral GHH fracture was not significantly associated with the atypical knot position (aOR = 1.521, 95% CI 0.884-2.617, $p > 0.05$), when adjusted for the presence of isolated STH fracture (aOR = 0.803, 95% CI 9.483-1.336, $p > 0.05$) and for the presence of simultaneous STH ad GHH fractures (aOR = 0.803, 95% CI 0.676-2.177, $p > 0.05$). This model correctly classified 57.3% of cases ($\chi^2 = 7.481$, df = 3, $p > 0.05$; Hosmer & Lemeshow Test: $\chi^2 = 5.044$, df = 3, $p > 0.05$).

4.2.1.2. The hangings with thyrohyoid or cervical spine fractures – Dataset II-w

In the subgroup of subjects in which at least one thyrohyoid or cervical spine fracture was observed, subjects older than 40 years were equally distributed between the two groups (typical vs. atypical hangings, $\chi^2 = 0.829$, df = 1, $p > 0.05$).

Age showed statistically significant weak positive correlation with the total number of GHH fractures (range 0-2, $\rho = 0.200$, $p < 0.05$). The positive correlation between subjects' body weight and the total number of STH fractures was statistically significant but negligible (range 0-2, $\rho = 0.199$, $p < 0.05$).). Body height did not significantly correlate with the number of thyrohyoid fractures, overall and when considered separately (STH and GHH, $p > 0.05$ – for all).

On the univariable binary logistic regression analysis, a statistically significant association with the atypical knot position was observed with the presence of unilateral GHH fracture (OR = 1.977, 95% CI 1.176 – 3.321, $p < 0.05$), and the absence of isolated STH fracture (OR = 1.793, 95% CI 1.068 – 3.009, $p < 0.05$). The presence of simultaneous STH and GHH fracture was included in the multivariable analysis, as the p-value was < 0.1.

On the multivariable binary logistic regression analysis, none of the three considered variables were an independent predictor of the atypical knot position: unilateral GHH fracture (aOR = 1.775, 95% CI 0.836 – 3.770, $p > 0.05$), simultaneous STH and GHH fractures (aOR = 1.343, 95% CI 0.681 – 2.648, $p > 0.05$), and the absence of isolated STH fracture (aOR = 1.014, 95% CI 0.429 – 2.396, $p > 0.05$). This model correctly classified 58.7% of cases ($\chi^2 = 7.705$, df = 3, $p > 0.05$; Hosmer & Lemeshow Test: $\chi^2 = 5.977$, df = 3, $p > 0.05$).

4.2.1.3. *The atypical hangings with thyrohyoid or cervical spine fractures – Dataset III-w*

The subgroup of Dataset III-w comprised only atypical hanging cases with at least one thyrohyoid or cervical spine fracture, and here, the anterior and lateral hanging groups were compared in between. Subjects older than 40 years of age were equally distributed between the two groups ($\chi^2 = 1.51$, df = 1, $p > 0.05$).

In Dataset III-w, subjects' age, body weight, and body height did not correlate significantly with the number of thyrohyoid fractures, either combined, or considered separately (STH and GHH fractures, p-values > 0.05).

On the univariable binary logistic regression analysis, a statistically significant association with the anterior knot position was observed with the total number of GHH fractures (OR = 0.206, 95% CI 0.043 – 0.977, $p < 0.05$), total number of thyrohyoid fractures (OR = 0.143, 95% CI 0.035 – 0.587, $p < 0.05$), and the presence of the cervical spine fracture (OR = 33.667, 95% CI 6.214 – 182.402, $p < 0.001$). In addition to these variables, subjects' sex was included in the multivariable analysis, as the p-value for this variable was < 0.1.

On the multivariable binary logistic regression analysis, the presence of cervical spine fracture remained independently associated with the anterior knot position, compared to the lateral (aOR = 66.829, 95% CI 5.111 – 873.808, $p = 0.001$), adjusted for subjects' sex (aOR = 0.123, 95% CI 0.011 – 1.334, $p > 0.05$), as well as for the total number of GHH fractures (aOR = 0.274, 95% CI 0.032 – 2.374, $p > 0.05$) and the total number of thyrohyoid fractures (aOR = 0.770, 95% CI 0.187 – 3.174, $p > 0.05$). This model correctly classified 93.9% of cases ($\chi^2 = 25.938$, df = 4, $p < 0.001$; Hosmer & Lemeshow Test: $\chi^2 = 3.340$, df = 7, $p > 0.05$).

4.2.1.4. *The lateral hangings with thyrohyoid and cervical spine fractures – Dataset IV-w*

Subjects older than 40 years of age were equally distributed between the two groups ($\chi^2 = 0.008$, df = 1, $p > 0.05$).

Subjects' age, body weight, and body height did not correlate significantly with the number of thyrohyoid fractures, either combined, or considered separately (STH and GHH fractures, p-values > 0.05).

On the univariable binary logistic regression analysis, none of the coded variables was significantly associated with the left lateral hangings, and because not a single p-value was < 0.1 the multivariable regression analysis was not performed.

Table 4.2.2. *The descriptives of the coded variables: thyrohyoid and cervical fractures and basic subject characteristics for Datasets I-w, II-w, and III-w.*

		DATASET I-w *THE ENTIRE SAMPLE*			***DATASET II-w*** *HANGINGS WITH FRACTURES*			***DATASET III-w*** *ATYPICAL HANGINGS*		
		Knot Position			***Knot Position***			***Knot Position***		
		Typical *N = 197 (53.5%)*	***Atypical*** *N = 171 (46.5%)*	***p-value***	***Typical*** *N = 128 (52.9%)*	***Atypical*** *N = 114 (47.1%)*	***p-value***	***Anterior*** *N = 8 (7.0%)*	***Lateral*** *N = 106 (93.0%)*	***p-value***
Sex	Male	155 (78.7%)	128 (74.9%)		99 (77.3%)	88 (77.2%)		4 (50.0%)	84 (79.2%)	
	Female	42 (21.3%)	43 (25.1%)		29 (22.7%)	26 (22.8%)		4 (50.0%)	22 (20.8%)	
Age (years)		55.0 (18-90)	58.0 (16-94)		57.0 (22-90)	61.5 (16-94)		66.0 (57-82)	60.5 (16-94)	
Body weight (kg)		70 (34-148)	71.0 (38-112)		70 (41-146)	70.5 (38-112)		67.5 (38-94)	70.5 (40-112)	
Body height (cm)		176.0 (145-205)	176.0 (151-195)		175.0 (145-205)	176 (152-195)		172.5 (154-181)	176 (152-195)	
THYROHYOID AND CERVICAL SPINE FRACTURE PATTERNS										
Isolated	Yes	63 (32.0%)	40 (23.4%)		**63 (49.2%)**	**40 (35.1%)**	**< 0.05**	3 (37.5%)	37 (34.9%)	
STH fracture(s)	No	134 (68.0%)	131 (76.6%)		**65 (50.8%)**	**74 (64.9%)**		5 (62.5%)	69 (65.1%)	
Unilateral	Yes	63 (32.0%)	51 (29.8%)		63 (49.2%)	51 (44.7%)		3 (37.5%)	48 (45.3%)	
STH fracture	No	134 (68.0%)	120 (70.2%)		65 (50.8%)	63 (55.3%)		5 (62.5%)	58 (54.7%)	
Bilateral	Yes	33 (16.8%)	31 (18.1%)		33 (25.8%)	31 (27.%)		1 (12.5%)	39 (28.3%)	
STH fracture	No	140 (81.9%)	164 (83.2%)		95 (74.2%)	83 (72.8%)		7 (87.5%)	76 (71.7%)	
Total N⁰ of STH fractures (0 – 2)		0 (0-2)	(0-2)		1 (0-2)	1 (0-2)		**0.5 (0-2)**	**1 (0-2)**	**< 0.05**
Isolated		30 (15.2%)	28 (16.4%)		30 (23.4%)	28 (24.6%)		1 (12.5%)	27 (25.5%)	
GHH fracture(s)		167 (84.8%)	143 (83.6%)		98 (76.6%)	86 (75.4%)		7 (87.5%)	79 (74.5%)	
Unilateral	Yes	**43 (21.8%)**	**57 (33.3%)**	**< 0.05**	**43 (33.6%)**	**57 (50.0%)**	**< 0.05**	2 (25.0%	55 (51.9%)	
GHH fracture	No	**154 (78.2%)**	**114 (66.7%)**		**85 (66.4%)**	**57 (50.0%)**		6 (75.0%)	51 (48.1%)	
Bilateral	Yes	20 (10.2%)	13 (7.6%)		20 (15.6%)	13 (11.4%)		0 (0%)	13 (12.3%)	
GHH fracture	No	177 (89.8%)	158 (92.4%)		108 (84.4%)	101 (88.6%)		8 (100%)	93 (87.7%)	
Total N⁰ of GHH fractures (0 – 2)		(0-2)	(0-2)		0 (0-2)	1 (0-2)		0 (0-1)	1 (0-2)	
Total N⁰ of TyHy fractures (0 – 4)		1 (0-4)	1 (0-4)		1 (0-4)	2 (0-4)		**0 (0-2)**	**2 (0-4)**	**< 0.05**
Simultaneous STH and GHH fractures	Yes	33 (16.8%)	42 (24.6%)		33 (25.8%)	42 (36.8%)		1 (12.5%)	41 (38.7%)	
	No	164 (83.2%)	129 (75.4%)		95 (74.2%)	72 (63.2%)		7 (87.5%)	65 (61.3%)	
Contralateral Thyrohyoid fracture								Yes: 0 (0%)	11 (10.4%)	
								No: 8 (100%)	95 (89.6%)	
Cervical spine fracture	Yes	6 (3.0%)	10 (5.8%)		6 (4.7%)	10 (8.8%)		**5 (62.5%)**	**5 (4.7%)**	**< 0.001**
	No	191 (97.0%)	161 (94.2%)		122 (95.3%)	104 (91.2%)		**3 (37.5%)**	**101 (95.3%)**	

Note: *The categorical data is presented as frequency and ratio, and numerical as average ± standard deviation or median and range. For comparison of categorical data, the χ^2 or Fisher's Exact test were performed, while the Mann-Whitney U test was performed for numerical data. The missing p-values are > 0.05.*

Abbreviations: *STH – Superior thyroid cartilage horn; GHH – Greater hyoid bone horn; TyHy – Thyrohyoid.*

Table 4.2.3. *Characteristics of the lateral hanging cases with thyrohyoid or cervical spine fractures (Dataset IV-w).*

N = 106			***Left lateral N = 54 (50.9%)***	***Right lateral N = 52 (49.1%)***	***p-value***
Sex	Male	84 (79.2%)	45 (83.3%)	39 (75.0%)	
	Female	22 (20.8%)	9 (16.7%)	13 (25.0%)	
Age (years)		60.5 (16-94)	60.5 (18-94)	60.5 (16-87)	
Body weight (kg)		70.5 (40-112)	72.5 (49-112)	70.0 (40-103)	
Body height (cm)		176.0 (152-195)	178 (153-195)	174.5 (152-195)	
THYROHYOID AND CERVICAL SPINE FRACTURE PATTERNS					
Thyrohyoid fractures present	Yes	105 (99.1%)	53 (98.1%)	52 (100%)	
	No	1 (0.9%)	1 (1.9%)	0 (0%)	
STH fracture present	Yes	78 (73.6%)	42 (77.8%)	37 (69.2%)	
	No	28 (26.4%)	12 (22.2%)	16 (30.8%)	
GHH fracture present	Yes	68 (64.2%)	35 (64.8%)	33 (63.5%)	
	No	38 (35.8%)	19 (35.2%)	19 (36.5%)	
Left GHH fracture	Yes	41 (38.7%)	24 (44.4%)	17 (32.7%)	
	No	65 (61.3%)	30 (55.6%)	35 (67.3%)	
Right GHH fracture	Yes	40 (37.7%)	19 (35.2%)	21 (40.4%)	
	No	66 (62.3%)	35 (64.8%)	31 (59.6%)	
Left STH fracture	Yes	52 (49.1%)	27 (50.0%)	25 (48.1%)	
	No	54 (50.9%)	27 (50.0%)	27 (51.9%)	
Right STH fracture	Yes	56 (52.8%)	31 (57.4%)	23 (42.6%)	
	No	50 (47.2%)	25 (48.1%)	27 (51.9%)	
Isolated GHH fracture	Yes	27 (25.5%)	11 (20.4%)	16 (30.8%)	> 0.05
	No	79 (74.5%)	43 (79.6%)	36 (69.2%)	
Isolated STH fracture	Yes	37 (34.9%)	18 (33.3%)	19 (36.5%)	
	No	69 (65.1%)	37 (66.7%)	33 (63.5%)	
Simultaneous STH and GHH fracture	Yes	41 (38.7%)	24 (44.4%)	17 (32.7%)	
	No	65 (61.3%)	30 (55.6%)	35 (67.3%)	
Unilateral GHH fracture	Yes	55 (55.9%)	27 (50.0%)	28 (53.8%)	
	No	51 (48.1%)	27 (50.0%)	24 (46.2%)	
Unilateral STH fracture	Yes	48 (45.3%)	26 (48.1%)	22 (42.3%)	
	No	58 (54.7%)	28 (51.9%)	30 (57.7%)	
Bilateral GHH fracture	Yes	13 (12.3%)	8 (14.8%)	5 (9.6%)	
	No	93 (87.7%)	46 (85.2%)	47 (90.4%)	
Bilateral STH fracture	Yes	30 (28.3%)	16 (29.6%)	14 (26.9%)	
	No	76 (71.7%)	38 (70.4%)	38 (73.1%)	
Ipsilateral GHH fracture	Yes	32 (30.2%)	16 (29.6%)	16 (30.8%)	
	No	74 (69.8%)	38 (70.4%)	36 (69.2%)	
Contralateral STH fracture	Yes	26 (24.5%)	15 (27.8%)	11 (21.2%)	
	No	80 (75.5%)	39 (72.2%)	41 (78.8%)	
Contralateral thyrohyoid fractures	Yes	11 (10.4%)	7 (13.0%)	4 (7.7%)	
	No	95 (89.6%)	47 (87.0%)	48 (92.3%)	
Cervical spine fracture	Yes	5 (4.7%)	3 (5.6%)	2 (3.8%)	
	No	101 (95.3%)	51 (94.4%)	50 (96.2%)	

Note: *The categorical data is presented as frequency and ratio, and numerical as average ± standard deviation or median and range. For comparison of categorical data, the χ^2 test or Fisher's exact test were performed, while the Mann-Whitney U test was performed for numerical data. All the p-values are > 0.05.* ***Abbreviations:*** *STH – Superior thyroid cartilage horn; GHH – Greater hyoid bone horn.*

4.2.2. Machine learning algorithms

In the second part of the study, due to the smaller sample size, the machine learning models were developed only for Datasets I-w and II-w, while for Datasets III-w and IV-w only 'conventional' statistical methods were used for analysis and these are already reported in the previous subsection of the results. The characteristics of the Datasets I-w and II-w with regards to the coded variables and test/training group division are shown in Supplement B. The SMOTE algorithm was used in both datasets (I-w and II-w).

In Dataset I-w, the initial frequency proportion between the group of cases of atypical hangings and the group of cases of typical hangings – 1:1.2 (46.5% atypical hangings to 53.5% typical hangings) was processed to form the sample of 385 cases, with the ratio of 1:1.05. In Dataset II-w, the initial frequency proportion between the group of cases of atypical hangings and the group of cases of typical hangings – 1:1.12 (47.1% atypical hangings to 52.9% typical hangings) was processed to form the sample of 250 cases, with the ratio of 1:1.05. In the following text, the results on machine learning algorithms are reported in the previously established order.

4.2.2.1. Genetic Algorithm-optimized Artificial Neural Networks

Performance characteristics analyses of the GA-optimized ANNs, for Datasets I-w and II-w are reported in Table 4.2.4 and Table 4.2.5, respectively.

Table 4.2.4. *Performance characteristics of ANN developed in MATLAB for knot position classification in the entire sample (Dataset I-w).*

GA-optimized ANN									
DATASET I-w		***Accuracy (95% CI)***	***Sn***	***Sp***	***PPV***	***NPV***	***LR+***	***LR-***	***AUC (95% CI)***
Body weight & body height ***considered***	**Overall**	54.8% (49.7-59.9)	55.3%	54.3%	53.6%	56.0%	1.2	0.8	0.56 (0.50-0.61)
	Test	55.7% (46.1-64.9)	62.9%	47.2%	58.2%	52.1%	1.2	0.8	0.51 (0.40-0.62)
	Training	54.4% (48.3-60.5)	51.6%	56.9%	51.2%	57.3%	1.2	0.8	0.57 (0.50-0.64)
Body weight & body height ***NOT considered***	**Overall**	56.6% (51.5-61.6)	66.0%	47.7%	54.6%	59.5%	1.3	0.7	0.58 (0.53-0.64)
	Test	56.5% (47.0-65.7)	69.4%	41.5%	58.1%	53.7%	1.2	0.7	0.52 (0.41-0.63)
	Training	56.7% (50.5-62.7)	64.3%	50.0%	52.9%	61.5%	1.3	0.7	0.60 (0.54-0.67)

Note: *The atypical knot position was considered as the positive state in confusion matrix performance calculations. There was no statistically significant difference in ROC curve analysis of the predicted outcome probabilities between the training and the test group ($p > 0.05$).* ***Abbreviations:*** *GA – Genetic algorithm; Sn – sensitivity; Sp – specificity; PPV – positive predictive value, NPV – negative predictive value, LR+ – positive likelihood ratio, negative LR- – negative likelihood ratio, AUC – Area under the curve, CI – Confidence Interval.*

The GA-optimized ANN for Dataset I-w that considered subjects' body weight and body height selected following variables (n = 13) to be included in the model: subject's sex and age, body weight and body height, presence of unilateral STH fracture, presence of bilateral STH fracture, presence of isolated STH fracture, total number of STH fractures, presence of unilateral GHH fracture, presence of bilateral GHH fractures, presence of isolated GHH fracture, total number of GHH fractures, presence of simultaneous STH and GHH fracture.

The GA-optimized ANN for Dataset I-w that did not consider subjects' body weight and body height selected following variables (n = 5) to be included in the model: subject's sex, presence of unilateral STH fracture, presence of isolated STH fracture, the total number of thyrohyoid fractures, and the presence of cervical spine fracture.

Table 4.2.5. *Performance characteristics of ANN developed in MATLAB for knot position classification in the hangings with fractures (Dataset II-w).*

GA-optimized ANNs DATASET II-w		***Accuracy (95% CI)***	***Sn***	***Sp***	***PPV***	***NPV***	***LR+***	***LR-***	***AUC (95% CI)***
Body weight & body height ***considered***	***Overall***	62.4% (56.1 – 68.4)	75.4%	50.0%	59.0%	68.1%	1.5	0.5	0.62 (0.55-0.69)
	Test	68.0% (56.2 – 78.3)	81.1%	55.3%	63.8%	75.0%	1.8	0.3	0.67 (0.54-0.79)
	Training	60.0% (52.3 – 67.3)	72.9%	47.8%	56.9%	65.2%	1.4	0.6	0.61 (0.53-0.70)
Body weight & body height ***NOT considered***	***Overall***	62.4% (56.1 – 68.4)	69.7%	55.5%	59.9%	65.7%	1.6	0.5	0.64 (0.57-0.71)
	Test	68.0% (56.2 – 78.3)	73.0%	63.2%	65.9%	70.6%	2.0	0.4	0.66 (0.53-0.78)
	Training	60.0% (52.3 – 67.3)	68.2%	52.2%	57.4%	63.5%	1.4	0.6	0.63 (0.54-0.71)

Note: *The atypical knot position was considered as the positive state in confusion matrix performance calculations. There was no statistically significant difference in ROC curve analysis of the predicted outcome probabilities between the training and the test group ($p > 0.05$).* ***Abbreviations:*** *GA – Genetic algorithm; Sn – sensitivity; Sp – specificity; PPV – positive predictive value, NPV – negative predictive value, LR+ – positive likelihood ratio, negative LR- – negative likelihood ratio, AUC – Area under the curve, CI – Confidence Interval.*

The GA-optimized ANN for Dataset II-w that considered subjects' body weight and body height selected following variables (n = 6) to be included in the model: subject's age and body weight, presence of isolated STH fracture, total number of STH fractures, presence of isolated GHH fracture, and the total number of thyrohyoid fractures.

The GA-optimized ANN for Dataset II-w that did not consider subjects' body weight and body height selected following variables (n = 7) to be included in the model: subject's sex and age, presence of isolated STH fracture, presence of bilateral GHH fracture, total number of thyrohyoid fractures, presence of simultaneous STH and GHH fractures, and presence of the cervical spine fracture.

4.2.2.2. MLP-ANN, Decision Tree, k-NN, and Naïve Bayes algorithms

Table 4.2.6 and Table 4.2.7 provide information on the performance characteristics of the machine learning algorithms developed in SPSS software, for Datasets I-w and II-w, respectively.

Figure 4.2.4 shows ROC curve analysis of each reported ML algorithm, separately for both datasets (I-w and II-w).

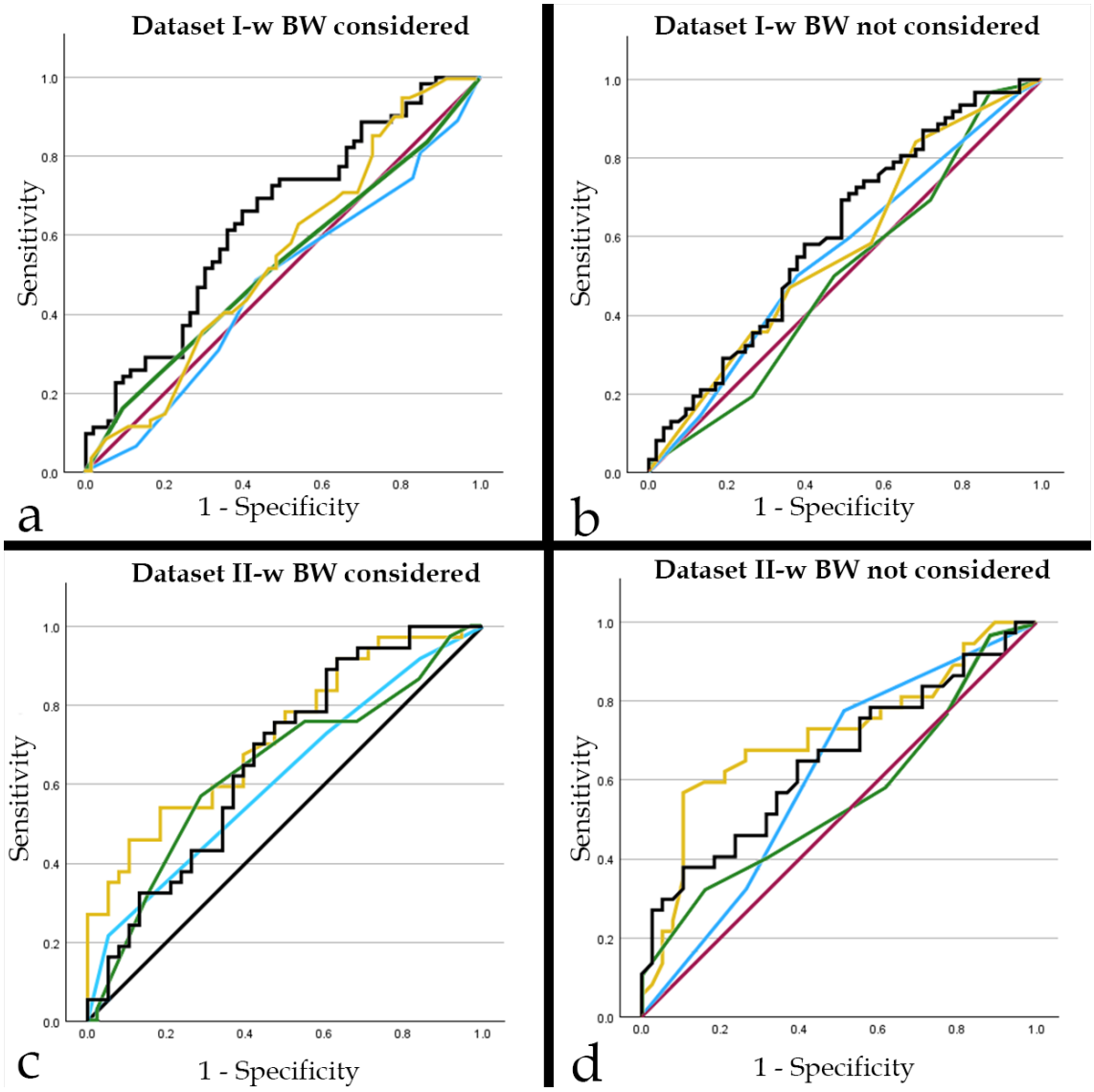

Figure 4.2.4. *The Receiver Operating Characteristic (ROC) and Area under the curve (AUC) analysis of developed machine learning models in Test samples of analyzed sets – (**a** and **b**) Dataset I, and (**b** and **c**) Dataset II. The AUCs with 95% Confidence Intervals are listed in Tables 4.2.6 and 4.2.7.* ***Legend:*** *black line (MLP-ANN), blue line (DT), green line (k-NN), yellow line (NB), red line (reference).*

Table 4.2.6. *The performance characteristics of the machine learning models developed in SPSS, for the knot in a noose position classification in Dataset I-w.*

MLAs – Dataset I – w			Accuracy (95% CI)	Sn	Sp	PPV	NPV	LR+	LR-	AUC (95% CI)
MLP-ANN	**Overall**	**w**	57.1% (52.0-62.1)	38.8%	74.6%	59.3%	56.1%	1.5	0.8	0.60 (0.54-0.66)
		w/o	58.7% (53.6-63.7)	50.0%	67.0%	59.1%	58.4%	1.5	0.7	0.62 (0.56-0.67)
	Test	**w**	57.4% (47.8-66.6)	46.8%	69.8%	64.4%	52.9%	1.5	0.8	0.64 (0.54-0.74)
		w/o	57.4% (47.8-66.6)	54.8%	60.4%	61.8%	53.3%	1.4	0.7	0.61 (0.50-0.71)
	Training	**w**	57.0 (50.9-63.2)	34.9%	76.4%	56.4%	57.3%	1.5	0.9	0.58 (0.51-0.65)
		w/o	59.3% (53.1-65.2)	47.6%	69.4%	57.7%	60.2%	1.6	0.7	0.62 (0.55-0.69)
Decision Tree	**Overall**	**w**	61.6% (56.5-66.4)	51.6%	71.1%	63.0%	60.6%	1.8	0.7	0.64 (0.59-0.70)
		w/o	59.5% (54.4-64.4)	52.7%	66.0%	59.6%	59.4%	1.5	0.7	0.62 (0.56-0.67)
	Test	**w**	52.2% (42.7-61.6)	48.4%	56.6%	56.6%	48.4%	1.1	0.9	0.47 (0.36-0.58)*
		w/o	55.7% (46.1-64-9)	50.0%	62.3%	60.8%	51.6%	1.3	0.8	0.56 (0.45-0.66)
	Training	**w**	65.6% (59.6-71.2)	53.2%	76.4%	66.3%	65.1%	2.3	0.6	0.72 (0.66-0.78)*
		w/o	61.1% (55.0-67.0)	54.0%	67.4%	59.1%	62.6%	1.6	0.7	0.64 (0.58-0.71)
k-NN	**Overall**	**w**	51.4% (46.3-56.5)	51.6%	51.3%	50.3%	52.6%	1.1	0.9	0.52 (0.47-0.58)
		w/o	53.5% (48.4-58.6)	48.4%	58.4%	52.6%	54.2%	1.2	0.9	0.52 (0.46-0.57)
	Test	**w**	52.2% (42.7-61.6)	51.6%	52.8%	56.1%	48.3%	1.1	0.9	0.52 (0.42-0.63)
		w/o	51.3% (41.8-60.7)	50.0%	52.8%	55.4%	47.5%	1.1	0.9	0.50 (0.39-0.61)
	Training	**w**	51.1% (45.0-57.2)	51.6%	50.7%	47.8%	54.5%	1.0	0.9	0.52 (0.45-0.59)
		w/o	54.4% (48.3-60.5)	47.6%	60.4%	51.3%	56.9%	1.2	0.9	0.52 (0.45-0.59)
Naïve Bayes	**Overall**	**w**	57.4% (52.3-62.4)	37.2%	76.6%	60.3%	56.1%	1.6	0.8	0.59 (0.53-0.64)
		w/o	57.7% (52.6-62.7)	54.3%	60.9%	57.0%	58.3%	1.4	0.7	0.60 (0.54-0.65)
	Test	**w**	54.8% (45.7-63.8)	31.7%	76.6%	55.9%	53.3%	1.3	0.9	0.57 (0.46-0.67)
		w/o	55.2% (45.2-65.0)	52.1%	57.9%	51.0%	58.9%	1.2	0.8	0.54 (0.43-0.65)
	Training	**w**	58.6% (52.4-64.7)	39.8%	76.7%	62.2%	57.0%	1.7	0.8	0.59 (0.52-0.66)
		w/o	58.6% (52.6-64.4)	55.0%	6.1%	59.2%	58.0%	1.5	0.7	0.61 (0.55-0.68)
Logistic Regression	**Overall**		57.3% (52.1-62.4)	33.3%	78.2%	57.0%	57.5%	1.5	0.8	0.57 (0.51-0.63)

Notes: *The atypical knot position was considered as a positive state in confusion matrix performance calculations. There was no statistically significant difference in Area under the ROC curve analysis between training and test samples ($p > 0.05$), except in a Decision Tree model that considered body weight (forced input variable) – * – no DT model that considered body weight met this criterion.* ***Abbreviations:*** *MLP–ANN – Multilayer Perceptron – Artificial Neural Network, k-NN – k Nearest Neighbors, Logistic Regression – Multivariable Logistic Regression analysis, w – the model considered body weight and body height, w/o – the model did not consider the body weight and body height, Sn – sensitivity, Sp – specificity, PPV – positive predictive value, NPV – negative predictive value, LR+ – positive likelihood ratio, negative LR- – negative likelihood ratio, AUC – Area under the curve, CI – Confidence Interval.*

Table 4.2.7. *The performance characteristics of the machine learning models developed in SPSS, for the knot in a noose position classification in Dataset II-w.*

MLAs – Dataset II – w			Accuracy (95% CI)	Sn	Sp	PPV	NPV	LR+	LR-	AUC (95% CI)
MLP-ANN	**Overall**	**w**	62.8% (56.5 – 68.8)	68.0%	57.8%	60.6%	65.5%	1.6	0.6	0.69 (0.63-0.76)
		w/o	60.0% (53.6 – 66.1)	59.0%	60.9%	59.0%	60.9%	1.5	0.7	0.63 (0.56-0.70)
	Test	**w**	64.0% (52.1 – 74.8)	70.3%	57.9%	61.9%	66.7%	1.7	0.5	0.66 (0.54-0.79)
		w/o	60.0% (52.3 – 67.3)	60.0%	60.0%	0.6	0.6	1.5	0.7	0.65 (0.52-0.77)
	Training	**w**	62.3% (54.7 – 69.5)	67.1%	57.8%	60.0%	65.0%	1.6	0.6	0.71 (0.63-0.79)
		w/o	60.0% (43.3 – 75.1)	56.8%	63.2%	60.0%	60.0%	1.5	0.7	0.62 (0.54-0.71)
Decision Tree	**Overall**	**w**	60.8% (54.4 – 66.9)	70.5%	51.6%	58.1%	64.7%	1.5	0.6	0.65 (0.58-0.72)
		w/o	59.6% (53.2 – 65.7)	77.0%	43.0%	56.3%	66.3%	1.4	0.5	0.6 (0.53-0.67)
	Test	**w**	56.0% (44.1 – 67.5)	73.0%	39.5%	54.0%	60.0%	1.2	0.7	0.61 (0.49-0.74)
		w/o	62.7% (50.7 – 73.6)	78.4%	47.4%	59.2%	69.2%	1.5	0.5	0.61 (0.48-0.74)
	Training	**w**	62.9% (55.2 – 70.0)	69.4%	56.7%	60.2%	66.2%	1.6	0.5	0.67 (0.59-0.75)
		w/o	58.3% (50.6 – 65.7)	76.5%	41.1%	55.1%	64.9%	1.3	0.6	0.59 (0.51-0.68)
k-NN	**Overall**	**w**	61.6% (55.3 – 67.7)	68.0%	55.5%	59.3%	64.5%	1.5	0.6	0.58 (0.50-0.65)
		w/o	55.2% (48.8 – 61.5)	41.8%	68.0%	55.4%	55.1%	1.3	0.9	0.541 (0.469-0.613)
	Test	**w**	60.0% (48.0 – 71.1)	75.7%	44.7%	57.1%	65.4%	1.4	0.5	0.63 (0.51-0.76)
		w/o	54.7% (42.7 – 66.2)	40.5%	68.4%	55.6%	54.2%	1.3	0.9	0.55 (0.42-0.69)
	Training	**w**	62.3% (54.7 – 69.5)	64.7%	60.0%	60.4%	64.3%	1.6	0.6	0.56 (0.47-0.65)
		w/o	55.4% (47.7 – 62.9)	42.4%	67.8%	55.4%	55.5%	1.3	0.9	0.53 (0.45-0.62)
Naïve Bayes	**Overall**	**w**	61.2% (54.9 – 67.3)	62.3%	60.2%	59.8%	62.6%	1.6	0.6	0.67 (0.603-0.736)
		w/o	63.2% (56.9 – 69.2)	57.4%	68.8%	63.6%	62.9%	1.8	0.6	0.65 (0.582-0.717)
	Test	**w**	59.1% (46.3 – 71.0)	59.4%	58.8%	57.6%	60.6%	1.4	0.7	0.72 (0.61-0.84)
		w/o	62.0% (50.4 – 72.7)	60.9%	63.6%	70.0%	53.8%	1.7	0.6	0.71 (0.59-0.83)
	Training	**w**	62.0% (54.5 – 69.0)	63.3%	60.6%	60.6%	63.3%	1.6	0.6	0.65 (0.56-0.73)
		w/o	63.7% (56.1 – 70.9)	55.3%	70.5%	60.0%	66.3%	1.9	0.6	0.62 (0.54-0.70)
Logistic Regression	**Overall**		58.7% (52.2 – 64.9)	50.0%	66.4%	57.0%	59.9%	1.5	0.8	0.60 (0.53-0.67)

Notes: *The atypical knot position was considered as a positive state in confusion matrix performance calculations. There was no statistically significant difference in Area under the ROC curve analysis between training and test samples ($p > 0.05$).* ***Abbreviations:*** *MLP–ANN – Multilayer Perceptron – Artificial Neural Network, k-NN – k Nearest Neighbors, Logistic Regression – Multivariable Logistic Regression analysis, w – the model considered body weight and body height, w/o – the model did not consider the body weight and body height, Sn – sensitivity, Sp – specificity, PPV – positive predictive value, NPV – negative predictive value, LR+ – positive likelihood ratio, negative LR- – negative likelihood ratio, AUC – Area under the curve, CI – Confidence Interval.*

4.2.2.3. GA-optimized ANN and MLP-ANN ROC analysis comparison

The comparison analysis between the ROC curves of the GA-optimized ANN models and the ROC curves of the MLP-ANN models for Dataset I-w and Dataset II-w are shown in Figure 4.2.5.

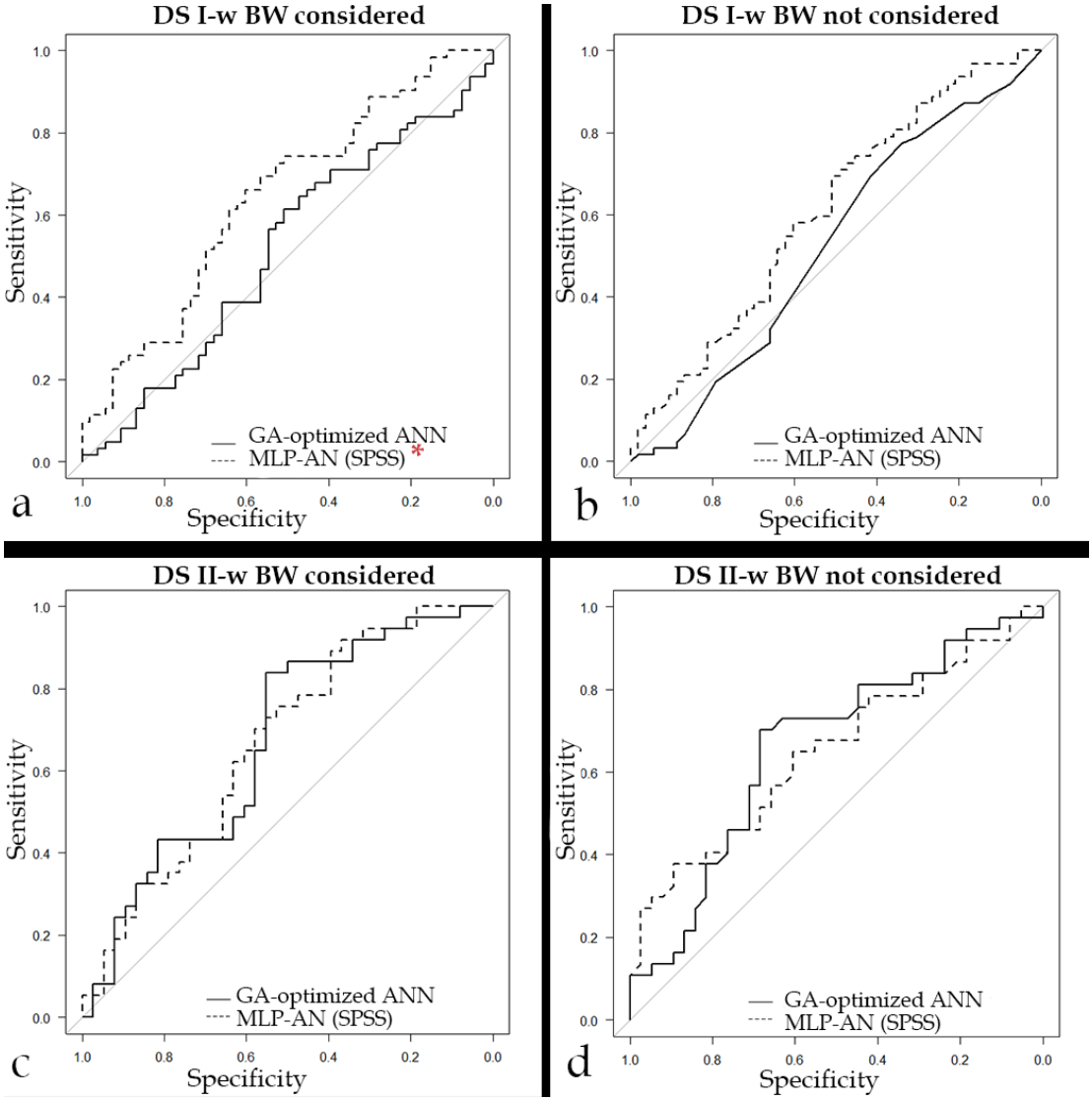

Figure 4.2.5. *Comparison of ROC curves of the two Artificial Neural Network models developed for the knot position classification (atypical vs. typical hangings) in Dataset I-w, for models that (**a**) did consider and (**b**) did not consider subjects' body weight and height, and in Dataset II-w, for models that (**c**) did consider and (**d**) did not consider subjects' body weight and height: The GA-optimized ANN developed in MATLAB and the MLP-ANN developed in SPSS.*

* *There was a statistically significant difference between the outcome predicted probabilities on ROC curve analysis of the models that considered subjects' body weight and height - one developed in MATLAB (GA-ANN) and the other (MLP-ANN) in SPSS ($Z = -2.4978$, $p < 0.05$).*

There was no statistically significant difference between the ROC curves between the remaining models developed in MATLAB and SPSS:

Dataset I-w with subjects' body weight and height not considered, $Z = 1.4154$, $p > 0.05$;

Dataset II-w with subjects' body weight and height considered, $Z = 0.059016$, $p > 0.05$;

Dataset II-w with subjects' body weight and height not considered, $Z = 0.23823$, $p > 0.05$;

4.2.2.4. *Comparison of analogous machine learning models: Models with & models without consideration of subjects' body weight & height*

There was no significant difference in the ROC curves analyses in test samples between the analogous ML models that did consider and did not consider subjects' body weight and height in Datasets I-w and II-w. This holds true for GA-optimized ANNs (Figure 4.2.6), as well as for MLP-ANNs, DTs, k-NN, and NB (Figures 4.2.7. and 4.2.8, for Dataset I-w and Dataset II-w, respectively).

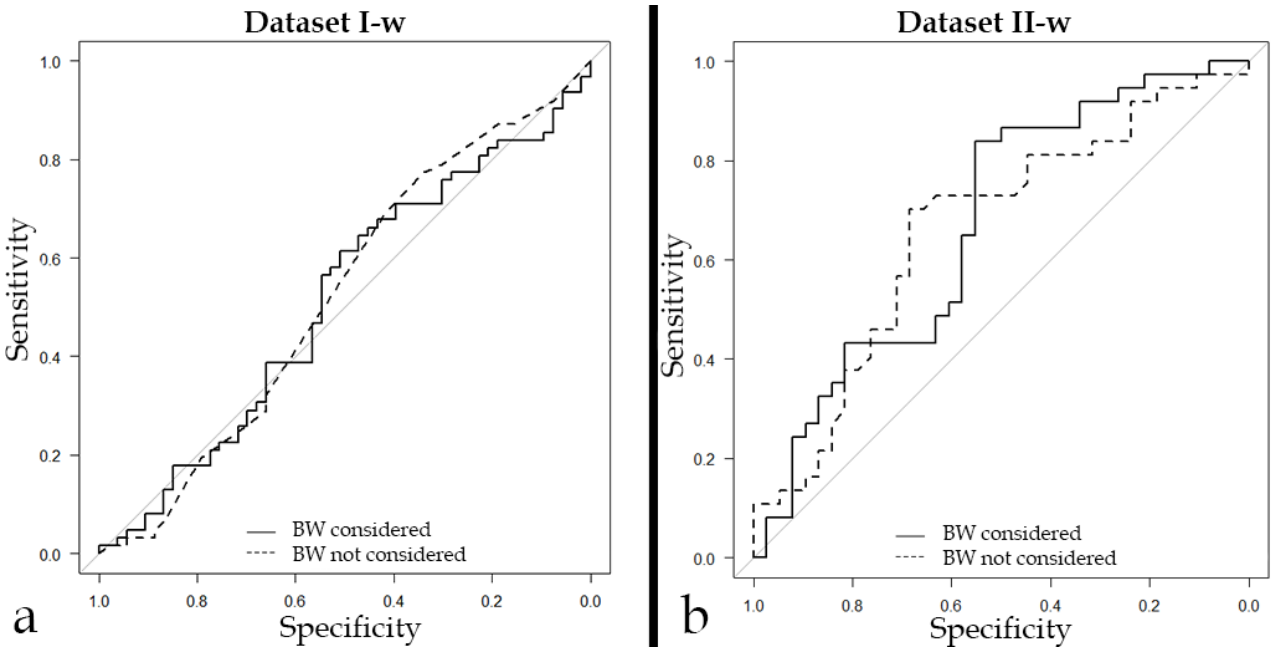

Figure 4.2.6. *The comparison of the ROC curves of two analogous GA-ANN models developed in MATLAB, one considering subjects' body weight and body height, and one that does not consider them, in (**a**) Dataset I-w, and in (**b**) Dataset II-w.*

There was no statistically significant difference in the ROC curve analysis between the two analogous models. (Dataset I-w: Z = -0.17407, p > 0.05; Dataset II-w: Z = 0.059016, p > 0.05).

4.2.2.5. *Machine learning models' variable importance and settings*

Table 4.2.8. lists up to the top five ranked input variables for each of these algorithms, according to the variable's independent importance.

The hyperparameters settings for all used algorithms developed in SPSS (MLP-ANN, DT, k-NN, and NB), in both datasets (I-w and II-w, respectively) are shown in Table 4.2.9.

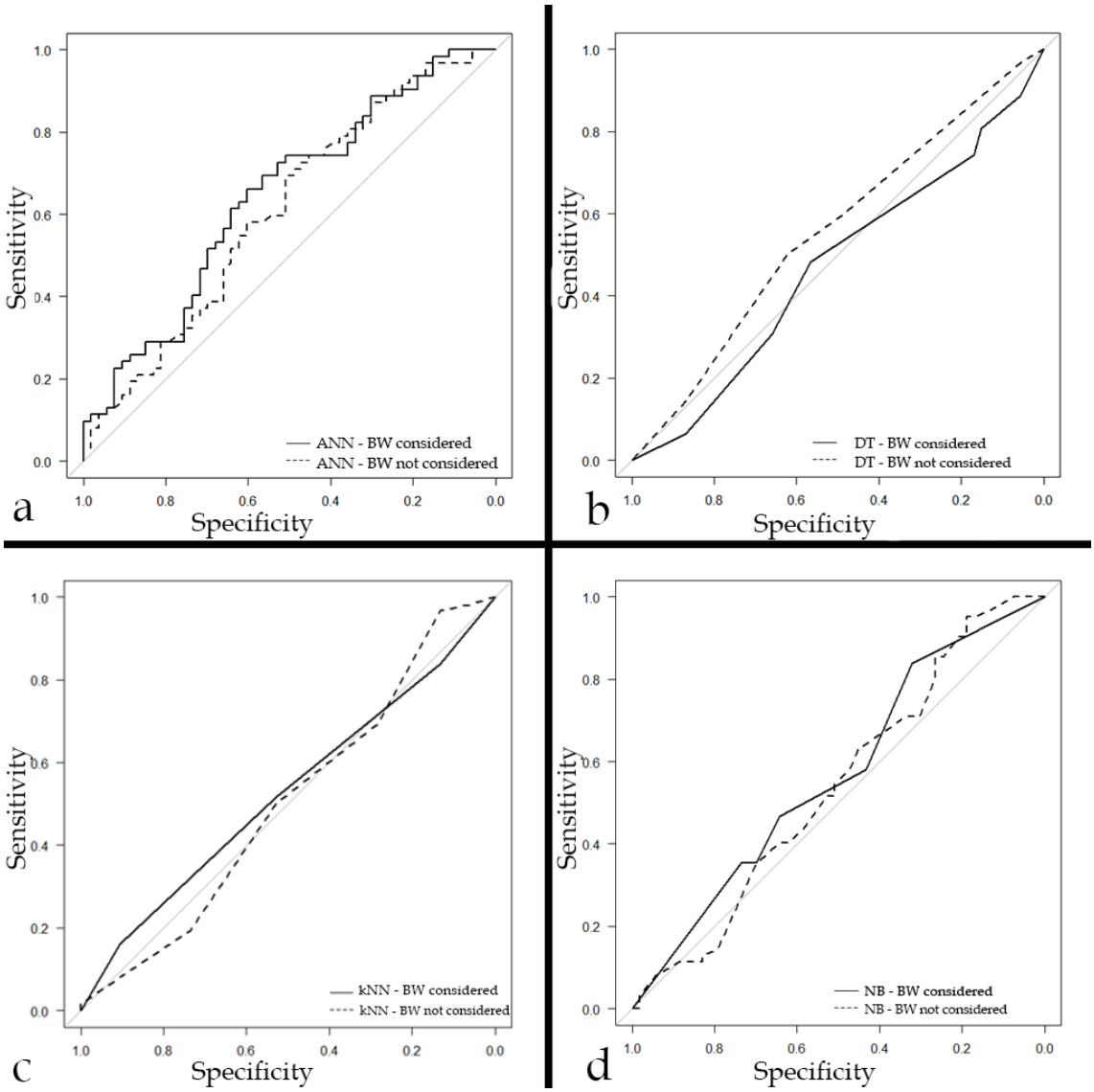

Figure 4.2.7. *The comparison of the ROC curves of two analogous machine learning models developed in SPSS, one considering the subjects' body weight and body height, and one that does not consider them, in Dataset I-w: MLP-ANN (**a**), Decision Tree (**b**), k-Nearest Neighbors (**c**), and Naïve Bayes (**d**).*

There was no statistically significant difference in the ROC curve analysis between any of the analogous models:

MLP-ANN, Z = 0.66786, p > 0.05;
Decision Tree, Z = -1.4334, p > 0.05;
k-Nearest Neighbors, Z = 0.48151, p > 0.05;
Naïve Bayes, Z = 0.32563, p > 0.05;

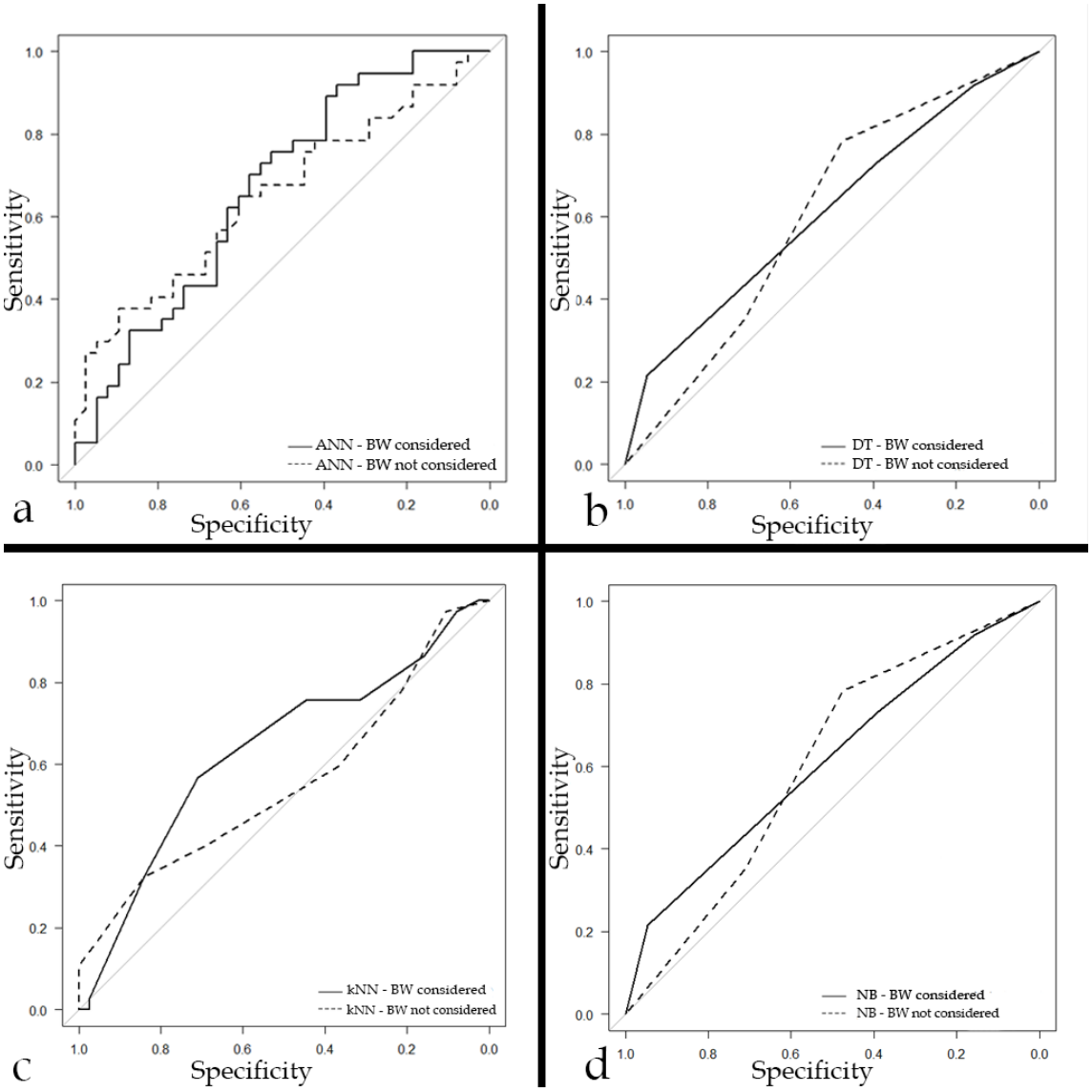

Figure 4.2.8. *The comparison of the ROC curves of two analogous machine learning models developed in SPSS, one considering the subjects' body weight and body height, and one that does not consider them, in Dataset II-w: MLP-ANN (**a**), Decision Tree (**b**), k-Nearest Neighbors (**c**), and Naïve Bayes (**d**).*

There was no statistically significant difference in the ROC curve analysis between any of the analogous models:

MLP-ANN, Z = 0.28063, p > 0.05;
Decision Tree, Z = 0.064592, p > 0.05;
k-Nearest Neighbors, Z = 0.90233, p > 0.05;
Naïve Bayes, Z = 0.2654, p > 0.05;

Table 4.2.8. *The top five ranked input variables based on their relative importance for utilized machine learning models.*

	DATASET I-w considering BW & BH				*DATASET I-w not considering BW & BH*				*DATASET II-w considering BW & BH*				*DATASET II-w not considering BW & BH*			
	MLP	**DT**	**k-NN**	**NB**	**MLP**	**DT***	**k-NN**	**NB**	**MLP**	**DT**	**k-NN**	**NB**	**MLP**	**DT**	**k-NN**	**NB**
1st	BH	BW	Spine	BW	Age	UL-Hy	Age	Tot.Fr. N^0	BH	BW	UL-Hy	Tot.Fr. N^0	Age	Age	Hy N^0	UL-Hy
2nd	Age	UL-Hy	sTy&Hy	BH	Tot.Fr. N^0	Age	Sex	iHy	BW	Age	BL-Hy	iHy	Spine	UL-Ty	BL-Hy	iTy
3rd	Tot.Fr. N^0	Hy N^0	Hy N^0	Tot.Fr. N^0	BL-Hy	sTy&Hy	Spine	BL-Hy	Hy N^0	Tot.Fr. N^0	Hy N^0	BL-Hy	sTy&Hy	iTy	UL-Hy	sTy&Hy
4th	BW	Age	iHy	UL-Ty	Hy N^0	/	sTy&Hy	Sex	Tot.Fr. N^0	BH	iHy	UL-Ty	Hy N^0	sTy&Hy	iHy	BL-Hy
5th	iTy	sTy&Hy	BL-Hy	UL-Hy	BL-Ty	/	Hy N^0	UL-Ty	Age	Ty N^0	Tot.Fr. N^0	sTy&Hy	UL-Hy	Hy N^0	Tot.Fr. N^0	Spine

Note: Some models included less than 5 variables, and these empty fields in table are labeled by "/" sign.

Abbreviations: *BW – Body Weight, BH – Body Height, BL-Hy – bilateral greater hyoid horn fractures, BL-Ty – bilateral superior thyroid horn fractures, CL-Ty - superior thyroid cartilage horn contralateral to the knot position, Hy N^0 – Total number of greater hyoid horn fractures, iTy – isolated superior thyroid horn fracture(s), IL-Hy - greater hyoid bone horn ipsilateral to the knot position, IL-Ty – superior thyroid cartilage horn ipsilateral to the knot position, L-Hy – left greater hyoid bone horn, L-Ty – left superior thyroid cartilage horn, R-Hy – right greater hyoid bone horn, sTy&Hy – simultaneous superior thyroid horn and greater hyoid horn fractures, Spine – Cervical spine fracture, Tot.Fr.N^0 – Total number of thyrohyoid fractures, Ty N^0 – Total number of superior thyroid horn fractures, UL-Hy – unilateral greater hyoid horn fracture, UL-Ty – unilateral superior thyroid horn fracture.*

**Selecting Exhaustive CHAID growing method for DT model does not provide information on variable importance ranking.*

Table 4.2.9. *Hyperparameter settings in the reported machine learning algorithms (developed in SPSS).*

		Nº of hidden layers	Nº of neurons in a hidden layer	Activation function	Training type	Training algorithm	Initial learning rate	Momentum
MLP ANN	**DATASET I-w** *BW considered*	1	5	Hyperbolic tangent	Batch	Gradient descent	0.4	0.9
	DATASET I-w *BW not consd.*	1	10	Hyperbolic tangent	Batch	Gradient descent	0.4	0.9
	DATASET II-w *BW considered*	1	9	Hyperbolic tangent	Online	Gradient descent	0.5	0.7
	DATASET II-w *BW not consd.*	1	10	Hyperbolic tangent	Online	Gradient descent	0.5	0.7

		Growing method	Tree depth	Min. samples of parent node	Min. samples of child node	Nº of nodes	Nº of terminal nodes
Decision Tree	**DATASET I-w** *BW considered*	CRT	4	50	10	13	7
	DATASET I-w *BW not consd.*	Exhaustive CHAID	3	70	10	9	5
	DATASET II-w *BW considered*	CRT	3	25	10	7	4
	DATASET II-w *BW not consd.*	CRT	2	25	10	5	3

		Nº of Neighbors to consider	Distance metrics	Search Algorithm (Feature selection - Stopping criterion)
k-NN	**DATASET I-w** *BW considered*	3	Euclidean	Select all features
	DATASET I-w *BW not consd.*	13	Euclidean	Select all features
	DATASET II-w *BW considered*	13	Euclidean	5 features selected
	DATASET II-w *BW not consd.*	10	Euclidean	Select all features

		Maximum memory (Mb)	Nº of bins for scale predictors	Nº of selected predictors
Naïve Bayes	**DATASET I-w** *BW considered*	1024	5	1
	DATASET I-w *BW not consd.*	1024	5	5
	DATASET II-w *BW considered*	1024	10	10
	DATASET II-w *BW not consd.*	1024	10	13

Abbreviations: *MLP-ANN - Multilayer Perceptron – Artificial neural network, k-NN – k Nearest Neighbors.*

4.3. PART III of the study: Analysis of the sternocleidomastoid muscles' origin hemorrhage in knot position-related fracture patterns assessment

The characteristics of included cases regarding the subjects' sex, age, body weight and body height, thyrohyoid and cervical spine fracture occurrence, ligature knot position, as well as the presence of the hemorrhages of the sternocleidomastoid muscle origins at the clavicles are shown in Table 4.3.1.

4.3.1. Descriptive, basic inferential, and logistic regression analysis of the thyrohyoid and cervical spine fracture patterns

Following the reporting of the previous study parts, the distribution of the analyzed variables (thyrohyoid and cervical spine fractures), including the presence of sternocleidomastoid muscle origin hemorrhages, in terms of the coded variables for study subgroups (Datasets I-m – III-m) is shown in Table 4.3.2, and Table 4.3.3. (Dataset IV-m), and the additional basic and logistic regression analyses are reported here.

4.3.1.1. The entire sample (hangings with and without fractures or sternocleidomastoid muscle hemorrhages) – Dataset I-m

In the Dataset I-m, comprising 126 hangings with and without thyrohyoid complex and cervical spine fractures, in overall, the thyrohyoid complex fractures were significantly more frequent in subjects older than 40 years of age than in the younger subjects (N = 68, 73.9% subjects older than 40 years of age vs. N = 17, 50.0% of younger subjects, $\chi^2 = 6.47$, df = 1, $p < 0.05$). Further analysis revealed that the significant difference in fracture occurrence between these two age groups existed only for the greater hyoid horn fractures: GHH fractures were significantly more frequent in older than 40 years of age compared to younger individuals (N = 37, 40.2% subjects older than 40 years of age vs. N = 4, 11.8% of younger subjects, $\chi^2 = 9.16$, df = 1, $p < 0.05$). Contrary, no significant difference was observed in the frequency of STH fractures (N = 51, 55.4% of subjects older than 40 years of age vs. N = 16, 47.1% of younger subjects, $\chi^2 = 0.69$, df = 1, $p > 0.05$). There was no statistically significant difference in the frequency of SCM muscle hemorrhages between these two groups, too (N = 79, 85.9% subjects older than 40 years of age vs. N = 29, 85.3% of younger subjects, $\chi^2 = 0.01$, df = 1, $p > 0.05$). The overall occurrence of thyrohyoid fractures did not significantly differ between the two analyzed groups (typical vs. atypical hangings, $\chi^2 = 1.46$, df = 1, $p > 0.05$), the distribution of subjects older than 40 years of age was equal between these groups ($\chi^2 = 0.09$, df = 1, $p > 0.05$), and the frequency of SCM hemorrhage occurrence was similar ($\chi^2 = 0.19$, df = 1, $p > 0.05$).

On the ROC analysis, subjects' age and body weight were statistically significant predictors of thyrohyoid fracture occurrence, which is not true for subject's body height. Of these anthropometric variables, only the body weight was a statistically significant predictor of sternocleidomastoid muscle hemorrhage at the origin on the clavicles. The ROC curve analyses are shown in Figures 4.3.1 – 4.3.3. for subjects' age, body weight, and body height, regarding the analyzed fractures, respectively, while the predictive value of these variables for the occurrence of SCM hemorrhages is shown in Figure 4.3.4.

Table 4.3.1. *Basic subjects' and injury characteristics – the study sample of Dataset I-m.*

N = 126

Sex	Male	99 (78.6%)
	Female	27 (21.4%)
Age (years)		55.0 (17 – 94)
Body weight (kg)		70.0 (40 – 125)
Body height (cm)		176.0 (145 – 205)
THYROHYOID AND CERVICAL SPINE FRACTURES		
Thyrohyoid fractures present	Yes	85 (67.5%)
	No	41 (32.5%)
STH fracture present	Yes	67 (53.2%)
	No	59 (46.8%)
GHH fracture present	Yes	41 (32.5%)
	No	85 (67.5%)
Isolated STH fracture(s)	Yes	44 (34.9%)
	No	82 (65.1%)
Isolated GHH fracture(s)	Yes	18 (14.3%)
	No	108 (85.7%)
Simultaneous STH and GHH fractures	Yes	23 (18.3%)
	No	103 (81.7%)
Left GHH fracture	Yes	25 (19.8%)
	No	101 (80.2%)
Right GHH fracture	Yes	27 (21.4%)
	No	99 (78.6%)
Left STH fracture	Yes	37 (29.4%)
	No	89 (70.6%)
Right STH fracture	Yes	54 (42.9%)
	No	72 (57.1%)
Cervical Spine fracture	Yes	3 (2.4%)
	No	123 (97.6%)
STERNOCLEIDOMASTOID MUSCLE HEMORRHAGES		
SCM hemorrhage present	Yes	108 (85.7%)
	No	18 (14.3%)
Left SCM hemorrhage	Yes	78 (61.9%)
	No	48 (38.1%)
Right SCM hemorrhage	Yes	88 (69.8%)
	No	38 (30.2%)
KNOT POSITION		
Anterior		7 (5.6%)
Posterior		62 (49.2%)
Left lateral		33 (26.2%)
Right lateral		24 (19.0%)

Note: *The data is presented as frequency and ratio.*
Abbreviations: *STH – Superior thyroid cartilage horn; GHH – Greater hyoid bone horn; SCM – sternocleidomastoid muscle.*

Table 4.3.2. *The descriptives of the coded variables: thyrohyoid and cervical fractures and basic subject characteristics for Datasets I-m, II-m, and III-m.*

		DATASET I-m *THE ENTIRE SAMPLE OF STUDY PART III*			***DATASET II-m*** *HANGINGS WITH FRACTURES OR SCM HEMORRHAGES*			***DATASET III-m*** *ATYPICAL HANGINGS*		
		Knot Position			***Knot Position***			***Knot Position***		
		Typical *N = 62 (49.2%)*	***Atypical*** *N = 64 (50.8%)*	***p*-value**	***Typical*** *N = 59 (50.4%)*	***Atypical*** *N = 58 (49.6%)*	***p*-value**	***Anterior*** *N = 6 (10.3%)*	***Lateral*** *N = 52 (89.7%)*	***p*-value**
Sex	Male	49 (79.0%)	50 (78.1%)		46 (78.0%)	46 (79.3%)		5 (83.3%)	41 (78.8%)	
	Female	13 (21.%)	14 (21.9%)		13 (22.0%)	12 (20.7%)		1 (16.7%)	11 (21.2%)	
Age (years)		55.5 (20 – 90)	54.5 (17 – 94)		56.0 (20 – 90)	54.5 (24 – 94)		57.5 (31 – 91)	54.0 (23 – 94)	
Body weight (kg)		68 (41 -125)	72 (40 – 112)		69.0 (41 – 125)	72.5 (40 – 112)		85.5 (60 – 94)	72.0 (40 – 112)	
Body height (cm)		175 (145 – 205)	177 (151 – 190)		175.0 (145 – 205)	177.5 (151 – 190)		179.5 (164 – 190)	177.0 (151 – 190)	
THYROHYOID AND CERVICAL SPINE FRACTURE PATTERNS										
Isolated	Yes	22 (35.5%)	22 (34.4%)		22 (37.3%)	22 (37.9%)		2 (33.3%)	20 (38.5%)	
***STH** fracture(s)*	No	40 (64.5%)	42 (65.6%)		37 (62.7%)	36 (62.1%)		4 (66.7%)	32 (61.5%)	
Unilateral	Yes	21 (33.9%)	20 (31.3%)		21 (35.6%)	20 (34.5%)		1 (16.7%)	19 (36.5%)	
***STH** fracture*	No	41 (66.1%)	44 (68.8%)		38 (64.4%)	38 (65.5%)		5 (83.3%)	33 (63.5%)	
Bilateral	Yes	12 (19.4%)	12 (18.8%)		12 (20.3%)	12 (20.7%)		1 (16.7%)	11 (21.2%)	
***STH** fracture*	No	50 (80.6%)	52 (81.2%)		47 (79.7%)	46 (79.3%)		5 (83.3%)	41 (78.8%)	
Total N⁰ of STH fractures (0 – 2)		1 (0 – 2)	1 (0 – 2)		1 (0 – 2)	1 (0 – 2)		0 (0 – 2)	1 (0 – 2)	
Isolated		12 (19.4%)	6 (9.4%)		12 (20.3%)	6 (10.3%)		1 (16.7%)	5 (9.6%)	
***GHH** fracture(s)*		50 (80.6%)	58 (90.6%)		47 (79.7%)	52 (89.7%)		5 (83.3%)	47 (90.4%)	
Unilateral	Yes	17 (27.4%)	11 (17.2%)		17 (28.8%)	11 (19.0%)		1 (16.7%)	10 (19.2%)	
***GHH** fracture*	No	45 (72.6%)	53 (82.8%)		42 (71.2%)	47 (81.0%)		5 (83.3%)	42 (80.8%)	
Bilateral	Yes	6 (9.7%)	5 (7.8%)		6 (10.2%)	5 (8.6%)		0 (0.0%)	5 (9.6%)	
***GHH** fracture*	No	56 (90.3%)	59 (92.2%)		53 (89.8%)	53 (91.4%)		6 (100.0%)	47 (90.4%)	
Total N⁰ of GHH fractures (0 – 2)		0 (0 – 2)	0 (0 – 2)		0 (0 – 2)	0 (0 – 2)		0 (0 – 1)	0 (0 – 2)	
Total N⁰ of TyHy fractures (0 – 4)		1 (0 – 4)	1 (0 – 4)		1 (0 – 4)	1 (0 – 4)		0.5 (0 – 2)	1 (0 – 4)	
Simultaneous	Yes	11 (17.7%)	12 (18.8%)		11 (18.6%)	12 (20.7%)		0 (0.0%)	12 (23.1%)	
***STH and GHH** fractures*	No	51 (82.3%)	52 (81.3%)		48 (81.4%)	46 (79.3%)		6 (100.0%)	40 (76.9%)	
Contralateral thyrohyoid fracture							Yes	0 (0.0%)	6 (11.5%)	
							No	6 (100.0%)	46 (88.5%)	
***Cervical spine** fracture*	Yes	1 (1.6%)	2 (3.1%)		1 (1.7%)	2 (3.4%)		1 (16.7%)	1 (1.9%)	
	No	61 (98.4%)	62 (96.9%)		58 (98.3%)	56 (96.6%)		5 (83.3%)	51 (98.1%)	

Table 4.3.2. *Continued*

		DATASET I-m *THE ENTIRE SAMPLE OF STUDY PART III*			**DATASET II-m** *HANGINGS WITH FRACTURES OR SCM HEMORRHAGES*			**DATASET III-m** *ATYPICAL HANGINGS WITH FRACTURES OR SCM HEMORRHAGES*		
		Knot Position			***Knot Position***			***Knot Position***		
		Typical *N = 62 (49.2%)*	***Atypical*** *N = 64 (50.8%)*	**p-value**	***Typical*** *N = 59 (50.4%)*	***Atypical*** *N = 58 (49.6%)*	**p-value**	***Anterior*** *N = 6 (10.3%)*	***Lateral*** *N = 52 (89.7%)*	**p-value**
STERNOCLEIDOMASTOID MUSCLES' ORIGIN HEMORRHAGES										
Unilateral	Yes	21 (33.9%)	29 (45.3%)		21 (35.6%)	29 (50.0%)		1 (16.7%)	28 (53.8%)	
SCM hemorrhages	No	41 (66.1%)	35 (54.7%)		38 (64.4%)	29 (50.0%)		5 (83.3%)	24 (46.2%)	
Bilateral	Yes	33 (53.2%)	25 (39.1%)		33 (55.9%)	25 (43.1%)		5 (83.3%)	20 (38.5%)	
SCM hemorrhages	No	29 (46.8%)	39 (60.9%)		26 (44.1%)	33 (56.9%)		1 (16.7%)	32 (61.5%)	
Total N⁰ of SCM hemorrhages (0 – 2)		2 (0 – 2)	1 (0 – 2)		2 (0 – 2)	1 (0 – 2)		**2 (1 – 2)**	**1 (0 – 2)**	**< 0.05**

Note: *The categorical data is presented as frequency and ratio, and numerical as average ± standard deviation or median and range. For comparison of categorical data, the χ^2 or Fisher's Exact test were performed, while the Mann-Whitney U test was performed for numerical data. The missing p-values are > 0.05.*

Abbreviations: *STH – Superior thyroid cartilage horn; GHH – Greater hyoid bone horn; SCM – sternocleidomastoid muscle.*

Table 4.3.3. *Characteristics of the lateral hangings in Dataset IV-m.*

N = 52			***Left lateral N = 30 (57.7%)***	***Right lateral N = 22 (42.3%)***	***p-value***
Sex	Male	41 (78.8%)	26 (86.7%)	15 (68.2%)	
	Female	11 (21.2%)	4 (13.3%)	7 (31.8%)	
Age (years)		54.0 (24 – 94)	51.5 (24 – 94)	54.0 (25 – 85)	
Body weight (kg)		72.0 (40 – 112)	71.5 (49 – 112)	72.5 (40 – 103)	
Body height (cm)		177.0 (151 – 190)	179.0 (151 – 190)	176.0 (153 – 190)	
THYROHYOID AND CERVICAL SPINE FRACTURE PATTERNS					
Thyrohyoid fractures present	Yes	37 (71.2%)	21 (70.0%)	16 (72.7%)	
	No	15 (28.8%)	9 (30.0%)	6 (27.3%)	
STH fracture present	Yes	32 (61.5%)	19 (63.3%)	13 (59.1%)	
	No	20 (38.5%)	11 (36.7%)	9 (40.9%)	
GHH fracture present	Yes	17 (32.7%)	10 (33.3%)	7 (31.8%)	
	No	35 (67.3%)	20 (66.7%)	15 (68.2%)	
Isolated STH fractures	Yes	20 (38.5%)	11 (36.7%)	9 (40.9%)	
	No	32 (61.5%)	19 (63.3%)	13 (59.1%)	
Isolated GHH fractures	Yes	5 (9.6%)	2 (6.7%)	3 (13.6%)	
	No	47 (90.4%)	28 (93.3%)	19 (86.4%)	
Left GHH fracture	Yes	13 (25.0%)	8 (26.7%)	5 (22.7%)	
	No	39 (75.0%)	22 (73.3%)	17 (77.3%)	
Right GHH fracture	Yes	9 (17.3%)	5 (16.7%)	4 (18.2%)	
	No	43 (82.7%)	25 (83.3%)	18 (81.8%)	
Left STH fracture	Yes	17 (32.7%)	9 (30.0%)	8 (36.4%)	
	No	35 (67.3%)	21 (70.0%)	14 (63.6%)	
Right STH fracture	Yes	26 (50.0%)	16 (53.3%)	10 (45.5%)	
	No	26 (50.0%)	14 (46.7%)	12 (54.5%)	
Unilateral GHH fracture	Yes	10 (19.2%)	7 (23.3%)	3 (13.6%)	
	No	42 (80.8%)	23 (76.7%)	19 (86.4%)	
Unilateral STH fracture	Yes	19 (36.5%)	13 (43.3%)	6 (27.3%)	
	No	33 (63.5%)	17 (56.7%)	16 (72.7%)	
Bilateral GHH fracture	Yes	5 (9.6%)	3 (10.0%)	2 (9.1%)	
	No	47 (90.4%)	27 (90.0%)	20 (90.9%)	
Bilateral STH fracture	Yes	11 (21.2%)	6 (20.0%)	5 (22.7%)	
	No	41 (78.8%)	24 (80.0%)	17 (77.3%)	
Ipsilateral GHH fracture	Yes	6 (11.5%)	5 (16.7%)	1 (4.5%)	
	No	46 (88.%)	25 (83.3%)	21 (95.5%)	
Contralateral STH fracture	**Yes**	**12 (23.1%)**	**10 (33.3%)**	**2 (9.1%)**	**< 0.05**
	No	**40 (76.9%)**	**20 (66.7%)**	**20 (90.9%)**	
Contralateral thyrohyoid fractures	Yes	6 (11.5%)	5 (16.7%)	1 (4.5%)	
	No	46 (88.5%)	25 (83.3%)	21 (95.5%)	
Simultaneous STH and GHH fracture	Yes	12 (23.1%)	8 (26.7%)	4 (18.2%)	
	No	40 (76.9%)	22 (73.3%)	18 (81.8%)	
Total N⁰ of STH fractures (0 – 2)		1 (0 – 2)	1 (0 – 2)	1 (0 – 2)	
Total N⁰ of GHH fractures (0 – 2)		0 (0 – 2)	0 (0 – 2)	0 (0 – 2)	
Total N⁰ of thyrohyoid fractures (0 – 4)		1 (0 – 4)	1.5 (0 – 4)	1 (0 – 3)	
Cervical spine fracture	Yes	1 (1.9%)	1 (3.3%)	0 (0.0%)	
	No	51 (98.1%)	29 (96.7%)	22 (100.0%)	
STERNOCLEIDOMASTOID MUSCLE'S ORIGIN HEMORRHAGES					
SCM hemorrhage present	Yes	48 (92.3%)	28 (93.3%)	20 (90.9%)	
	No	4 (7.7%)	2 (6.7%)	2 (9.1%)	
Left SCM hemorrhage	Yes	31 (59.6%)	**23 (76.7%)**	**8 (36.4%)**	**< 0.05**
	No	21 (40.4%)	**7 (23.3%)**	**14 (63.6%)**	
Right SCM hemorrhage	Yes	37 (71.2%)	**17 (56.7%)**	**20 (90.9%)**	**< 0.05**
	No	15 (28.8%)	**13 (43.3%)**	**2 (9.1%)**	
Unilateral SCM hemorrhage	Yes	28 (53.8%)	16 (53.3%)	12 (54.5%)	
	No	24 (46.2%)	14 (46.7%)	10 (45.5%)	
Bilateral SCM hemorrhage	Yes	20 (38.5%)	12 (40.0%)	8 (36.4%)	
	No	32 (61.5%)	18 (60.0%)	14 (63.6%)	
Ipsilateral SCM hemorrhage	Yes	23 (44.2%)	11 (36.7%)	12 (54.5%)	
	No	29 (55.8%)	19 (63.3%)	10 (45.5%)	
Total N⁰ of SCM hemorrhages (0 – 2)		1 (0 – 2)	1 (0 – 2)	1 (0 – 2)	

Note: *The categorical data is presented as frequency and ratio, and numerical as average ± standard deviation or median and range. For comparison of categorical data, the χ^2 test or Fisher's exact test were performed, while the Mann-Whitney U test was performed for numerical data. All the p-values are > 0.05.* ***Abbreviations:*** *STH – Superior thyroid cartilage horn; GHH – Greater hyoid bone horn; SCM – Sternocleidomastoid muscle.*

Age was a significant predictor for overall thyrohyoid complex fracture occurrence (AUC 0.622, 95% CI 0.511 – 0.733, $p < 0.05$) – cutoff value was age of ≥ 54.5 years (sensitivity 75.3%, specificity 51.2%), as well as for the occurrence of GHH fracture (AUC 0.664, 95% CI 0.568 – 0.760, $p = 0.001$) – cutoff value was age of ≥ 52.5 years (sensitivity 75.6%, specificity 55.3%). However, age was not a good predictor of STH fracture occurrence considered separately (AUC 0.479, 95% CI 0.374 – 0.584, $p > 0.05$). Here, age was not a significant predictor of cervical spine fracture occurrence, too (AUC 0.533, 95% CI 0.293 – 0.772, $p > 0.05$).

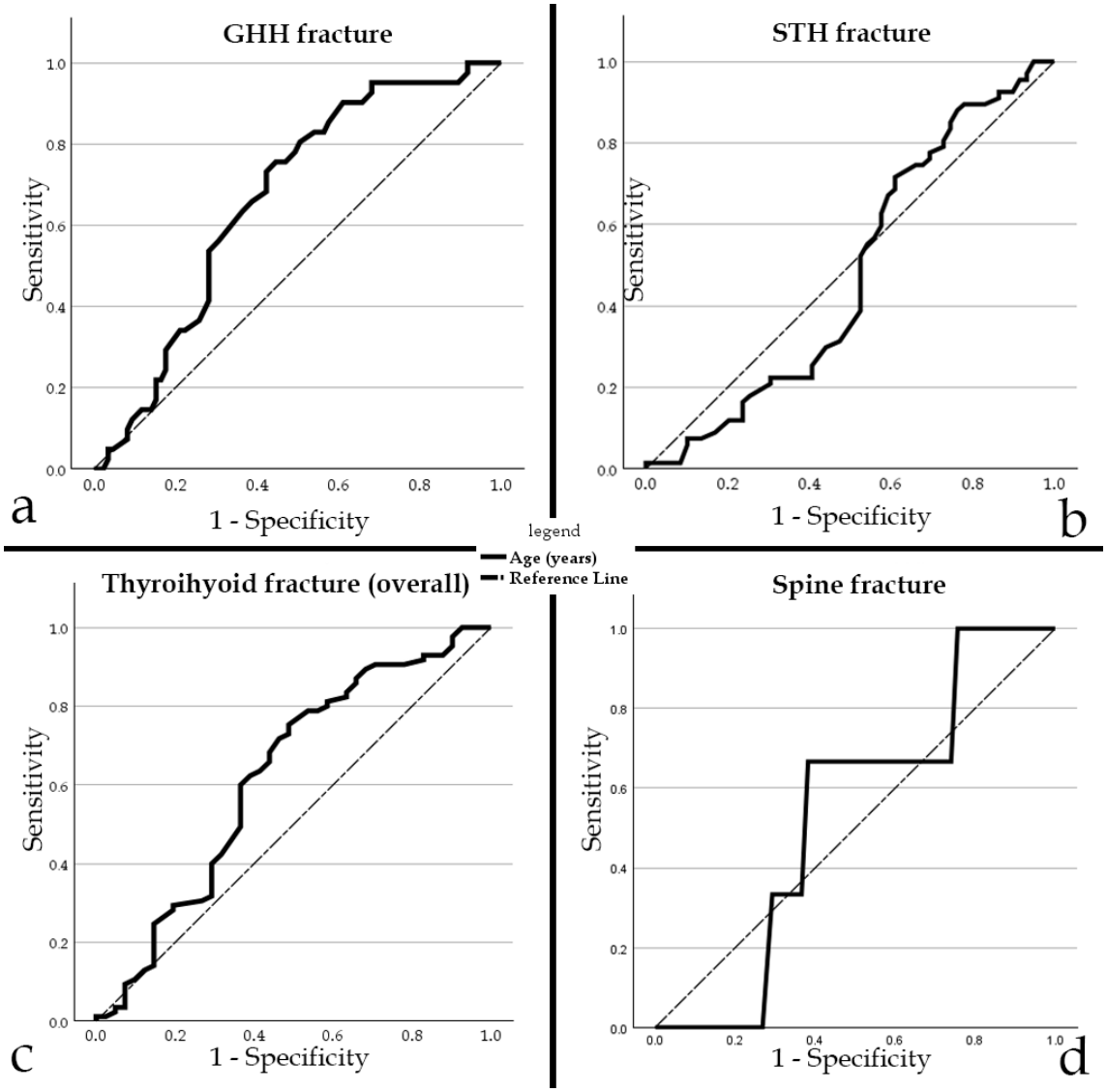

Figure 4.3.1. *The ROC curve analyses of the subjects' age as a predictor for* ***(a)*** *the occurrence of GHH fractures,* ***(b)*** *the occurrence of STH fractures,* ***(c)*** *the occurrence of thyrohyoid fractures in general, as well as* ***(d)*** *the cervical spine fracture occurrence, in Dataset I-m.* ***Abbreviations:*** *GHH – Greater hyoid bone horn, STH – Superior thyroid cartilage horn.*

Age showed a negligible statistically significant positive correlation with the total number of thyrohyoid fractures (range 0-4 – sum of STH and GHH fractures, $\rho = 0.188$, $p < 0.05$), and a weak correlation with the total number of GHH fractures (range 0-2, $\rho = 0.248$, $p < 0.05$), but did not correlate with the total number of STH fractures (range 0-2, $\rho = 0.023$, $p > 0.05$). Also, subjects' age did not correlate significantly with the number of SCM hemorrhages (range 0-2, $\rho = 0.007$, $p > 0.05$).

Subjects' body weight was a significant predictor for the occurrence of STH fracture (AUC 0.640, 95% CI 0.544 – 0.737, $p < 0.05$) – cutoff value was body weight of ≥ 65.5 kg (sensitivity 74.6%, specificity 52.5%). However, body weight was not a good predictor of overall thyrohyoid complex fracture occurrence (AUC 0.556, 95% CI 0.453 – 0.659, $p > 0.05$) and of GHH fracture occurrence considered separately (AUC 0.482, 95% CI 0.373 – 0.591, $p > 0.05$). Also, body weight was not a significant predictor of cervical spine fracture occurrence, too (AUC 0.537, 95% CI 0.257 – 0.817, $p > 0.05$).

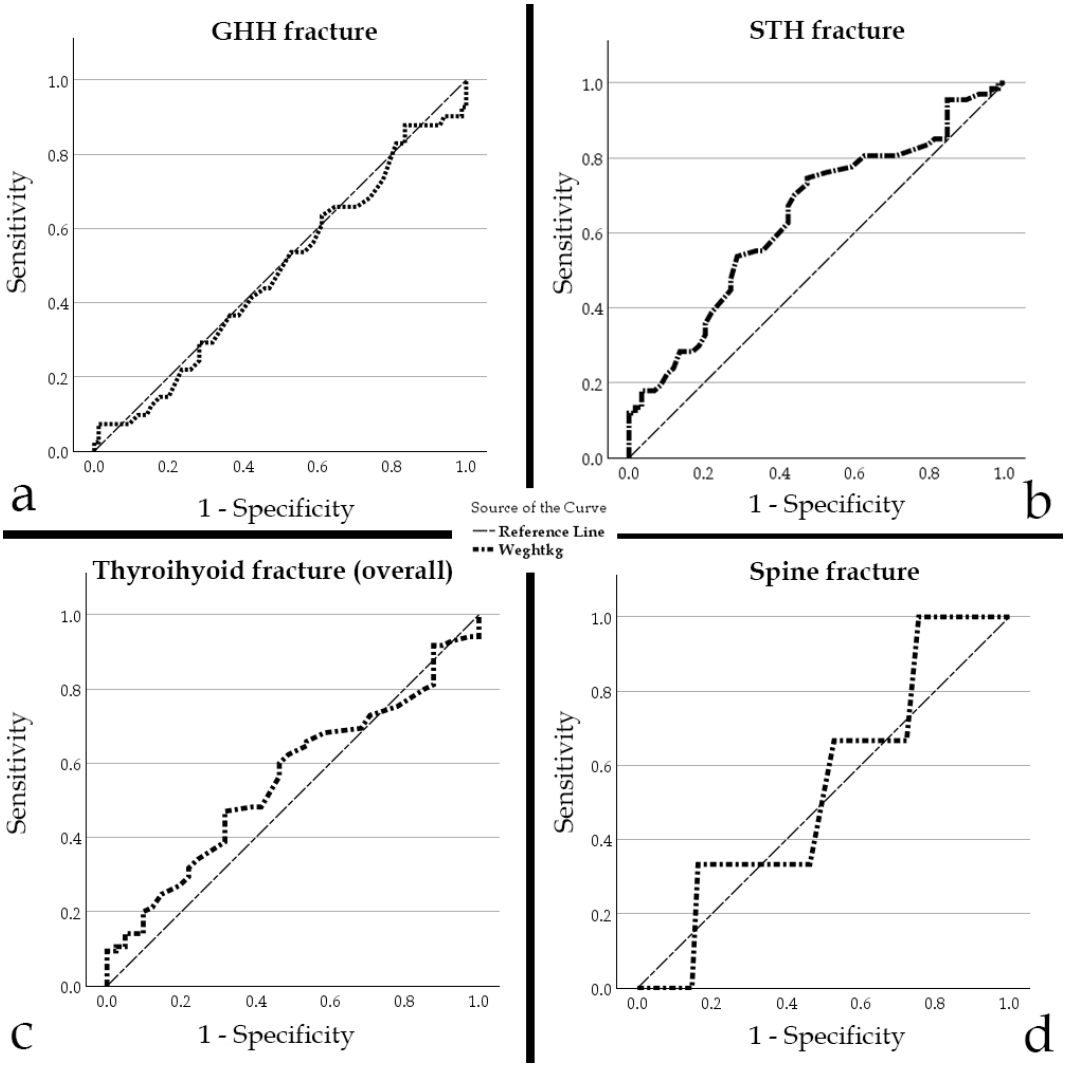

Figure 4.3.2. *The ROC curve analyses of the subjects' body weight as a predictor for (**a**) the occurrence of GHH fractures, (**b**) the occurrence of STH fractures, (**c**) the occurrence of thyrohyoid fractures in general, as well as (**d**) the cervical spine fracture occurrence, in the Dataset I-m.* ***Abbreviations:*** *GHH – Greater hyoid bone horn, STH – Superior thyroid cartilage horn.*

A statistically significant but negligible positive correlation was observed only between subjects' body weight and the total number of STH fractures (range 0-2, $\rho = 0.197$, $p < 0.05$). There were no statistically significant correlations of body weight with the total number of thyrohyoid fractures (range 0-4 – sum of STH and GHH fractures, $\rho = 0.083$, $p > 0.05$), total number of GHH fractures considered alone (range 0-2, $\rho = -0.049$, $p > 0.05$), as well as with the total number of SCM muscle hemorrhages (range 0-2, $\rho = 0.141$, $p > 0.05$).

Body height was not a significant predictor for any of the considered variables: overall thyrohyoid fracture occurrence (AUC 0.534, 95% CI 0.430 – 0.639, p > 0.05), GHH fracture occurrence considered separately (AUC 0.518, 95% CI 0.410 – 0.625, p > 0.05), STH fracture occurrence considered separately (AUC 0.575, 95% CI 0.475 – 0.676, p > 0.05), and cervical spine fracture occurrence (AUC 0.541, 95% CI 0.317 – 0.765, p > 0.05).

Body height did not significantly correlate with the number of thyrohyoid fractures, overall and when considered separately (STH and GHH, p > 0.05 – for all), as well as with the total number of SCM muscle hemorrhages (range 0-2, ρ = 0.112, p > 0.05).

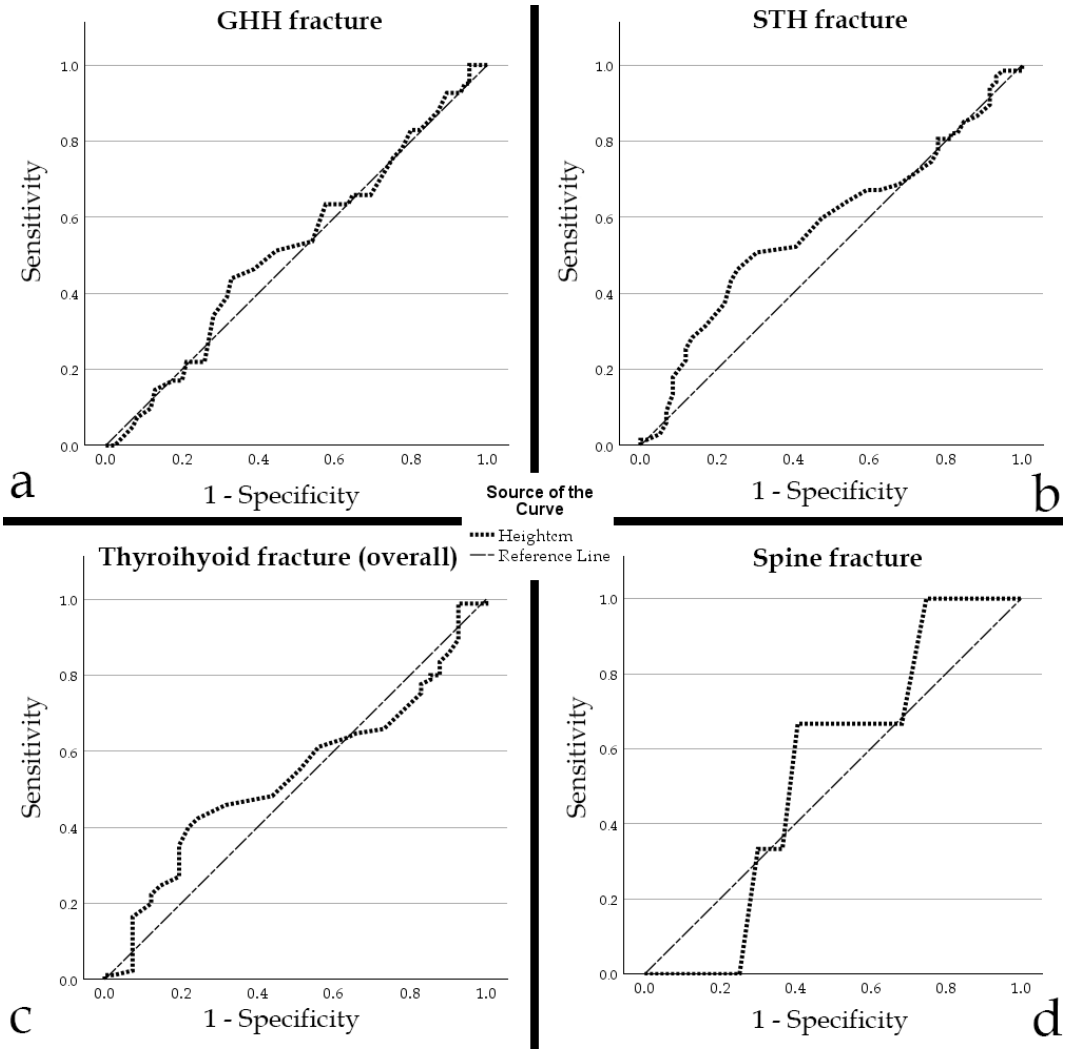

Figure 4.3.3. *The ROC curve analyses of the subjects' body height as a predictor for (**a**) the occurrence of GHH fractures, (**b**) the occurrence of STH fractures, (**c**) the occurrence of thyrohyoid fractures in general, as well as (**d**) the cervical spine fracture occurrence, in the Dataset I-m.* ***Abbreviations:*** *GHH – Greater hyoid bone horn, STH – Superior thyroid cartilage horn.*

Regarding the predictive value on the occurrence of sternocleidomastoid muscle's origin hemorrhages – subjects' age was not a statistically significant predictor of hemorrhages at the origin of SCM muscles (AUC 0.463, 95% CI 0.316 – 0.610, p > 0.05). Body weight was a statistically significant predictor of hemorrhages at the origin of SCM muscles (AUC 0.639, 95% CI 0.505 – 0.772, p < 0.05) – cutoff value was body weight of ≥ 67.5 kg (sensitivity 62.0%, specificity 66.7%). Subjects' body height was not a statistically significant predictor of hemorrhages at the origin of SCM muscles (AUC 0.619, 95% CI 0.492 – 0.745, p > 0.05).

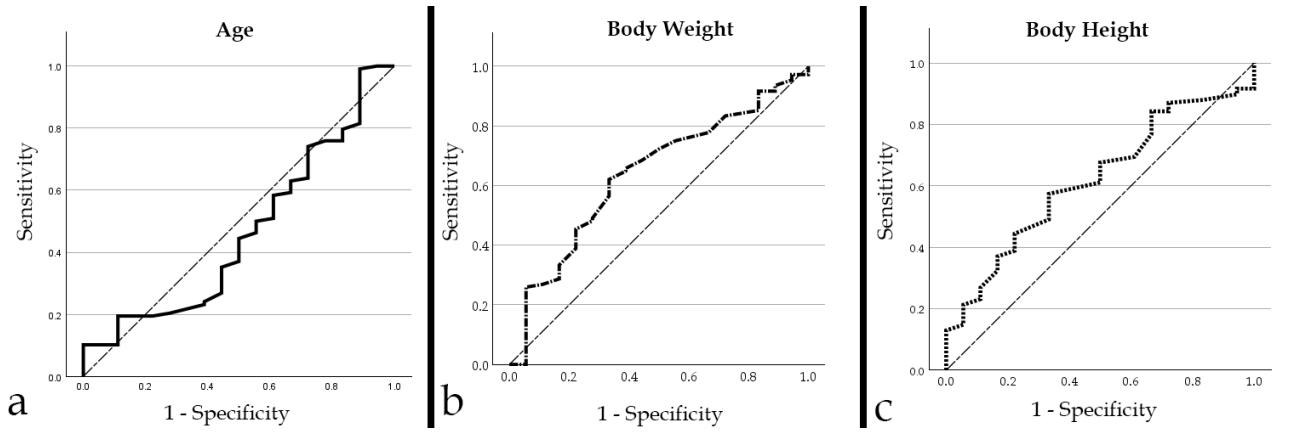

Figure 4.3.4. *The ROC curve analyses the subjects' age (**a**), body weight (**b**), and body height (**c**) as predictors for the occurrence of sternocleidomastoid muscle's origin hemorrhages, in Dataset I-m.*

On the univariable logistic regression analysis, none of the defined coded variables showed statistically significant association with the knot in a noose position ($p > 0.05$, for all), and because all the p-values were above 0.1, multivariable logistic regression analysis was not performed.

4.3.1.2. The hangings with thyrohyoid or cervical spine fractures or sternocleidomastoid muscle hemorrhages – Dataset II-m

In the subgroup of subjects in which at least one thyrohyoid or cervical spine fracture or SCM muscle hemorrhage was observed, subjects older than 40 years were equally distributed between the two groups (typical vs. atypical hangings, $\chi^2 = 0.003$, df = 1, $p > 0.05$).

Subjects' age had a weak statistically significant positive correlation with the number of GHH fractures (range 0-2, $\rho = 0.249$, $p < 0.05$). The body weight and body height did not correlate with the number of thyrohyoid fractures overall, and if GHH and STH were considered separately ($p > 0.05$, for all). The number of SCM hemorrhages (range 0 – 2) did not significantly correlate with the subjects' age, body weight, and body height ($p > 0.05$, for all).

On the univariable logistic regression analysis, none of the defined coded variables showed statistically significant association with the knot in a noose position ($p > 0.05$, for all), and because all the p-values were above 0.1, multivariable logistic regression analysis was not performed.

4.3.1.3. The atypical hangings with thyrohyoid or cervical spine fractures or sternocleidomastoid muscle hemorrhages – Dataset III-m

The subgroup of Dataset III-m comprised only atypical hanging cases with at least one thyrohyoid or cervical spine fracture or at least one sternocleidomastoid muscle hemorrhage, and it this dataset the anterior and lateral hanging groups were compared in between. Subjects older than 40 years of age were equally distributed between the two groups ($\chi^2 = 0.29$, df = 1, $p > 0.05$).

In Dataset III-m, subjects' age showed statistically significant weak positive correlation with the total number of thyrohyoid complex fractures (range 0-4, $\rho = 0.293$, $p < 0.05$), but did not significantly correlate with the total number of GHH or STH fractures if these were considered separately (both p-values > 0.05). Subjects' body weight, and body height did not correlate significantly with the number of thyrohyoid fractures, either combined, or considered separately (STH and GHH fractures, p-values > 0.05).

Also, subjects' age, body weight, and body height did not significantly correlate with the total number of sternocleidomastoid muscle hemorrhages (all three p-values were > 0.05).

On the univariable binary logistic regression analysis none of the coded variables was significantly associated with the (atypical) knot in a noose position (all p-values were > 0.05). The p-values for bilateral sternocleidomastoid muscle hemorrhages and total number of SCM hemorrhages (range 0-2) were < 0.1 but greater than 0.05 (OR 8.000 95% CI 0.870-73.550, p = 0.066, and OR 7.316 95% CI 0.836 – 64.034, p = 0.072, respectively), and the multivariable logistic regression analysis was not performed.

4.3.1.4. The lateral hangings with thyrohyoid and cervical spine fractures or sternocleidomastoid muscle hemorrhages – Dataset IV-m

Subjects older than 40 years of age were equally distributed between the two groups ($\chi^2 = 0.341$, df = 1, p > 0.05).

Subjects' age showed statistically significant weak positive correlation with the total number of thyrohyoid complex fractures (range 0 – 4, $\rho = 0.334$, $p < 0.05$), but did not significantly correlate with the total number of GHH or STH fractures when these were considered separately (both p-values > 0.05). Subjects' body weight, and body height did not correlate significantly with the number of thyrohyoid fractures, either combined, or considered separately (STH and GHH fractures, p-values > 0.05).

In Dataset IV-m, subjects' age, body weight, and body height did not significantly correlate with the total number of SCM muscle hemorrhages (all three p-values were > 0.05).

On the univariable logistic regression analysis, statistically significant association with left lateral knot position had the presence of left SCM muscle hemorrhages (OR 5.750, 95% CI 1.710 – 19.333, p < 0.05), and the absence of right SCM muscle hemorrhages (OR 7.647, 95% CI 1.509 – 38.759, p < 0.05). The presence of STH fracture contralateral to the knot position was included in the multivariable analysis due to p-value < 0.01.

On the multivariable logistic regression analysis, the hemorrhages of left SCM muscle (aOR 5.625, 95% CI 1.390 – 22.759), absence of right SCM muscle hemorrhages (aOR 8.652, 95% CI 1.462 – 51.204), and presence of the STH fracture contralateral to the knot in a noose position were all independently associated with the left lateral knot position. This model correctly classified 69.2% of cases ($\chi^2 = 20.263$, df = 3, $p < 0.05$; Hosmer & Lemeshow Test: $\chi^2 = 5.718$, df = 4, p > 0.05).

4.3.2. Machine learning algorithms

In the third part of the study, the machine learning models were developed only for Dataset I-m. The characteristics of this dataset regarding the coded variables and test/training group division are shown in Supplement C. The data were considered balanced in terms of the outcome frequency distribution, and the oversampling by SMOTE algorithm was not performed. In the following text, the results on machine learning algorithms are reported in the previously established order.

4.3.2.1. Genetic Algorithm-optimized Artificial Neural Networks

Performance characteristics analyses of the GA-optimized ANNs, for Datasets I-m are reported in Table 4.3.4.

Table 4.3.4. *Performance characteristics of ANN developed in MATLAB for knot position classification in the entire sample (Dataset I-m).*

GA-optimized ANN DATASET I-m		***Accuracy (95% CI)***	***Sn***	***Sp***	***PPV***	***NPV***	***LR+***	***LR-***	***AUC (95% CI)***
SCM muscle hemorrhages ***considered***	**Overall**	69.8% (61.0-77.7)	70.3%	69.4%	70.3%	69.4%	2.3	0.4	0.73 (0.64-0.82)
	Test	65.8% (48.6-80.4)	66.7%	65.0%	63.2%	68.4%	1.9	0.5	0.71 (0.54-0.88)
	Training	71.6% (61.0-80.7)	71.7%	71.4%	73.3%	69.8%	2.5	0.4	0.73 (0.62-0.84)
SCM muscle hemorrhages ***NOT considered***	**Overall**	63.5% (54.4-71.9)	75.0%	51.6%	61.5%	66.7%	1.6	0.5	0.65 (0.55-0.74)
	Test	63.2% (46.0-78.2)	88.9%	40.0%	57.1%	80.0%	1.5	0.3	0.67 (0.50-0.85)
	Training	63.6% (52.7-73.6)	69.6%	57.1%	64.0%	63.2%	1.6	0.5	0.64 (0.52-0.76)

Note: *The atypical knot position was considered as the positive state in confusion matrix performance calculations. There was no statistically significant difference in ROC curve analysis of the predicted outcome probabilities between the training and the test group ($p > 0.05$).* ***Abbreviations:*** *GA – Genetic algorithm; Sn – sensitivity; Sp – specificity; PPV – positive predictive value, NPV – negative predictive value, LR+ – positive likelihood ratio, negative LR- – negative likelihood ratio, AUC – Area under the curve, CI – Confidence Interval, SCM – sternocleidomastoid.*

The GA-optimized ANN for Dataset I-m that considered the SCM muscle hemorrhages selected following variables (n = 8) to be included in the model: subjects' body height, presence of unilateral STH fracture, presence of bilateral STH fractures, presence of isolated STH fracture, total number of STH fractures, presence of simultaneous STH and GHH fractures, presence of bilateral SCM muscle hemorrhages, and total number of SCM muscle hemorrhages.

The GA-optimized ANN for Dataset I-m that did not consider the SCM muscle hemorrhages selected following variables (n = 6) to be included in the model: subjects' sex, age, body weight, total number of STH fractures, presence of bilateral GHH fractures, and presence of isolated GHH fracture.

4.3.2.2. MLP-ANN, Decision Tree, k-NN, and Naïve Bayes algorithms

Table 4.3.5. shows information on the performance characteristics of the machine learning algorithms developed in SPSS software, for Dataset I-m.

Figure 4.3.5. shows ROC curve analysis of each of these reported ML algorithms.

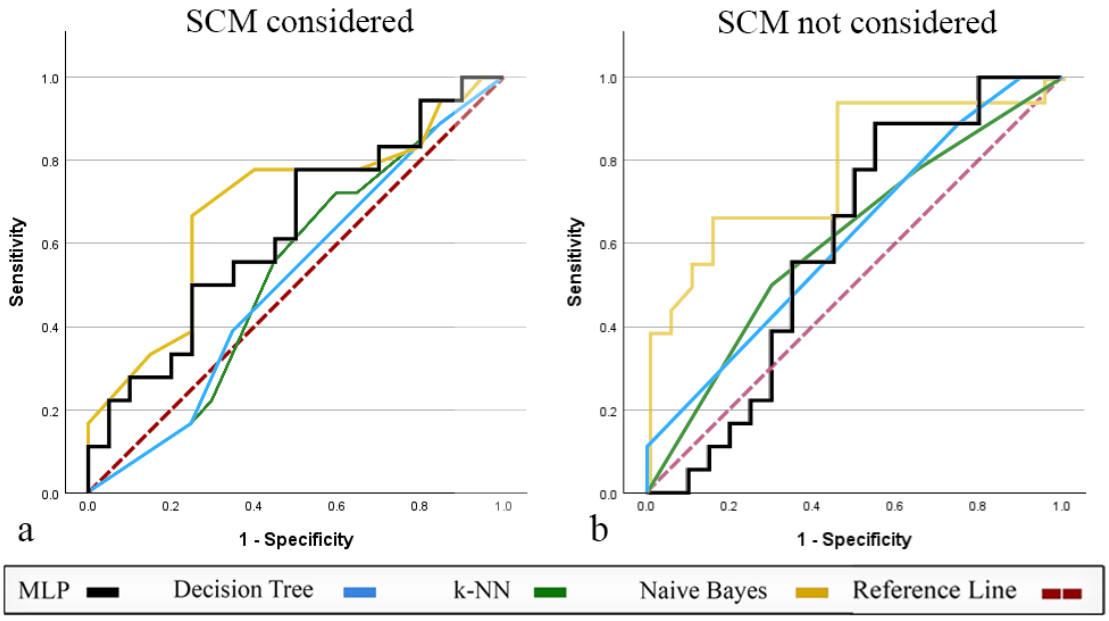

Figure 4.3.5. *The Receiver Operating Characteristic (ROC) and Area under the curve (AUC) analysis of developed machine learning models in test samples of each of four datasets. The AUCs with 95% Confidence Intervals are listed in Table 4.3.5. There was no statistically significant difference in analysis between any training and test sample (p > 0.05).* ***Abbreviations****: MLP – Multilayer Perceptron- Artificial Neural Network, k-NN – k Nearest Neighbors.*

Table 4.3.5. *The performance characteristics of the machine learning models developed in SPSS, for the knot in a noose position classification in Dataset I-m.*

MLAs – Dataset I–m			*Accuracy (95% CI)*	*Sn*	*Sp*	*PPV*	*NPV*	*LR+*	*LR-*	*AUC (95% CI)*
MLP-ANN	**Overall**	**w**	61.1% (52.0-69.7)	75.0%	46.8%	59.3%	64.4%	1.4	0.5	0.69 (0.60-0.78)
		w/o	65.1% (56.1-73.4)	84.4%	45.2%	61.4%	73.7%	1.5	0.3	0.61 (0.51-0.71)
	Test	**w**	60.5% (43.4-76.0)	66.7%	55.0%	57.1%	64.7%	1.5	0.6	0.63 (0.45-0.81)
		w/o	60.5% (43.4-76.0)	72.2%	50.0%	56.5%	66.7%	1.4	0.6	0.60 (0.41 – 0.78)
	Training	**w**	61.4% (50.4-71.6)	78.3%	42.9%	60.0%	64.3%	1.4	0.5	0.71 (0.60-0.81)
		w/o	67.0% (56.2-76.7)	89.1%	42.9%	63.1%	78.3%	1.6	0.3	0.62 (0.50-0.74)
Decision Tree	**Overall**	**w**	61.9% (52.8-70.4)	54.7%	69.4%	64.8%	59.7%	1.8	0.7	0.63 (0.54-0.73)
		w/o	60.3% (51.2-68.9)	89.1%	30.6%	57.0%	73.1%	1.3	0.4	0.62 (0.52-0.72)
	Test	**w**	52.6% (35.8-69.0)	38.9%	65.0%	50.0%	54.2%	1.1	0.9	0.51 (0.32-0.70)
		w/o	55.3% (38.3-71.4)	88.9%	25.0%	51.6%	71.4%	1.2	0.4	0.62 (0.44-0.80)
	Training	**w**	65.9% (55.0-75.7)	60.9%	71.4%	70.0%	62.5%	2.1	0.5	0.69 (0.58-0.80)
		w/o	62.5% (51.5-72.6)	89.1%	33.3%	59.4%	73.7%	1.3	0.3	0.62 (0.51-0.74)
k-NN	**Overall**	**w**	54.0% (44.9-62.9)	57.8%	50.0%	54.4%	53.4%	1.2	0.8	0.57 (0.46-0.67)
		w/o	60.3% (51.2-68.9)	79.7%	40.3%	58.0%	65.8%	1.3	0.5	0.58 (0.48-0.68)
	Test	**w**	55.3% (38.3-71.4)	55.6%	55.0%	52.6%	57.9%	1.2	0.8	0.52 (0.34-0.71)
		w/o	55.3% (38.3-71.4)	77.8%	35.0%	51.9%	63.6%	1.2	0.6	0.61 (0.43-0.79)
	Training	**w**	53.4% (42.5-64.1)	58.7%	47.6%	55.1%	51.3%	1.1	0.9	0.58 (0.46-0.70)
		w/o	62.5% (51.5-72.6)	80.4%	42.9%	60.7%	66.7%	1.4	0.5	0.57 (0.45-0.69)
Naïve Bayes	**Overall**	**w**	61.1% (52.0-69.7)	75.0%	46.8%	59.3%	64.4%	1.4	0.5	0.64 (0.54-0.74)
		w/o	67.5% (58.5-75.5)	71.9%	62.9%	66.7%	68.4%	1.9	0.4	0.74 (0.65-0.83)
	Test	**w**	55.2% (35.7-73.6)	69.2%	43.8%	50.0%	63.6%	1.2	0.7	0.69 (0.51-0.86)
		w/o	57.6% (39.2-74.5)	62.5%	52.9%	55.6%	60.0%	1.3	0.7	0.79 (0.64-0.94)
	Training	**w**	62.9% (52.5-72.5)	76.5%	47.8%	61.9%	64.7%	1.5	0.5	0.62 (0.50-0.73)
		w/o	71.0% (60.6-79.9)	75.0%	66.7%	70.6%	71.4%	2.3	0.4	0.7 (0.60-0.82)

Note: Notes: The atypical knot position was considered as a positive state in confusion matrix performance calculations. There was no statistically significant difference in Area under the ROC curve analysis between training and test samples ($p > 0.05$). Abbreviations: MLP–ANN – Multilayer Perceptron – Artificial Neural Network, k-NN – k Nearest Neighbors, Logistic Regression – Multivariable Logistic Regression analysis, w – model considered sternocleidomastoid muscle origin hemorrhages w/o – model did not consider sternocleidomastoid muscle hemorrhages, Sn – sensitivity, Sp – specificity, PPV – positive predictive value, NPV – negative predictive value, LR+ – positive likelihood ratio, negative LR- – negative likelihood ratio, AUC – Area under the curve, CI – Confidence Interval.

4.3.2.3. *GA-optimized ANN and MLP-ANN ROC analysis comparison*

The comparison analysis between the ROC curves of the GA-optimized ANN models and the ROC curves of the MLP-ANN models for Dataset I-m are shown in Figure 4.3.6.

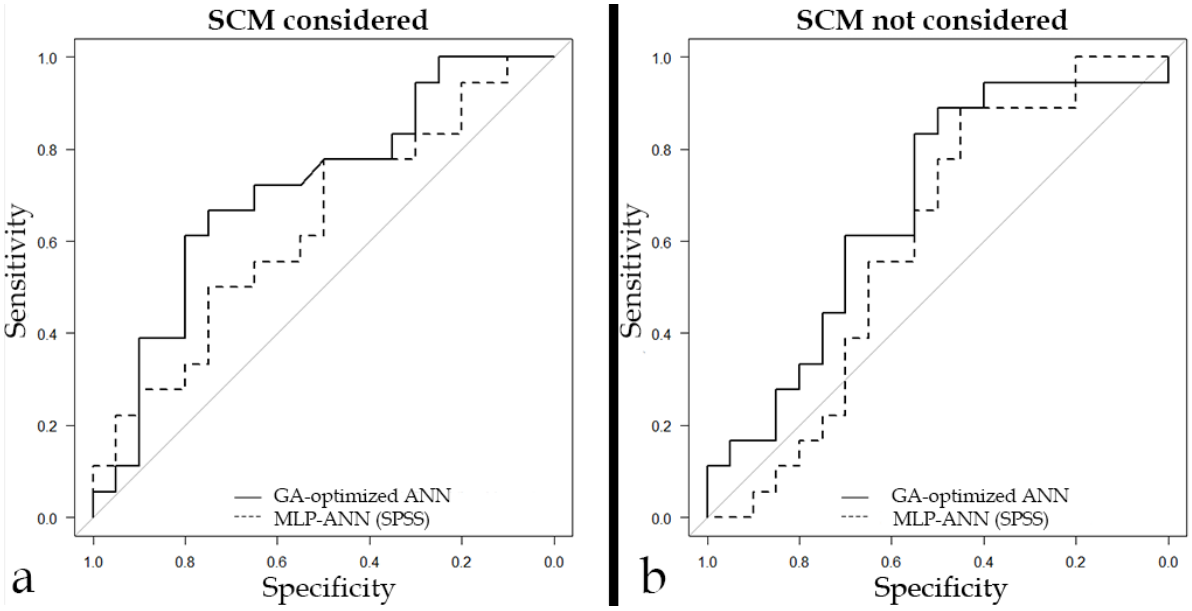

Figure 4.3.6. *The comparison of the ROC curves of two Artificial Neural Network models developed for the knot position classification (atypical vs. typical hangings) in Dataset I-m: the GA-optimized ANN developed in MATLAB and the MLP-ANN developed in SPSS.* ***(a)*** *The comparison of models that considered sternocleidomastoid muscle origin's hemorrhages* ***(b)*** *The comparison of models that did not consider sternocleidomastoid muscle origin's hemorrhages.*

There was no statistically significant difference between the ROC curves developed in MATLAB and SPSS:

Dataset I-m with SCM hemorrhages considered, $Z = 0.65384$, $p > 0.05$;
Dataset I-m with SCM hemorrhages not considered, $Z = 0.52077$, $p > 0.05$;

4.3.2.4. *Comparison of analogous machine learning models: Models with & models without consideration of SCM muscle hemorrhages*

There was no significant difference in the ROC curves analyses in test samples between the ML models that considered presence of sternocleidomastoid muscles origin's hemorrhages and the ML models that did not considered these hemorrhages in Dataset I-m. This holds true for GA-ANN (Figure 4.3.7), MLP-ANN, DT, k-NN, and NB (Figure 4.3.8).

4.3.2.5. *Machine learning models' variable importance and settings*

The hyperparameters settings for all used algorithms developed in SPSS (MLP-ANN, DT, k-NN, and NB), in Dataset I-m are shown in Table 4.3.6. Table 4.3.7. lists up to the top five ranked input variables for each of these algorithms, according to the variable's independent importance.

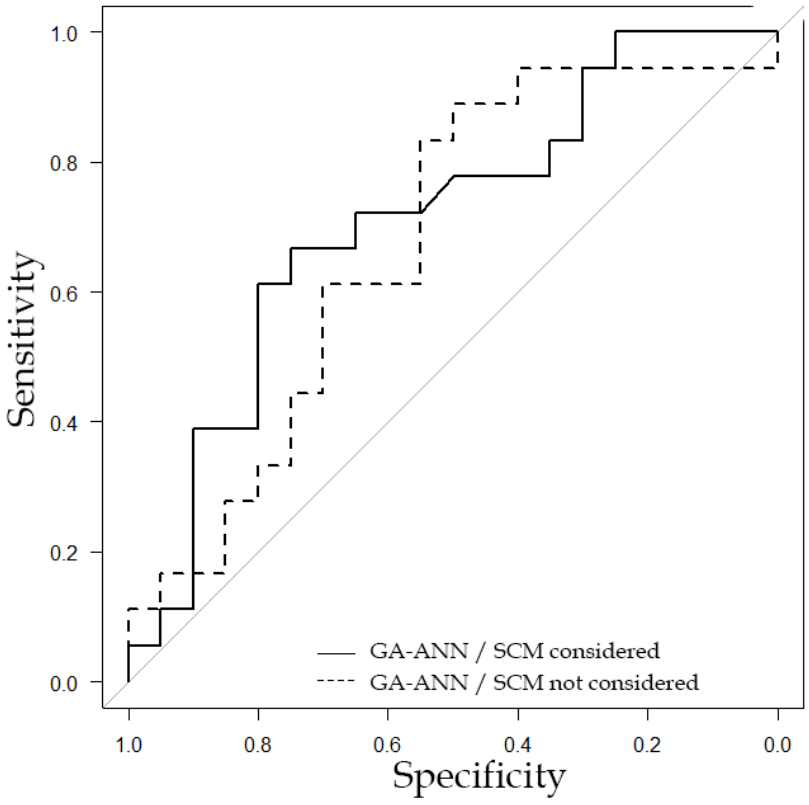

Figure 4.3.7. *The comparison of the ROC curves of two analogous GA-ANN models developed in MATLAB, one considering the presence of sternocleidomastoid muscles origin hemorrhages, and one that does not consider them, in Dataset I-m.*

There was no statistically significant difference in the ROC curve analysis between the two analogous models ($Z = 0.28849$, $p > 0.05$).

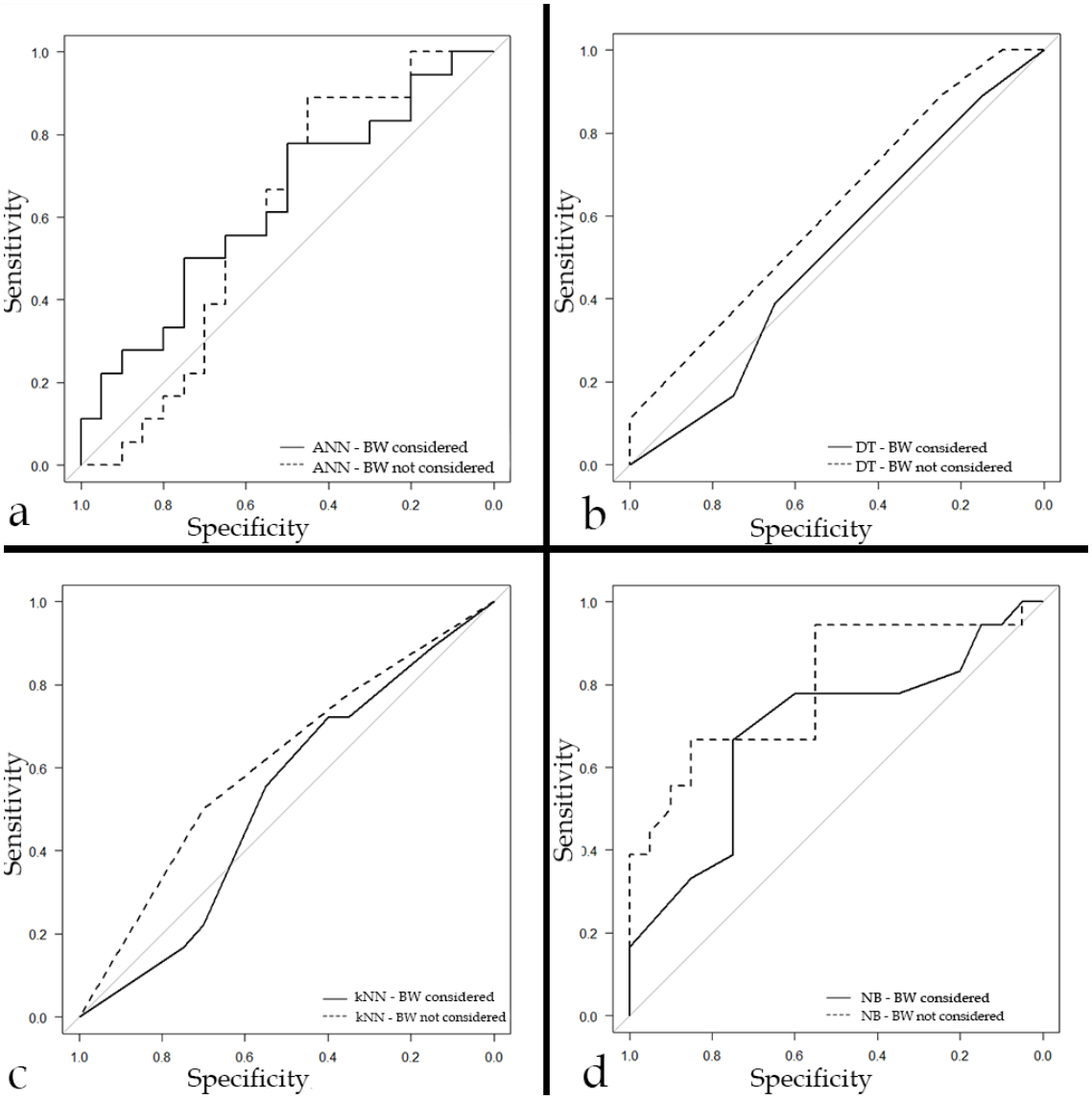

Figure 4.3.8. *The comparison of the ROC curves of two analogous machine learning models developed in SPSS, one considering the presence of sternocleidomastoid muscles origin hemorrhages, and one that does not consider them, in Dataset I-m: MLP-ANN (**a**), Decision Tree (**b**), k-Nearest Neighbors (**c**), and Naïve Bayes (**d**).*

There was no statistically significant difference in the ROC curve analysis between any of the analogous models:

MLP-ANN, Z = 0.40384, p > 0.05;
Decision Tree, Z = -1.0258, p > 0.05;
k-Nearest Neighbors, Z = -0.64212, p > 0.05;
Naïve Bayes, Z = -1.1272, p > 0.05;

Table 4.3.6. *Hyperparameter settings in the reported machine learning algorithms (developed in SPSS).*

		N⁰ of hidden layers	N⁰ of neurons in a hidden layer	Activation function	Training type	Training algorithm	Initial learning rate	Momentum
MLP ANN	**DATASET I-m** *SCM hemorrhage considered*	2	2	Hyperbolic tangent	Online	Gradient descent	0.4	0.9
	DATASET I-m *SCM hemorrhage not considered*	1	2	Hyperbolic tangent	Online	Gradient descent	0.4	0.3

		Growing method	Tree depth	Min. samples of parent node	Min. samples of child node	Nº of nodes	Nº of terminal nodes
Decision Tree	**DATASET I-m** *SCM hemorrhage considered*	CRT	3	8	4	7	4
	DATASET I-m *SCM hemorrhage not considered*	CRT	2	8	4	7	4

		Nº of Neighbors to consider	Distance metrics	Search Algorithm (Feature selection - Stopping criterion)
k-NN	**DATASET I-m** *SCM hemorrhage considered*	11	Euclidean	Change in Absolute Error Ratio ≤0.01
	DATASET I-m *SCM hemorrhage not considered*	2	Euclidean	5 features selected

		Maximum memory (Mb)	N⁰ of bins for scale predictors	N⁰ of selected predictors
Naïve Bayes	**DATASET I-m** *SCM hemorrhage considered*	1024	10	2
	DATASET I-m *SCM hemorrhage not considered*	1024	10	3

Abbreviations: *MLP-ANN - Multilayer Perceptron – Artificial neural network, k-NN – k Nearest Neighbors, SCM – sternocleidomastoid muscle.*

Table 4.3.7. *The top five ranked input variables based on their relative importance for utilized machine learning models.*

	DATASET I-m SCM origin hemorrhage considered				***DATASET I-m SCM origin hemorrhage not considered***			
	MLP	**DT**	**k-NN**	**NB**	**MLP**	**DT**	**k-NN**	**NB**
1st	BH	Tot.Fr.N^0	Tot.Fr.N^0	BW	BH	UL-Hy	BL-Hy	Age
2nd	Age	UL-SCM	BL-Ty	UL-SCM	Tot.Fr.N^0	Hy N^0	Sex	UL-Hy
3rd	Tot.Fr.N^0	iHy	Spine	UL-Hy	Hy N^0	BH	Spine	Tot.Fr.N^0
4th	BW	SCM N^0	SCM N^0	BH	UL-Hy	iHy	iHy	BH
5th	BL-Ty	BL-SCM	/	Age	BW	Tot.Fr.N^0	BH	BW

Note: *Some models included fewer than 5 variables, and the empty fields in the table are labeled with a "/" sign.*

Abbreviations: *BW – Body Weight, BH – Body Height, BL-Hy – bilateral greater hyoid horn fractures, BL-Ty – bilateral superior thyroid horn fractures, CL-Ty - superior thyroid cartilage horn contralateral to the knot position, Hy N^0 – Total number of greater hyoid horn fractures, iTy – isolated superior thyroid horn fracture(s), IL-Hy - greater hyoid bone horn ipsilateral to the knot position, IL-Ty – superior thyroid cartilage horn ipsilateral to the knot position, L-Hy – left greater hyoid bone horn, L-Ty – left superior thyroid cartilage horn, R-Hy – right greater hyoid bone horn, sTy&Hy – simultaneous superior thyroid horn and greater hyoid horn fractures, Spine – Cervical spine fracture, Tot.Fr.N^0 – Total number of thyrohyoid fractures, Ty N^0 – Total number of superior thyroid horn fractures, UL-Hy – unilateral greater hyoid horn fracture, UL-Ty – unilateral superior thyroid horn fracture. SCM N^0 – Total number of sternocleidomastoid muscle origin's hemorrhages; UL-SCM - unilateral sternocleidomastoid muscle origin's hemorrhage, BL-SCM - bilateral sternocleidomastoid muscle origin's hemorrhage*

5. DISCUSSION

The focus of this research and thesis was on the analysis of the potential association of the injuries to the neck organs, particularly the thyrohyoid complex and the cervical spine, and their possible distribution patterns with the position of the knot in a noose that was used in suicidal hanging cases without a long drop. The research was conducted on retrospectively obtained autopsy data by "conventional" (standard) statistical methods but also by using machine learning algorithms and experimentally developing several machine learning models in an attempt to correctly classify the knot in a noose position through the neck injury patterns. It is helpful to approach the analysis by immediately defining the main problems to properly scrutinize the issue that this thesis considered. If these are addressed properly, it provides a foundation and a good context for interpreting and synthesizing the numerous reported results, divided into three distinct study segments. These problems essentially are: the limited understanding of fracture distribution patterns of the thyrohyoid complex and cervical spine with regards to the knot position, the variability of general characteristics of these injuries in hangings that were observed in previous studies, the contribution of major anthropometric characteristics (subject's sex, age, body weight, and body height) to the injury occurrence and thus, indirectly, their patterns, then, the usefulness of additional autopsy findings in knot position assessment (this research analyzed the hemorrhages at the origin of sternocleidomastoid muscles), and finally, what also may make this thesis a significant one, usefulness of machine learning models which could potentially better predict the knot position through the injury patterns. So, firstly, the basic characteristics of the neck's hard-tissue injuries in general will be discussed, as well as the medicolegal usefulness in knot position reconstruction. Then, it will be looked at the thyrohyoid complex and cervical spine fracture characteristics in the sample this study analyzed, in general, but also in the context of the basic and crude statistical analyses, as well as the machine learning analyses. By considering the analogous findings of the three study parts and interpreting these results not only separately and independently but simultaneously due to similar designs and performed analyses, the practical and academic implications will be commented on, providing answers to the defined aims. The following text will deal with the issues described, roughly respecting the order presented above.

Common pathomorphology in deaths by hanging comprises a range of local (neck) and general autopsy findings [2–4, 9, 12, 22, 38, 54]. However, one exceptionally straightforward set of injuries characteristic of neck strangulation is confined to the laryngohyoid, or more precisely – the thyrohyoid complex [3, 9, 46, 52, 55, 58, 66]. In this research, the terms *laryngohyoid* and *thyrohyoid* were considered interchangeable. As described in more detail in the introduction section, thyroid cartilage and hyoid bone, located at the anterior neck midline, have a pair of structures (left and right): superior horns and greater horns, respectively, interconnected with ligaments and membranes, and surrounding soft tissue into a biomechanical functional unit [3, 6, 34, 47]. Because detecting these injuries is simple and is a binominal phenomenon (that is, a fracture is either present or absent), it would be ideal to observe any fracture distribution pattern associated with distinct hanging cases. More specifically – associated with the anatomical distribution of the suspension force a noose applies to the neck structures: the noose can be tied around the neck to form the knot

(i.e., the suspension point) either behind the occiput (so-called posterior or typical hanging), on a lateral side of the head (left or right), or anteriorly, in the jaw midline (the lateral and anterior hangings are so-called atypical hangings) The site of the noose opposing the knot is where the greatest force is applied on suspension, and the thyrohyoid injury pattern may reflect its position [43, 46, 51, 52, 58]. Fractures of the thyrohyoid complex may differ, depending on the distribution of different forces applied – direct compression or indirect, by stretching the soft tissue and remote structures of the complex or even compression against the cervical spine column [2, 3, 50].

If the noose applies enough pressure on the neck for some time after death (for example, more than 20 – 30 minutes), the ligature mark, *a furrow*, is formed that can clearly indicate the highest suspension points and knot position [9]. However, if the ligature is removed shortly after death (suspicious "hanging" deaths in custody, for example), if it is unavailable, the furrow is subtle, faded, or the body is found in a severely decomposed state (even skeletonized and detached from the loop – see Figure 5.1), the other means to assess where the knot was (and, therefore, where the greatest pressure was applied) in the noose would be of significant assistance to reconstruct the event, confirming or ruling out some of the possible or presumed circumstances [25, 43, 46, 51, 52, 55–57, 67, 69]. Therefore, the pattern of thyrohyoid and cervical spine fractures occurring at the moment of hanging or during the short agony could be useful in determining the knot position in these circumstances. This may also prove helpful in the event of a near-hanging and examination of victims of other types of non-fatal strangulation. In addition to the injury of the thyrohyoid complex, a cervical spine injury may be particularly important in the discussed terms, as it is already recognized to be more frequent in anterior atypical hangings.

Being one of the most common suicide methods worldwide, autopsy cases of deaths by hanging are routine in any forensic pathologist practice, and this has been a broadly explored research topic [2, 3, 6, 14–18, 25, 38, 40–43, 51, 52, 54–58, 64–73, 99–110], from the epidemiological to forensic and pathological aspects. Nevertheless, as Zátopková et al. excellently sum up the issue: "*laryngohyoid fractures in hanging victims are one of the most studied and paradoxically contradictory topics in forensic pathology*" [58]. Previous attempts to observe any fracture pattern provided extremely limited results, with statistical analyses mainly describing the thyrohyoid fracture frequency or crudely suggesting an association between the fracture occurrence and the knot position if any at all. Even the overall prevalence of the fractures is surprisingly inconsistent among the studies of suicidal hanging cases, from less than 5% to over 75% of analyzed cases [43, 46, 51, 52, 54–58, 64, 66, 68–70, 72, 73, 102, 107, 111–118]! We can unambiguously claim that if there were any straightforward answers (patterns), we would have them by now.

Nevertheless, before we conclude that thyrohyoid and cervical spine injuries are so heterogeneous irrespective of the ligature knot position that they should be considered stochastic essentially and of no medicolegal significance, it would be fair to supplement the conventional statistics and exhaust some more complex analyses (that is, machine learning models) on larger datasets with strictly uniform methodology.

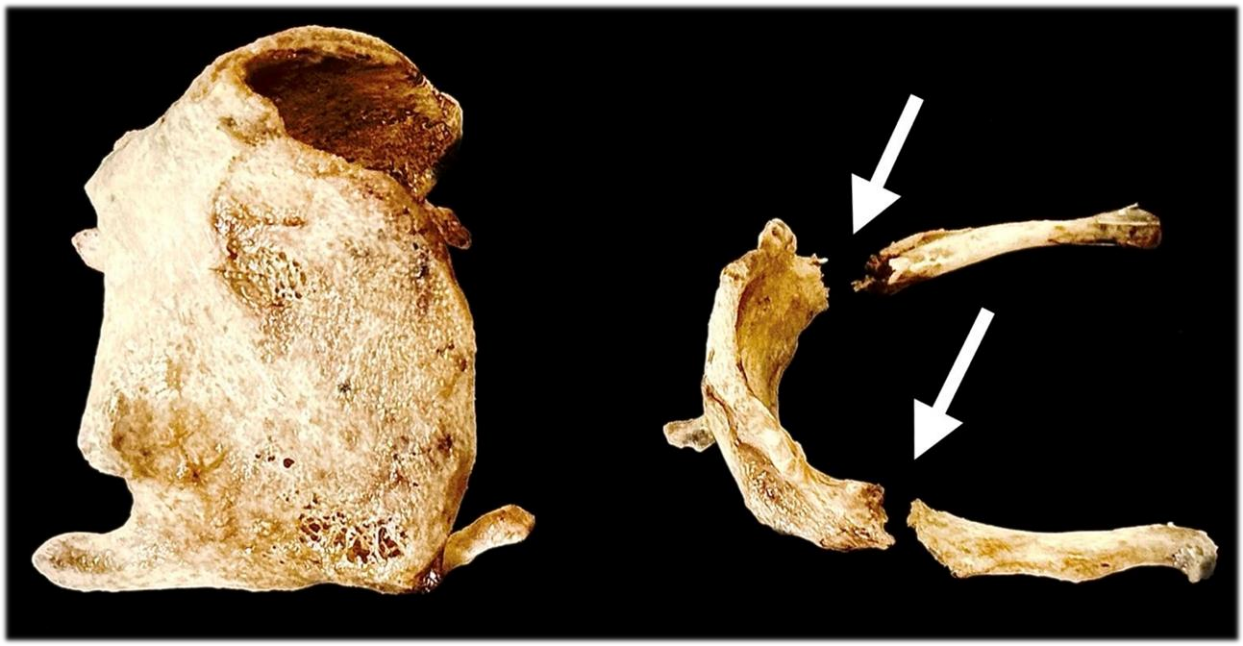

Figure 5.1. *The almost entirely skeletonized remains of a middle-aged man were found at the scene of a suspected suicidal short drop hanging. The noose was still hanging from a fixed point, while the human remains were on the ground in immediate vicinity. The anthropological and pathological examination reconstructed the skeleton of the thyrohyoid complex and further revealed jagged edged "disarticulation" of the greater horns from the body of the hyoid bone, indicating potential fractures (white arrows). Currently, there is no mean by which it can be stated with how much certainty the injuries could correspond to the neck constriction by the found noose regarding the position of its knot (e.g., is it a typical or atypical hanging). From: Institute of Forensic Medicine, University of Belgrade, Faculty of Medicine, Belgrade, Serbia.*

So, as directly implied from the defined aims, this research primarily aimed to utilize machine learning algorithms in an attempt to reconstruct (classify) the position of the knot in suicidal hangings. But it also presented many descriptive and inferential statistical analyses. And the reason for these numerous results should be clarified entirely first. Obviously, standard, often performed, and most importantly, relatively easily understandable and interpretable, crude and multivariable analyses can point directly to significant associations between variables. This is useful alone and in the context of a so-called black-box machine learning algorithm's output, which is not explainable by common logic (this will be referred to later). However, these descriptive and inferential statistical analyses are a solid foundation for the appropriate overall research interpretation in the light of very heterogenous results on data of our interest, which were previously reported in studies [3, 43, 44, 46, 51–58, 64, 66, 69, 73, 102, 106–108, 111–114, 116–118]. Ultimately, the eventually developed machine learning algorithms – models will be put in the appropriate context regarding the overall prevalence and distribution of thyrohyoid and cervical spine fractures and knot in a noose positions. Besides the fact that this would be a prerequisite to reflect on already published findings, it will be useful for later comparison by future studies, as the machine learning-based problem-solving approach will become a significant tool in forensic pathology research [95, 96, 119, 120].

The reported overall prevalence of thyrohyoid complex fractures, which is of greater hyoid bone horns (GHH) and superior horns of the thyroid cartilage (STH), is surprisingly heterogeneous and of a wide range. This data comes from numerous, mainly single-center, autopsy studies. Among the retrospective ones, the reported frequency of thyrohyoid

fractures (presence of either STH or GHH fracture, or a combination) ranged from less than 1% to over 75% [51, 58]. The heterogeneity of this prevalence was observed in both older and in relatively recently published studies. So, for example, we have observations dating back to 1881, when Maschka [121] reported the overall fracture prevalence of 2.0% on a sample of 153 cases, Ushakov's reported prevalence from the year 1900 [122] of 16.7% on a sample of 48 cases but also Reuters's study dating back to 1901, [123] which reported a frequency of 52.5% on a 200-subject sample. One might presume that the autopsy technique from the first decades of forensic pathology practice as an organized and recognized separate specialization has improved and become more standardized [2, 3, 5, 124–126]. However, the reported frequencies continued to vary in the second half of the 20th century and the last few decades. For example, Tualpunt et al. in 2017 [127] reported a prevalence of these fractures to be 0.8% on a sample of 244 subjects, Tugaleva et al. in 2016 [118] a prevalence of 7.3% on a sample of 632 subjects, Duband et al. in 2005 [128] frequency of 69% of cases on a 29-cases sample, Uzun et al. in 2007 [100] 58.6% on a 761-subject sample, and Azmak et al in 2006 [102], reporting a prevalence of 76.8% in 56 cases. There are even some studies on hangings that reported only cases without any of the thyrohyoid fractures [109, 129]! Probably the largest sample retrospective autopsy study reporting thyrohyoid complex fracture prevalence was published in 2015 by Taktak et al. comprising a total of 4,502 cases with an observed fracture prevalence of 52.3% [64].

In their article on thyrohyoid fractures in hangings, Zátopková et al. summarized these reports from 54 retrospective studies [58]. The same authors also found and analyzed 27 additional prospective studies on this issue. We may expect to observe more consistent or at least only higher reported prevalences in a prospectively designed observation, with a focused and unambiguously defined methodology for fracture inspections. However, even in these studies, there are single-digit percentage prevalence reports, reports of no fractures at all, and higher prevalences from c. 40-70% of analyzed cases or more [58, 73, 130–135]. So among these, for example, Patel et al. in 2012 [132] reported no fractures in 320 hanging cases, Hlavaty et al. in 2016 [73] 2.7% in 75 cases, Missliwetz 67.8% in 599 subjects (year 1981) [131], Zátopková et al. 72.5% in 178 cases [58]. One's impression can be that in prospective studies, a considerable number of studies report a prevalence higher than 20%, mostly ranging from about 40% to 60%.

Often, the most reliable data, in general, and so is the case in this particular issue, comes from a meta-analysis. The meta-analysis by Wilson et al. was published very recently, and it estimated the overall prevalence of thyrohyoid complex fractures to be 37.5% but with a relatively wide confidence interval (95% CI 27.4% – 48.3%) [51]. It is hard to explain such a striking heterogeneity in reported fracture prevalences in autopsy studies. Probably the most obvious reason may be the differences in methodology – the details of the dissection and inspection of autopsies in different institutions, the number of pathologists who performed the examinations, the systematics of autopsy findings documentation, or the number of analyzed cases [51, 58]. One direct explanation can also be the different approach when it comes to differentiating between artifactual and intravital thyrohyoid fractures – some authors considered all fractures in analyses, some excluded those without the surrounding soft tissue hemorrhages, while in some research, this was not specified [58]. Some studies relied on postmortem imaging [112, 133, 135–137], but this did not seem to solve the problem.

At the Institute of Forensic Medicine in Belgrade, where the present research was conducted, one study analyzed cervical spine injuries in short drop hangings, while other two studies on thyrohyoid fractures in hangings were already published by Nikolić et al. [46, 52]. In the first published study with the smallest sample an overall prevalence of these fractures reported to be about 68.0% based on the sample of 175 retrospectively analyzed cases [46]. The second study was on a larger sample of 557 retrospectively analyzed cases [52], where the frequency of the thyrohyoid complex fractures was reported to be about 57.3%. And in the last, third published study was on a sample of 766 retrospectively analyzed cases [43], where the frequency of the thyrohyoid complex fractures was reported to be about 58%. In the present research – this thesis, the most extensive retrospective study of autopsy hanging cases was conducted at this institution, and the main sample (the study part I) comprised a total of 1,235 subjects. Here, the thyrohyoid fractures were overall observed in c. 60% of cases. In addition to the uniform methodology, providing many cases would be detrimental to the analysis of such heterogeneous results. As we formed a three-part study, with two samples derived from the largest (1,235 cases, Dataset I), it can be appreciated that in the study parts II and III, in the smaller subsets (Dataset I-w and Dataset I-m, respectively), the overall frequency of thyrohyoid fractures slightly increased as the number of cases analyzed decreased, from 60.6% to 64.1% in Dataset I-w (368 cases), and to 67.5% in Dataset I-w (126 cases), as shown in Tables 4.1.1, 4.1.2, and 4.1.3. So, with a limited number of individuals included to analyze these injuries, a true prevalence can be easily underestimated or overestimated. Given that this sample partially overlaps with those comprising previous studies by Nikolić et al. [43, 46, 52], it is not surprising that the observed fracture prevalences were quite similar. Additionally, more than doubling the number of cases from the previous study likely impacts the better actual prevalence estimation. Actually, given that these are all retrospective analyses, it strongly points to consistency and systematicity in autopsy technique, special neck dissection uniformity among the personnel performing autopsies, and eventually, the autopsy reports *per se.* This is not a surprise, as good autopsy practice at the Institute of Forensic Medicine in Belgrade, its revision, and adequate supervision of it has been insisted on for many decades now (in the year 2023, the Department of the Forensic Medicine of the University of Belgrade Faculty of Medicine marked 100th year since its establishment) [138–140].

Why is all this of particular importance here? Well, the significant part of current research is the form of an experiment (program – software/computer-based), as will be referred to later in the discussion. However, that sort of experiment, in this case, relies solely on the retrospectively obtained data. So, in terms of the quality of the obtained data, this is essentially a retrospective study, and it will directly reflect on the results of the experimental study part, and obviously the conventional statistical analysis, and thus directly on the synthesized conclusions derived from all the parts of the study. Looking only at the overall prevalence of thyrohyoid complex fractures and the described methodology in the presented research (see section 3. Materials and Methods), and thus the systematic approach to the autopsies of hanging cases at the Institute (the observational period was relatively long – from 1995 to 2023), we can conclude that the obtained data was quite uniform, and matched those observed in a single-institutional, well designed prospective autopsy studies on the issue of thyrohyoid fractures in hangings. The frequency surpasses that of the recent meta-analysis (i.e., of average estimates), which is expected as this average value relies on the data from the studies that reported quite variable prevalences [51, 58]. Simply put – this means that in the present study, significant disadvantages of retrospectively obtained data

(e.g., failure to detect events – i.e., fractures) were overcome by a systematic, single-institutional, uniform autopsy procedure and findings documentation, all supervised by experienced forensic medicine specialists and that we provided adequate and large study sample without any missing data. Detecting analyzed fractures is straightforward on autopsy, which strongly diminishes (inter)investigator bias [58]. With a proper technique – in situ, neck dissection, *en bloc* evisceration and dissection of the thyrohyoid complex, and finally, inspection and palpation of the defleshed greater hyoid bone horns and superior thyrohyoid cartilage horns – detecting the fractures of interest is simple and should be invariably performed. Of note is, and it should be highlighted, that of our interest and consideration here are only suicidal hangings with a short drop or cases in which there is no drop at all. Because injury and death onset mechanisms, in essence, differ from those of long drop hangings [22, 25, 45]. If not explicitly stated otherwise, the comments and discussion refer to short-drop hangings and those essentially without a drop, and of a suicidal manner.

Scrutinizing further the observed prevalence of thyrohyoid fractures in this research, we can see that in the present sample and based on the 1,235 analyzed cases of suicidal hangings (study part I), the fractures of the superior horns of the thyroid cartilage (STH) occurred more frequently than the fractures of the hyoid bone's greater horns (GHH), in 44.5% and 34.4% of cases, respectively. The isolated STH fractures were more common than isolated GHH fractures, 26.2% vs. 16.1% of cases, while in 18.3% of cases in this sample, STH and GHH fractures co-occurred (both structures were fractured in a single subject). And while the overall thyrohyoid fracture prevalence slightly increased in study parts II and III, the distribution of these fractures (whether they were isolated or simultaneous) was nearly identical (compare frequencies in Tables 4.1.1, 4.2.1, and 4.3.1), and this will ease drawing synthesized conclusions from thee study parts. Moreover, despite the overall heterogeneity of reported fracture prevalences in previous studies, this sort of fracture distribution seems to be mainly consistent – isolated STH fractures are, to some small extent, more common than isolated GHH fractures, but the existence of statistical significance is in question. So, what this research contributes to is also yet another information on fracture prevalence from a large, uniform, complete (complete data in all included cases), and reliable sample. In addition to thyrohyoid complex fractures, this may be particularly important for the cervical spine fracture in hangings (Table 4.1.1), which is generally a rare finding but is known to show some association with the knot position, particularly the anterior one [43].

The proportions of the analyzed hanging types (i.e., the knot in a noose position) can influence the reported overall fracture prevalence, as the knot position may affect the fracture occurrence [25, 43, 49]. In this thesis, the largest proportion of cases were so-called typical hangings (the knot was located posteriorly in almost 60% of cases in Dataset I), the lateral hangings were the second most common (about a third of the Dataset I sample), while the smallest proportion of cases were with the anterior knot in a noose position (about 10% of the Dataset I sample), as shown in Table 4.1.1. Importantly, decreasing the sample in the present research (from study part I to study parts II and III) led to a significant decrease in the proportion of atypical hangings – it halved from about 10.0% in the first study part to about 5.0% of all considered cases in study parts II and III, which should be kept in mind. Thankfully, due to the uniformity of autopsy findings records in this research, the estimation of the knot in a noose position was identical in all derived subsets, and this minimized the risk of a bias of this kind affecting the observed prevalences.

Can the "conventional" statistical analysis on our sample discover any regularity in the thyrohyoid fracture pattern and the knot in a noose position? The very beginning of the study – defining the observations (variable coding) and outcome (knot position groups comparison), significantly differed from previous research attempts. Earlier studies focused on discrimination between the four-knot positions (posterior, anterior, left, and right lateral side of the head) or even eight positions [46, 52, 58, 64], the stepwise approach was made here through the four separate steps (in each study part). Firstly, it was assessed if any difference in fracture patterns existed between typical hangings on one side and all atypical hangings (anterior and lateral, combined) on the other side, also taking into account cases in which no neck structure fractures existed. The second step was to exclude these cases without any fractures so that the patterning difference could become more apparent: if there are no events to be observed – no fractures exist, then the association may be hidden and strongly and significantly underestimated. Only after this analysis between the typical and atypical hangings, we turned to fracture pattern discrimination between anterior atypical and lateral atypical hangings (left and right lateral combined). Ultimately, we looked for discriminative fracture patterns between the left and right lateral hangings with the fractures of the neck hard-tissue structures (i.e., the thyrohyoid complex and the cervical spine). The variable coding was per this approach: instead of immediately defining on which side a particular horn was fractured (left or right), we initially only defined if the fractures were unilateral or bilateral, thus increasing the possibility of detecting not-so-obvious differences in these fracture frequencies regarding the knot position, and in this manner suggesting an underlying pattern. The composition of the study – division into separate study parts was also constructed to systematically analyze the potential confounding effects of the major anthropometric factors – subjects' sex and age (study part I), body weight, and body height (study part II).

Starting from study part I (see sections 3.1 and 4.1.), which has considered the largest sample, the crude statistical comparison of thyrohyoid complex fracture patterns between typical and atypical hangings showed that unilateral fracture of the hyoid bone's greater horn and simultaneous fracture of the hyoid bone's greater horn(s) and thyroid cartilage superior horn(s) occur significantly more often in atypical than in typical hangings. On the other hand, in typical hangings, it is considerably more likely to observe an isolated fracture(s) of the thyroid cartilage's superior horn(s) without a hyoid bone fracture. Since we also included those who, in fact do not have any thyrohyoid fractures in this analysis (the first step), only the substantially large sample provided insight into these statistical significances – firstly we can see (in Table 4.1.2) that "statistically significantly more frequent" holds true but was not an overt and straightforward observation: in atypical hangings, in fact, only c. 30.0% of subjects (about every third case) had a unilateral GHH fracture compared to as much as 23.3% of typical hanging (about every fourth case), while the simultaneous fractures of GHH and STH, although significantly more common in atypical hangings, were present only in every fifth subject with atypically positioned knot (compared to 15.6% frequency observed in typical hangings). However, these differences were much more appreciable in Dataset II of the first study part, where the cases without any thyrohyoid and cervical spine fractures were excluded. Here, the same statistically significant frequency differences in fracture patterns were present between the typical and atypical hangings, but the ratios were different: every second hanging case with the atypical knot position had the unilateral fracture of the hyoid bone's greater horn, compared to about every third subject (38.1%) with the typical knot position. Furthermore, every third atypical

hanging case (34.1%) had the simultaneous fractures of GHH and STH, compared to every fourth one (25.4%) with the typical knot position. On the other side, in every second typical hanging case, there was an isolated fracture of the thyroid cartilage superior horn(s) (48.7%), which was, at the same time, observed in every third case of the atypical hanging (33.2%) (for counts see Table 4.1.2).

How these non-so obvious differences could remain undetected is best observed when looking at the subset of this large sample, which was used in the second part of the study (Dataset I-w). Here, in the 368 analyzed cases of hangings, most of the significant associations were lost – the only statistically significant difference in thyrohyoid fracture patterns between typical and atypical hangings was observed in the frequency of the unilateral fracture of the hyoid bone's greater horn – it was present in every third case of the atypical hanging (33.3%) compared to about every fifth case of the typical hanging (21.8%); when excluding cases without any fractures (in Dataset II-w) these proportions were more obvious and comparable to those in Dataset II of the first study part – GHH fractures were present in every second case with the atypical knot position, and in every third case with the typical knot position (Dataset II-w, part II of the study, see Table 4.2.2). In this smaller sample, only the exclusion of the cases without the fractures revealed the significantly more frequent isolated fractures of thyroid cartilage's superior horns in typical hangings compared to atypical ones (49.2% vs. 35.1%, respectively). Ultimately, in the third part of the study this thesis comprises of, there was no observable statistically significant association of the coded variables (thyrohyoid fracture patterns) with typical or atypical knot position (see Table 4.3.2, Datasets I-m and II-m).

It was emphasized earlier that intravital cervical spine fracture in hanging, although of extremely low prevalence, may be very useful in predicting the position of the knot in a noose [22, 43, 45, 128]. It is particularly associated with anterior hangings, and therefore with atypical knot position in general [43]. According to the data from the first study part, we can see that the cervical spine fracture was statistically very significantly associated with atypical knot position, where it was present in 6.4% - 10.0% of cases (depending on if the cases without fractures were considered, i.e., Datasets I or II), which was much more frequent than in typical hangings (1.4% - 2.3% of typical hangings), as shown in Table 4.1.2.

It should be considered that anthropometric characteristics of the sample, such as subjects' sex and age, may strongly influence the occurrence of the thyrohyoid and cervical spine fractures [2, 3, 9, 43, 46, 48, 51, 52, 58, 61, 67, 69, 70, 98, 100, 107, 111, 112, 128, 141–144], so this must be considered a strong confounding factor, and requires analysis with adjustments. The significance of sex in thyrohyoid complex fracture occurrence lies within the sexual dimorphism observed in morphology, thyroid cartilage calcification and hyoid bone ossification patterns [58, 60, 61, 70, 98, 143–145]. The morphology variations of thyrohyoid complex may influence the occurrence of fractures, such as the length of the hyoid bone, greater hyoid horns' steepness, and importantly the overall shape – so-called V-shaped hyoid bones fracture more often than so-called U-shape hyoid bones. Incidentally or not, these subtypes show sexual dimorphism, which makes factorial analysis adjustment more convenient [58–60, 63, 98, 143, 145]. The calcification and ossification pattern differences between males and females have been suggested but also some studies reported the more frequent thyrohyoid fractures in one sex than in other (there are studies with greater prevalence in males, and studies with greater prevalence in females) [58, 66, 68, 70,

110, 118] but there are also studies reporting no differences in the prevalence of these fractures [58, 107, 110, 146]. A recent meta-analysis did not reveal consistent patterns associated with age, but also sex, suspension, and ligature knot position [51]. Whatever the case is, it is recommended to consider subjects' sex in a multifactorial analysis, which this research did take into account. More importantly, a subject's age is easily the most significant single anthropometric factor that can affect the thyrohyoid complex and the cervical spine fracture occurrence [58]. Aging leads to calcification, ossification, reduced elasticity, increased brittleness and easier fracture occurrence [48, 52, 58, 130, 142, 143, 147]. Whatsoever, it is usually only after the age of 20 years that the hyoid bone's corpus and greater horns fusion starts to happen [48, 58, 61, 143]. The latter can affect both the occurrence of the fracture and the misinterpretation of the unfused horn hypermobility on autopsy (a false positive finding). The former was considered when the statistics were done, while the latter was avoided by the uniform neck autopsy procedure and supervision by experienced forensic pathologists in this research. The thyroid cartilage calcification begins earlier in males, culminating by the end of 6th decade of life, while in females, calcification occurs more slowly and is not complete [48, 58]. The thyroid cartilage morphology slightly alters with age, which may influence the distribution of the applied force and thus, potentially, the fracture occurrence or even fracture patterns [48, 58, 61, 143].

In the literature, the cutoff value for thyrohyoid fracture occurrence comparison was often set at 40 years of age [51, 58]. So, we conducted the same analysis in all datasets in all three parts of this study. In all three study parts, the thyrohyoid complex fractures occurred significantly more frequently in subjects older than 40 years of age than in younger subjects. When considered separately, GHH and STH fractures showed the same trend, but only in GHH fracture occurrence there was a significant association; this consistency was observed throughout all the study parts. The cervical spine fracture also occurred significantly more often in subjects older than 40 years of age, but this was not observed in all datasets – most likely due to the very low prevalence of this injury in hangings and, thus, in the analyzed subsamples. A very important fact, as well, was that all the groups that were compared (based on the knot position) had an equal distribution of subjects older and subjects younger than 40 years of age.

Considering the largest sample in this research (Dataset I, study part I), when all hanging cases were considered combined, of all the thyrohyoid and cervical spine fractures, age was the best predictor for cervical spine fracture occurrence. Based on the ROC curve analysis, the data from 1,235 short-drop hanging cases suggest that the cutoff age of 64.5 years or more is a good predictor for the presence of cervical spine fracture (AUC of 0.709, 95% CI 0.639 – 0.779) with a threshold sensitivity of 65.9%, and specificity of 70.6%. The statistically significant prediction of thyrohyoid complex fractures overall and GHH fractures alone was also observed, but these predictions were less accurate. Age of ≥ 36.5 years indicated the presence of thyrohyoid fracture with a sensitivity of 85.7% and specificity of 27.0%, while the age of ≥ 37.5 years indicated the presence of hyoid bone's greater horn fracture with a sensitivity of 87.8% and specificity of 25.6% (see Figure 4.1.1). In the remaining two study parts, the age showed a statistically significant association with overall thyrohyoid fracture occurrence and GHH fracture occurrence if considered separately (Figures 4.2.1, and 4.3.1), but the cutoff for the GHH fractures was slightly higher – in the early fifties. No association was observed between the subjects' age and the occurrence of the thyroid cartilage superior horn fractures in all study parts. These findings contradict the report of Zátopková et al.,

who showed a significant association between age and STH fractures but not between age and GHH fractures [58]. However, our findings can be explained by the fact that the mean subjects' age was over 50 years, the age when the ossification of the hyoid bone culminates, particularly in males, who comprised three-quarters of our sample. So, this crude analysis of age contribution on the neck solid structures fractures, as well as referenced literature data, invariably requires the abovementioned thyrohyoid fracture patterns to be interpreted with regards to the subject's age and adjusted for this variable.

The discussion on the subjects' age importance is even more significant if we consider that there was a statistically significant difference in age between the compared groups, where we discovered some fracture patterns associated with the atypical knot in a noose position. As can be seen in Table 4.1.2, subjects in whom the knot was in an atypical position on the neck were slightly older than subjects whose knot was in a typical (posterior) location (a considerable confounding!). Not surprisingly, age showed a significant association with atypical knot position on univariable logistic regression analysis. So, the multifactorial analysis provided more exact and reliable fracture patterns (see section 4.2.1). Therefore, after considering age and previously commented significant fracture patterns (unilateral GHH fracture, simultaneous GHH and STH fractures, cervical spine fracture, and isolated STH fracture), the multivariable logistic regression analysis revealed that the associated variables with atypical knot position were only unilateral fracture of the hyoid bone's greater horn and the cervical spine, but both independently of subjects' age and independent of the presence or absence of simultaneous STH and GHH fractures, as well as of isolated STH fractures. The odds for unilateral fracture of the hyoid bone's greater horn were c. 37% higher to occur in atypical, compared to typical hangings, while the odds for the cervical spine fractures were as much as 4.3 times higher than in typical. This was observed in Dataset I, where the cases without any fractures were included. If these cases were excluded (Dataset II), the same pattern was observed, and not surprisingly, with a slightly higher odds ratio. It should be noted that, however, the wide confidence interval still suggests that these associations (i.e., patterns) are not so evident in a daily case-to-case practice analysis. This is further well demonstrated in the second study part, with a significantly smaller sample size – in Dataset I-w, none of the "significant" fracture patterns was independently associated with the atypical knot position when adjusted for the presence of other mentioned fractures. Ultimately, in the third study part, conventional statistics did not reveal any statistically significant fracture patterns to discriminate between typical and atypical knot positions (Tables 4.3.2, and 4.3.3).

Further step-by-step analysis on thyrohyoid and cervical spine fractures considered possible pattern differences between anterior atypical hangings and lateral atypical hangings. These can be most appropriately appreciated only from the first part of the study (Dataset III) since the second study part (Dataset III-w) and the third study part (Dataset III-m) each comprised less than ten anterior hanging cases included in these subsets (eight and six cases, respectively; Tables 4.2.1, and 4.3.1). The most striking and statistically significant discriminator was the cervical spine fracture, present in 40.7% of cases with anterior knot position, compared to only 4.2% of cases with left or right lateral knot position (Table 4.1.2). Additionally, isolated and unilateral fractures of the thyroid cartilage's superior horns were more frequent in lateral than anterior hangings, with more STH fractures occurring in lateral hangings. When these variables were adjusted in multivariable logistic regression analysis, the cervical spine fracture essentially remained the only but strong independent predictor

of anterior knot position, with an odds ratio of c. 10 (95% CI 4.032 – 25.588). This association was even apparent in the second part of the study, despite only eight anterior hanging cases being compared to 106 lateral hanging cases (Dataset III-w).

Finally, the last and fourth step of each part of the study was a comparison of lateral hanging cases to find associations of fracture patterns with left or right lateral knot position, or more precisely, to discriminate between the left and the right lateral hangings. The straightforward and interesting finding was the association of the left GHH fracture and right STH fracture with the left lateral knot position (Table 4.1.3). The frequency occurrence of these fractures was not with too overt differences (frequency proportions of about 40% vs. 30% for both cases), and the odds ratios on multivariable analysis were c. 90% higher, but this may be an important finding in the context of machine learning analysis later considered. The unequal occurrence of the STH fracture contralateral to the knot position was observed in the smallest sample of this research – in Dataset IV-m of the study part III (Table 4.3.3) but this can be explained by a much smaller sample where this kind of discrepancy between two biomechanically mirror-imaged groups could happen by chance.

It should be highlighted that before we turn to machine learning algorithms, we need to reflect on the potential contribution of two additional major anthropometric factors not considered above – subjects' body weight and body height, to thyrohyoid complex fracture occurrence and thus the fracture patterns. Both factors, body weight, and height, could influence fracture occurrence indirectly but similarly by impacting the amount of force a noose applies to the neck [51, 53, 58]. When a person initiates suspension, the body or, more precisely, *the neck* falls *freely* until the ligature constricts it, tightened by the gravitational drag of the own body (whole body or a part of it) [6]. Presuming the person is not lying down (that is, a force is generated solely by the weight of a head), even in incomplete hangings, the heavier subjects will thus "generate" greater compression force than the lighter subjects for a given drop length. The body weight contribution seems straightforward. But how can the body height influence the force constricting the neck? One assumption can be that in taller people, the distance the neck travels before it completely stops due to the tightened loop is longer than in shorter people. Imagine a short-drop complete hanging context in which two subjects, one taller than the other, will invariably have a fool suspension. Each person climbs on a chair that is on the same level and puts a loop that is at the end of the ropes of the same length. The taller person will have a higher starting point at the beginning of the drop than a shorter person, but both will have the same endpoint, and the neck of the taller person will have a longer drop. On the other hand, if two people of the same height are in the previous situation, the heavier one will obviously generate a greater potential energy during the "free fall". So, between these two scenarios, which variable – weight (i.e., mass load) or height (i.e., drop length) would be of more importance? Figure 5.2. shows an illustrative example of ten cases of two short drop hanging scenarios. In one scenario the hanged subject body weight is constant while the drop length is variable, while in the other scenario the drop length is constant, and the body weight is variable. When the generated work (W) is calculated, it seems that the change in a drop from 2.5 cm to 50 cm forms a steeper increase in generated work than an increase in mass load to the neck from 10 kg to 100 kg. In this manner, the scenario covers various body weights and therefore diverse types of incomplete hangings – the different proportional weights are considered to cover a range of partial suspensions (e.g., lying, kneeling, sitting, standing). But these are all theoretical considerations. What does the evidence from research point?

The answer to this question also explains why the entire first part of the study in this thesis did not consider body weight, but its results can still be argued as valid. It has been experimentally demonstrated that for a fracture of the superior horn of the thyroid cartilage, the force generated needs to be about 30 N, which corresponds to a load of only 3 kg [99]! This was shown by Bockholdt et al. on more than 120 thyroid cartilage samples. There were some differences in samples from males and females – the critical force for an STH fracture to occur was higher in men by c. 6-7 N, corresponding to the load of c. 600-700 g [99].

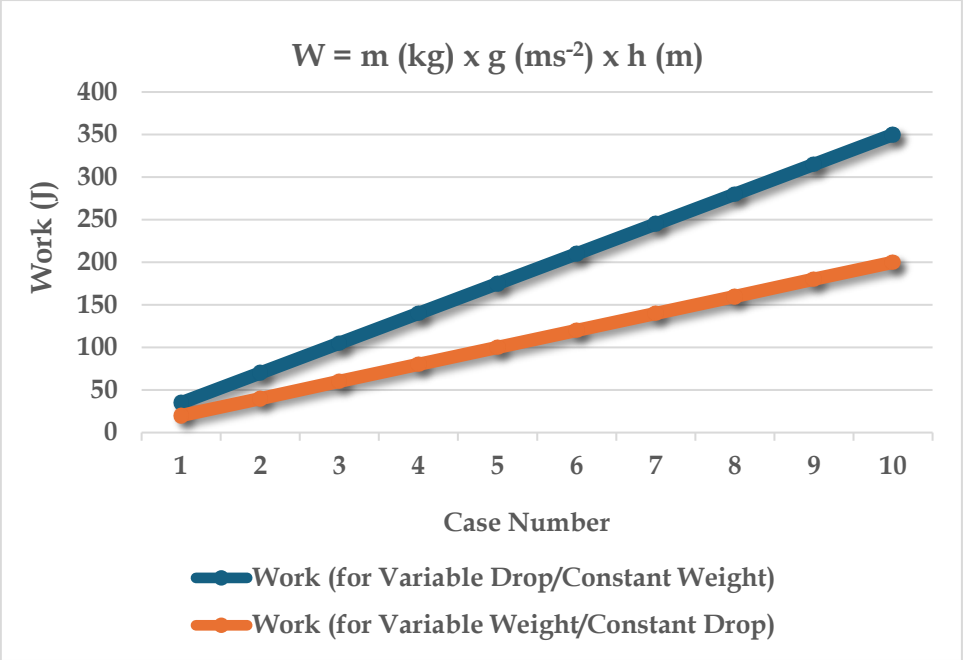

Figure 5.2. *The change in generated work (in Joules), depending on:*

The blue line *– the change in a drop length – the free fall of the person's neck, starting from the drop of 5 cm (Case 1), and increasing it by 5 cm until 50 cm is reached (Case 10), for a constant weight of 70 kg.*
The orange line *– the change in a weight load – increase in the load, starting from 10 kg (Case 1), and increasing it by 10 kg, until 100 kg is reached (Case 10), for a constant drop length of 20 cm.*
Abbreviation: *g – gravitational force (a constant).*

This is another reason for sex to be considered a confounding factor and included in the multifactorial analysis, including the machine learning models. The data on hyoid bone's greater horn critical load for a fracture to occur could be similar, again approximately about 3 kg [147]. On fresh thyrohyoid samples, experiments, however, by Travis et al. showed that loads needed to be several times greater than these 3 kgs – between about 14 kg and 19 kg [148]. Leberton-Chakour et al. experimentally demonstrated that a crushing force of 30.55 ± 18.189 N, or, again, a mean load of about 3 kg, is enough to cause a GHH fracture [147]. They also found some correlation between the anthropometric characteristics other than sex and age – body weight and body height that were associated with variability of hyoid bone shape, and thus probably and indirectly the fracture susceptibility. Although they discussed manual strangulation and hyoid bone fracture, their comment can be significant in the context considered here – a force necessary to generate a GHH fracture. They state the following: "*The forces measured in our study showed that the grip strength of an individual, man or woman, with no motor deficiency, is generally sufficient to generate a fracture of the hyoid bone by direct pressure. These findings tend to show that to produce fracture, the pressure required is at least 1.5 greater than simple, sustained grip pressure* [147]." So, given that the head alone

generates a weight load on a neck that is greater than 3 kg (about 5 kg, on average in adults) [6, 12, 21], we can argue that in short-drop hangings, including majority of incomplete hangings, enough force is directly applied on some point of the neck to cause a thyrohyoid complex fracture – therefore, a position of the loop (and the knot) should define this highest pressure point and cause a distinct fracture pattern [21, 135].

However, some studies on hanging cases suggested that fractures tend to occur almost exclusively in those weighing more than 50 kg and that occur significantly more often in overweight and obese subjects (based on the Body Mass Index – BMI) [57, 118, 128]. This year, Commins et al. published an article reporting the analysis of the association between body weight and body height with the occurrence of thyrohyoid fractures [53]. For this issue, they considered exclusively complete hangings. This, in fact, could be quite a similar scenario to the one theoretically considered in this discussion and shown in Figure 5.2. What the study results suggested by logistic regression analysis was that for each increase in body weight unit (i.e., for each additional kg of weight), the odds for the occurrence of the thyrohyoid fractures increased by about 1.7% (OR = 1.0166) or, if the BMI was considered, for each BMI unit increase, the odds for fracture increased by about 6.1% (OR = 1.0607) [53]. Additionally, regarding the body height contribution, the authors reported that the odds ratio for thyrohyoid fracture to occur for each unit increase in body height was 4.64 [53]! However, two critical things remained unclear – the authors did not state if the analysis considered height in meters or centimeters and did not report the p-value of the logistic regression analysis but reported only wide 95% CI, with the lower interval being < 1, thus indicating no statistically significant association (reported 95% CI was 0.29 – 73.95) [53]. Eventually, they did not perform multivariable analysis after these findings, and it remained unknown if the variable adjustment would yield a more definitive answer.

Therefore, we conducted a study, part II here, to investigate if there are any associations between body weight and height with the thyrohyoid complex and cervical spine fracture occurrence, and in this manner, a contribution to the fracture patterns with regards to the position of the knot in a noose. The information on the body weight was available only in some hanging cases and was omitted in study part I to form a sample with complete data, mainly in order to create a representative sample for machine learning analysis. So, as the information on body weight for subjects autopsied at our Institute was available from the end of the year 2014, we included all the relevant cases in the second part of the study, comprising a total of 368 hanged subjects.

The sample of Dataset I-w was derived from Dataset I (first study part) and, therefore, had a significant overlapping characteristic, which is a good element for results comparison, as previously discussed. We already commented that in this second part of the study, the age remained the good predictor of general thyrohyoid complex fracture occurrence (cutoff value was the age of ≥ 41.5 years), and for GHH fractures alone (cutoff value was the age of ≥ 52.5 years – more than 10 years higher than in the first step – note the difference in the ratio of sensitivity and specificity on ROC curve analysis) but here the focus was on the body weight and height. While body height did not show any significant correlation with the number of thyrohyoid fractures in general, nor was it a predictor of their presence, the body weight did show some statistically significant association. To be precise, body weight was a predictor of thyroid cartilage's superior horn fracture presence, with a determined cutoff value of ≥ 72.5 kg showing sensitivity of 51.1% and specificity of 61.6% (i.e., correctly

detecting approximately every second case). But weight did not have any association with GHH and cervical spine fracture occurrence. The same observations were detected in our smallest subset, in Dataset I-m of the study part III (Figure 4.3.1). Here the predictive value was slightly different for STH fracture occurrence, with better ROC curve analysis performance for a cutoff value of ≥ 65.5 kg, with a sensitivity of 74.6% and a specificity of 52.5%. Although we showed some correlation between weight and STH fracture occurrence exist, we must highlight that these correlations were essentially negligible ($\rho = 0.139$, $p < 0.05$ in Dataset I-w, and $\rho = 0.197$, $p < 0.05$ in Dataset I-m). Nevertheless, having in mind experimental data, autopsy studies, and the results reported here, this variable should be considered in multivariable analyses and particularly in machine learning model development, in a tool capable of detecting non-obvious associations and regularities (see further) [75, 76, 78, 80, 94].

The final set of variables that were considered in this research were the characteristics and distribution of the soft-tissue hemorrhages, sometimes detected at the periosteal surface of the sternocleidomastoid muscles (SCM) origin at the clavicles. These are considered one of the most common autopsy findings on autopsy of deaths by hanging and could, therefore, be a significant tool in knot position assessment [2, 3, 40, 54, 149]. While the first part of the study was directed solely to thyrohyoid complex and cervical spine fractures, and the second part of the study additionally considered body weight and body height, this third and final part of the study aimed to assess the significance of these SCM muscle hemorrhages regarding the knot in a noose position. The issue here is the fact that, in contrast to straightforward fracture detection on autopsy, the presence of the hemorrhages is more prone to subjective interpretation, regarding both its presence at all and the extent. Therefore, the cases were carefully selected and included only if the presence of the macroscopically visible hemorrhages was unambiguously established and described directly on autopsy or by the revision of autopsy photography documentation. Although the smallest of all the samples in the present research (main sample of 126 cases and smaller derived subsets), presence of these hemorrhages was observed in more than 85% of cases.

Contrary to the previously analyzed variables (fractures and anthropometrics), the distribution pattern of these hemorrhages was already relatively clearly described, particularly in lateral hanging cases [40, 149]. Keil et al. [149] and Hejna & Zátopková [40] demonstrated that hemorrhages were more often present at the side of the knot (i.e., the highest point in lateral hangings, where "*the strain at the points of clavicular attachment of sternocleidomastoid muscles*" is highest [40] on suspension and due to the "*forced lateroflexion of the head*." Since these hemorrhages are present in other types of hangings, he suggested that the additional mechanism for the appearance is "*forced dorsiflexion of the head in cases of anterior hanging*" [40] – these tend to occur bilaterally often if the knot is placed anteriorly. Our results correspond very well with these conclusions. In Dataset I-m, their presence and distribution did not aid in crude comparison between typical and atypical hangings. But, when the anterior knot position was compared to the lateral ones, it was demonstrated that in the former the total number of these hemorrhages was significantly greater than in the lateral ones (medians of 2 vs. 1) directly pointing that most often, in anterior hangings there are bilateral SCM hemorrhages (seen in 83.3% of anterior hangings compared to 38.5% of lateral hangings, despite the insignificant difference on a Fischer's exact test – the sample of anterior hanging cases was too small). Moreover, in lateral hangings, where unilateral SCM hemorrhages occurred in every second case (53.8%) while bilateral SCM hemorrhages were

present in about every third case (38.5%), a statistically significant association was detected with the hemorrhage ipsilateral to the knot position (i.e., the left SCM hemorrhage in the left lateral hangings) (Table 4.3.3). Considering this with thyrohyoid fractures, it should be noted that in Dataset IV-m, in lateral hangings, the unilateral STH fracture contralateral to the knot's position was significantly more frequent in the left compared to the right lateral hangings (Table 4.3.3). Having in mind patterns recognized in the first study part (Dataset IV), we can argue that this is a consequence of the much smaller sample (in Dataset IV-m), with an incidental grouping of these cases into one group (simply by chance).

Our results differed from Hejna's & Zátopková's in one segment. They did not detect any association with sex, age, and body weight regarding the SCM hemorrhage presence [40]. In Dataset I-m, body weight was a statistically significant predictor of SCM hemorrhage occurrence – those weighing 67.5 kg or more were most likely to have these hemorrhages. This cutoff value had a predictive significance with a sensitivity of 62.0% and a specificity of 66.7% (AUC 0.639, 95% CI 0.505 – 0.772, Figure 4.3.4). From this cutoff value, it may seem that a greater mass load is required to produce SCM hemorrhages than some thyrohyoid complex fractures, but we should remember that these were observed in at least 8 – 9 of 10 subjects, while the overall prevalence of thyrohyoid fractures was less than that (Tables 4.1.1, 4.2.1, and 4.3.1). To be precise, in Dataset I-m of the third part of the study, body weight was a statistically significant predictor only of STH fracture occurrence, with a determined cutoff value of ≥ 65.5 kg (sensitivity 74.6%, specificity 52.5%). Despite almost identical cutoff values of the subject's body weight for STH fracture occurrence and for the occurrence of SCM muscle hemorrhages, the latter was c. 30% more common in the sample. Besides the fact that this was the smallest sample in the entire research, a possible explanation could be that SCM muscles are superficial but initially absorb a more significant portion of the kinetic energy than structures of the thyrohyoid complex. Moreover, the elastic properties of the skeletal muscles significantly differ from those of bone and cartilage, and this may be a straightforward explanation. But this should be explored in further studies and adjustments for the knot position.

Only after detailed consideration of all the characteristics of the sample we can now turn to the final and crucial part of the thesis – do machine learning models supplement the conventional statistical analyses in the knot in a noose prediction, and if so, do they suggest any additional conclusions regarding the decision-making process for a forensic pathologist, and do they point to additional significant associations between analyzed variables? Answering these questions was the main reason for a specific three-part study design. In each part, a uniform sample with absolutely complete data of interest (i.e., the coded variables) was formed and was as large as possible for this single-institutional research. The first part focused on the sole assessment of thyrohyoid complex fracture distribution in relation to the knot in a noose position, considering only the subjects' age as an additional input. The second part complemented the previous analysis by adding information on each subject's body weight and height. The third part of the study further broadened the inputs by adding information on the presence and distribution of SCM muscle hemorrhages at their origins in the clavicles. So, on the one side, we could evaluate if providing the additional inputs could improve the predictive capabilities of the machine learning models and see if, in the same datasets, analogous models where some variables were omitted (e.g., body weight and height) preserved the same or very similar classification performances. The only unfortunate thing was that while increasing the input,

the total sample size decreased. However, the inclusion of only relevant cases with complete data lies behind this fact, and it is one of the most important parts of the machine learning models development process.

Technically, the ultimate goal is to provide an input on detected neck organ fracture distributions, and some of additional information (sex, age, weight, height), and to expect a multiclass output: there are four possible outcomes – knot located on a posterior, anterior, left lateral or right lateral side of the head/neck. Regarding the design of machine learning models, it should be highlighted that we did not approach the solution by creating multi-class output: the four-class output of a single model, according to the four defined knot positions (anterior, posterior, left lateral, or right lateral). We instead defined a "stepwise" decision-making process. Since the process in the first study part represents the most complete one, that was later replicated and "pruned" in the second and the third part of the study, we will discuss the issue here on study part I. The stepwise decision-making process in machine learning classification meant that initially (ML models for Datasets I and II) the goal was to discriminate between cases of typical (knot located posteriorly) and atypical hangings (knot located anteriorly or laterally), and then to separately try to differentiate between anterior and lateral knot positions (Dataset III), or only between left and right lateral knot positions (Dataset IV). In the first part of the study, except for Dataset III, this provided a relatively large number of cases with a well-balanced distribution among the two outcome possibilities (the knot positions, Supplement A). The Datasets I and II differed, as already explained, in a manner that in the latter, the cases without any fractures were eliminated: if there is no event in any classes to be observed, it may strongly underestimate the true power of a model to correctly classify it from a set of same defined events.

Additionally, with a small number of fracture pattern characteristics detected by "conventional" (standard) statistics in mind, it was first decided to include all coded variables as available inputs for models' development. This, of course, increased the possibility of developing models that overfit the data on training [75–77]. One step in avoiding this was the set inclusion condition – for any model to be accepted, there must not be a statistically significant difference in ROC curves between the training and the test sample based on the outcome-predicted probabilities for each sample. Of course, this was a single metric, but it was an important supplement to other reported metrics of models' performance characteristics [76]. Regarding the sample splitting into training and independent testing divisions, it should be noted that before modeling, each dataset engaged in machine learning analysis was divided into a portion of 70% of cases for training the model and 30% of cases for testing the developed model. Again, to avoid the overfitting and to enable comparison of the performance characteristics of different machine learning algorithms, another condition was made – the training and test samples were pre-defined and did not have any statistically significant differences in the coded variables characteristics in-between (see Supplements for each study part). Except for the Naïve Bayes models developed in SPSS, which could not be set to use these pre-defined training and test sample divisions (it always automatically performed random sample splitting), all other developed ML models in all three study parts were trained and tested on the same samples described in the Supplementary tables. As a rule, many machine learning models presume the prevalences of different outcomes are similar ("50-50 chances") [75–77]. In the first part of the study, the frequency of the analyzed outcomes was similar in Datasets I, II, and IV, and the data did not need to be balanced. But, in Dataset III, the SMOTE algorithm was used

to oversample the minority group (atypical hangings), while in the second part of the study, a small number of SMOTE-generated cases of atypical hangings were added into the initial dataset – here not only to balance out the outcome frequencies but also to increase the total sample size slightly. As the Dataset I-m of the third study part was small, compared to the previous parts of the study, and outcome frequencies were balanced, the SMOTE-based oversampling was avoided – it would not be appropriate for SMOTE-generated cases to be a majority in the test sample.

Furthermore, in addition to developing several different machine learning algorithms (e.g., neural networks, k-nearest neighbors, decision trees), this research involved the development of two quite similar artificial neural networks – one using MATLAB, which automatically optimized model's hyperparameters by genetic algorithm, and the second, Multilayer Perceptron – Artificial Neural Network, developed in SPSS. Although comprising a similar algorithm, the optimization by genetic algorithm theoretically leads to better hyperparameter optimization than partially manual, more time-consuming with fewer modeling attempts – optimization performed in SPSS [79, 80, 84, 85]. So, in addition to analyzing different algorithms, we could compare two artificial neural networks developed in different software solutions using different optimization methods.

Once the models were developed, their classification performance was assessed through several metrics (for example, overall accuracy, sensitivity, specificity, positive and negative predictive value, and ROC curve analysis) [76]. While the ROC curve analysis was performed on the predicted outcome probabilities (for each case, a probability ranges from 0 to 1), the other classification metrics were calculated based on the predicted group (binary outcome, e.g., typical or atypical hanging). The cutoff for this dichotomous classification was not modified – it remained at a probability of 0.5. Therefore, we provided classification performance based on this cutoff value, but reported the classification metric which is not dependent on this binary outcome, too – the ROC curve analysis on predicted outcome probabilities, making the interpretation more flexible [76].

The first part of the study had a complete four-step approach in machine learning-based reconstruction of the knot in a noose position: in the first two steps discrimination between typical and atypical knot positions, in third step discrimination between anterior and lateral knot positions, and in final, fourth step a discrimination between left lateral and right lateral knot position. In the second study part, the analogous analysis was performed only on the first two steps (discrimination between the typical and atypical knot positions), while in the third part of the study only the first step was applied, being limited with the significant decrease in sample sizes. And, instead of considering each study part separately, it may be clearer to "vertically" analyze machine learning models – comparing first steps in each of the three study parts (Datasets I, I-w, and I-m), then turning to the second steps in the first and the second part of the study (Datasets II, and II-w, respectively), and, at the end, considering the exclusive analysis of the first part of the study – machine learning models developed on Datasets III and IV, and discriminative power in atypical and only lateral hanging cases, respectively. The focus should be on the models' classification performances, variable selections, and their importance, to extract some practical conclusions.

The first step in each study part regarding the machine learning models was to develop – train, and then test them on a sample that also contains cases without any fractures of the

thyrohyoid complex or the cervical spine. The high expectation was on the performance in the first part of the study, in Dataset I, which was the largest of all (1,235 cases included), with a well-balanced outcome frequency. Here, the overall accuracy of essentially all developed models (ANN optimized by genetic algorithm and models developed in SPSS – MLP-ANN, k-NN, DT, and NB) was c. 60.0%, which is about the proportion of the typical hangings in Dataset I. What first meets the eye is that these models' decision-making processes may be equivalent to guessing based only on the knowledge of outcome prevalences in the sample. However, this approach would mean that the model predicts the same outcome (e.g., typical knot position) for all cases in training and test samples, thus yielding an overall accuracy of 60%. However, this would lead to a "test" with a sensitivity of 100% and a specificity of 0%! If we look at Table 4.1.4, and Table 4.1.8, we can see the developed models did not perform this way. What differed between the models most strikingly was the balance between the sensitivity and specificity, and other calculated metrics. For example, in these terms, artificial neural networks did not surpass the performance of the multivariable logistic regression analysis (Table 4.1.8), but, on the other hand, the k-Nearest Neighbors model showed more balanced values of the test sensitivity and specificity. In Dataset I of the first study part, almost all developed models could generalize from training to independent test samples without evident signs of overfitting [76]. Furthermore, even in the test sample, the ROC curve analysis had a lower 95% confidence interval above 0.5 (indicating a significant predictor), and based on calculations from contingency tables, the overall test performances did not have a lower 95% confidence interval below 50%. So, in general, as a first attempt to utilize machine learning algorithms in predicting the knot in a noose position solely by the distribution of thyrohyoid and cervical spine fractures and subjects' age, the results of this analysis can be considered satisfactory. Also, it should be noted that there was no statistically significant difference in the ROC curve of GA-optimized ANN developed in MATLAB and the ROC curve of MLP-ANN developed in SPSS on the same sample – Dataset I (Figure 4.1.3). So, we can say that less systematic experiments on MLP-ANN development in terms of hyperparameter settings successfully met the "standard" of systematic hyperparameter settings achieved through genetic algorithm optimization. Another characteristic of ANN developed in MATLAB is that the script provides output on the variables selected for the best-developed ANN (the one reported in this research). Looking at these, we can see the GA-optimized ANN in Dataset I achieved the reported metrics by considering only six of thirteen available variables – inputs, including sex, age, and variables considering the number and distribution of only GHH fractures. But remember that even on a conventional statistical analysis, a unilateral GHH fracture was a significant discriminator between the typical and atypical position of the knot and that this needed to be adjusted for age on multivariable logistic regression analysis (see section 4.1.1.1)! The models developed in SPSS for discrimination between typical and atypical hangings in Dataset I of the first study part also highly ranked the importance of some variables recognized as significant in conventional statistics (Table 4.1.12). For example, cervical spine fractures and the simultaneous presence of STH and GHH fractures. The not-so-comprehensible concept of the variable importance in ML models will be commented on later. For now, we can say that these selected variables can suggest the models did not achieve the reported metrics simply by chance, that the generalization to the test sample was good, and that similar performances were achieved by different approaches (that is, different models ranked coded variables differently regarding their importance), and some models did this despite the presence of irrelevant data "noise" (non-associated – irrelevant variables) [75, 76, 94].

Considering the same type of analysis in the second part of this study (analysis on Dataset I-w) firstly and directly should be highlighted that the developed machine learning models did not perform better if they considered subjects' body weight and height (Tables 4.2.4, and 4.2.6, and Figures 4.2.6, and 4.2.7). Two facts, however, should be additionally clarified. First, the overall accuracy of the models was lower than in Dataset I (study part I); the lower 95% confidence intervals of the accuracies were almost always under the threshold of 50%, and the intervals were wide, and the lower 95% confidence intervals of the ROC curve analyses in most developed models were below the threshold of a 0.5 on AUC analysis – indicating a questionable overall predictive value of the developed models. And second, this was the only segment of the present research in which a statistically significantly different classification performance was observed between the artificial neural network developed in MATLAB (GA-ANN) and analogous neural network developed in SPSS (MLP-ANN) (Figure 4.2.5).

To assess the contribution of body weight (and height) for machine learning models' improvement in classification (knot position estimation) probably, a good approach is to develop two analogous models on the exact same dataset (including these variables in one while omitting them in the other). This is precisely what was done in this research, rather than directly comparing the models from different parts of the study. This also provided the opportunity to statistically-mathematically compare classification performances (areas under the ROC curves) of the two analogous models (one that considered weight and height and the other that did not). So, this was used as an objective measure to detect significant improvements or worsening of models' classification performances. If done otherwise, the differences in other metrics could be easily misinterpreted as an improvement. For example, there is a better balance of sensitivity and specificity in Dataset I-w than in Dataset I (see Tables 4.1.6, and 4.2.6).

The concept in machine learning model development for Dataset I (part I of the study) and Dataset I-w (part II of the study) was technically identical, but by forming the Dataset I-w, the total number of cases was decreased by more than three times (from c. 1200 to c. 380 cases). Of the included cases, a portion of them did not have any thyrohyoid or cervical spine fractures (this may have contributed to the underestimation). Moreover, the models that considered the body weight and body height had two more input variables, potentially causing additional noise of irrelevant information for models to handle, all on a smaller sample. Hence, a slight decrease in performance metrics was expected. All of this contributed to wider confidence intervals estimates (i.e., less precise estimations).

Of the developed models, the most robust to these changes were MLP-ANNs, the one which considered subjects' body weight and height, as well as the analogous one for which these two variables were omitted. These two ANNs showed the best classification performances, without a significant difference between them, even with the ROC curve analyses like those achieved in the first part of the study (Table 4.2.6, Figure 4.2.7). Only in these two models did the algorithm manage to generalize the classification ability from the training to the test sample [76], which preserved statistically significant predictive ability on the ROC curve analysis (the lower 95% confidence intervals remained greater than 0.5, Table 4.2.6). These models had almost identical overall accuracies as the multivariable logistic regression analysis but showed more balanced sensitivity/specificity metrics (Table 4.2.6) Additionally, the ANN that did not consider body weight and height was developed,

optimized by genetic algorithm, with a very similar performance metrics (there was no statistically significant difference in area under the ROC curve analyses for predicted outcome probabilities compared to the analogous MLP-ANN algorithm, Figure 4.2.6, and 4.2.7). This GA-optimized ANN considered only six variables when predicting the knot position (sex, cervical spine fracture, total number of thyrohyoid fractures, isolated and unilateral STH fractures) – the optimization eliminated many irrelevant variables. On the one side, we see the GA-optimized ANN "canceled out" the noise of many irrelevant information-variables by excluding them, and on the other, the analogous MLP-ANN (SPSS) successfully handled all the input variables to provide the same classification performances in the experiment without the body weight and body height despite the same "noise" (Tables 4.2.4 and 4.2.6, and Figure 4.2.5). However, out of GA-optimized ANNs, which took into account the body weight and body height variables, the selected model (i.e., the best one developed) did not perform better and included 13 input variables (more than double the analogous GA-ANN model did). Moreover, this GA-optimized ANN had a significantly worse classification ability compared to the analogous MLP-ANN developed in SPSS (which considered body weight), as shown in Table 4.2.4, and 4.2.6), and as can be observed by a direct comparison of the two models' AUC ROC curves (shown in Figure 4.2.5). One explanation is that the reported model, which considered the body weight variable, was included "by force" to demonstrate if this variable contributes to the better performance of a model or if it only produces the "noise" of irrelevant information to the model. The other can be that the experiment in SPSS was done on more optimal hyperparameter settings (achieved by chance) or the software automatically handled the numerous irrelevant variables better (which is also possible to occur by chance). Of note is that the developed models, if considered body weight and height, most often highly ranked their importance for prediction (Table 4.2.8), with some giving advantage to body height compared to weight (remember the theoretical examples from Figure 5.2. – this could explain the phenomenon). On the other hand, the ML models in the second study part, if not provided with information on subjects' body weight and height, used primarily variables shown to be statistically significant for knot position discrimination in the previous (the first) part of the study. This was observed in Dataset I-w even though most of these significant associations were not present in the same dataset on the "conventional" statistical analysis – it is hard to believe that these have been selected stochastically.

How the data on body weight (and height) may be irrelevant in knot position assessment probably best shows the development of decision tree models. Aside from their low overall performance (Table 4.2.6) we can clearly see the overt discrepancy between the metrics achieved in the training compared to the test sample. Particularly for the model, which considered body weight and body height. The model, forced to use the information on subjects' body weight as a relevant, directly associated body weights of the subjects in the training group with the knot's positions. Once given the new, independent test sample, this caused a drastic deterioration of the classification performance – a very poor generalization capability. In fact, this was the only model in which there was a statistically significant difference in predictive capability in the training sample compared to the test sample. The other machine learning models developed on Dataset I-w showed satisfactory generalization [76] to the test sample but overall had lower accuracies and wide confidence intervals of the calculated accuracy and AUCs (Table 4.2.6).

So, it seems that taking into account subjects' body weight and height does not contribute to better prediction of the knot in a noose position, although in the same sample of this research, we saw some crude predictive significance of body weight to the occurrence of STH fractures. On the other hand, it was demonstrated that the presence and distribution of the SCM muscle origin's hemorrhages can assist in knot position estimation to some extent. So, it remains to be seen if the SCM muscle hemorrhages can improve the machine learning-based knot position classification performance. Following the same methodology for model development that was applied in the second part of the study (on Dataset I-w), the models were developed on the third part of the study, on Dataset I-m. These models were provided with additional variables – information on the SCM muscle hemorrhages but were at the same time developed on a yet smaller sample – of only 126 cases (see Supplementary Table C.1). Here, again, the most robust showed to be artificial neural networks. There was no statistically significant difference between the AUCs of the GA-optimized ANNs developed in MATLAB, and analogous MLP-ANNs developed in SPSS. However, we can see in Table 4.3.4. that the GA-optimization resulted in the highest overall accuracies (lower 95% CI was just below 50%), and more importantly, ROC analysis showed that these statistically were a significant predictor in knot position assessment (lower 95% CIs above the value of 0.5). Moreover, as was the case with MLP-ANN (SPSSS), the models generalized the classification ability from the training to test sample well. The GA-ANN selected a modest number of important variables (eight), amongst which were the body height, distribution and number of STH fractures, presence of simultaneous STH and GHH fractures, but also the distribution and number of SCM muscle hemorrhages. The analogous GA-ANN algorithm – model without information on SCM muscles, achieved very similar results by using only six variables, including age, body weight, and variables both on STH and on GHH fractures. It should be again noted that the study design with development of two analogous models of each ML algorithm (i.e., one considering SCM muscle hemorrhages, and other that did not have this input) provides better understanding of the variable's significance. If we would compare only model performances achieved in the first study part (Dataset I) with the performances from the third study part (Dataset I-m), we would overestimate the significance of additional variables since the overall accuracy of artificial neural networks in Dataset I-m were over 65% (vs. c. 60% in Dataset I). This might be a consequence of a much smaller sample with a grouping of some "easier" cases, but also, there might be some minor contribution of additional variables [75–77]. Although, we failed to demonstrate that this contribution is crucial, by developing analogous models in the same dataset with statistically same predictive capabilities. Moreover, the variables on SCM muscle hemorrhages were not amongst the top five variables ranked by importance in the reported MLP-ANN (Table 4.3.6). Of the models other than neural networks in the third part of the study, Naïve Bayes provided better results than others (k-NN and DT), but this should be interpreted with caution. As already explained, the settings in SPSS prevented the NB algorithm from constantly using manually predefined sample division into the training and test groups. The model automatically formed new groups each time in a defined proportion of approximately 70% to 30%.

So, considering the first step in machine learning algorithms development in all three study parts, the impression is that the artificial neural networks showed the best robustness but also indicated the classification performance did not significantly improve if additional anthropometrics (weight and height) and some autopsy finding other than presence and distribution of the neck fractures (i.e., SCM muscle hemorrhages) were considered. The next

step was to see if the inclusion of cases without any lesions to detect – the fractures strongly impacted the predictive capabilities of the models. So, the models developed on Dataset II (study part I) and Dataset II-w (study part II) comprised only cases with at least one thyrohyoid or cervical spine fracture. By doing this, the overall accuracy of all models in Dataset I (part I) increased minimally – by a couple of percent (all being around 62.0.% of overall accuracy). However, the sensitivity and specificity balance improved, which was particularly appreciable in both artificial neural networks (see Tables 4.1.5, and 4.1.8). In Dataset II, a similar trend was observed (Tables 4.2.4, and 4.2.7). Here, it was also observed that some models performed slightly better on a test than on the training sample, which should be cautiously considered. But let's remember the condition of the methodology was to include the models in which there was no statistically significant difference between the area under the ROC curve analysis in training compared to the test sample. What is more important when looking at Dataset II-w (part II) is that the models that considered information on subjects' body weight and body height did not perform better than the analogous model–algorithms without information on this variable. Thus, further indicating their low importance in knot position assessment by machine learning. Some algorithms (k-NN) developed a model (with the weight and height considered) with a slightly better overall accuracy than the analogous model without these variables (still, this was a statistically insignificant difference) but, as shown in Table 4.2.8, we can see that these variables were not considered to be among the top five most important of all the used.

While we can say that in the first two steps (discrimination between typical and atypical hangings), the machine learning models' prediction was modest, at most, the ability to correctly classify the knot position was much better in attempts to discriminate between anterior and lateral knot position (Dataset III), as well as discriminating between left and right knot position in a separate analysis of lateral hangings (Dataset IV), that was particularly good (first part of the study). The overall accuracies for discrimination between anterior and lateral hangings substantially increased to about 85.0% of correctly classified cases, which was also possible to achieve through multivariable logistic regression analysis. Given the imbalance in the sample Dataset III, the high accuracy of the developed models can, to some extent, be attributed to this limitation of the sample. However, in Dataset IV, with equal distribution of left lateral and right lateral hangings and with a low accuracy of the logistic regression model, a substantial result is the development of models with overall accuracies over 90.0% (Table 4.1.12). With no overt evidence of models' overfitting [76, 77], with good generalization from the training to test sample, we can consider these findings promising. But, having in mind a vast amount of information presented, the usefulness of metrics' characteristics alone and in combination with conventional statistics will be further discussed, pointing to some implications for practice and for future research.

There are two aspects on which the summary of the presented research should reflect – the practical implications and the additional academic significance this thesis provides. The application of these results directly in current practice is limited from the professional, medicolegal perspective. In cases where an expert opinion is not possible to confirm a single scenario (e.g., due to low test sensitivity), but to "only" exclude or significantly lower the probability of one of four possible events can be decisive. For example, an opinion that a thyrohyoid and cervical spine injury pattern in a body found hanged with an anteriorly placed knot in the noose, without evident ligature mark, is very unlikely to be a consequence of this hanging event (potentially a concealed homicide by neck strangulation, with later

simulation hanging of a dead body) can be supported by a highly specific test (that is, to exclude a single distinct scenario). The essential problem with machine learning algorithms is *the black box* concept – the inability to comprehend their decision-making process and underlying "rules" to make a same decision by a common sense, and therefore, these models can be considered untrustworthy [76, 77, 87, 90, 92, 93, 119]. Particularly as the case in our study is, with artificial neural networks, some k-NNs or NBs showing the best performances overall and /the first two) especially in lateral hanging analysis. And with a lack of consistent and broader evidence – with good reason. The black boxes, lacking argumentation comprehensible by forensic experts, not only limit the "courtroom" usefulness of ML models but also do not explain *per se* the decision-making process that can point to currently undefined biomechanics of thyrohyoid fracture occurrence in hangings [119, 120]. On the other hand, developing a decision tree model with a very high accuracy would be quite a useful in these terms, as this model provides understandable, step-by-step instructions on making decisions with a defined event certainty through the concept *if-then*. Unfortunately, this was not achieved in the present study.

For now, we should probably interpret the characteristics of the developed models only alongside the detected significant associations of the knot in a noose position with defined variables. The variables we used and coded for these analyses are easily and directly observable by a forensic pathologist performing an autopsy, and on-the-spot decision-making based on the thyrohyoid complex and cervical spine fractures pattern would be instrumental in directing the further body examination and investigation. Therefore, we could point out the key elements to further investigate alongside crude and multivariable analysis of fracture patterns (descriptives and logistic regression) and the knowledge about the relative importance of coded variables for machine learning algorithms (Tables 4.1.12, 4.2.8, and 4.3.7). Finally, this can indirectly point to the biomechanics underlying the occurrence of neck fractures in hangings and the distribution of the force a noose applies to the neck. These facts are the most important findings of the present study.

The research presented in this thesis provides several comprehensible answers for forensic pathology research on the long-standing problem of thyrohyoid complex injury in hangings:

- Until now, researchers who tried to figure out the thyrohyoid complex fracture patterns often designed the studies by analyzing variables that were expected to directly discriminate between the four or even eight-knot positions in a single step – by immediately defining on which side a particular horn was fractured (left or right). Instead, here it is demonstrated that the distribution pattern can be analyzed by combining biomechanically similar scenarios (left and right hangings are biomechanical mirror images – the same outcome). Avoiding the use of two sides (left/right – biomechanically "mirror-images") and defining if the fractures were unilateral or bilateral made some insight into fracture patterns possible to observe on a large sample.

- The single most significant and directly observable finding on autopsy, about five times more likely to occur in the atypical than in the typical hangings, was the fracture of the cervical spine. It was followed by the unilateral fracture of the hyoid bone's greater

horn, which was about 1.4 – 1.7 times more likely to occur if the knot was placed atypically. Both findings were valid irrespective of the subject's age and independent of the presence or absence of the thyroid cartilage's superior horns (see sections 4.1.1.1 and 4.1.1.2). With less certainty of true independent association with an atypical knot, the position was also the simultaneous fractures of the hyoid bone's greater horns and thyroid cartilage's superior horns. On the other hand, a similar association with the typical knot position was the presence of isolated fractures of the thyroid cartilage's superior horn (while the hyoid bone remains uninjured). Still, adjustments for the subject's age and the presence of other injuries failed to confirm the last two results unambiguously.

- The cervical spine fracture was useful not only in discriminating between atypical and typical knot positions but also between anterior and lateral knot positions. It was at least ten times more likely to occur if the knot was placed anteriorly compared to left or right lateral knot positions and independently of the thyrohyoid fractures (see section 4.1.1.3). The isolated fractures of the thyroid cartilage's superior horns (without other neck hard structure injury), while rare in anterior hangings, were significantly more common in typical hangings and in lateral hangings.

- If the knot was located at the lateral sides, the fractures of the thyroid cartilage's superior horns tended to be unilateral (but this is not always the case!) and were almost two times (1.8) more likely to occur on the side opposite to the knot position (contralaterally). Irrespective of this, in lateral hangings, the fractures of the hyoid bone's greater horns, despite not occurring only unilaterally, were almost two times (1.9) more likely to happen at the side of the knot (ipsilaterally; see section 4.1.1.4).

- Of the other analyzed autopsy findings, the discrimination between left and right lateral knot position could be improved by considering the distribution of the hemorrhages at the periosteum of the clavicles – the origins of sternocleidomastoid muscles, which were more likely to occur on the side of the knot (left or right).

- There are several implications for the hanging biomechanics. One on a cervical spine mechanism fracture corresponds to the previous suggestions – it is most likely caused by a hyperextension occurring when the knot is placed anteriorly [6, 22, 40, 43, 45, 58]. Findings can implicate the biomechanics of thyrohyoid complex fractures in lateral hangings – the fractures of the superior horns of thyroid cartilage occur most probably due to direct pressure of the ligature (compressive fractures) either on the cartilage or on the thyrohyoid membrane. At the same time, greater hyoid bone's horn fractures, if not directly compressed by the ligature loop, could occur either indirectly – due to the traction of adjacent soft tissue (traction fractures) or by compression against the cervical portion of the spine column [26, 49, 50, 59, 98, 142, 147]. Postmortem imaging studies could also corroborate the latter claim [49, 50, 135]. The direct compressive fractures of the thyroid cartilage would also explain their low occurrence in anterior hangings (characteristically without a significant direct compression by the ligature) [43], as will their significantly more frequent and isolated occurrence in typical hangings observed in this research.

- The major anthropometric factors can contribute to thyrohyoid complex and cervical spine fracture occurrence, but their clear significance in reconstructing the knot position was not observed. Regarding age – the most significant of three considered anthropometrics, it

was already well-demonstrated that subjects older than 40 years were more prone to these fractures. The present research adds to this by demonstrating that age significantly impacted only the occurrence of hyoid bone's greater horns fractures (more likely after the age of about 37 – by approaching the forties) and cervical spine fractures (more likely after the age of about 65 years). The body weight was associated only with the fractures of the thyroid cartilage's superior horns (more likely in persons heavier than 65 – 72 kg) and with the appearance of sternocleidomastoid muscle hemorrhages at their origin – the periosteum of the collarbones (more likely in persons heavier than about 67 kg).

- The present study also demonstrated that it is possible to develop machine learning models for classification purposes of the knot in a noose position that are capable of generalization from training to test samples. This was achieved in genetic algorithm-optimized artificial neural networks developed in MATLAB, as well as in artificial neural networks and several other algorithms in SPSS. The ANN was probably the most robust of all developed models, with some successful results also observed in, for example, k-Nearest Neighbors models. Although the overall accuracy of some classification attempts was relatively low or modest (discrimination between typical and atypical hangings) and comparable to logistic regression, very high accuracy for some discriminations was achieved, especially for the knot side estimation in the lateral hangings (discrimination between left lateral and right lateral knot position). Even though far from a solution for a 'witness' or 'expert' opinion in a courtroom, some probable biomechanics explanations for thyrohyoid fracture patterns occurrence are suggested. Firstly, it was directly demonstrated that information on the subjects' body weight and body height did not improve models' classification performances, despite presumed theoretical explanations for their significance and despite presented findings on the crude associations with fracture occurrence. Additionally, the information on the presence and distribution of SCM muscle-origin hemorrhages did not improve classification performance for discrimination between typical and atypical hangings. However, with further analysis and discussed biomechanics in lateral hangings in mind, this must be explored further. Most developed models either selected or ranked highly important coded variables, which were significant discriminators in standard statistical analyses. And the conclusions based on the conventional statistics are in fact further corroborated by the variables' relative importance in many MLA models analyzed herein. Given that the aims were to assess the predictive usefulness of machine learning models in a problem previously unexplored by this method, which was not possible to explain by conventional descriptive analyses, the present study provided useful and even promising results.

To the best of the author's knowledge, this is the first attempt to determine the thyrohyoid and cervical spine fracture patterns in hangings concerning the position of the ligature's knot using machine learning algorithms. Considering this, the information about the achieved hyperparameter MLA settings for these distinct datasets and variable coding that showed some valuable results may prove helpful in further studies of this specific problem. Particularly with conventional statistical software solutions now capable of machine learning modeling, with graphic user interfaces becoming relatively easy to operate on by less experienced users (but preferably not completely lay), that forensic pathologists are, with appropriate supervision. Ultimately, the in-detail report on methodology (e.g., variable coding), sample characteristics (basic descriptives and

inferential statistics), and developed machine learning algorithm models characteristics (e.g., hyperparameter settings) ensure study transparency, accuracy, and reproducibility, which is a prerequisite for Artificial Intelligence-based research.

At the very end, the study limitations should be discussed. Data on which the machine learning experiments and other analyses were performed were obtained retrospectively. The quality of the data source defines the quality of the experiment. Fortunately, the systematic approach at the Institute provided a complete and uniform source. Information on subjects' body weight, height, and particularly hemorrhages of the sternocleidomastoid muscles was available for a small portion of the sample, which probably impacted the models' classification performances. The priority was to give an advantage to uniform and complete data sets over many missing inputs. Finally, additional data could be significant and lead to better model development. But the exact circumstances data are often unavailable and non-systematically obtainable (e.g., point of suspension and completeness of hanging, a drop length, ligature diameter, and softness/hardness – the material) it may further improve machine learning models' performances and knot in a noose position assessment. On the other hand, some recent reports suggest that, for example, a ligature diameter did not impact thyrohyoid fracture occurrence. An additional increase in sample size without missing significant data probably requires multicenter studies, but representative samples could be obtained with broadly applied standards in autopsy practice. These collaborations should be highly encouraged. The future collaboration of forensic experts and engineers in machine learning may prove very useful in academic research and general practice.

5.1. Study implications and perspective

The present study was the first attempt to utilize machine learning algorithms to reconstruct the knot in a noose position by analyzing the distribution and pattern of the thyrohyoid complex and cervical spine fractures. Before this is considered, it should be noted that the initial step in forming machine learning models – the data acquisition and data set forming was done distinctly – the variables coding the presence and distribution of thyrohyoid complex fractures were designed to specify the biomechanical characteristic (e.g., the general relation of the fracture to the knot position), and not to only directly specify the exact side of the knot – the knot is not only located on the left or right side, but it is, for example an unilateral fracture in general or it is a fracture at the same – ipsilateral side to the knot in lateral hangings. By this variable coding, not only was the development of several valid supervised machine learning models possible, but some crude significant patterns of the fractures and knot positions were also revealed, and some previous observations were confirmed.

The developed machine learning models are, nevertheless, of limited to no direct applicability in routine practice – either the accuracies were modest, or the algorithm and model that performed the best in classification do not provide an understandable decision-

making process (e.g., artificial neural networks) – these are the black boxes. So, further attempts could be made to develop highly accurate, comprehensible models, such as decision trees, with potentially sound step-by-step decisions for forensic pathologists. The potential variables that could be of limited use or create the "noise" are also pointed out here, including some major anthropometric factors.

Apart from this, how the present research adds in the current form should be considered. When providing expert opinion on some topic - forensic expertise claims cannot always be made on a discrete particular level of probability, and sometimes it is even based on a case-based anecdotal experience. Providing objective measures of certainty is welcome in contrast to such a biased approach. The present research can also be a proof-of-concept for this sort of reasoning in modern forensic expertise of various issues in forensic medicine and pathology. The applicability and potential benefits of artificial intelligence-based and assisted methods should invariably be further explored, including the topic considered in this research. If it fails to prove useful, it could be the ultimate sign that one is heading through a dead-end street.

6. CONCLUSIONS

I Based on the analysis of the systematically obtained data on 1,235 suicidal hangings with a short drop or without a drop, the overall frequency of thyrohyoid fractures was estimated to be 60.6%, with fractures of the superior horns of the thyrohyoid complex being more frequent than the fractures of the greater horns of the hyoid bone – 44.5% and 34.4% of cases, respectively. In the same sample, cervical spine fracture was observed in 3.6% of cases. The sample comprised 57.2% hangings with a typical (posterior) knot position, 33.4% with lateral knot positions (left and right positions almost identical in frequency), and 9.4% of cases with anteriorly placed knots.

On a conventional analysis, subjects' age significantly impacted only the occurrence of hyoid bone's greater horns fractures, which were more likely after the age of about 38 years, and cervical spine fractures, which were more likely after the age of about 65 years. It is an essential contributor to thyrohyoid fracture susceptibility.

By analyzing the association of the coded variables and knot in a noose position, the following significant associations were identified: for discrimination between atypical (anterior and lateral) and typical (posterior) hangings, significant were cervical spine fracture, unilateral hyoid horn fracture, simultaneous thyroid and hyoid horns fractures, all with higher odds to occur in atypical hangings but of course not exclusive to them. Of those, only the cervical spine and unilateral hyoid horn fractures indicated atypical knot position independently of other fractures and the subject's age. The independent association of other mentioned variables was less clear. In typical hangings, on the other side, isolated thyroid horn fractures were more likely to occur than in atypical.

Finally, in lateral hangings, the hyoid and thyroid horn fractures occurred with higher odds on the ipsilateral and contralateral sides to the knot position, respectively.

II It is possible to develop machine learning models capable of classification of the knot in a noose position in suicidal hangings based on the thyrohyoid complex and cervical spine fractures.

In the first part of the study, this was achieved by considering only fracture presence, the subject's sex, and age. All the developed models (GA-optimized ANN, MLP-ANN, k-NN, DT, NB) could adequately generalize from training to test samples. The genetic algorithm-based ANN hyperparameter optimization in MATLAB did not result in a significantly better model than partially manual adjustment experiments performed in SPSS for MLP-ANN, based on the Receiver Operating Characteristic curve analysis.

The discrimination between typical and atypical hangings was modest, with overall accuracies of about 60.0%, and this performance improved only slightly (to about 62%) if the cases without any fractures were excluded. However, the overall classification accuracies improved significantly in discriminating between anterior and lateral atypical hangings, and then particularly between left and right lateral hangings. In the latter case, the ANN and k-NN achieved accuracies higher than 90%, with areas under the receiver operating characteristic curve in the test sample of 0.98 and 0.97, respectively. Most of the developed models highly ranked the importance of variables observed to be significant for discrimination by the conventional (standard) statistical methods.

In addition to the input on fractures, age should be invariably considered.

III The analogous machine learning algorithm models developed on the same smaller dataset of the study part II, one with additional inputs on subjects' body weight (and body height) and one without them, did not statistically significantly differ in the classification performance, based on the ROC curve comparison, in discriminating between typical and atypical hangings. This holds true irrespective of considering cases without any thyrohyoid or cervical spine fracture.

The study's results imply that considering the body weight and height does not significantly improve machine learning classification between typical and atypical knot positions – it is possible to develop valid models of similar classification capabilities only through the fracture distribution and subject's age. Indirectly, this suggests that body weight and height are not of vast importance in reconstructing the knot position through thyrohyoid fracture patterns.

In fact, the decision tree algorithm overfitted the model if forced to consider body weight. Moreover, most of the developed models highly ranked the importance of classifying variables that were detected to be significant by conventional (standard) statistical methods in the first study part, even though most of these crude associations were not possible to detect in the sample of the second part of the study.

However, body weight was significantly associated with the superior horns of the thyroid cartilage fracture occurrence on a conventional statistical analysis: these were more likely to occur in persons heavier than 65 – 72 kg. This could be a rationale for including the variable in more complex models (on a larger sample with more inputs).

IV The analogous machine learning algorithm models developed on the same smaller dataset of the study part III, one with additional inputs on the presence and distribution of the periosteal hemorrhages at the sternocleidomastoid muscle origin at the clavicles and one without them, did not statistically significantly differ in their classification performance based on the ROC curve comparison, in discriminating between typical and atypical hangings (considering cases with fractures and without fractures, and with and without the muscle hemorrhages).

The study's results imply that considering the sternocleidomastoid muscle hemorrhages does not improve discrimination between typical and atypical knot positions. Indirectly, it suggests this input is not crucial in differentiating typical from atypical knot positions through thyrohyoid fracture patterns. However, given the significant pattern in hemorrhage distribution in lateral hangings - which were more likely to occur on the side of the knot, these should be considered in a more complex model to discriminate between left and right lateral hangings and maybe even between anterior and lateral hangings.

Again, most of the developed models highly ranked the importance of classifying variables that were detected to be significant by conventional (standard) statistical methods in the former study parts, even though most of these crude associations were not possible to detect in the sample of the second part of the study.

Of potentially significant additional associations between the input variables, body weight was significantly associated with the appearance of sternocleidomastoid muscle hemorrhages at their origin—the periosteum of the clavicles, which were more frequent in persons heavier than about 67 kg.

7. REFERENCES

[1] Speake J, LaFlaur M. The Oxford Essential Dictionary of Foreign Terms in English. Oxford: Oxford University Press; 2002.

[2] Madea B (Ed). Handbook of forensic medicine, 2nd ed. Hoboken, NJ: Wiley; 2022.

[3] Saukko P, Knight B. Knight's Forensic Pathology, 4th ed. Boca Raton: CRC Press; 2015.

[4] Sauvageau A, Boghossian E. Classification of Asphyxia: The Need for Standardization. J Forensic Sci. 2010;55:1259–67. https://doi.org/10.1111/j.1556-4029.2010.01459.x.

[5] Ely SF, Gill JR. Approach to asphyxial deaths. In: Ely SF, Gill JR (Eds). Principles of Forensic Pathology: From investigation to certification. London: Academic Press, an imprint of Elsevier; 2023, pp. 279–305.

[6] Nikolić S, Živković V. Injuries and vital reactions patterns in hanging. Srp Arh Celok Lek. 2015;143:93–9. https://doi.org/10.2298/SARH1502093N.

[7] Madea B (Ed). Asphyxiation, Suffocation, and Neck Pressure Deaths. Boca Raton: CRC Press; 2020.

[8] DiMaio VJM, Kimberley Molina D. DiMaio's Forensic Pathology, 3rd ed. Boca Raton: CRC Press; 2021.

[9] Dettmeyer RB, Verhoff MA, Schütz HF. Neck Trauma. In: Dettmeyer RB, Verhoff MA, Schütz HF. Forensic Medicine Fundamentals and Perspectives. Berlin, Heidelberg: Springer Berlin Heidelberg; 2014, pp. 171–89.

[10] Spitz WU, Diaz FJ (Eds). Spitz and Fisher's Medicolegal Investigation of Death: Guidelines for the Application of Pathology to Crime Investigation, 5th ed. Springfield, IL: Charles C Thomas; 2020.

[11] Shkrum MJ, Ramsay DA. Forensic Pathology of Trauma. Totowa, NJ: Humana Press; 2007.

[12] Sauvageau A. Death by hanging. In: Rutty GN (Ed). Essentials of Autopsy Practice. Springer-Verlage, 2014, pp. 22–38.

[13] World Health Organization. Suicide [Internet]. Available at: https://www.who.int/news-room/fact-sheets/detail/suicide. (accessed July 22, 2024).

[14] World Health Organization. Suicide worldwide in 2019: Global Health Estimates. [Internet]. World Health Organization, Geneva 2019:4–9. Available from: https://www.who.int/publications/i/item/9789240026643. (accessed July 22, 2024).

[15] Dhungel B, Sugai MK, Gilmour S. Trends in Suicide Mortality by Method from 1979 to 2016 in Japan. Int J Environ Res Public Health. 2019;16:1794. https://doi.org/10.3390/ijerph16101794.

[16] Morovatdar N, Moradi-Lakeh M, Malakouti SK, Nojomi M. Most Common Methods of Suicide in Eastern Mediterranean Region of WHO: A Systematic Review and Meta-Analysis. Arch Suicide Res. 2013;17:335–44. https://doi.org/10.1080/13811118.2013.801811.

[17] Moftakhar L, Mirahmadizadeh A, Amiri S, Rezaei F, Azarbakhsh H. Epidemiology of Suicide by Hanging in Fars Province, Iran (2011-2019): A Population-based Cross-sectional Study. J Prev Med Public Health. 2023;56:264–71. https://doi.org/10.3961/jpmph.22.519.

[18] Varnik A, Kolves K, van der Feltz-Cornelis CM, Marusic A, Oskarsson H, Palmer A, et al. Suicide methods in Europe: a gender-specific analysis of countries participating in the "European Alliance Against Depression." J Epidemiol Community Health. 2008;62:545–51. https://doi.org/10.1136/jech.2007.065391.

[19] Vieira DN, Pinto AE, Oliveira Sá F. Homicidal Hanging. Am J Forensic Med Pathol 1988;9:287–9. https://doi.org/10.1097/00000433-198812000-00003.
[20] Rayes M, Mittal M, Rengachary SS, Mittal S. Hangman's fracture: a historical and biomechanical perspective. J Neurosurg Spine. 2011;14:198–208. https://doi.org/10.3171/2010.10.SPINE09805.
[21] Khokhlov VD. Calculation of tension exerted on a ligature in incomplete hanging. Forensic Sci Int. 2001;123:172–7. https://doi.org/10.1016/S0379-0738(01)00543-6.
[22] Hellier C, Connolly R. Cause of death in judicial hanging: a review and case study. Med Sci Law 2009;49:18–26. https://doi.org/10.1258/rsmmsl.49.1.18.
[23] Brouardel P. La pendaison, la strangulation, la suffocation, la submersion. Paris: Libraire J.-B. Baillière et fils; 1897.
[24] Rauschke J. Uber den Eintritt der Bewusstlosigkeit bei atypischer Erhängung [Incipient loss of consciousness in atypical hanging]. Dtsch Z Gesamte Gerichtl Med. 1957;46(2):206-11. https://pubmed.ncbi.nlm.nih.gov/13437822.
[25] Clément R, Redpath M, Sauvageau A. Mechanism of Death in Hanging: A Historical Review of the Evolution of Pathophysiological Hypotheses. J Forensic Sci. 2010;55:1268–71. https://doi.org/10.1111/j.1556-4029.2010.01435.x.
[26] Schwarzacher W. Beiträge zum Mechanismus des Erhängungstodes. Dtsch Z Gesamte Gerichtl Med. 1928;11:145–53. https://doi.org/10.1007/BF01748806.
[27] Brinkmann B, Koops E, Wischhusen F, Kleiber M. Halskompression und arterielle Obstruktion. Z Rechtsmed. 1981;87:59–73. https://doi.org/10.1007/BF00201211.
[28] Brinkmann B, Püschel K, Bause HW, Doehn M. Zur Pathophysiologie der Atmung und des Kreislaufs bei Tod durch obstruktive Asphyxie. Z Rechtsmed. 1981;87:103–16. https://doi.org/10.1007/BF00201215.
[29] Ikeda N, Harada A, Suzuki T. The course of respiration and circulation in death due to typical hanging. Int J Leg Med. 1992;104:313–5. https://doi.org/10.1007/BF01369548.
[30] Sauvageau A. Agonal Sequences in Four Filmed Hangings: Analysis of Respiratory and Movement Responses to Asphyxia by Hanging. J Forensic Sci. 2009;54:192–4. https://doi.org/10.1111/j.1556-4029.2008.00910.x.
[31] Sauvageau A, Ambrosi C, Kelly S. Autoerotic Nonlethal Filmed Hangings. Am J Forensic Med Pathol. 2012;33:159–62. https://doi.org/10.1097/PAF.0b013e3181ea1aa6.
[32] Sauvageau A, Kelly S, Ambrosi C. A Filmed Hanging Without Decerebrate and Decorticate Rigidity. Am J Forensic Med Pathol. 2012;33:176–8. https://doi.org/10.1097/PAF.0b013e3181efbc3b.
[33] Sauvageau A, LaHarpe R, King D, Dowling G, Andrews S, Kelly S, et al. Agonal Sequences in 14 Filmed Hangings With Comments on the Role of the Type of Suspension, Ischemic Habituation, and Ethanol Intoxication on the Timing of Agonal Responses. Am J Forensic Med Pathol. 2011;32:104–7. https://doi.org/10.1097/PAF.0b013e3181efba3a.
[34] Standring S (Ed). Gray's anatomy : The Anatomical Basis of Clinical Practice, 40th Ed. Edinburgh: Churchill Livingstone/Elsevier; 2008.
[35] Leković A, Nikolić S. Autonomous nervous system-related vital reactions in short-drop hangings. Med Podml. 2025;76(6). https://doi.org/10.5937/mp76-48972. (Accepted for publication)

[36] Suárez-Peñaranda JM, Cordeiro C, Rodríguez-Calvo M, Vieira DN, Muñoz-Barús JI. Cardiac inhibitory reflex as a cause/mechanism of death. J Forensic Sci. 2013;58:1644–7. https://doi.org/10.1111/1556-4029.12212.
[37] Doberentz E, Madea B. Traumatic carotid sinus reflex and postmortem investigation of the glomus caroticum in cases of pressure to the neck. In: Rutty GN (Ed). Essentials of Autopsy Practice: Reviews, Updates and Advances. London: Springer-Verlage, 2019, pp. 67–88.
[38] Lockyer BE. Death by hanging: examination of autopsy findings and best approach to the post-mortem examination. Diagn Histopathol. 2019;25:423–30. https://doi.org/10.1016/j.mpdhp.2019.07.006.
[39] Nikolić S, Živković V, Babić D, Juković F. Cervical soft tissue emphysema in hanging – a prospective autopsy study. J Forensic Sci. 2012;57:132–5. https://doi.org/10.1111/J.1556-4029.2011.01911.X.
[40] Hejna P, Zátopková L. Significance of Hemorrhages at the Origin of the Sternocleidomastoid Muscles in Hanging. Am J Forensic Med Pathol. 2012;33:124–7. https://doi.org/10.1097/PAF.0b013e31820b8fb8.
[41] Hejna P. Amussat's Sign in Hanging-A Prospective Autopsy Study. J Forensic Sci. 2011;56:132–5. https://doi.org/10.1111/j.1556-4029.2010.01548.x.
[42] Asirdizer M, Kartal E. Neck vascular lesions in hanging cases: A literature review. J Forensic Leg Med. 2022;85:102284. https://doi.org/10.1016/j.jflm.2021.102284.
[43] Nikolić S, Živković V. Cervical spine injuries in suicidal hanging without a long-drop-patterns and possible underlying mechanisms of injury: An autopsy study. Forensic Sci Med Pathol. 2014;10:193–7. https://doi.org/10.1007/S12024-014-9550-Y.
[44] Chikhani M, Winter R. Injury after non-judicial hanging. Trauma. 2014;16:164–73. https://doi.org/10.1177/1460408614530941.
[45] James R, Nasmyth-Jones R. The occurrence of cervical fractures in victims of judicial hanging. Forensic Sci Int. 1992;54:81–91. https://doi.org/10.1016/0379-0738(92)90083-9.
[46] Nikolić S, Micić J, Atanasijević T, Djokić V, Djonić D. Analysis of Neck Injuries in Hanging. Am J Forensic Med Pathol. 2003;24:179–82. https://doi.org/10.1097/01.PAF.0681069550.31660.f5.
[47] Djurić M, Milisavljević M, Maliković A, Djonić D, Milovanović P. Anatomija glave i vrata. Beograd: Medicinski fakultet Univerziteta u Beogradu; 2020.
[48] de Bakker BS, de Bakker HM, Soerdjbalie-Maikoe V, Dikkers FG. Variants of the hyoid-larynx complex, with implications for forensic science and consequence for the diagnosis of Eagle's syndrome. Sci Rep. 2019;9:15950. https://doi.org/10.1038/s41598-019-52476-z.
[49] Meredith M, Harris P, Day C, Milne N, Watkins T, Ong BB. A Possible Mechanism of Laryngohyoid Fractures in Hanging. Am J Forensic Med Pathol. 2024. https://doi.org/10.1097/PAF.0000000000000944.
[50] Cianci V, Mondello C, Cracò A, Cianci A, Bottari A, Gualniera P, et al. Hyoid Bone Fracture Pattern Assessment in the Forensic Field: The Importance of Post Mortem Radiological Imaging. Diagnostics. 2024;14:674. https://doi.org/10.3390/diagnostics14070674.
[51] Wilson R, McFadden C, Rowbotham S. A meta-analytic review of the frequency and patterning of laryngohyoid and cervical fractures in cases of suicide by hanging. J Forensic Sci. 2023;68:731-42. https://doi.org/10.1111/1556-4029.15234.

[52] Nikolić S, Živković V, Babić D, Juković F, Atanasijević T, Popović V. Hyoid-laryngeal fractures in hanging: where was the knot in the noose? Med Sci Law. 2011;51:21–5. https://doi.org/10.1258/msl.2010.010016.
[53] Commins C, Bolster M, Mulligan L. To investigate the pattern of neck injuries and the role of toxicology in cases of hanging and manual/homicidal ligature strangulation in Ireland between 2016 – 2020: A retrospective review and analysis. J Forensic Leg Med. 2024;103:102686. https://doi.org/10.1016/j.jflm.2024.102686.
[54] Crudele GDL, Amadasi A, Franceschetti L, Cattaneo C. Pathological Findings in Hanging: Is the Traditional Knowledge Correct? Diagnostics. 2024;14:318. https://doi.org/10.3390/diagnostics14030318.
[55] Paparo GP, Siegel H. Neck markings and fractures in suicidal hangings. Forensic Sci Int. 1984;24:27–35. https://doi.org/10.1016/0379-0738(84)90148-8.
[56] Green H, James RA, Gilbert JD, Byard RW. Fractures of the hyoid bone and laryngeal cartilages in suicidal hanging. J Clin Forensic Med. 2000;7:123–6. https://doi.org/10.1054/JCFM.2000.0419.
[57] Clément R, Guay J-P, Sauvageau A. Fracture of the neck structures in suicidal hangings: A Retrospective study on contributing variables. Forensic Sci Int. 2011;207:122–6. https://doi.org/10.1016/j.forsciint.2010.09.016.
[58] Zátopková L, Janík M, Urbanová P, Mottlová J, Hejna P. Laryngohyoid fractures in suicidal hanging: A prospective autopsy study with an updated review and critical appraisal. Forensic Sci Int. 2018;290:70–84. https://doi.org/10.1016/j.forsciint.2018.05.043.
[59] Pollanen M, Ubelaker D. Forensic Significance of the Polymorphism of Hyoid Bone Shape. J Forensic Sci. 1997;42:890–2. https://doi.org/10.1520/JFS14225J.
[60] Mukhopadhyay PP. Morphometric features and sexual dimorphism of adult hyoid bone: A population specific study with forensic implications. J Forensic Leg Med. 2010;17:321–4. https://doi.org/10.1016/j.jflm.2010.04.014.
[61] Garvin HM. Ossification of Laryngeal Structures as Indicators of Age. J Forensic Sci. 2008;53:1023–7. https://doi.org/10.1111/j.1556-4029.2008.00793.x.
[62] Leković A, Vukićević A, Nikolić S. Assessing the knot in a noose position by thyrohyoid and cervical spine fracture patterns in suicidal hangings using machine learning algorithms: A new insight into old dilemmas. Forensic Sci Int. 2024;357:111973. https://doi.org/10.1016/j.forsciint.2024.111973.
[63] Pollanen MS, Chiasson DA. Fracture of the Hyoid Bone in Strangulation: Comparison of Fractured and Unfractured Hyoids from Victims of Strangulation. J Forensic Sci. 1996;41:13904J. https://doi.org/10.1520/JFS13904J.
[64] Taktak S, Kumral B, Unsal A, Ozdes T, Buyuk Y, Celik S. Suicidal hanging in Istanbul, Turkey: 1979–2012 Autopsy results. J Forensic Leg Med. 2015;33:44–9. https://doi.org/10.1016/j.jflm.2015.03.008.
[65] Tumram NK, Ambade VN, Bardale RV, Dixit PG. Injuries over neck in hanging deaths and its relation with ligature material: Is it vital? J Forensic Leg Med. 2014;22:80–3. https://doi.org/10.1016/j.jflm.2013.12.021.
[66] Sharma BR, Harish D, Sharma A, Sharma S, Singh H. Injuries to neck structures in deaths due to constriction of neck, with a special reference to hanging. J Forensic Leg Med. 2008;15:298–305. https://doi.org/10.1016/j.jflm.2007.12.002.
[67] Saternus K-S, Maxeiner H, Kernbach-Wighton G, Koebke J. Traumatology of the superior thyroid horns in suicidal hanging – An injury analysis. Leg Med. 2013;15:134–9. https://doi.org/10.1016/j.legalmed.2012.10.008.

[68] Godin A, Kremer C, Sauvageau A. Fracture of the Cricoid as a Potential Pointer to Homicide. Am J Forensic Med Pathol. 2012;33:4–7. https://doi.org/10.1097/PAF.0b013e3181d3dc24.
[69] Jayaprakash S, Sreekumari K. Pattern of Injuries to Neck Structures in Hanging—An Autopsy Study. Am J Forensic Med Pathol. 2012;33:395–9. https://doi.org/10.1097/PAF.0b013e3182662761.
[70] Simonsen J. Patho-anatomic findings in neck structures in asphyxiation due to hanging: A survey of 80 cases. Forensic Sci Int. 1988;38:83–91. https://doi.org/10.1016/0379-0738(88)90012-6.
[71] Maxeiner H, Bockholdt B. Homicidal and suicidal ligature strangulation—a comparison of the post-mortem findings. Forensic Sci Int. 2003;137:60–6. https://doi.org/10.1016/S0379-0738(03)00279-2.
[72] Sharma BR, Singh VP, Harish D. Neck Structure Injuries in Hanging – Comparing Retrospective and Prospective Studies. Med Sci Law. 2005;45:321–30. https://doi.org/10.1258/rsmmsl.45.4.321.
[73] Hlavaty L, Kasper W, Sung L. Current Analysis of Hangings That Deviates From Recently Published Studies. Am J Forensic Med Pathol. 2016;37:299–305. https://doi.org/10.1097/PAF.0000000000000270.
[74] Nikolić S, Živković V, Juković F, Babić D, Stanojkovski G. Simon's bleedings: A possible mechanism of appearance and forensic importance-a prospective autopsy study. Int J Leg Med. 2009;123:293–7. https://doi.org/10.1007/S00414-009-0318-Y.
[75] Lidströmer N, Aresu F, Ashrafian H. Basic Concepts of Artificial Intelligence: Primed for Clinicians. In: Lidströmer N, Ashrafian H (Eds). Artificial Intelligence in Medicine. Cham: Springer, 2022, pp. 3–20. https://doi.org/10.1007/978-3-030-64573-1_1.
[76] Harrison JH, Gilbertson JR, Hanna MG, Olson NH, Seheult JN, Sorace JM, et al. Introduction to Artificial Intelligence and Machine Learning for Pathology. Arch Pathol Lab Med. 2021;145:1228–54. https://doi.org/10.5858/ARPA.2020-0541-CP.
[77] Jiang T, Gradus JL, Rosellini AJ. Supervised Machine Learning: A Brief Primer. Behav Ther. 2020;51:675–87. https://doi.org/10.1016/J.BETH.2020.05.002.
[78] Hanna MG, Hanna MH. Current applications and challenges of artificial intelligence in pathology. Human Pathology Reports. 2022;27:300596. https://doi.org/10.1016/J.HPR.2022.300596.
[79] Vukicevic AM, Jovicic GR, Stojadinovic MM, Prelevic RI, Filipovic ND. Evolutionary assembled neural networks for making medical decisions with minimal regret: Application for predicting advanced bladder cancer outcome. Expert Syst Appl. 2014;41:8092–100. https://doi.org/10.1016/j.eswa.2014.07.006.
[80] Vukicevic AM, Stojadinovic M, Radovic M, Djordjevic M, Cirkovic BA, Pejovic T, et al. Automated development of artificial neural networks for clinical purposes: Application for predicting the outcome of choledocholithiasis surgery. Comput Biol Med. 2016;75:80–9. https://doi.org/10.1016/j.compbiomed.2016.05.016.
[81] Stiglic G, Kocbek S, Pernek I, Kokol P. Comprehensive Decision Tree Models in Bioinformatics. PLoS One. 2012;7:e33812. https://doi.org/10.1371/journal.pone.0033812.
[82] John GH, Langley P. Estimating Continuous Distributions in Bayesian Classifiers arXiv. 2013;1302.4964. https://doi.org/10.48550/arXiv.1302.4964.
[83] Cover T, Hart P. Nearest neighbor pattern classification. IEEE Trans Inf Theory. 1967;13:21–7. https://doi.org/10.1109/TIT.1967.1053964.

[84] Vukićević AM. Razvoj metoda za trodimenzionalnu rekonstrukciju koronarnih arterija za potrebe numeričke analize protoka i procene mehaničkog integriteta stenta [dissertation], Kragujevac, Serbia: University of Kragujevac; 2016. Available from: https://phaidrakg.kg.ac.rs/view/o:590. Accessed July 16, 2024.
[85] Yang XS. Nature-Inspired Optimization Algorithms. London: Elsevier; 2014.
[86] Jodas DS, Passos LA, Adeel A, Papa JP. PL-kNN: PL-kNN: A Python-based implementation of a parameterless k-Nearest Neighbors classifier. Softw Impacts. 2022;15:100459. https://doi.org/10.1016/j.simpa.2022.100459.
[87] Shehab M, Abualigah L, Shambour Q, Abu-Hashem MA, Shambour MKY, Alsalibi AI, et al. Machine learning in medical applications: A review of state-of-the-art methods. Comput Biol Med. 2022;145:105458. https://doi.org/10.1016/j.compbiomed.2022.105458.
[88] Park C, Lee J, Park W, Lee D. Fire accelerant classification from GC–MS data of suspected arson cases using machine–learning models. Forensic Sci Int. 2023;346:111646. https://doi.org/10.1016/j.forsciint.2023.111646.
[89] Knecht S, Santos F, Ardagna Y, Alunni V, Adalian P, Nogueira L. Sex estimation from long bones: a machine learning approach. Int J Leg Med. 2023;137:1887–95. https://doi.org/10.1007/S00414-023-03072-4.
[90] Nikita E, Nikitas P. On the use of machine learning algorithms in forensic anthropology. Leg Med. 2020;47:101771. https://doi.org/10.1016/j.legalmed.2020.101771.
[91] Yeow WL, Mahmud R, Raj RG. An application of case-based reasoning with machine learning for forensic autopsy. Expert Syst Appl. 2014;41:3497–505. https://doi.org/10.1016/j.eswa.2013.10.054.
[92] Casali M, Malchiodi D, Spada C, Zanaboni AM, Cotroneo R, Furci D, et al. A pilot study for investigating the feasibility of supervised machine learning approaches for the classification of pedestrians struck by vehicles. J Forensic Leg Med. 2021;84:102256. https://doi.org/10.1016/j.jflm.2021.102256.
[93] Dempsey N, Bassed R, Amarasiri R, Blau S. Exploring the use of machine learning for the assessment of skeletal fracture morphology and differentiation between impact mechanisms: A pilot study. J Forensic Sci. 2022;67:683–96. https://doi.org/10.1111/1556-4029.14996.
[94] Klauschen F, Dippel J, Keyl P, Jurmeister P, Bockmayr M, Mock A, et al. Toward Explainable Artificial Intelligence for Precision Pathology. Annu Rev Pathol-Mech. 2024;19:541–70. https://doi.org/10.1146/annurev-pathmechdis-051222-113147.
[95] Tournois L, Trousset V, Hatsch D, Delabarde T, Ludes B, Lefèvre T. Artificial intelligence in the practice of forensic medicine: a scoping review. Int J Leg Med. 2023:1–15. https://doi.org/10.1007/s00414-023-03140-9.
[96] Piraianu A-I, Fulga A, Musat CL, Ciobotaru O-R, Poalelungi DG, Stamate E, et al. Enhancing the Evidence with Algorithms: How Artificial Intelligence Is Transforming Forensic Medicine. Diagnostics. 2023;13:2992. https://doi.org/10.3390/diagnostics13182992.
[97] Carter J V., Pan J, Rai SN, Galandiuk S. ROC-ing along: Evaluation and interpretation of receiver operating characteristic curves. Surgery. 2016;159:1638–45. https://doi.org/10.1016/J.SURG.2015.12.029.
[98] Urbanová P, Hejna P, Zátopková L, Šafr M. Can the morphology of the hyoid bone be helpful in assessing mechanisms of injuries. 19th IAFS Meeting, Madeira, Portugal, 2011.

[99] Bockholdt B, Hempelmann M, Maxeiner H. Experimental investigations of fractures of the upper thyroid horns. Leg Med. 2003;5:S252–5. https://doi.org/10.1016/S1344-6223(02)00142-6.
[100] Üzün İ, Büyük Y, Gürpinar K. Suicidal hanging: Fatalities in Istanbul Retrospective analysis of 761 autopsy cases. J Forensic Leg Med. 2007;14:406–9. https://doi.org/10.1016/j.jflm.2007.01.002.
[101] Kootbodien T, Naicker N, Wilson KS, Ramesar R, London L. Trends in Suicide Mortality in South Africa, 1997 to 2016. Int J Environ Res Public Health. 2020;17:1850. https://doi.org/10.3390/ijerph17061850.
[102] Azmak D. Asphyxial Deaths. Am J Forensic Med Pathol. 2006;27:134–44. https://doi.org/10.1097/01.paf.0000221082.72186.2e.
[103] Gunnell D, Bennewith O, Hawton K, Simkin S, Kapur N. The epidemiology and prevention of suicide by hanging: a systematic review. Int J Epidemiol. 2005;34:433–42. https://doi.org/10.1093/ije/dyh398.
[104] Baker SP, Hu G, Wilcox HC, Baker TD. Increase in Suicide by Hanging/Suffocation in the U.S., 2000–2010. Am J Prev Med. 2013;44:146–9. https://doi.org/10.1016/J.AMEPRE.2012.10.010.
[105] Li X, Xiao Z, Xiao S. Suicide among the elderly in mainland China. Psychogeriatrics. 2009;9:62–6. https://doi.org/10.1111/J.1479-8301.2009.00269.X.
[106] Gorgiard C, Taccoen M, Ludes B. Fracture du cartilage thyroïde et pendaison incomplète : à propos d'un cas et revue de la littérature. La Revue de Médecine Légale. 2016;7:33–7. https://doi.org/10.1016/j.medleg.2015.12.001.
[107] Kurtulus A, Nilufer Yonguc G, Boz B, Acar K. Anatomopathological findings in hangings: a retrospective autopsy study. Med Sci Law. 2013;53:80–4. https://doi.org/10.1258/msl.2012.012030.
[108] Akshay Kumar Ramtake, B.S. Patil, Tikendra Dewangan. A Study of Deaths Due to Hanging: A Retrospective Study. Indian J Forensic Med Toxicol. 2024;18:9–12. https://doi.org/10.37506/0ykbp376.
[109] Bowen D. Hanging — A review. Forensic Sci Int. 1982;20:247–9. https://doi.org/10.1016/0379-0738(82)90124-4.
[110] Ambade VN, Kolpe D, Tumram N, Meshram S, Pawar M, Kukde H. Characteristic Features of Hanging: A Study in Rural District of Central India. J Forensic Sci. 2015;60:1216–23. https://doi.org/10.1111/1556-4029.12772.
[111] Samarasekera A, Cooke C. The pathology of hanging deaths in Western Australia. Pathology. 1996;28:334–8. https://doi.org/10.1080/00313029600169294.
[112] Morild I. Fractures of neck structures in suicidal hanging. Med Sci Law. 1996;36:80–4. https://doi.org/10.1177/002580249603600115.
[113] Suárez-Peñaranda JM, Álvarez T, Miguéns X, Rodríguez-Calvo MS, De Abajo BL, Cortesão M, et al. Characterization of Lesions in Hanging Deaths. J Forensic Sci. 2008;53:720–3. https://doi.org/10.1111/j.1556-4029.2008.00700.x.
[114] Meera T, Bapin Kumar Singh M. Pattern of neck findings in suicidal hanging a study in Manipur. J Indian Forensic Sci. 2011; 33(4):352-354.
[115] Kumar A, Bommanahalli BP, Jatti VB, et al. Suicidal Hanging in Franco da Rocha, Brazil-a six-year prospective and retrospective study. Indian J Forensic Med Toxicol. 2011;5(2):14-17
[116] Abd-Elwahab Hassan D, Ghaleb SS, Kotb H, Agamy M, Kharoshah M. Suicidal hanging in Kuwait: Retrospective analysis of cases from 2010 to 2012. J Forensic Leg Med. 2013;20:1118–21. https://doi.org/10.1016/j.jflm.2013.09.021.

[117] Russo MC, Verzeletti A, Piras M, De Ferrari F. Hanging Deaths. Am J Forensic Med Pathol. 2016;37:141–5. https://doi.org/10.1097/PAF.0000000000000239.
[118] Tugaleva E, Gorassini DR, Shkrum MJ. Retrospective Analysis of Hanging Deaths in Ontario. J Forensic Sci. 2016;61:1498–507. https://doi.org/10.1111/1556-4029.13179.
[119] Leković A, Nikolić S. Commentary on "The integration and implications of artificial intelligence in forensic science." Forensic Sci Med Pathol. 2024. https://doi.org/10.1007/s12024-024-00781-z. Epub ahead of print.
[120] Tynan P. The integration and implications of artificial intelligence in forensic science. Forensic Sci Med Pathol 2024. https://doi.org/10.1007/s12024-023-00772-6. Epub ahead of print.
[121] Maschka J. Der Tod durch Erstickung. In: Maschka J, editor. Handbuch der Gerichtlichen Medizin, Tübingen: Verlag der H. Laupp'schen Buchhandlung; 1881, p. 601–2.
[122] Ushakov FS. Cadaveric Material in Medico-Legal Department of the Military Medical Academy for 15 years (1885–1900) [dissertation]. St. Petersburg; 1900.
[123] Reuter F. Über die anatomische Befunde beim Tode durch Erdrosseln und durch Erhängen. Z Heilkunde. 1901;22:145–72.
[124] Bauer G. Austrian forensic medicine. Forensic Sci Int. 2004;144:143–9. https://doi.org/10.1016/j.forsciint.2004.04.048.
[125] Brinkmann B. Harmonisation of medico-legal autopsy rules. Int J Leg Med. 1999;113:1–14. https://doi.org/10.1007/S004140050271.
[126] Peterson GF, Clark SC. Forensic Autopsy Performance Standards. Am J Forensic Med Pathol. 2006;27:200–25. https://doi.org/10.1097/01.paf.0000243580.43150.3c.
[127] Tulapunt N, Phanchan S, Peonim V. Hanging Fatalities in Central Bangkok, Thailand: A 13-Year Retrospective Study. Clin Med Insights Pathol. 2017;10:117955571769254. https://doi.org/10.1177/1179555717692545.
[128] Duband S, Peoc'h M, Movsessian J, Debout M. Lésions cervicales au cours des pendaisons et des strangulations: Étude rétrospective sur quatre années. J Med Leg Droit Med. 2005;48:29–35.
[129] Elfawal MA, Awad OA. Deaths from Hanging in the Eastern Province of Saudi Arabia. Med Sci Law. 1994;34:307–12. https://doi.org/10.1177/002580249403400406.
[130] Charoonnate N, Narongchai P, Vongvaivet S. Fractures of the hyoid bone and thyroid cartilage in suicidal hanging. J Med Assoc Thai. 2010;93:1211–6.
[131] Missliwetz J. Morphologie der Verletzungen von Kehlkopf und Zungenbein beim Erhängen (unter besonderer Berücksichtigung der Ringknorpelbrüche). Beitr Gerichtl Med. 1981;39:357–63.
[132] Patel AP, Bansal A, Shah K.A. Study of Hanging Cases in Ahmedabad Region. J Indian Acad Forensic Med. 2012;34:342–5.
[133] Kempter M, Ross S, Spendlove D, Flach PM, Preiss U, Thali MJ, et al. Post-mortem imaging of laryngohyoid fractures in strangulation incidents: First results. Leg Med. 2009;11:267–71. https://doi.org/10.1016/j.legalmed.2009.07.005.
[134] Talukder MA, Mansur MA, Kadir MM. Incidence of typical and atypical hanging among 66 hanging cases. Mymensingh Med J. 2008;17:149–51.
[135] Khokhlov VD. Injuries to the hyoid bone and laryngeal cartilages: Forensic Sci Int. 1997;88:173–83. https://doi.org/10.1016/S0379-0738(97)00101-1.
[136] Le Blanc-Louvry I, Thureau S, Duval C, Papin-Lefebvre F, Thiebot J, Dacher JN, et al. Post-mortem computed tomography compared to forensic autopsy findings: A French experience. Eur Radiol. 2013;23:1829–35. https://doi.org/10.1007/S00330-013-2779-0.

[137] Rao D. An autopsy study of death due to Suicidal Hanging – 264 cases. Egypt J Forensic Sci. 2016;6:248–54. https://doi.org/10.1016/j.ejfs.2015.01.004.
[138] Jovanović Simić J, Nikolić S. Mortui Vivos Docent – When the dead teach the living. Belgrade: Museum of Science and Technology/University of Belgrade, Faculty of Medicine; 2023.
[139] Nikolić S, Leković A. Katedra za sudsku medicinu: 1923-2023. Belgrade: University of Belgrade, Faculty of Medicine; 2023.
[140] Leković A. The exhibition catalog "Mortui Vivos Docent – When the dead teach the living" authored by Jelena Jovanović Simić and Slobodan Nikolić. Health Care. 2023;52:14–9. https://doi.org/10.5937/zdravzast52-47453.
[141] Luke J, Reay D, Eisele J, Bonnell H. Correlation of Circumstances with Pathological Findings in Asphyxial Deaths by Hanging: A Prospective Study of 61 Cases from Seattle, WA. J Forensic Sci. 1985;30:1140–7. https://doi.org/10.1520/JFS11055J.
[142] Ubelaker D. Hyoid Fracture and Strangulation. J Forensic Sci. 1992;37:1216–22. https://doi.org/10.1520/JFS13308J.
[143] Miller K, Walker P, O'Halloran R. Age and Sex-Related Variation in Hyoid Bone Morphology. J Forensic Sci. 1998;43:1138–43. https://doi.org/10.1520/JFS14376J.
[144] Naimo P, O'Donnell C, Bassed R, Briggs C. The use of computed tomography in determining developmental changes, anomalies, and trauma of the thyroid cartilage. Forensic Sci Med Pathol. 2013;9:377–85. https://doi.org/10.1007/s12024-013-9457-z.
[145] Urbanová P, Hejna P, Zátopková L, Šafr M. What is the appropriate approach in sex determination of hyoid bones? J Forensic Leg Med. 2013;20:996–1003. https://doi.org/10.1016/j.jflm.2013.08.010.
[146] Ma J, Jing H, Zeng Y, Tao L, Yang Y, Ma K, et al. Retrospective analysis of 319 hanging and strangulation cases between 2001 and 2014 in Shanghai. J Forensic Leg Med. 2016;42:19–24. https://doi.org/10.1016/j.jflm.2016.05.001.
[147] Lebreton-Chakour C, Godio-Raboutet Y, Torrents R, Chaumoitre K, Boval C, Bartoli C, et al. Manual strangulation: Experimental approach to the genesis of hyoid bone fractures. Forensic Sci Int. 2013;228:47–51. https://doi.org/10.1016/j.forsciint.2013.02.014.
[148] Travis LW, Olson NR, Melvin JW, Snyder RG. Static and dynamic impact trauma of the human larynx. Trans Sect Otolaryngol Am Acad Ophthalmol Otolaryngol. 1975;80:382–90.
[149] Keil W, Forster A, Meyer HJ, Peschel O. Characterization of haemorrhages at the origin of the sternocleidomastoid muscles in hanging. Int J Leg Med. 1995;108:140–4. https://doi.org/10.1007/BF01844825.

SUPPLEMENTS

Supplement A – Part I of the study

Supplementary Table A.1. *Training and test groups in Dataset I: the coded variables characteristics comparison.*

Characteristics		***Total*** *(N = 1,235)*	***Training*** *(N = 865, 70%)*	***Test*** *(N = 370, 30 %)*	***p-value***
Sex	Male	937 (75.9 %)	654 (75.6%)	283 (76.5 %)	> 0.05
	Female	298 (24.1 %)	211 (24.4 %)	87 (23.5%)	
Age (years)		54.2 ± 17.9	53.8 ± 17.6	55.3 ± 18.5	> 0.05
THYROHYOID and CERVICAL SPINE FRACTURE PATTERNS					
Unilateral STH fracture	Yes	369 (29.9 %)	262 (30.3 %)	107 (29.0 %)	> 0.05
	No	866 (70.1 %)	603 (69.7 %)	263 (71.0 %)	
Bilateral STH fracture	Yes	181 (14.7 %)	129 (14.9 %)	52 (14.1 %)	> 0.05
	No	1054 (85.3 %)	736 (85.1 %)	318 (85.9 %)	
Total N of STH fractures (0 – 2)		0 (0 – 2)	0 (0 – 2)	0 (0 – 2)	> 0.05
Unilateral GHH fracture	Yes	339 (27.4 %)	241 (27.9 %)	98 (26.5 %)	> 0.05
	No	896 (72.6 %)	624 (72.1 %)	272 (73.5 %)	
Bilateral GHH fracture	Yes	86 (7.0 %)	59 (6.8 %)	27 (7.3 %)	> 0.05
	No	1149 (93.0 %)	806 (93.2 %)	343 (92.7 %)	
Total N of GHH fractures (0 – 2)		0 (0 – 2)	0 (0 – 2)	0 (0 – 2)	> 0.05
Total N of TyHy fractures (0 – 4)		1 (0 – 4)	1 (0 – 4)	1 (0 – 4)	>0.05
Isolated STH fracture(s)	Yes	324 (26.2%)	225 (26.0%)	99 (26.8%)	> 0.05
	No	911 (73.8%)	640 (74.0%)	271 (73.2%)	
Isolated GHH fracture(s)	Yes	199 (16.1%)	134 (15.5%(	65 (17.6%)	> 0.05
	No	1036 (83.9%)	731 (84.5%)	305 (82.4%)	
Simultaneous STH and GHH fractures	Yes	226 (18.3%)	166 (19.2%)	60 (16.2%)	> 0.05
	No	1,009 (81.7%)	699 (80.8%)	310 (83.8%)	
Cervical Spine fracture	Yes	44 (3.6 %)	32 (3.7 %)	12 (3.2 %)	> 0.05
	No	1,191 (96.4 %)	833 (96.3 %)	358 (96.8 %)	
KNOT POSITION					
Knot position – Hanging type	**Typical**	707 (57.2 %)	497 (57.5 %)	210 (56.8 %)	> 0.05
	Atypical	528 (42.8 %)	368 (42.5 %)	160 (43.2 %)	

Note: The categorical data is presented as frequency and ratio, and numerical as average ± standard deviation or median and range. For comparison of categorical data, the χ^2 test was performed, while the Student's t-test for two independent samples or Mann-Whitney U test were performed for numerical data.

Abbreviations: STH – Superior thyroid cartilage horn; GHH – Greater hyoid bone horn; TyHy – Thyrohyoid.

Adopted from: Leković et al. [62]

Supplementary Table A.2. *Training and Test groups in Dataset II: the coded variables characteristics comparison.*

Characteristics		***Total*** *(N = 773)*	***Training*** *(N = 540, 69.9 %)*	***Test*** *(N = 233, 30.1 %)*	***p-value***
Sex	Male	600 (77.6%)	419 (77.6%	181 (77.7%)	> 0.05
	Female	173 (22.4%)	121 (22.4%)	52 (22.3%)	
Age (years)		56.1 ± 16.9	55.5 ± 16.9	57.3 ± 17.0	> 0.05
THYROHYOID and CERVICAL SPINE FRACTURE PATTERNS					
Unilateral STH fracture	Yes	369 (47.7%)	257 (47.6%)	112 (48.1%)	> 0.05
	No	404 (52.3%)	283 (52.4%)	121 (51.9%)	
Bilateral STH fracture	Yes	181 (23.4%)	124 (23.0%)	57 (24.5%)	> 0.05
	No	592 (76.6%)	416 (77.0%)	176 (75.1%)	
Total N of STH fractures (0 – 2)		1 (0 – 2)	1 (0 – 2)	1 (0 – 2)	> 0.05
Unilateral GHH fracture	Yes	339 (43.9%)	233 (43.1%)	106 (45.5%)	> 0.05
	No	434 (56.1%)	307 (56.9%)	127 (54.5%)	
Bilateral GHH fracture	Yes	86 (11.1%)	59 (10.9%)	27 (11.6%)	> 0.05
	No	687 (88.9%)	481 (89.1%)	206 (88.4%)	
Total N of GHH fractures (0 – 2)		1 (0 – 2)	1 (0 – 2)	1 (0 – 2)	>0.05
Total N of TyHy fractures (0 – 4)		1 (0 – 4)	1 (0 – 4)	1 (0 – 4)	>0.05
Isolated STH fracture(s)	Yes	324 (41.9%)	233 (43.1%)	91 (39.1%)	>0.05
	No	449 (58.1%)	307 (56.9%)	142 (60.9%)	
Isolated GHH fracture(s)	Yes	199 (25.7%)	144 (26.7%)	55 (23.6%)	>0.05
	No	574 (74.3%)	396 (73.3%)	178 (76.4%)	
Simultaneous STH and GHH fractures	Yes	226 (29.2%)	148 (27.4%)	78 (33.5%)	>0.05
	No	547 (70.8%)	392 (72.6%)	155 (66.5%)	
Cervical Spine fracture	Yes	44 (5.7%)	28 (5.2%)	16 (6.9%)	> 0.05
	No	729 (94.3%)	512 (94.8%)	217 (93.1%)	
KNOT POSITION					
Knot position – Hanging type	**Typical**	433 (56.0%)	298 (55.2%)	135 (57.9%)	> 0.05
	Atypical	340 (44.0%)	242 (44.8%)	98 (42.1%)	

Note: The categorical data is presented as frequency and ratio, and numerical as average ± standard deviation or median and range. For comparison of categorical data, the χ^2 test was performed, while the Student's t-test for two independent samples or Mann-Whitney U test were performed for numerical data.

Abbreviations: STH – Superior thyroid cartilage horn; GHH – Greater hyoid bone horn; TyHy – Thyrohyoid.

Adopted from: Leković et al. [62]

Supplementary Table A.3. *Training and Test groups in Dataset III: the coded variables characteristics comparison.*

Characteristics		***Total*** *(N = 340)*	***Training*** *(N = 238, 70 %)*	***Test*** *(N = 102, 30 %)*	***p-value***
Sex	Male	271 (79.7%)	193 (81.1%)	78 (76.5%)	> 0.05
	Female	69 (20.3%)	45 (18.9%)	24 (23.5%)	
Age (years)		58.00 (16 – 94)	58.5 (19 – 94)	56.0 (16 – 86)	> 0.05
THYROHYOID and CERVICAL SPINE FRACTURE PATTERNS					
Unilateral STH fracture	Yes	156 (45.9%)	108 (45.4%)	48 (47.1%)	> 0.05
	No	184 (54.1%)	130 (54.6%)	54 (52,9%)	
Bilateral STH fracture	Yes	73 (21.5%)	48 (20.2%)	25 (24.5%)	> 0.05
	No	267 (78.5%)	190 (79.8%)	77 (75.7%)	
Total N of STH fractures (0 – 2)		1 (0 – 2)	1 (0 – 2)	1 (0 – 2)	> 0.05
Unilateral GHH fracture	Yes	174 (51.2%)	125 (52.5%)	49 (48.0%)	> 0.05
	No	166 (48.8%)	113 (47.5%)	53 (52.0%)	
Bilateral GHH fracture	Yes	33 (9.7%)	22 (9.2%)	11 (10.8%)	> 0.05
	No	307 (90.3%)	216 (90.8%)	91 (89.2%)	
Total N of GHH fractures (0 – 2)		1 (0 – 2)	1 (0 – 2)	1 (0 – 2)	>0.05
Total N of TyHy fractures (0 – 4)		1 (0 – 4)	1 (0 – 4)	2 (0 – 4)	>0.05
Isolated STH fracture(s)	Yes	113 (33.2%)	78 (32.8%)	35 (34-3%)	>0.05
	No	227 (66.8%)	160 (67.2%)	67 (65.7%)	
Isolated GHH fracture(s)	Yes	91 (26.8%)	69 (29.0%)	22 (21.6%)	>0.05
	No	249 (73.2%)	169 (71.0%)	80 (78.4%)	
Simultaneous STH and GHH fractures	Yes	116 (34.1%)	78 (32.8%)	38 (37.3%)	>0.05
	No	224 (65.9%)	160 (67.2%)	64 (62.7%)	
Cervical Spine fracture	Yes	34 (10.0%)	24 (10.1%)	10 (9.8%)	> 0.05
	No	306 (90%)	214 (89.9%)	92 (90.2%)	
KNOT POSITION					
Knot position – Hanging type	**Anterior**	54 (15.9%)	37 (15.5%)	17 (16.7%)	> 0.05
	Lateral	286 (84.1%)	201 (84.5%)	85 (83.3%)	

Note: The categorical data is presented as frequency and ratio, and numerical as average ± standard deviation or median and range. For comparison of categorical data, the χ^2 test was performed, while the Mann-Whitney U test was performed for numerical data. Only the preprocessed sample characteristics are shown. After the SMOTE algorithm was performed to reduce the disproportion of the group sample sizes, the absence of statistically significant difference in the analyzed variables was preserved (not shown, see Results, section 3.2.).

Abbreviations: STH – Superior thyroid cartilage horn; GHH – Greater hyoid bone horn; TyHy – Thyrohyoid.

Adopted from: Leković et al. [62]

Supplementary Table A.4. *Training and test groups in Dataset IV: the coded variables characteristics comparison.*

Characteristics		***Total*** *(N = 286)*	***Training*** *(N = 201, 70 %)*	***Test*** *(N = 85, 30 %)*	***p-value***
Sex	Male	233 (81.5%)	166 (82.6%)	67 (78.8%)	> 0.05
	Female	53 (18.5%)	35 (17.4%)	18 (21.2%)	
Age (years)		57.0 (16 – 94)	56.0 (18.0 – 94.0)	59.0 (16.0 – 94.0)	> 0.05
THYROHYOID and CERVICAL SPINE FRACTURE PATTERNS					
Unilateral STH fracture	Yes	138 (48.3%)	101 (50.2%)	37 (43.5%)	> 0.05
	No	148 (51.7%)	100 (49.8%)	48 (56.5%)	
Bilateral STH fracture	Yes	65 (22.7%)	43 (21.4%)	22 (25.9%)	> 0.05
	No	221 (77.3%)	158 (78.6%)	63 (74.1%)	
Total N of STH fractures (0 – 2)		1 (0 – 2)	1 (0 – 2)	1 (0 – 2)	> 0.05
Contralateral STH fracture	Yes	80 (28.0%)	58 (28.9%)	22 (25.9%)	> 0.05
	No	206 (72.0%)	143 (71.1%)	63 (74.1%)	
Left STH fracture	Yes	136 (47.6%)	95 (47.3%)	41 (42.2%)	> 0.05
	No	150 (52.4%)	106 (52.7%)	44 (51.8%)	
Right STH fracture	Yes	132 (46.2%)	92 (45.8%)	40 (47.1%)	> 0.05
	No	154 (53.8%)	109 (54.2%)	45 (52.9%)	
Unilateral GHH fracture	Yes	152 (53.1%)	108 (53.7%)	44 (51.8%)	> 0.05
	No	134 (46.9%)	93 (46.9%)	41 (48.2%)	
Bilateral GHH fracture	Yes	26 (9.1%)	18 (9.0%)	8 (9.4%)	> 0.05
	No	260 (90.9%)	183 (91.0%)	77 (90.6%)	
Total N of GHH fractures (0 – 2)		1 (0 – 2)	1 (0 – 2)	1 (0 – 2)	>0.05
Left GHH fracture	Yes	99 (34.6%)	69 (34.3%)	30 (35.3%)	> 0.05
	No	187 (63.3%)	132 (65.7%)	55 (64.7%)	
Right GHH fracture	Yes	105 (36.7%)	75 (37.3%)	30 (35.3%)	> 0.05
	No	181 (63.3%)	126 (62.7%)	55 (64.7%)	
Ipsilateral GHH fracture	Yes	90 (31.5%)	62 (30.8%)	28 (23.9%	> 0.05
	No	196 (68.5%)	139 (69.2%)	57 (67.1%)	
Total N of TyHy fractures (0 – 4)		1 (0 – 4)	1 (0 – 4)	2 (0 – 4)	>0.05
Isolated STH fracture(s)	Yes	103 (36.0%)	72 (35.8%)	31 (36.5%)	>0.05
	No	183 (64.0%)	129 (64.2%)	54 (63.5%)	
Isolated GHH fracture(s)	Yes	78 (27.3%)	54 (26.9%)	24 (28.2%)	>0.05
	No	208 (72.7%)	147 (73.1%)	61 (71.8%)	
Simultaneous STH and GHH fractures	Yes	100 (35.0%)	72 (35.8%)	28 (32.9%)	>0.05
	No	186 (65.0%)	129 (64.2%)	57 (67.1%)	
Cervical Spine fracture	Yes	12 (4.2%)	9 (4.5%)	3 (3.5)	> 0.05
	No	274 (95.8%)	192 (95.5%)	82 (96.5%)	
KNOT POSITION					
Knot position – Hanging type	**Left Lateral**	140 (49.0%)	101 (50.2%)	39 (45.9%)	> 0.05
	Right Lateral	146 (51.0%)	100 (49.8%)	46 (54.1%)	

Note: The categorical data is presented as frequency and ratio, and numerical as average ± standard deviation or median and range. For comparison of categorical data, the χ^2 test was performed, while the Mann-Whitney U test was performed for numerical data.
Abbreviations: STH – Superior thyroid cartilage horn; GHH – Greater hyoid bone horn; TyHy – Thyrohyoid. Adopted from: Leković et al. [62]

Supplement B – Part II of the study

Supplementary Table B.1. *Training and test groups in Dataset I-w: the coded variables characteristics comparison.*

Characteristics		***Total*** *(N = 385)*	***Training*** *(N = 270, 70.1%)*	***Test*** *(N = 115, 29.9%)*	***p-value***
Sex	Male	298 (77.4%)	207 (76.7%)	91 (79.1%)	> 0.05
	Female	87 (22.6%)	63 (23.3%)	24 (20.9%)	
Age (years)		57.0 (16-94)	56.5 (16-94)	58.0 (20-90)	> 0.05
Body weight (kg)		71.0 (34-148)	70.0 (34-148)	72.0 (46-108)	> 0.05
Body height (cm)		176.0 (145-205)	176.0 (145-205)	175.0 (153-195)	> 0.05
THYROHYOID and CERVICAL SPINE FRACTURE PATTERNS					
Unilateral STH fracture	Yes	116 (30.1%)	82 (30.4%)	34 (29.6%)	> 0.05
	No	269 (69.9%)	188 (69.6%)	81 (70.4%)	
Bilateral STH fracture	Yes	65 (16.9%)	47 (17.4%)	18 (15.7%)	> 0.05
	No	320 (83.1%)	223 (82.6%)	97 (84.3%)	
Total N of STH fractures (0 – 2)		0 (0-2)	0 (0-2)	0 (0-2)	
Unilateral GHH fracture	Yes	101 (26.2%)	72 (26.7%)	29 (25.2%)	> 0.05
	No	284 (73.8%)	198 (73.3%)	86 (74.8%)	
Bilateral GHH fracture	Yes	33 (8.6%)	23 (8.5%)	10 (8.7%)	> 0.05
	No	352 (91.4%)	247 (91.5%)	105 (91.3%)	
Total N of GHH fractures (0 – 2)		0 (0-2)	0 (0-2)	0 (0-2)	> 0.05
Total N of TyHy fractures (0 – 4)		1 (0-4)	1 (0-4)	1 (0-4)	> 0.05
Isolated STH fracture(s)	Yes	106 (27.5%)	79 (29.3%)	27 (23.5%)	> 0.05
	No	279 (72.5%)	191 (70.7%)	88 (76.5%)	
Isolated GHH fracture(s)	Yes	59 (15.3%)	45 (16.7%)	14 (12.2%)	> 0.05
	No	326 (84.7%)	225 (83.3%)	101 (87.8%)	
Simultaneous STH and GHH fractures	Yes	75 (19.5%)	50 (18.5%)	25 (21.7%)	> 0.05
	No	310 (80.5%)	220 (81.5%)	90 (78.3%)	
Cervical Spine fracture	Yes	16 (4.2%)	10 (3.7%)	6 (5.2%)	> 0.05
	No	369 (95.8%)	260 (96.3%)	109 (94.8%)	
KNOT POSITION					
Knot position – Hanging type	**Typical**	197 (51.2%)	144 (53.3%)	53 (46.1%)	> 0.05
	Atypical	188 (48.8%)	126 (46.7%)	62 (53.9%)	

Note: The categorical data is presented as frequency and ratio, and numerical as average ± standard deviation or median and range. For comparison of categorical data, the χ^2 test was performed, while the Mann-Whitney U test or Student's t test were performed for numerical data.

Abbreviations: STH – Superior thyroid cartilage horn; GHH – Greater hyoid bone horn; TH – Thyrohyoid.

Supplementary Table B.2. *Training and test groups in Dataset II-w:* the coded variables characteristics comparison.

Characteristics		***Total*** *N =250*	***Training*** *N = 175 (70.0%)*	***Test*** *N = 75 (30.0%)*	***p-value***
Sex	Male	193 (77.2%)	134 (76.6%)	59 (78.7%)	> 0.05
	Female	57 (22.8%)	41 (23.4%)	16 (21.3%)	
Age (years)		58.2 ± 17.9	59.4 ± 18.0	55.6 ± 17.6	> 0.05
Body weight (kg)		70.5 (38 – 146)	72.0 (38 – 146)	70.0 (46 – 117)	> 0.05
Body height (cm)		176 (145 – 205)	175 (145 – 205)	176 (152 – 200)	> 0.05
THYROHYOID and CERVICAL SPINE FRACTURE PATTERNS					
Unilateral STH fracture	Yes	118 (47.2%)	81 (46.3%)	37 (49.3%)	> 0.05
	No	132 (52.8%)	94 (53.7%)	38 (50.7%)	
Bilateral STH fracture	Yes	65 (26.0%)	45 (25.7%)	20 (26.7%)	> 0.05
	No	185 (74.0%)	130 (74.3%)	55 (73.3%)	
Total N of STH fractures (0 – 2)		1 (0 – 2)	1 (0 – 2)	1 (0 – 2)	
Unilateral GHH fracture	Yes	105 (42.0%)	72 (41.1%)	33 (44.0%)	> 0.05
	No	145 (58.0%)	103 (58.9%)	42 (56.0%	
Bilateral GHH fracture	Yes	33 (13.2%)	24 (13.7%)	9 (12.0%)	> 0.05
	No	217 (86.8%)	151 (86.3%)	66 (88.0%)	
Total N of GHH fractures (0 – 2)		1 (0 – 2)	1 (0 – 2)	1 (0 – 2)	> 0.05
Total N of TyHy fractures (0 – 4)		1 (0 – 4)	1 (0 – 4)	2 (0 – 4)	> 0.05
Isolated STH fracture(s)	Yes	106 (42.4%)	74 (42.3%)	32 (42.7%)	> 0.05
	No	144 (57.6%)	101 (57.7%)	54 (57.3%)	
Isolated GHH fracture(s)	Yes	61 (24.4%)	44 (25.1%)	17 (22.7%)	> 0.05
	No	189 (75.6%)	131 (74.9%)	58 (77.3%)	
Simultaneous STH and GHH fractures	Yes	77 (30.8%)	52 (29.7%)	25 (33.3%)	> 0.05
	No	173 (69.2%)	123 (70.3%)	50 (66.7%)	
Cervical Spine fracture	Yes	16 (6.4%)	13 (7.4%)	3 (4.0%)	> 0.05
	No	234 (93.6%)	162 (92.6%)	72 (96.0%)	
KNOT POSITION					
Knot position – Hanging type	**Typical**	128 (51.2%)	90 (51.4%)	38 (50.7%)	> 0.05
	Atypical	122 (48.8%)	85 (48.6%)	37 (49.3%)	

Note: The categorical data is presented as frequency and ratio, and numerical as average ± standard deviation or median and range. For comparison of categorical data, the χ^2 test was performed, while the Mann-Whitney U test or Student's t test were performed for numerical data.

Abbreviations: STH – Superior thyroid cartilage horn; GHH – Greater hyoid bone horn; TH – Thyrohyoid.

Supplement C – Part III of the study

Supplementary Table C.1. *Training and test groups in Dataset I-m: the coded variables characteristics comparison.*

Characteristics		***Total*** *(N = 126)*	***Training*** *(N = 88, 69.8%)*	***Test*** *(N = 38, 30.2%)*	***p-value***
Sex	Male	99 (78.6%)	72 (81.8%)	27 (71.1%)	> 0.05
	Female	27 (21.4%)	16 (18.2%)	11 (28.9%)	
Age (years)		55.0 (18 – 94)	55.5 (17 – 94)	54.0 (20 – 90)	> 0.05
Body weight (kg)		70.0 (40 – 125)	70.0 (40 – 125)	70.0 (41 – 124)	> 0.05
Body height (cm)		176.0 (145 – 205)	176.5 (145 – 190)	173.5 (151 - 205)	> 0.05
THYROHYOID and CERVICAL SPINE FRACTURE PATTERNS					
Unilateral STH fracture	Yes	41 (32.5%)	26 (29.5%)	15 (39.5%)	> 0.05
	No	85 (67.5%)	62 (70.5%)	23 (60.5%)	
Bilateral STH fracture	Yes	24 (19.0%)	19 (21.6%)	5 (13.2%)	> 0.05
	No	102 (81.0%)	69 (78.4%)	33 (86.8%)	
Total N⁰of STH fractures (0 – 2)		1 (0 – 2)	1 (0 – 2)	1 (0 – 2)	> 0.05
Unilateral GHH fracture	Yes	28 (22.2%)	22 (25.0%)	6 (15.8%)	> 0.05
	No	98 (77.8%)	66 (75.0%)	32 (84.2%)	
Bilateral GHH fracture	Yes	11 (8.7%)	7 (8.0%)	4 (10.5%)	> 0.05
	No	115 (91.3%)	81 (92.0%)	34 (89.5%)	
Total N⁰ of GHH fractures (0 – 2)		0 (0 – 2)	0 (0 – 2)	0 (0 – 2)	> 0.05
Total N⁰ of TyHy fractures (0 – 4)		1 (0 – 4)	1 (0 – 4)	1 (0 – 4)	> 0.05
Isolated STH fracture(s)	Yes	44 (34.9%)	30 (34.1%)	14 (36.8%)	> 0.05
	No	82 (65.1%)	58 (65.9%)	24 (63.2%)	
Isolated GHH fracture(s)	Yes	18 (14.3%)	14 (15.9%)	4 (10.5%)	> 0.05
	No	108 (85.7%)	74 (84.1%)	34 (89.5%)	
Simultaneous STH and GHH fractures	Yes	23 (18.3%)	16 (18.2%)	7 (18.4%)	> 0.05
	No	103 (81.7%)	72 (81.8%)	31 (81.6%)	
Cervical Spine fracture	Yes	3 (2.4%)	2 (2.3%)	1 (2.6%)	> 0.05
	No	123 (97.6%)	86 (97.7%)	37 (97.4%)	
STERNOCLEIDOMASTOID MUSCLE'S ORIGIN HEMORRHAGES					
Unilateral SCM hemorrhage	Yes	50 (39.7%)	36 (40.9%)	14 (36.8%)	> 0.05
	No	76 (60.3%)	52 (59.1%)	24 (63.2%)	> 0.05
Bilateral SCM hemorrhage	Yes	58 (46.0%)	39 (44.3%)	19 (50.0%)	> 0.05
	No	68 (54.0%)	49 (55.7%)	19 (50.0%)	> 0.05
Total N⁰ of SCM hemorrhages (0 – 2)		1 (0 – 2)	1 (0 – 2)	1.5 (0 – 2)	> 0.05
Knot position – Hanging type	**Typical**	62 (49.2%)	46 (52.3%)	18 (47.4%)	> 0.05
	Atypical	64 (50.8%)	42 (47.7%)	20 (52.6%)	

Note: The categorical data is presented as frequency and ratio, and numerical as average ± standard deviation or median and range. For comparison of categorical data, the χ^2 test was performed, while the Mann-Whitney U test was performed for numerical data. ***Abbreviations:*** STH – Superior thyroid cartilage horn; GHH – Greater hyoid bone horn; TH – Thyrohyoid; SCM – sternocleidomastoid muscle.

PhD candidate's brief biography

Aleksa Leković was born on October 10, 1995, in Belgrade. After graduating from the gymnasium, he enrolled at the University of Belgrade - Faculty of Medicine in 2014 and graduated in 2020 with an average grade of 9.80. He enrolled in specialist academic studies in Forensic pathology and expertise diagnostics at the Faculty of Medicine in Belgrade in 2020 and graduated in 2022, defending his thesis entitled "Forensic significance of burn index, burns characteristics and carboxyhemoglobin levels in fire deaths." Since February 2022, he has been employed at the Institute of Forensic Medicine *Milovan Milovanović*. On December 15, 2021, Aleksa became a Teaching Associate at the Department of Forensic Medicine at the Faculty of Medicine, University of Belgrade, and was reelected to the same position on December 15, 2022. On October 18, 2023, he became a Teaching Assistant. In 2021, he enrolled in PhD studies at the University of Belgrade – Faculty of Medicine (course: Skeletal Biology). Since April 2023, he is also enrolled in the Forensic Medicine residency program (Faculty of Medicine in Belgrade). Aleksa Leković is one of the research team members on the *BoFraM project* (Changes in bone structure and composition leading to increased fracture risk in aged population with chronic comorbidities; PI Prof. Marija Djurić) funded by the Science Fund of the Republic of Serbia. According to the Scopus index database, Aleksa Leković has published 16 research papers in journals with impact factor (access date: August 25, 2024).

Кратка биографија докторанда

Алекса Лековић рођен је 10. октобра 1995. године у Београду. Након завршене гимназије, 2014. године уписао је Медицински факултет Универзитета у Београду. Дипломирао је 2020. године, са просечном оценом 9,80. Специјалистичке академске студије из форензичке патологије и експертизне дијагностике на Медицинском факултету у Београду уписао је 2020, а дипломирао 2022. године, одбраном завршног рада под називом „Форензички значај индекса опечености, карактеристика опекотина и вредности карбоксихемоглобина у случајевима смрти у пожару.“ Од фебруара 2022. године запослен је у Институту за судску медицину *Милован Миловановић.* У звање сарадника у настави на Катедри за судску медицину Медицинског факултета Универзитета у Београду изабран је 15. децембра 2021. године и реизабран следеће године, а 18. октобра 2023. године изабран је у звање асистента. Године 2021. уписао је докторске академске студије на Медицинском факултету у Београду, модул „Биологија скелета.“ Такође, специјализант је судске медицине (Медицински факултет у Београду) од априла 2023. године. Тренутно је члан пројектног тима на пројекту *BoFram (Changes in bone structure and composition leading to increased fracture risk in aged population with chronic comorbidities*; руководилац проф. др Марија Ђурић), који је финансиран од стране Фонда за науку Републике Србије. Према индексној бази Скопус, Алекса Лековић објавио је 16 научно-истраживачких радова у часописима са импакт фактором (приступ 25. августа 2024. године).

Currently published papers resulting from the work on this research and dissertation

Original paper

Leković A, Vukićević A, Nikolić S. Assessing the knot in a noose position by thyrohyoid and cervical spine fracture patterns in suicidal hangings using machine learning algorithms: A new insight into old dilemmas. Forensic Sci Int. 2024;357:111973. https://doi.org/10.1016/j.forsciint.2024.111973.

Letter to the editor

Leković A, Nikolić S. Commentary on "The integration and implications of artificial intelligence in forensic science." Forensic Sci Med Pathol. 2024. https://doi.org/10.1007/s12024-024-00781-z. Epub ahead of print.

Mini-review article (Medical Youth)

Leković A, Nikolić S. Autonomous nervous system-related vital reactions in short-drop hangings. Med Podml. 2025;76(6). https://doi.org/10.5937/mp76-48972.
(Accepted for publication)

образац изјаве о ауторству

Изјава о ауторству

Име и презиме аутора **Алекса Лековић**

Број индекса **дс215022**

Изјављујем

да је докторска дисертација под насловом:

„Алгоритми машинског учења у форензичкој експертизи: процена положаја чвора омче у самоубилачким вешањима на основу распореда прелома тиреохиоидног комплекса и вратне кичме“ (енгл. ***Machine learning algorithms in forensic expertise: Assessing noose knot's position in suicidal hangings through fracture patterns of the thyrohyoid complex and the cervical spine***):

- резултат сопственог истраживачког рада;
- да дисертација у целини ни у деловима није била предложена за стицање друге

дипломе према студијским програмима других високошколских установа;

- да су резултати коректно наведени и
- да нисам кршио ауторска права и користио интелектуалну својину других лица.

Потпис аутора

У Београду,

30. августа 2024. године _____

Изјава о истоветности штампане и електронске верзије докторског рада

Име и презиме аутора **Алекса Лековић**

Број индекса **дс215022**

Студијски програм **Биологија скелета**

Наслов рада **„Алгоритми машинског учења у форензичкој експертизи: процена положаја чвора омче у самоубилачким вешањима на основу распореда прелома тиреохиоидног комплекса и вратне кичме“** (енгл**.** ***Machine learning algorithms in forensic expertise: Assessing noose knot's position in suicidal hangings through fracture patterns of the thyrohyoid complex and the cervical spine***)

Ментор **проф. др Слободан Николић**

Изјављујем да је штампана верзија мог докторског рада истоветна електронској верзији коју сам предао ради похрањивања у Дигиталном репозиторијуму Универзитета у Београду.

Дозвољавам да се објаве моји лични подаци везани за добијање академског назива доктора наука, као што су име и презиме, година и место рођења и датум одбране рада.

Ови лични подаци могу се објавити на мрежним страницама дигиталне библиотеке, у електронском каталогу и у публикацијама Универзитета у Београду.

Потпис аутора

У Београду,

30. августа 2024. године _____

образац изјаве о коришћењу

Изјава о коришћењу

Овлашћујем Универзитетску библиотеку „Светозар Марковић“ да у Дигитални репозиторијум Универзитета у Београду унесе моју докторску дисертацију под насловом: **„Алгоритми машинског учења у форензичкој експертизи: процена положаја чвора омче у самоубилачким вешањима на основу распореда прелома тиреохиоидног комплекса и вратне кичме“** (енгл. ***Machine learning algorithms in forensic expertise: Assessing noose knot's position in suicidal hangings through fracture patterns of the thyrohyoid complex and the cervical spine***),

која је моје ауторско дело.

Дисертацију са свим прилозима предао сам у електронском формату погодном за трајно архивирање. Моју докторску дисертацију похрањену у Дигиталном репозиторијуму Универзитета у Београду и доступну у отвореном приступу могу да користе сви који поштују одредбе садржане у одабраном типу лиценце Креативне заједнице *(Creative Commons)* за коју сам се одлучио.

1. Ауторство (CC BY)

2. Ауторство – некомерцијално (CC BY-NC)

3. Ауторство – некомерцијално – без прерада (CC BY-NC-ND)

4. Ауторство – некомерцијално – делити под истим условима (CC BY-NC-SA)

5. Ауторство – без прерада (CC BY-ND)

6. Ауторство – делити под истим условима (CC BY-SA)

(Молимо да заокружите само једну од шест понуђених лиценци.
Кратак опис лиценци је саставни део ове изјаве).

Потпис аутора

У Београду,

30. августа 2024. године _____

1. **Ауторство.** Дозвољавате умножавање, дистрибуцију и јавно саопштавање дела, и прераде, ако се наведе име аутора на начин одређен од стране аутора или даваоца лиценце, чак и у комерцијалне сврхе. Ово је најслободнија од свих лиценци.

2. **Ауторство – некомерцијално.** Дозвољавате умножавање, дистрибуцију и јавно саопштавање дела, и прераде, ако се наведе име аутора на начин одређен од стране аутора или даваоца лиценце. Ова лиценца не дозвољава комерцијалну употребу дела.

3. **Ауторство – некомерцијално – без прерада.** Дозвољавате умножавање, дистрибуцију и јавно саопштавање дела, без промена, преобликовања или употребе дела у свом делу, ако се наведе име аутора на начин одређен од стране аутора или даваоца лиценце. Ова лиценца не дозвољава комерцијалну употребу дела. У односу на све остале лиценце, овом лиценцом се ограничава највећи обим права коришћења дела.

4. **Ауторство – некомерцијално – делити под истим условима.** Дозвољавате умножавање, дистрибуцију и јавно саопштавање дела, и прераде, ако се наведе име аутора на начин одређен од стране аутора или даваоца лиценце и ако се прерада дистрибуира под истом или сличном лиценцом. Ова лиценца не дозвољава комерцијалну употребу дела и прерада.

5. **Ауторство – без прерада.** Дозвољавате умножавање, дистрибуцију и јавно саопштавање дела, без промена, преобликовања или употребе дела у свом делу, ако се наведе име аутора на начин одређен од стране аутора или даваоца лиценце. Ова лиценца дозвољава комерцијалну употребу дела.

6. **Ауторство – делити под истим условима.** Дозвољавате умножавање, дистрибуцију и јавно саопштавање дела, и прераде, ако се наведе име аутора на начин одређен од стране аутора или даваоца лиценце и ако се прерада дистрибуира под истом или сличном лиценцом. Ова лиценца дозвољава комерцијалну употребу дела и прерада. Слична је софтверским лиценцама, односно лиценцама отвореног кода.